CARDIFF UNIVERSITY
PRIFYSGOL CAERDYDD

BINDING SERVICES
Tel +44 (0)29 2087 4949
Fax +44 (0)29 20371921
e-mail bindery@cardiff.ac.uk

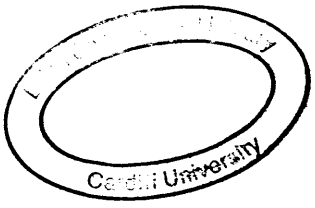

Novel Transglutaminases: A potential route to healthy skin

Sally Rosser-Davies B.Sc.

Matrix Biology and Tissue Repair

Cardiff Dental School

University of Wales, Cardiff

July 2005

Ph.D .Thesis

Supervisors: Prof. D. Aeschlimann
Dr. R. Ginger

Funded by: Biotechnology and Biological Sciences Research Council
Unilever

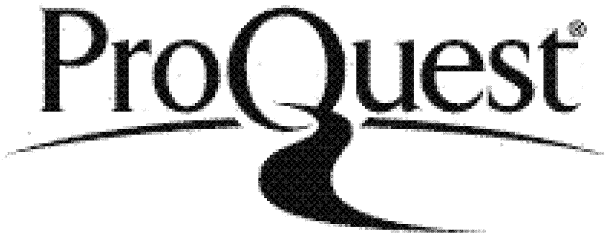

ProQuest LLC
789 East Eisenhower Parkway
P.O. Box 1346
Ann Arbor, MI 48106-1346

Novel Transglutaminases: A potential route to healthy skin

Contents Page

Acknowledgements

Firstly I must thank my supervisors, Prof. Daniel Aeschlimann (University of Wales, Cardiff) and Dr. Rebecca Ginger (Unilever, Colworth). I would also like to thank Dr. Clive Harding (Unilever, Colworth) for his continued input throughout this project.

Concerning specific sections of work, I would like to thank Dr. William Parish (Unilever, Colworth), Dr. Ian Mackenzie and Dr. Matthew Locke (Cardiff, Dental School) for sharing their expertise on skin equivalent cultures. Kath Allsop (Cardiff, Pathology Department) must be acknowledged for the time she generously spent sectioning skin equivalent samples. I would also like to thank Dr. Elke Schöhnerr for her help in developing a keratinocyte migration model.

Finally, I must express thanks to Martin Langley M.Phil, Dr. Ryan Mosley and Dr. Stewart Jones (University of Wales, Cardiff) for their daily advice and my family for their continued support.

Summary

The transglutaminases (TGs) constitute a family of enzymes capable of post-translationally modifying proteins through the formation of cleavage-resistant γ-glutamyl-ε-lysine bonds. Interest in these enzymes as therapeutic targets is increasing and they have been implicated in a number of skin disorders, including lamellar ichthyosis and the autoimmune disease, dermatitis herpetiformis. This thesis has focused specifically on the role of TG enzymes in skin homeostasis.

Limited data exists concerning the most recently identified isoforms, TG6 and TG7. Peptide antibodies have successfully been generated against these enzymes and their expression within human dermis and epidermis has been demonstrated. In addition to this, immunohistochemical studies have identified an upregulation of TG7 in the epidermis of dermatitis herpetiformis patients.

In vitro experiments have demonstrated the C-terminal β-barrel regions of TG5, TG6 and TG7 are capable of binding actin. This chapter of work does not support the hypothesis that these domains are involved in substrate selection as has formerly been suggested.

Previous studies have reported the existence of a mature form of corneocyte within the epidermis. The putative role these cells have in the skin-barrier function has attracted some interest. Based on data revealing an increase in γ-glutamyl-ε-lysine bonds within these "mature" cells, work was carried out to identify TGs that are potentially responsible. Western blot analysis revealed increased levels of the TG3 zymogen and its cleavage products in the more superficial layers of the stratum corneum. This same profile was not evident in samples harvested from an environmentally exposed region of skin.

Investigations into the function of mesenchymal-TG2 in epidermal formation and keratinocyte migration were established with varying success using coculture systems. Results indicate TG2 overexpression increases the rate of keratinocyte migration via an as yet unidentified soluble factor. Conversely, the presence of fibroblasts overexpressing this TG have demonstrated an inhibitory effect on keratinocyte migration.

List of Abbreviations

AEC	3-amino-9-ethyl-carbozide
BSA	Bovine serum albumin
BCA	Bicinchoninic acid
CBL	Covalently bound lipid
CE	Cornified envelope
CHAPS	3-[(3-Cholamidopropyl)dimethylammonio]propanesulonate
CIAP	Calf Intestinal Alkaline Phosphatase
CNBr	Cyanogen bromide
DEJ	Dithiothretol
DTT	Dermo-epidermal junction
DMSO	Dimethyl sulfoxide
ELISA	Enzyme-linked immunosorbent assay
ECM	Extracellular matrix
EDC	1-ethyl-3-(3-dimethylaminopropyl)-carbiimide
EDTA	Ethylenediaminetetraacetic acid
EGF	Epidermal growth factor
EGTA	Ethyl glycol-bis(2-aminoethylether)-N,N,N',N'-tetraacetic acid
FAM	Fluorencin
FBS	Fetal bovine serum
FGF	Fibroblast growth factor
FITC	Fluorescein
FN	Fibronectin
FPLC	Fast protein liquid chromatography
GM-CSF	Granulocyte macrophage colony stimulating factor
GST	Glutathione S-transferase
HEPES	N-2-hydroxyethlpiperazine-N'-2-ethane sulphonic acid monosodium salt
HGF	Hepatocyte growth factor
HPLC	High performance liquid chromatography
IGF	Insulin-like growth factor
IL	Interleukin
IPTG	Isopropyl β D-thiogalactoside
K	Keratin
KGF	Keratinocyte growth factor
KHL	Keyhole limpet
LI	Lamellar ichthyosis
MDC	Monodansyl cadaverine
NEM	N-ethyl malemide
PBS	Phosphate buffered saline
PM	Plasma membrane
PMSF	Phenylmethyl sulphonylfluoride
PSG	Penicillin-Streptomycin-Glutamine
RGD	Arginine-Glycine-Aspartate
SDS	Sodium dodecyl sulfate
SE	Skin equivalent
SFM	Serum free medium
SPR	Small proline rich
Sulfo-NHS	N-hydroxysulfosuccinimide
Sulfo-GMBS	(N-[g-Maleimidobutyryloxy]sulfosuccinimide ester)
TAE buffer	Tris/acetate/EDTA buffer
TAMRA	Tetramethylrhodamine

TBS	Tris buffered saline
TBE	Tris-Borate-EDTA
TCA	Trichloroacetic acid
TGF	Transforming growth factor
TG	Transglutaminase
TNF	Tumour neucrosis factor
UV	Ultra violet

Chapter 1:

A review of current literature

1.1 The Transglutaminase Family

The transglutaminase (TG) enzymes have been described as nature's biological glues (Griffin *et al.*, 2002), alluding to their ability to post-translationally modify proteins by intra and inter-molecular cross-linking. These covalent bonds are predominantly formed between the side chains of peptide-linked glutamine (Gln) and lysine (Lys) residues and have been termed γ-glutamyl-ε-lysine isopeptide bonds (Folk and Finlayson, 1977). The activity of these enzymes is dependent on calcium binding (Folk *et al.*, 1967; Lorand and Conrad, 1984; Chang and Chung, 1986) with an estimated 500 μM required for enzyme activity. This would suggest that TGs are rendered virtually inactive under normal physiological conditions since intra-cellular calcium levels rarely exceed 100 nM (Nemes *et al.*, 1999b).

The transamidation reaction proceeds via an acyl intermediate, formed between the γ-carboxamide-group of Gln and the thiol group of an active cysteine residue within the TG. The release of ammonia at this stage, and its subsequent protonation, generates the driving force of the reaction. During a second step the enzyme is liberated by the nucleophilic attack of the primary amine group within a Lys side chain (Folk and Finlayson, 1977; Lorand and Conrad 1984). Once formed these isopeptide bonds have proved resistant to mechanical and proteolytic cleavage, often producing large, insoluble polymers (Tokunaga *et al.*, 1993; Cariello *et al.*, 1997; Kobayashi *et al.*, 1998; Makarova *et al.*, 1999). It has been observed that other primary amines, such as spermidine and putrescine, are capable of acting as acyl acceptors (Folk, 1980), demonstrating a flexibility not seen with the donors. The selection of target Gln residues by TGs is restricted by the composition and charge of surrounding residues (Folk and Finlayson, 1977; Folk, 1980;Gorman *et al.*, 1981; 1984; Aeschlimann *et al.*, 1992). In contrast, residues flanking Lys residues do not have a pronounced affect on the substrate properties, providing some insight as to why small primary amines may serve equally well as substrates (Folk *et al.*, 1999).

Formation of mono or bis(γ-glutamyl)polyamine cross-links do not generate the formation of polymers as demonstrated between protein chains (Greenberg *et al.*, 1991). Instead, this modification may affect the biological activity or turnover of the protein targeted (Aeschlimann and Paulsson, 1994). The selectivity of TG enzymes for a nucleophile group in the second step of the transamidation reaction is by no means limited to amine groups. These enzymes have been observed to utilise water molecules in the absence of primary amines, hydrolysing Gln side chains to form glutamate (Glu) (Tamaki *et al.*, 1982; Paramesworan *et al.*, 1997). In addition to this, TG enzymes can catalyse the esterification of hydroxyl groups (Nemes and Steinert, 1999), which is particularly pertinent in the later stages of keratinocyte differentiation and will be discussed in relevant sections. A summary of these reactions is included (Fig. 1).

To date nine members of the transglutaminase family have been identified and sequenced in humans (summarised in Table. 1). The numerical system of nomenclature is now largely accepted, designating these enzymes TG1-7, factor XIII and band 4.2 (B4.2), and will be used throughout this thesis (alternate designations are summarised in Table. 1). The active site of the TGs comprises of a catalytic triad of cysteine (Cys), histidine (His) and aspartate (Asp) (Pedersen *et al.*, 1994). A Cys to Ala substitution in B4.2 has resulted in the only cross-linking deficient member of the enzyme group (Korsgren, *et al.*, 1990). TG enzymes have been implicated in a wide range of physiological processes including semen coagulation (Williams-Ashman, 1984), fibrin clot formation (Pisano *et al.*, 1968; Chen and Doolittle, 1971; Shainoff *et al.*, 1991), wound healing (Raghunath *et al.*, 1996; Haroon *et al.*, 1999) and generation of cornified envelopes in keratinocyte differentiation (Steinert and Marekov, 1995; 1997; Candi *et al.*, 1999). Some members of this family appear to fulfil specialised functions, with correspondingly limited expression patterns. For example B4.2 and its structural role in the cytoskeleton of hemopoetic cells (Aeschlimann *et al.*, 2001). In contrast other members, such as TG2 and TG5, have a far more ubiquitous expression (Thomazy and Fesus, 1989; Grenard *et al.*, 2001; Candi *et al.*, 2004). Often more than one TG is expressed in the same tissue and when the generation of a TG2 knockout mouse produced no overt phenotype (De Laurenzi and Melino, 2000) it was hypothesised that redundancy exists within the family. Indeed, these enzymes demonstrate high sequence homology (Table. 2) and domain

conservation (Fig. 2). These proteins are thought to have evolved from cysteine proteases occurring early in evolution (Pedersen *et al.*, 1994) (Fig. 3). TG-like enzymes have been identified in invertebrates, plants, unicellular eukaryotes and bacteria, although, determining the primary structure of bacterial TG has revealed evolution by a separate lineage to the eukaryotic enzymes (Kanaji *et al.*, 1993). For the purposes of this work the focus will remain on the mammalian forms and more particularly the human TGs where data is available. TG genes have been found clustered on five different chromosomes, most likely evolving by successive duplications (Grenard *et al.*, 2001).

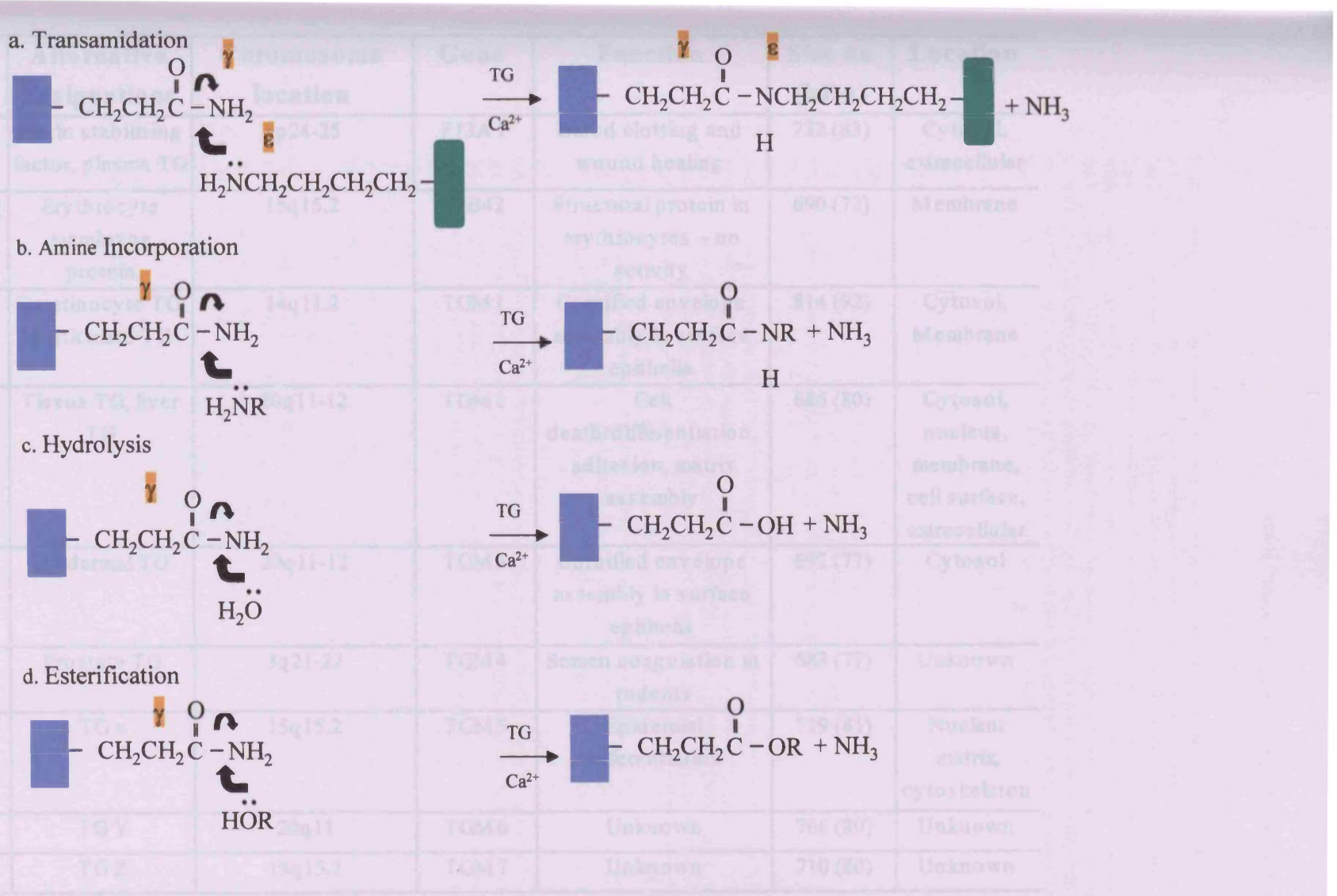

Fig. 1 Transglutaminases are capable of catalysing various post-translational modifications: Cross-links can be formed between glutamine residues (blue rectangle) and (a) protein linked lysine (green rectangle) residues, forming g-glutamyl-e-lysine isopetide bonds (b) amines (H2NR) (diamines and polyamines may function as a bis-glutaminyl adducts between two proteins) (c) water molecules, resulting in deamidation d) alcohols to form ester linkages.

TG	Alternative designations	Chromosome location	Gene	Function	Size aa (kDa)	Location
Factor XIII	Fibrin stabilising factor, plasma TG	6p24-25	F13A1	Blood clotting and wound healing	732 (83)	Cytosol, extracellular
Band 4.2	Erythrocyte membrane protein	15q15.2	EPB42	Structural protein in erythrocytes – no activity	690 (72)	Membrane
1	Keratinocyte TG, particulate TG	14q11.2	TGM1	Cornified envelope assembly in surface epithelia	814 (92)	Cytosol, Membrane
2	Tissue TG, liver TG	20q11-12	TGM2	Cell death/differentiation, adhesion, matrix assembly	686 (80)	Cytosol, nucleus, membrane, cell surface, extracellular
3	Epidermal TG	20q11-12	TGM3	Cornified envelope assembly in surface epithelia	692 (77)	Cytosol
4	Prostate TG	3q21-22	TGM4	Semen coagulation in rodents	683 (77)	Unknown
5	TGx	15q15.2	TGM5	Epidermal differentiation	719 (81)	Nuclear matrix, cytoskeleton
6	TGY	20q11	TGM6	Unknown	706 (80)	Unknown
7	TGZ	15q15.2	TGM7	Unknown	710 (80)	Unknown

Table. 1 Summary table of the nine TG isoforms.

```
TG2    ------------------------------------------------------------    D1
B4.2   ------------------------------------------------------------
TG3    ------------------------------------------------------------
TG6    ------------------------------------------------------------
TG5    ------------------------------------------------------------
TG7    ------------------------------------------------------------
FXIII  ---SETSRTAFGGRRAVPPNNS-----------------------------NAAEDDL 26
TG1    MDGPRSDVGRWGGNPLQPPTTPSPEPEPEPDGRSRRGGGRSFWARCCGCCSCRNAADDDW 60
TG4    ------------------------------------------------------------
                                       1

TG2    ----------------------------------------                    D1
B4.2   ----------------------------------------
TG3    ----------------------------------------
TG6    ----------------------------------------
TG5    ----------------------------------------
TG7    ----------------------------------------
FXIII  PT--------------------VELQGVVPRG--VN-----                   38
TG1    GPEPSDSRGRGSSSGTRRPGSRGSDSRRPVSRGSGVNAAGDG                  103
TG4    ----------------------------------------

TG2    ---AEELVLERCDLELET---NGRDHHTADLCREKLVVRRGQPFWLTLHFEG--RNYEAS 52  D2
B4.2   ---GQALGIKSCDFQAAR---NNEEHHTKALSSRRLFVRRGQPFTIILYFRAPVRAFLPA 54
TG3    ----AALGVQSINWQTAF---NRQAHHTDKFSSQELILRRGQNFQVLMIMN---KGLGSN 50
TG6    ----AGIRVTKVDWQRSR---NGAAHHTQEYPCPELVVRRGQSFSLTLELS---RALDCE 50
TG5    ---AQGLEVALTDLQSSR---NNVRHHTEEITVDHLLVRRGQAFNLTLYFRN--RSFQPG 52
TG7    -DQVATLRLESVDLQSSR---NNKEHHTQEMGVKRLTVRRGQPFYLRLSFS---RPFQSQ 51
FXIII  --LQEFLNVTSVHLFKERWDTNKVDHHTDKYENNKLIVRRGQSFYVQIDLS---RPYDPR 95
TG1    TIREGMLVVNGVDLLSSRSDQNRREHHTDEYEYDELIVRRGQPFHMLLLLS---RTYESS 160
TG4    MDASKELQVLHIDFLNQ---DNAVSHHTWEFQTSSPVFRRGQVFHLRLVLN---QPLQSY 54
             : :   .        *   ***         .**** * : : :    :

TG2    VDSLTFSVVTGPAPSQEAGTKARFPLRDAVEEGDWTATVVDQQDCTLSLQLTTPANAPIG 112 D2
B4.2   LKKVALTAQTGEQPSKINRTQATFPISSLGDRKWWSAVVEERDAQSWTISVTTPADAVIG 114
TG3    -ERLEFIVSTGPYPSESAMTKAVFPLSNGSSG-GWSAVLQASNGNTLTISISSPASAPIG 109
TG6    -EILIFTVETGPRASEALHTKAVFQTSELERGEGWTAAREAQMEKTLTVSLASPPSAVIG 109
TG5    LDNIIFVVETGPLSDLALGTRAVFSLARHHSPSPWIAWLETNGATSTEVSLCAPPTAAVG 112
TG7    NDHITFVAETGPKPSELLGTRATFFLTRVQPGNVWSASDFTIDSNSLQVSLFTPANAVIG 113
FXIII  RDLFRVEYVIGRYPQENKGTYIPVPIVSELQSGKWGAKIVMREDRSVRLSIQSSPKCIVG 155
TG1    -DRITLELLIGNNPEVGKGTHVIIPVG-KGGSGGWKAQVVKASGQNLNLRVHTSPNAIIG 217
TG4    -HQLKLEFSTGPNPSIAKHTLVVLDPRTPSDHYNWQATLQNESGKEVTVAVTSSPNAILG 113
         . . .    *  ..    *   .          * *           : : :.. . :*

TG2    LYRLSLEAST---GYQGSSFVLGHFILLF                               138 D2
B4.2   HYSLLLQVSG---RKQ---LLLGQFTLLF                               137
TG3    RYTMALQIFS---QGGISSVKLGTFILLF                               134
TG6    RYLLSIRLSS---HRKHSNRRLGEFVLLF                               135
TG5    RYLLKIHIDSF--QGSVTAYQLGEFILLF                               139
TG7    HYTLKIEISQG--QGHSVTYPLGTFILLF                               140
FXIII  KFRMYVAVWTPYGVLRTSRNPETDTYILF                               184
TG1    KFQFTVRTQSDAGEFQLPFDPRNEIYILF                               246
TG4    KYQLNVKTGN-----HILKSEENILYLLF                               137
         : : :                  :**
```

```
TG2    NAWCPADAVYLDSEEERQEYVLTQQGFIYQGSAKFIKNIPWNFGQFEDGILDICLILLDV 198 D3
B4.2   NPWNREDAVFLKNEAQRMEYLLNQNGLIYLGTADCIQAESWDFGQFEGDVIDLSLRLLSK 197
TG3    NPWLNVDSVFMGNHAEREEYVQEDAGIIFVGSTNRIGMIGWNFGQFEEDILSICLSILDR 194
TG6    NPWCAEDDVFLASEEERQEYVLSDSGIIFRGVEKHIRAQGWNYGQFEEDILNICLSILDR 195
TG5    NPWCPEDAVYLDSEPQRQEYVMNDYGFIYQGSKNWIRPCPWNYGQFEDKIIDICLKLLDK 199
TG7    NPWSPEDDVYLPSEILLQEYIMRDYGFVYKGHERFITSWPWNYGQFEEDIIDICFEILNK 200
FXIII  NPWCEDDAVYLDNEKEREEYVLNDIGVIFYGEVNDIKTRSWSYGQFEDGILDTCLYVMDR 244
TG1    NPWCPEDIVYVDHEDWRQEYVLNESGRIYYGTEAQIGERTWNYGQFDHGVLDACLYILDR 306
TG4    NPWCKEDMVFMPDEDERKEYILNDTGCHYVGAARSIKCKPWNFGQFEKNVLDCCISLLTE 197
       *.*   * *::  .    **:  : *  : *    *    *.:***:  ::. .: ::

TG2    NPKFLKNAGRDCSRRSSPVYVGRVVSGMVNCNDDQGVLLGRWDNNYGDGVSPMSWIGSVD 258 D3
B4.2   D--------KQVEKWSQPVHVARVLGALLHFLKEQRVLPTPQTQATQEGALLNKRRGSVP 249
TG3    SLNFRRDAATDVASRNDPKYVGRVLSAMINSNDDNGVLAGNWSGTYTGGRDPRSWNGSVE 254
TG6    SPGHQNNPATDVSCRHNPIYVTRVISAMVNSNNDRGVVQGQWQGKYGGGTSPLHWRGSVA 255
TG5    SLHFQTDPATDCALRGSPVYVSRVVCAMINSNDDNGVLNGNWSENYTDGANPAEWTGSVA 259
TG7    SLYHLKNPAKDCSQRNDVVYVCRVVSAMINSNDDNGVLQGNWGEDYSKGVSPLEWKGSVA 260
FXIII  A-------QMDLSGRGNPIKVSRVGSAMVNAKDDEGVLVGSWDNIYAYGVPPSAWTGSVD 297
TG1    R-------GMPYGGRGDPVNVSRVISAMVNSLDDNGVLIGNWSGDYSRGTNPSAWVGSVE 359
TG4    S-------SLKPTDRRDPVLVCRAMCAMMSFEKGQGVLIGNWTGDYEGGTAPYKWTGSAP 250
                  .   * *.  .::   . . *:          *          **.

TG2    ILRRWKNHGCQRVKYGQCWVFAAVACTVLRCLGIPTRVVTNYNSAHDQNSNLLIEYFRNE 318 D3
B4.2   ILRQWLTGRGRPVYDGQAWVLAAVACTVLRCLGIPARVVTTFASAQGTGGRLLIDEYYNE 309
TG3    ILKNWKKSGFSPVRYGQCWVFAGTLNTALRSLGIPSRVITNFNSAHDTDRNLSVDVYYDP 314
TG6    ILQKWLKGRYKPVKYGQCWVFAGVLCTVLRCLGIATRVVSNFNSAHDTDQNLSVDKYVDS 315
TG5    ILKQWNATGCQPVRYGQCWVFAAVMCTVMRCLGIPTRVITNFDSGHDTDGNLIIDEYYDN 319
TG7    ILQQWSARGGQPVKYGQCWVFASVMCTVMRCLGVPTRVVSNFRSAHNVDRNLTIDTYYDR 320
FXIII  ILLEYRSSE-NPVRYGQCWVFAGVFNTFLRCLGIPARIVTNYFSAHDNDANLQMDIFLEE 356
TG1    ILLSYLRTG-YSVPYGQCWVFAGVTTTVLRCLGLATRTVTNFNSAHDTDTSLTMDIYFDE 418
TG4    ILQQYYNTK-QAVCFGQCWVFAGILTTVLRALGIPARSVTGFDSAHDTERNLTVDTYVNE 309
       **  :       *  **.**:*.   * :*.**:.:* :: : *.:.    * :: : :

TG2    FGEIQGD-KSEMIWNFHCWVESWMTRPDLQPGYEGWQALDPTPQEKSEGTYCCGPVPVRA 377 D3
B4.2   EGLQNGEGQRGRIWIFQTSTECWMTRPALPQGYDGWQILDPSAPNGGGVLGSCDLVPVRA 369
TG3    MGNPLD-KGSDSVWNFHVWNEGWFVRSDLGPSYGGWQVLDATPQERSQGVFQCGPASVIG 373
TG6    FGRTLEDLTEDSMWNFHVWNESWFARQDLGPSYNGWQVLDATPQEESEGVFRCGPASVTA 375
TG5    TGRILGNKKKDTIWNFHVWNECWMARKDLPPAYGGWQVLDATPQEMSNGVYCCGPASVRA 379
TG7    NAEMLSTQKRDKIWNFHVWNECWMIRKDLPPGYNGWQVLDPTPQQTSSGLFCCGPASVKA 380
FXIII  DGNVNSKLTKDSVWNYHCWNEAWMTRPDLPVGFGGWQAVDSTPQENSDGMYRCGPASVQA 416
TG1    NMKPLEHLNHDSVWNFHVWNDCWMKRPDLPSGFDGWQVVDATPQETSSGIFCCGPCSVES 478
TG4    NGEKITSMTHDSVWNFHVWTDAWMKRPDLPKGYDGWQAVDATPQERSQGVFCCGPSPLTA 369
                 :* ::   : *: *  *  .: *** :*.:. : .     *.  .: .

TG2    IKEGDLSTKYDAPFVFAEVNADVVDWIQQDDG---SVHKSINRSLIVGLKISTKSVGRDE 434 D3
B4.2   VKEGTVGLTPAVSDLFAAINASCVVWKCCEDG---TLELTDSNTKYVGNNISTKGVGSDR 426
TG3    VREGDVQLNFDMPFIFAEVNADRITWLYDNTTG--KQWKNSVNSHTIGRYISTKAVGSNA 431
TG6    IREGDVHLAHDGPFVFAEVNADYITWLWHEDES--RERVYS-NTKKIGRCISTKAVGSDS 432
TG5    IKEGEVDLNYDTPFVFSMVNADCMSWLVQGGK---EQK-LHQDTSSVGNFISTKSIQSDE 435
TG7    IREGDVHLAYDTPFVYAEVNADEVIWLLGDGQ---AQEILAHNTSSIGKEISTKMVGSDQ 437
FXIII  IKHGHVCFQFDAPFVFAEVNSDLIYITAKKDG---THVVENVDATHIGKLIVTKQIGGDG 473
TG1    IKNGLVYMKYDTPFIFAEVNSDKVYWQRQDDG---SFKIVYVEEKAIGTLIVTKAISSNM 535
TG4    IRKGDIFIVYDTRFVFSEVNGDRLIWLVKMVNGQEELHVISMETTSIGKNISTKAVGQDR 429
       ::.* :         ::: :*.. :                          :*  * ** :  :

TG2    REDITHTYKYPEGSSEEREAFTRANHLNKL-----------------AEKEE-------- 469 D3
B4.2   CEDITQNYKYPEGSLQEKEVLERVEKEKME-----------------REKDNGIRP---- 465
TG3    RMDVTDKYKYPEGSDQERQVFQKALGKLKP--------------NTPFAATSSMG----- 472
TG6    RVDITDLYKYPEGSRKERQVYSKAVNRLFG--------------VEASGRRIWIRRAGGR 478
TG5    RDDITENYKYEEGSLQERQVFLKALQKLKARSFHGSQRGAELQPSRPTSLSQDSPRS--- 492
TG7    RQSITSSYKYPEGSPEERAVFMKASRKMLG---------------PQRASLPFLDL--- 478
FXIII  MMDITDTYKFQEGQEEERLALETALMYGAKKP-------------LNTEGVMKSRS---- 516
TG1    REDITYLYKHPEGSDAERKAVETAAAHGSKP--------------NVYANRGSAE---- 576
TG4    RRDITYEYKYPEGSSEERQVMDHAFLLLSSE--------------REHRRPVKEN---- 470
         .:*  **. **.  *: .   .                                  ▲
                                                                 2
```

```
TG2    ----------------                                                469 D3
B4.2   ---------PSLETA--                                               471
TG3    ------LETEEQEPS--                                               681
TG6    CLWRDDLLEPATKPS--                                               493
TG5    ------LHTPSLRPSDV                                               503
TG7    ------LESGGLRDQ--                                               487
FXIII  ----------------                                                516
TG1    ----------------                                                576
TG4    ----------------                                                470


TG2    TGMAMRIRVGQSMNMGSDFDVFAHITNNTAEEYV-----CRLLLCARTVSYNGILGPECG 524 D4
B4.2   SPLYLLLKAPSSLPLRGDAQISVTLVNHSEQEKA-----VQLAIGVQAVHYNGVLAAKLW 526
TG3    --IIGKLKVAGMLAVGKEVNLVLLLKNLSRDTKT-----VTVNMTAWTIIYNGTLVHEVW 534
TG6    --IAGKFKVLEPPMLGHDLRLALCLANLTSRAQR-----VRVNLSGATILYTRKPVAEIL 546
TG5    VQVSLKFKLLDPPNMGQDICFVLLALNMSSQFK-----DLKVNLSAQSLLHDGSPLSPFW 558
TG7    -PAQLQLHLARIPEWGQDLQLLLRIQRVPDSTHPRGPIGLVVRFCAQALLHGGGTQKPFW 546
FXIII  --NVDMDFEVENAVLGKDFKLSITFRNNSHNRYT-----ITAYLSANITFYTGVPKAEFK 569
TG1    --DVAMQVEAQDAVMGQDLMVSVMLINHSSSRRT-----VKLHLYLSVTFYTGVSGTIFK 629
TG4    --FLHMSVQSDDVLLGNSVNFTVILKRKTAALQN-----VNILGSFELQLYTGKKMAKLC 523
                       . .     . .                      :

TG2    TKYLLNLNLEPFSEKSVPLCILYEKYRD---CLTESNLIKVRALLVEPVINSYLLAERDL 581 D4
B4.2   RKKLH-LTLSANLEKIITIGLFFSNFER---NPPENTFLRLTAMATHSESNLSCFAQEDI 582
TG3    KDSAT-MSLDPEEEAEHPIKISYAQYEK---YLKSDNMIRITAVCKVPD-ESEVVVERDI 589
TG6    HESHA-VRLGPQEEKRIPITISYSKYKE---DLTEDKKILLAAMCLVTK-GEKLLVEKDI 601
TG5    QDTAF-ITLSPKEAKTYPCKISYSQYSQ---YLSTDKLIRISALGEEKSSPEKILVNKII 614
TG7    RHTVR-MNLDFGKETQWPLLLPYSNYRN---KLTDEKLIRVSGIAEVEETGRSMLVLKDI 602
FXIII  KETFD-VTLEPLSFKKEAVLIQAGEYMG---QLLEQASLHFFVTARINETRDVLAKQKST 625
TG1    ETKKE-VELAPGASDRVTMPVAYKEYRP---HLVDQGAMLLNVSGHVKESGQVLAKQHTF 685
TG4    DLNKT-SQIQG-QVSEVTLTLDSKTYINSLAILDDEPVIRGFIIAEIVESKEIMASEVFT 581
              :        .  :    :         .  :

TG2    YLENPEIKIRILGEPKQKRKLVAEVSLQNPL                                612 D4
B4.2   AICRPHLAIKMPEKAEQYQPLTASVSLQNSL                                613
TG3    ILDNPTLTLEVLNEARVRKPVNVQMLFSNPL                                620
TG6    TLED-FITIKVLGPAMVGVAVTVEVTVVNPL                                631
TG5    TLSYPSITINVLGAAVVNQPLSIQVIFSNPL                                645
TG7    CLEPPHLSIEVSERAEVGKALRVHVTLTNTL                                633
FXIII  VLTIPEIIIKVRGTQVVGSDMTVTVQFTNPL                                656
TG1    RLRTPDLSLTLLGAAVVGQECEVQIVFKNPL                                716
TG4    SFQYPEFSIELPNTGRIGQLLVCNCIFKNTL                                612
        :    : : :               . *.*

TG2    PVALEGCTFTVEGAGLTEEQKTVEIPDPVEAGEEVKVRMDLLPLHMGLHKLVVNFESDKL 672 D5
B4.2   DAPMEDCVISILGRGLIHRERSYRFRS-VWPENTMCAKFQFTPTHVGLQRLTVEVDCNMF 672
TG3    DEPVRDCVLMVEGSGLLLGNLKIDVPT-LGPKEGSRVRFDILPSRSGTKQLLADFSCNKF 679
TG6    IERVKDCALMVEGSGLLQEQLSIDVPT-LEPQERASVQFDITPSKSGPRQLQVDLVSPHF 690
TG5    SEQVEDCVLTVEGSGLFKKQQKVFLGV-LKPQHQASIILETVPFKSGQRQIQANMRSNKF 704
TG7    MVALSSCTMVLEGSGLINGQIAKDLGT-LVAGHTLQIQLDLYPTKAGPRQLQVLISSNEV 692
FXIII  KETLRNVWVHLDGPGVTRP-----------------MKKMFREIRPN-----STVQWEEV 694
TG1    PVTLTNVVFRLEGSGLQRPKILNVGDI--GGNETVTLRQSFVPVRPGPRQLIASLDSPQL 774
TG4    AIPLTDVKFSLESLGISSLQTSDHGTV--QPGETIQSQIKCTPIKTGPKKFIVKLSSKQV 670
        : .  . : . *:                                 : .       .    .
```

```
TG2    KAVKGFRNVIIGPA---------------------------          686 D5
B4.2   QNLTNYKSVTVVAPELSA----------------------           690
TG3    PAIKAMLSIDVAE----------------------------          692
TG6    PDIKGFVIVHVATAK--------------------------          705
TG5    KDIKGYRNVYVDFAL--------------------------          719
TG7    KEIKGYKDIFVTVAGAP------------------------          709
FXIII  CRPWVELDVQIQRRPSM-----------------------           711
TG1    SQVHGVIQVDVAPAPGDGGFFSDAGGDSHLGETIPMASRGGA        816
TG4    KEINAQKIVLITK----------------------------          683
              : :
```

Fig. 2 Multiple alignment of the nine human transglutaminase sequences: An alignment of the nine characterised human gene products, TG2 (Gentile et al., 1991), band 4.2 (Korsgren et al., 1990), TG3 (Kim et al, 1993), TG6 long form (Thomas, H., Thesis, 2004), TG5 (Aeschlimann et al., 1998), TG7 (Grenard et al., 2001), factor XIII a-subunit (Grundmann et al., 1986; Takahashi et al., 1986), TG1 (Phillips et al., 1990; Kim et al., 1991) and TG4 (Grant et al., 1994) are shown. *Dashes* indicate gaps inserted for optimal sequence alignments. Residues conserved in all sequences are designated "*", those demonstrating conserved substitutions are designated ":" and semi-conserved substitutions are marked ".". The sequences are arranged to reflect the transglutaminase domain conservation based on the crystal structure of factor XIII a-subunit (Yee et al., 1994): N-terminal propeptide domain (D1), β-sandwich domain (D2), catalytic core domain (D3), and β-barrel domains 1 (D4) and 2 (D5). The active cysteine residue, required for transamidation reactions is shown in red. Identified cleavage sites are indicated with arrowheads (red); (1) sites identified in FXIII and TG1 (2) sites identified in FXIII, TG1 and TG3.

Table. 2

	1	2	3	4	5	6	7	FXIII	B 4.2
1	-	35	35	35	34	36	35	41	27
2	-	-	38	32	42	41	40	34	33
3	-	-	-	33	44	50	40	31	30
4	-	-	-	-	33	35	36	30	27
5	-	-	-	-	-	45	49	31	33
6	-	-	-	-	-	-	44	32	30
7	-	-	-	-	-	-	-	28	33
FXIII	-	-	-	-	-	-	-	-	24
B 4.2	-	-	-	-	-	-	-	-	-

Fig. 3

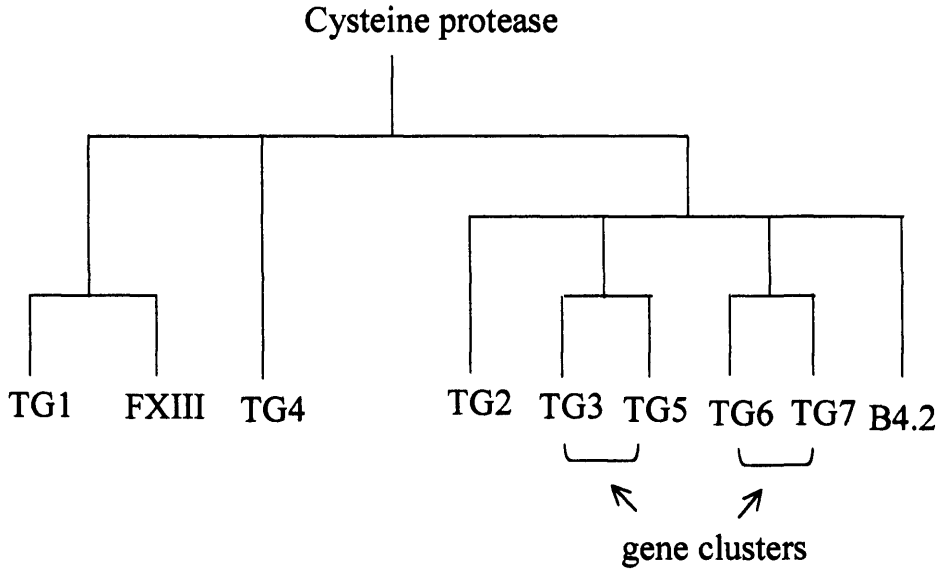

Table. 2 Percentage identity between protein sequences of transglutaminase isoforms: Relative identities between isoforms was calculated using ClustalW software (European Bioinformatics institute).

Fig. 3 Hypothetical representation of transglutaminase pedigree in vertebrates: Derived from sequence data concerning the relationship between individual gene products (adapted from Grenard *et al.*, 2001).

1.1.1 Structural features of transglutaminase enzymes

The 3D structure of the enzyme FXIII was the first to be identified from the TG family (Yee *et al.*, 1994; 1996) and was found to comprise of four distinct domains. As structures of other TGs have been elucidated it has been demonstrated that as with the primary sequence the domain structure is highly conserved (Fig. 4). An exception to this is the presence of an N-terminal flanking sequence, which is unique to FXIII and TG1 (Kim *et al.*, 1991; Yee *et al.*, 1994). This additional sequence has been shown to occlude the active site or act as a membrane anchoring region, respectively (Takagi and Doolittle, 1974; Chakravarty and Rice, 1989; Rice *et al.*, 1990).

The conserved TG structure comprises of a beta sandwich domain present at the N-terminus, which in conjunction with the largely alpha helical active domain 2, forms a 450 amino acid residue "core". The C-terminus of TG enzymes consists of two β-barrel domains, the first of which is linked to the catalytic domain by a highly flexible loop, particularly prone to protease cleavage (Kim *et al.*, 1993; Casadio *et al.*, 1999). Members of the TG family primarily differ in additional N-terminal sequences and their C-termini (Kim *et al.*, 1991). Furthermore, it is these structures that are thought to impact on substrate selection (Greenberg *et al.*, 1991; Reichert *et al.*, 1993; Kim *et al.*, 1995a), with suggestions that the acyl donor approaches from the C-terminal β-barrel regions thereby incurring the greater degree of enzyme-specificity (Lorand and Graham, 2003). In contrast, the acyl acceptor is thought to dock from the catalytic domain. It has been proposed that non-proline cis-peptide bonds present in close proximity to the active site (Weiss *et al.*, 1998; Ahvazi *et al.*, 2002; Liu *et al.*, 2002) may be involved in TG activation. The putative mechanism relies on the binding of calcium or substrates, which triggers a cis to trans isomerisation of these bonds and consequently exposes the active site (Weiss *et al.*, 1998). It has also been established that Trp^{241} is essential for TG2 activity, possibly through stabilisation of the enzymes transition state. Interestingly this residue is conserved throughout the TG family with the notable exception of the inactive B4.2 protein (Murthy *et al.*, 2002).

Studies have revealed two TGs may react with the same substrate but demonstrate different affinities (Gorman *et al.*, 1981; Gorman *et al.*, 1984) and/or target distinct residues (Shainoff *et al.*, 1991; Candi *et al.*, 1999; 2001). These differences have been attributed to structural and charge properties of flanking residues. Studies have revealed the requirements of FXIIIa to be more stringent than those of TG2 when concerning acyl donors (Gorman *et al.*, 1981; Gorman *et al.*, 1984; Fesus *et al.*, 1986).

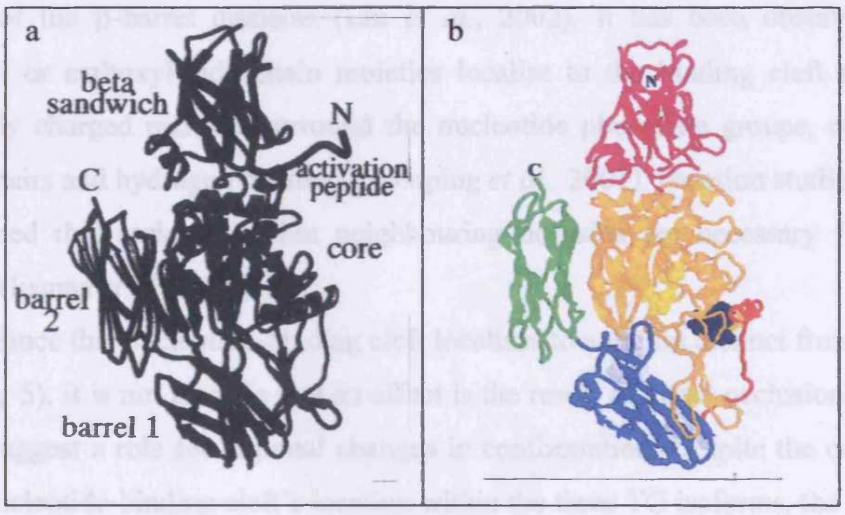

Fig. 4 The secondary structure of transglutaminase enzymes is conserved: The domain structure between isoenzymes are observed to conserve the N-terminal sandwich domain, catalytic domain and two C-terminal β-barrel domains as demonstrated by the backbone structure of a) the FXIII monomer (Yee *et al.*, 1994) and b) TG2, where the domains are coloured magenta, orange, blue and green respectively. The flexible loop connecting the catalytic domain and the 1st β-barrel domain is coloured red and the amino acids involved in the active site (Cys^{277}, His^{335} and Asp^{358}), $Ca2+$ binding (Ser^{449}, Pro^{446}, Glu^{451} and Glu^{452}) and interaction with GTP (Ser^{171}, Lys^{173}, Arg^{478}, Val^{479} and Arg^{580}) are coloured yellow, black and grey respectively (Griffin *et al.*, 2002).

1.1.2 Certain transglutaminases are negatively regulated by nucleotide binding

Despite low levels of sequence homology with classical G-proteins it has been found that TG2, 3 and 5 are negatively regulated by nucleotide triphosphate (NTP) binding and are capable of hydrolysing these molecules (NTPase). For some time this regulation was considered to be unique to TG2 (Achuthan and Greenberg, 1987; Nakaoka *et al.*, 1994; Smethurst and Griffin, 1996) but recent studies have disproved this (Ahvazi *et al.*, 2004; Candi *et al.*, 2004). The NTP binding occurs at a 1:1 ratio (Liu *et al.*, 2002; Ahvazi *et al.*, 2004) within corresponding sites in the three isoenzymes. The nucleotide-binding cleft resides between the catalytic domain and the 1st of the β-barrel domains (Liu *et al.*, 2002). It has been observed that no hydroxyl or carboxyl side chain moieties localise to the binding cleft and several positively charged residues surround the nucleotide phosphate groups, coordinating via ion pairs and hydrogen bonding (Shenping *et al.*, 2001). Deletion studies have also ascertained that residues within neighbouring domains are necessary for NTPase activity (Iismaa *et al.*, 2000).

Since this nucleotide-binding cleft localises to a region distinct from the active site (Fig. 5), it is not feasible that its effect is the result of direct occlusion. Instead, it would suggest a role for regional changes in conformation. Despite the conservation of the nucleotide-binding cleft's location within the three TG isoforms, the amino acid residues involved with nucleotide interactions are observed to vary. This would account for the differing affinities these enzymes demonstrate for adenosine triphosphate (ATP) and guanosine triphosphate (GTP) (Ahvazi *et al.*, 2004; Candi *et al.*, 2004). It has also been reported that although, TG3 and TG5 are capable of binding ATP and GTP they differ from TG2 in that they are only capable of hydrolysing GTP (Ahvazi *et al.*, 2004; Candi *et al.*, 2004).

X-ray crystallographic structure analysis of GDP bound TG2 demonstrates that under these binding conditions the transamidation site is obstructed by two loops within the β-barrel domain and the active Cys residue is hydrogen bonded to a Tyr residue (Shenping *et al.*, 2001; Liu *et al.*, 2002). This inhibition can be counteracted by Ca^{2+} (Achyuthan and Greenberg 1987; Singh *et al.*, 1995), most likely through conformational changes weakening NTP interactions (Casadio *et al.*, 1999). It would seem this divalent ion provides the switch between the two distinct functions of these

TGs. This dual regulation has interesting implications concerning the nature of TG activity with its location. The high concentration of NTPs within the cytoplasm accompanied with low Ca^{2+} levels may select the enzymes NTP-cycling activity, whereas the high Ca^{2+} levels in surrounding matrices would promote transamidating activity. It has also been suggested that local concentrations of Ca^{2+} and nucleotides may have an important role in TG regulation (Haroon *et al.*, 1999). Further to this, the distinct sensitivities of TG isoforms to these regulators could be physiologically relevant. *In vitro* TG5 demonstrates lower sensitivity to Ca^{2+} activation and GTP inhibition than TG2 (Candi *et al.*, 2004). Consequently, at physiological levels of Ca^{2+} TG5 retains 25 % of its maximal activity, compared to 75 % for TG2. Conversely at physiological GTP levels 45-55 % of TG5 enzyme activity is lost, compared to 90 % of TG2 (Candi *et al.*, 2004).

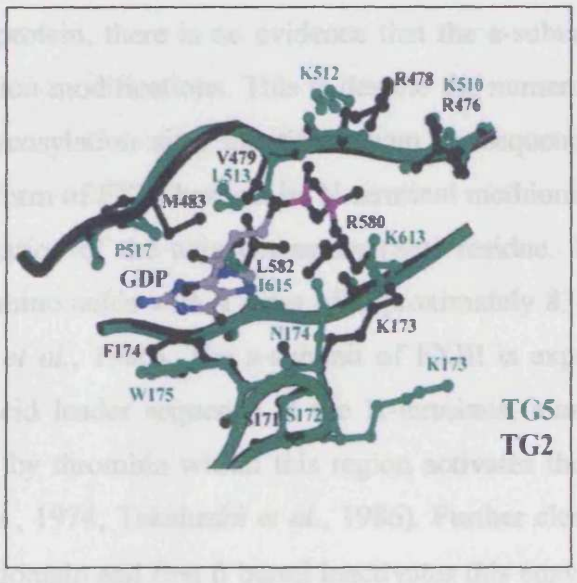

Fig. 5 Identification of the TG5 putative GTP-binding pocket: A computer generated 3D structure of TG5 superimposed onto the crystal structure of the nucleotide-binding pocket of TG2 (Candi *et al.*, 2004).

The following section summarises available data concerning the protein structure and physiological function of the nine TG isoforms identified to date.

1.1.3 Factor XIII

The primary sites of FXIII synthesis include platelets, peripheral blood monocytes and the liver (Weisberg *et al.*, 1987; Poon *et al.*, 1989). This enzyme is found in intracellular and extracellular forms, the former existing as a non-covalently associated dimer (a_2) and the latter residing in the plasma as a tetramer formed from two filamentous b-subunits associating with the dimer (a_2b_2) (Carrell *et al.*, 1989). To date the mechanism of the a-subunit secretion has not been identified, it lacks a typical hydrophobic leader sequence (Grundmann *et al.*, 1986; Ichinose *et al.*, 1986) and attempts to establish a yeast model incorporating such a predomain, produced aberrant post-translational modifications (Tharaud *et al.*, 1992). Consistent with FXIII being a cytoplasm protein, there is no evidence that the a-subunit contains disulfide bonds or glycosylation modifications. This is despite the numerous free Cys residues and potential N-glycosylation sites identified from its sequence (Takahashi *et al.*, 1986). The mature form of FXIII has lost its N-terminal methionine (Met) by cleavage and undergoes acylation of the adjacent serine (Ser) residue. The resulting protein comprises of 731 amino acids with a mass of approximately 83 kDa (Grundmann *et al.*, 1986; Ichinose *et al.*, 1986). The a-subunit of FXIII is expressed as a zymogen with a 37 amino acid leader sequence at the N-terminus, masking the active site. Limited proteolysis by thrombin within this region activates the enzyme, generating FXIIIa (Takagi *et al.*, 1974; Takahashi *et al.*, 1986). Further cleavage at the interface between the active domain and first β barrel inactivates this enzyme (Takahashi *et al.*, 1986).

FXIII is primarily involved with the final step of the blood coagulation cascade, where it catalyses the polymerisation of fibrin monomers (Pisano *et al.*, 1968; Chen and Doolittle, 1971; Doolittle *et al.*, 1979; Shainoff *et al.*, 1991). In addition to this it has an apparent role in mediating cell-matrix interactions during wound healing and is expressed within granulation tissue during the later stages of this process (Cohen *et al.*, 1982; Knox *et al.*, 1986; Mosher *et al.*, 1991; Corbett *et al.*, 1997).

1.1.4 Band 4.2

Deduction of the cDNA encoding B4.2 revealed a 691 amino acid protein with a mass of 77 kDa (Korsgren *et al.*, 1990). A Cys to alanine (Ala) substitution at residue 268 produces the only cross-linking deficient isoform identified to date. Post-translational modifications include the cleavage of the terminal Met and myristylation of the penultimate glycine (Gly) (Cohen *et al.*, 1993). It has been suggested that this isoform is stabilised by phosphorylation (Cohen *et al.*, 1993). B4.2 was the first member of the TG family for which alternative splicing was identified. A 30 amino acid insert following Gln^3 has been observed in some forms of the enzyme and has been designated B4.2L (Cohen *et al.*, 1993).

The loss of transamidating activity apparent in Band 4.2 highlights the potential structural function of TG enzymes. This TG associates with the cytoplasmic face of erythrocyte membranes, forming part of the cytoskeleton (Lorand and Conrad, 1984; White *et al.*, 1992; Cohen *et al.*, 1993). Mutations in this gene are accompanied by abnormally shaped red blood cells and the development of anaemia. As yet no functional difference between the two splice variants has been distinguished, although it has been proposed that post-translational modifications take place within the additional N-terminal sequence as observed with TG1 (Aeschlimann and Paulsson, 1994).

1.1.5 TG1

cDNA cloning of TG1 from humans identified a proenzyme with an 814 amino acid sequence and a predicted size of 92 kDa (Kim *et al.*, 1991). Comparison with the corresponding rat sequence revealed a high level of homology, 92 % (Aeschlimann and Paulsson, 1994). The TG1 protein has proved highly unstable in attempts to purify it (Thacher, 1989), consequently a number of studies have been carried out utilising a recombinant form of the enzyme (Kim *et al.*, 1994; 1995a; Nemes *et al.*, 1999a). TG1 is post-translationally modified within its N-terminus to incorporate the fatty acid palmitate or myristate via a thioester linkage (Phillips *et al.*, 1993). Treatment with protein synthesis inhibitors suggests that myristylation occurs cotranslationally, whilst palmitate labelling is a post-translational process (Steinert *et al.*, 1996b). A number of Ser residues in the N-terminus are also phosphorylated, but no corresponding alteration in activity is evident, suggesting a possible function in substrate interactions (Rice *et al.*, 1996). The detection of a 106 kDa form of the TG1 has led to speculation that the enzyme undergoes further and as yet unidentified modifications (Kim *et al.*, 1995a). The presence of a fatty acid anchor localises >95 % of TG1 to the membrane fraction of the cell (Steinert *et al.*, 1996a) and it has been postulated that this anchorage of the enzyme is necessary for subsequent processing (Kim *et al.*, 1995a). Studies have reported approximately 50 % of the membrane bound enzyme is present in its zymogen form, the remainder undergoes cleavage to produce three fragments with calculated masses of 10 kDa (N-terminal membrane anchoring region), 33 kDa (C-terminal β-barrels) and 67 kDa (containing the active domain) (Steinert *et al.*, 1996a). The majority of these cleavage products remain in complex to produce a highly active form of TG1 and this accounts for almost all its activity in keratinocytes (Steinert *et al.*, 1996a). Edman degradation sequencing identified these cleavage sites as residing between Arg^{573}-Gly^{574} and Arg^{93}-Gly^{94} (Kim *et al.*, 1995a; Steinert *et al.*, 1996a). Alignment with other human TG sequences demonstrated the first of these sites correlates with the thrombin activation of FXIII and the second with the inactivating cleavage of the same enzyme. However, the second site also aligns with the cleavage site of the TG3 zymogen by an unknown enzyme to generate the active form (Kim *et al.*, 1995a). Studies with antibodies distinguishing the N-terminus of the two TG1 fragments would suggest cleavage first occurs between residues 573-574 and then 93-94. It was also hypothesised that two

separate enzymes may be involved, or at least differential control of a single protease (Iizuka *et al.,* 2003). A smaller pool of soluble TG1 has also been studied, identifying the full-length enzyme and cleavage products. The ratio of these cleavage products compared to the full-length enzyme was observed to increase in keratinocytes committed to differentiation. It was therefore concluded that this process of activation is regulated (Kim *et al.*, 1995a, b; Steinert *et al.*, 1996a, b). Complexes between the 67 kDa with either the 33 kDa fragment or full-length enzyme have been obtained by coelution from Mono Q Fast protein liquid chromatography (FPLC) or coprecipitation and the specific activities calculated. The full-length enzyme is active, however the specific activity of the 67 kDa in isolation is 5 fold greater increasing to 10 fold when associated with the 33 kDa fragment. The 67 kDa fragment is also subject to negative regulation by binding of the full-length enzyme, which produced a reduction in enzyme activity (Kim *et al.,* 1995a). These processed forms of TG1 exhibited a significantly shortened half-life, estimated to be approximately 7 h in comparison with 20 h for the full-length form. To date, the enzyme responsible for this cleavage has not been identified, however plasmin, calpain and cathepsin D are possible candidates (Rice *et al.*, 1990; Garach-Jehoshua *et al.*, 1998; Horikoshi *et al.*, 1999). In the latter case, the generation of transgenic mice have lent credence to this enzyme's suggested function. TG activity within the epidermis of these cathepsin $D^{-/-}$ mice is severely diminished when compared to the wild-type control (Egberts *et al.,* 2004). Furthermore, the addition of exogenous cathepsin D has been demonstrated to increase TG1 activity in cultured keratinocytes (Egberts *et al.,* 2004).

Recent studies have suggested TG1 has a function in controlling the barrier properties of microvascular monolayers via its cross-linking activity within the intercellular junctions of myocardium endothelial cells. This has been demonstrated by inhibition of this enzyme with monodansylcadaverine and RNA silencing (Baumgarter *et al.* 2004). It is however the role of TG1 in the terminal differentiation of squamous epithelia that is best characterised (Simon and Green, 1985; Kim *et al.*, 1995a; 1995b; Steinert *et al.*, 1996a). *In vitro* studies have demonstrated that TG1 is capable of cross-linking a number of proteins expressed during this terminal differentiation, including involucrin, loricrin and small proline rich (SPR) proteins (Candi *et al.*, 1999; 2001). These proteins cross-link to form shell-like macromolecules termed cornified envelopes (CE), which impart stronger physical

attributes to the tissue and in conjunction with novel lipid lamellae produce an effective barrier to infection and water-loss. These features will be discussed in detail in Sections 1.2.3-1.2.4.

In addition to this role in CE formation, TG1 appears to possess a unique function in the TG family. Within an *in vitro* lipid vesicle system, this isoform has demonstrated the ability to catalyse the formation of ester linkages between a ω-hydroxyceramide analogue and a number of CE precursors, predominantly involucrin (Nemes *et al.*, 1999a) (Fig. 6). Similar linkages involving involucrin have been isolated from *ex vivo* samples and to a lesser extent the envelope precursors envoplakin and periplakin (Marekov and Steinert, 1998). In conjunction with CE formation the sequestering of covalently bound lipids (CBLs) to the surface of differentiating keratinocytes is an important step in the transition of cells into a hydrophobic environment. It has been demonstrated that TG1 ablation in mice produces a lethal phenotype as a consequence of defective skin barrier formation, with mice dying a matter of hours after birth (Matsuki *et al.*, 1998). This key role for TG1 in skin homeostasis and the absence of a compensatory mechanism will be discussed in more detail in Section 1.2.9.2.

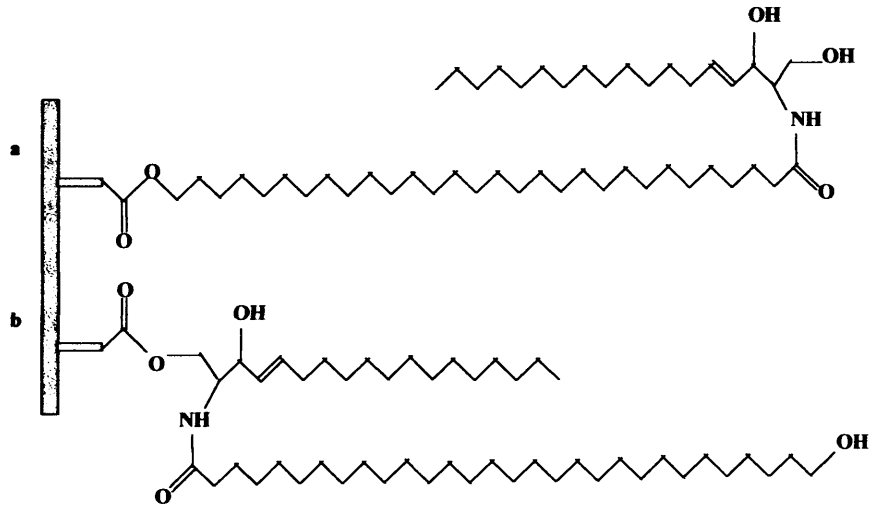

Fig. 6 Schematic representation of lipids covalently bound to the envelope precursor involucrin: It has been found that a number of lipids within the stratum corneum are attached to cornified envelopes via ester linkages. Primarily these cross-links occur with involucrin molecules (grey rectangle) and the reaction is thought to be catalysed by TG1. Two examples shown here include (a) a ω-hydroxyl linkage (b) a sphingosine-1-hydroxyl ester linkage (Swartzendruber *et al.*, 1987).

1.1.6 TG2

TG2 has been successfully cloned from a number of mammals including human, cow, mouse, guinea pig and chicken, identifying a polypeptide between 685 and 691 amino acid residues in size (~80 kDa) (Ikura *et al.*, 1988; Gentile *et al.*, 1991). Moderate conservation was observed between species (65-88 % when compared to human sequence) (Aeschlimann and Paulsson, 1994). TG2 is expressed as an active enzyme, the majority of which localises to the cytosol (80 %) but additional pools are found within the nucleus (5 %) or are membrane-associated (15 %), the latter may be partly due to fatty acid-linkages (Harsfalvi *et al.*, 1987). There is no evidence for glycosylation or the inclusion of disulfide bonds (Ikura *et al.*, 1988), and the N-terminus of this enzyme is blocked by the removal of the initiator Met and the acylation of the flanking Ala residue.

It has also been observed that TG2 can be externalised, localising at the cell surface or in association with extracellular matrix (ECM) components in a number of tissues (Aeschlimann and Paulsson, 1991; Barsigian *et al.*, 1991; Martinez *et al.*, 1994; Aeschlimann *et al.*, 1995; Gaudry *et al.*, 1999). As is the case for FXIII, a hydrophobic leader sequence is conspicuously absent. It has been proposed that the N^{α}-acetyl group may target the enzyme to an "alternative" secretory pathway (Muesch *et al.*, 1990). Other suggestions for the secretion of this enzyme include specialised pores within the plasma membrane or passive diffusion following transient stress-induced membrane ruptures (Kuchler and Thorner, 1990; Steinhardt *et al.*, 1994; Elliot and O'Hare, 1997). It has been postulated that the presence of cis-peptide bonds conserved within the TG family (discussed in Section 1.1.1) may be essential for the secretion of TG2 into the ECM (Balklava *et al.*, 2002). TG2 mutations of the active Cys residue ($Cys^{277}Ser$) or targeting the proposed cis-bond ($Tyr^{274}Ala$) have demonstrated that only the active form is retrieved in culture medium or detected in the ECM (Balklava *et al.*, 2002). This would suggest that transamidation activity and/or the tertiary conformation of the active site is required for complete secretion. Both mutant forms were able to localise to the plasma membrane.

TG2 is ubiquitously expressed and constitutively expressed at high levels in endothelial and smooth muscle cells (Thomazy and Fesus, 1989). With regard to regulation of TG2 levels, discrepancies between the relative mRNA (most abundant in lung, heart, kidney and red blood vessels) and protein quantities (most abundant in

liver and spleen) would suggest control at the translation level and/or the rate of protein turnover (Clarke *et al.*, 1959; Aeschlimann and Paulsson, 1994). To date, two alternatively spliced variants of TG2 have been identified, located within exons VI and X (Fraij and Gonzales, 1997). Studies of the neurodegenerative condition, progressive supranuclear palsy have detected significantly raised levels of mRNA encoding a short form of TG2, implicating a role for this splice variant (Zemaitaitis *et al.*, 2002). This truncated form lacks the nucleotide-binding cleft and in the absence of this negative regulation demonstrates high levels of cross-linking activity.

As was mentioned previously (Section 1.1.2) TG2 is capable of NTP-cycling, targeting ATP and GTP. This was the first member of the TG family to which this activity was attributed (Achyuthan and Greenberg, 1987). Although the structure of the inactive GDP bound form has been analysed by X-ray crystallography (Liu *et al.*, 2002) the corresponding Ca^{2+}-bound form has not been established. Protein dynamics simulation indicates that binding of this divalent ion produces major conformational changes moving apart domain 2 and 3, between which the active site is situated (Casadio *et al.*, 1999).

TG2 was the first member of the TG family to be identified in 1959 (Clark *et al.*, 1959) but its physiological function still remains something of an enigma. This is a consequence of its ubiquitous expression and the necessary delinearisation of its opposing activates as a transamidating enzyme and G-protein. This isoform has been implicated in signal transduction (Nakaoka *et al.*, 1994), cell adhesion, spreading and differentiation (Gentile *et al.*, 1992; Aeschlimann *et al.*, 1993; Jones *et* al, 1997; Stephens *et al.*, 2004), wound healing (Bowness *et al.*, 1988; Haroon *et al.*, 1999) and apoptosis. Concerning the latter case, the function of TG2 has not been established unambiguously. Studies have reported TG2 to promote (Gentile *et al.*, 1992; Melino *et al.*, 1994; Oliverio *et al.*, 1999) or inhibit this form of cell death (Antonyak *et al.*, 2001; Tucholski and Johnson, 2002). More recent work has suggested that this contradiction can be accounted for by enzyme localisation and activity. Cytosolic transamidating activity demonstrated pro-apoptotic tendencies corresponding to raised Ca^{2+} levels in late-stage apoptosis, whilst nuclear GTP-cycling proved to be anti-apoptotic (Milakovic *et al.*, 2004).

The following sections attempt to summarise current data available on the physiological functions of TG2.

1.1.6.1 Intracellular TG2 function

1. Cytosol

TG2 is capable of targeting a number of cellular proteins and loss of its calcium regulation in 3T3 fibroblasts results in large insoluble protein shells analogous to those formed in keratinocyte differentiation (Nicholas *et al.*, 2003). These structures may have an important role *in vivo*, stabilising cells prior to clearance by phagocytosis and limiting the potentially harmful release of cellular components into the surrounding tissue. The absence of this activity has led to reports of inflammatory and autoimmune responses (Piredda *et al.*, 1997). Experiments involving the overexpression of TG2 in fibroblasts and neuroblastoma cells have reported an increase in spontaneous and induced apoptosis (Gentile *et al.*, 1992; Melino *et al.*, 1994; Piredda *et al.*, 1997). Conversely, antisense silencing of TG2 in neuroblastoma and human promonocytes resulted in a decreased susceptibility to retinoic-acid induced apoptosis (Oliverio *et al.*, 1999).

In addition to its apparent function in apoptosis, TG2 has been implicated in cell adhesion, spreading and migration. It has been reported that TG2 impacts on vimentin recruitment to stress fibres via retinoic-acid-induced transamidation of RhoA. This occurs via the action of ROCK-2 and is accompanied by increased cell adhesion (Singh *et al.*, 2001). A more recent *in vitro* study utilising antisense techniques in HCA2 fibroblasts in conjunction with overexpression of TG2 or a cross-linking deficient form, has reported normal attachment in TG2 deficient cells but has identified delayed spreading (Stephens *et al.*, 2004). This phenotype was accompanied by defects in motility and both were demonstrated to be unrelated to the cross-linking activity of TG2. Blocking antibodies failed to induce similar defects in the wild type fibroblasts, indicating the involvement of the intracellular pool of TG2 (Stephens *et al.*, 2004). Further experiments revealed these TG2 deficient cells had defects in focal adhesion turnover and stress fibre formation. Accompanying this were alterations in the phosphorylation of focal adhesion kinase (FAK) and failure to activate protein kinase C α (Stephens *et al.*, 2004), an enzyme known to be involved in cell spreading.

2. membrane

As a membrane-associated G-protein TG2 couples α_{1b}- and α_{1d} – adrenoreceptors, thromboxane and oxytocin receptors to phospholipase C, mediating inositol phosphate production in response to agonist activation (Nakaoka *et al.*, 1994; Feng *et al.*, 1996).

3. nucleus

Concerning the nuclear pool of TG2, it has been suggested that it is transported with the help of importin-α3 (Peng *et al.*, 1999). The ability of TG2 to cross-link histones (Ballestar *et al.*, 1996; 2001), retinoblastoma (Oliverio *et al.*, 1997) and Sp1 proteins has lead to the hypothesis that this enzyme may have a direct role in chromatin modifications and/or gene expression regulation.

1.1.6.2 Extracellular TG2

In contrast with work carried out by Stephens *et al.* (2004) a number of studies support a case for TG2 involvement in cell adhesion. Fibroblasts overexpressing TG2 have been reported to demonstrate a decreased susceptibility to trypsin-treatment (Gentile *et al.*, 1992; Verderio *et al.*, 1998). Moreover, the use of antisense silencing techniques in endothelial cells resulted in a reduction in adhesion and spreading (Jones *et al.*, 1997). Initially it was postulated that the transamidating activity of TG2 and its remodelling of the pericellular matrix may be responsible for this enzymes function in cell adhesion and spreading (Jones *et al.*, 1997). Studies have demonstrated TG2 is capable of binding FN with a high affinity with the recognition sites for this glycoprotein residing within the enzymes N-terminus (Jeong *et al.*, 1995). TG2 colocalises with pericellular FN, whilst truncated TG2, lacking the FN binding site is not sequestered to this region (Gaudry *et al.*, 1999). However, more recent studies have discovered the existence of cell surface TG2/β integrin coreceptors for FN (Fig. 7a-b). The predominant complex forms with α5β1, and although TG2 may function cooperatively in this complex it cannot substitute for the action of these integrins in FN assembly (Akimov and Belkin, 2001). These TG2/β integrin receptors are calculated to comprise of a 1:1 ratio between the components and, dependent on cell type, up to 40 % of β1 integrins may complex in this way (Akimov *et al.*, 2000). These coreceptors have been observed to facilitate cell adhesion, spreading (Isobe *et al.*, 1999) and mobility (Balklava *et al.*, 2002). The majority of this work has been carried out on FN and these coreceptors may play a particularly prominent role on this substratum. This could account for apparent disparities with studies established on other ECM components or tissue grade plastic (Stephens *et al.*, 2004). Despite the ability of TG2 to cross-link FN (Barsigian *et al.*, 1991; Martinez *et al.*, 1994; Jones *et al.*, 1997) these functions are all found to be independent of transamidation activity (Akimov *et al.*, 2000; Balklava *et al.*, 2002), thus highlighting a structural role for TG2. A role for cell surface TG2 in fibroblast migration is further supported by *in vitro* wound healing studies carried out using transgenic mice (De Laurenzi *et al.*, 2001; Verderio *et al.*, 2005). Fibroblasts isolated from $TG2^{-/-}$ were found to re-populate wounds at a slower rate than the wild-type controls. However, this could be partly counteracted by the addition of exogenous

purified guinea pig liver TG2. This was observed to improve the stability of the cells sheets and shifted the pattern of healing toward the control phenotype.

Although originally, sequence data led to TG2 being considered a cytosolic protein, quantities of TG2 have been detected associated with the ECM of certain tissues. Here its function extends to wound healing, angiogenesis, remodelling and stabilisation (Upchurch *et al.*, 1991; Haroon *et al.*, 1999; Aeschlimann and Thomazy, 2000). The role of TG2 in wound healing will be discussed at length in Section 1.3.4.3. The ability of TG2 to remodel ECM tissue has been attributed to its cross-linking activity, demonstrated *in vitro* by its ability to contract floating collagen lattices. Cross-linking deficient forms of the enzyme produced by the substitution of Cys^{277} to a Ser residue demonstrate a reduced rate of contraction, accompanied by reduced levels of MT1-MMP and active MMP-2 (Stephens *et al.*, 2004). TG2 substrates within the ECM are many and varied including, FN (Jones *et al.*, 1997), vitronectin (Sane *et al.*, 1988) collagen (Kleman *et al.*, 1995), osteonectin (Aeschlimann *et al.*, 1995), osteopontin (Kaartinen *et al.*, 1997) and nidogen (Aeschlimann and Paulsson, 1991). The high affinity TG2 demonstrates for a number of basement membrane (BM) components lead to speculation that it is involved in stabilising the dermo-epidermal junction (DEJ) (Fig. 7c). Indeed, clinical studies have shown its activity correlates with increased stabilisation of human skin grafts (Raghunath *et al.*, 1996).

TG2 may also affect matrix deposition indirectly. The secreted enzyme is found to impact on the activation of transforming growth factor β (TGFβ), possibly through covalent modification of activating factors (Kojima *et al.*, 1993; Nunes *et al.*, 1997). This produces a positive feed back loop to TG2 expression and that of a number of other ECM genes (Ritter *et al.*, 1998; Akimov and Belkin, 2001).

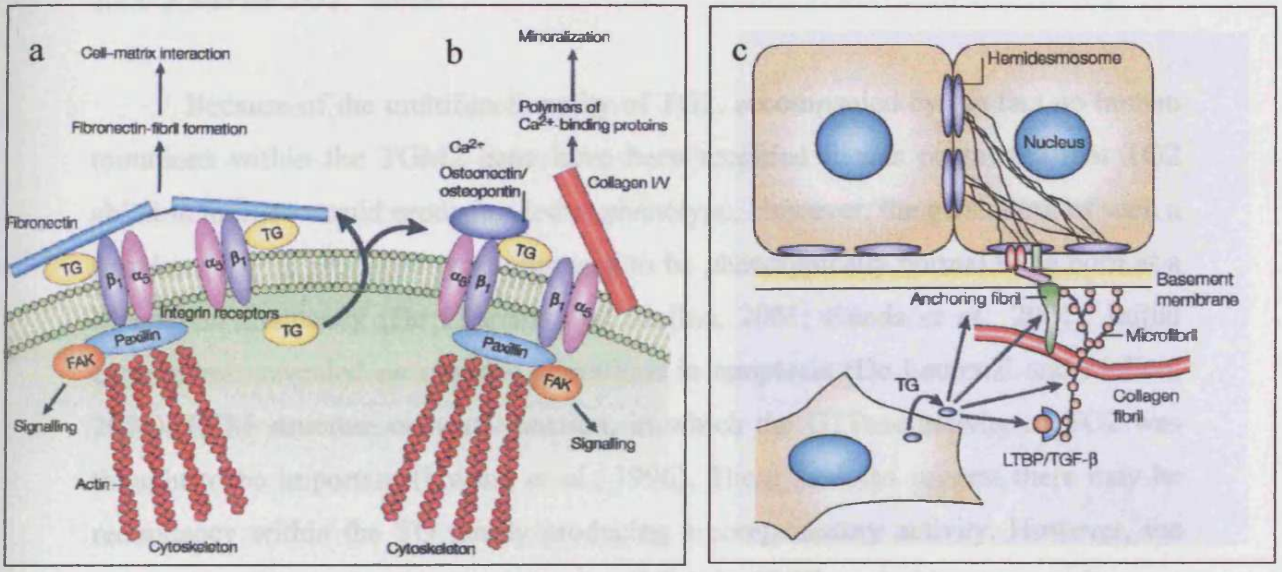

Fig. 7 Schematic representation of the role of extracellular TG2: Transglutaminase 2 (TG2) acts as an integrin coreceptor and binds fibronectin with a high affinity, thereby aiding the organisation of the extracellular matrix (ECM). Through interactions with adhesion components such as paxillin and FAK, the α5β1 integrin receptor can influence intracellular signalling and the cytoskeleton. Unlike the more reversible processes of cell-matrix interactions (a) that are dependent only on non-covalent associations with TG2, irreversible mineralisation (b) requires the covalent cross-linking of connective-tissue substrates (osteonectin/osteopontin and collagens) by the Ca^{2+}-activated enzyme (Figure courtesy of D. Aeschlimann, University of Wales, Cardiff, UK). (c) TG2 also stabilises the dermo-epidermal junction. This enzyme catalyses the covalent attachment of TGFβ, through its latent TGFβ protein (LTBP) subunit, to the microfibrils. As such, large stores of this growth factor can accumulate in the connective tissue from where it can be liberated by the action of proteases. Hemidesmosome-mediated attachment of cells to the basement membrane and the underlying connective tissue proteins (anchoring fibrils, microfibrils and collagen fibrils) – all of which are substrates for TG2 – are shown. (Lorand and Graham, 2003).

1.1.6.3 Murine TG2$^{-/-}$ model

Because of the multifunctionality of TG2, accompanied by the fact no human mutations within the TGM2 gene have been recorded it was postulated that TG2 ablation in mice would produce a lethal phenotype. However, the generation of such a knockout model produced what appeared to be phenotypically normal mice born at a Mendelian frequency (De Laurenzi and Melino, 2001; Nanda *et al.*, 2001). Initial experiments revealed no obvious alterations in apoptosis (De Laurenzi and Melino, 2001), ECM structure or heart function, in which the GTPase activity of TG2 was thought to be important (Hwang *et al.*, 1996). These findings suggest there may be redundancy within the TG family producing a compensatory activity. However, the only other TG to be localised to the ECM is FXIII and this enzyme has not demonstrated a capacity for NTP-cycling. Further studies of these mice have since identified a decrease in primary fibroblast adhesion (Nanda *et al.*, 2001) and impaired wound healing (Mearns *et al.*, 2002). It was also demonstrated that following dexamethasone-induction of apoptosis, phagocytic clearance by macrophages is defective within the thymus and the liver (Nanda *et al.*, 2001). This agrees with previous studies, suggesting TG2 cross-linking activity is important in stabilising apoptotic cells prior to clearance (Piredda *et al.*, 1997). Finally, knockout mice have demonstrated glucose intolerance as a result of reduced insulin secretion that correlates strongly with maturity-onset diabetes in humans (Bernassola *et al.*, 2002).

1.1.7 TG3

TG3 is expressed as a virtually inactive 692 amino acid (77 kDa) zymogen that localises to the cell cytosol (Kim *et al.*, 1993; Hitomi *et al.*, 2003). Activation of the enzyme relies on its cleavage at Ser^{469} to produce a 50 and 27 kDa fragment, accompanied by an increase in specific activity (Kim *et al.*, 1990; Kim *et al.*, 1993). Although the 50 kDa cleavage product, comprising of the N-terminal sandwich and catalytic domains is capable of catalysing transamidation reactions (Chung and Folk, 1972; Ogawa and Goldsmith, 1976), complexes with the 27 kDa C-terminal β-barrels demonstrate increased activity and the two fragments are reported to remain associated (Kim *et al.*, 1990; Ahvazi *et al.*, 2002). As yet the enzyme responsible for this cleavage *in vivo* has not been identified, but *in vitro* studies have utilised the bacterial protease, dispase to produce correlating cleavage products (Kim *et al.*, 1993). The cleavage site is a unique sequence of twelve polar amino acid residues residing in the flexible loop connecting the catalytic and β-barrel domain 1 (Kim *et al.*, 1993). As has been mentioned previously, this correlates strongly with cleavage sites found in TG1 and FXIII. Conservation of TG3 between species is comparatively low ranging from 50 – 75 % (Kim *et al.*, 1993) suggesting this enzyme is still undergoing rapid evolution (Aeschlimann and Paulsson, 1994). Particularly low homology is apparent within the protease cleavage site and is evidence of species evolving alternative activation mechanisms (Kim *et al.*, 1993). The recent resolution of a number of TG3 crystallographic structures has allowed a more comprehensive understanding of conformational changes accompanying altered activity. A total of three Ca^{2+} binding sites have been identified within the enzyme (Ahvazi *et al.*, 2002), the 1st of these (Asn^{224}- Asn^{229}) demonstrates constitutive binding (Kd 0.3 μM) and has a putative role in enzyme stabilisation. Ca^{2+} binding at sites 2 (Asn^{430}- Asn^{448}) and 3 (Asn^{393}, Glu^{443} and Glu^{448}) occurs following zymogen cleavage and cooperate to produce a movement of the β-strand Gly^{322} – Ser^{325}. This conformational change opens a channel through the enzyme (Fig. 8) and exposes two tryptophan (Trp) residues in close proximity to the active site. These are thought to be involved in stabilising the enzymes transition state. This conformational change also makes Asp^{324} accessible for coordination to the Ca^{2+} ion at site 3. It was demonstrated that the Ca^{2+} ions at site 2 and 3 could be substituted for lanthamides and in the case of the

latter Mg^{2+}. However, it was apparent that Ca^{2+} binding was required at site 3 for enzyme activation. Consequently, it has been proposed that Mg^{2+} binding of the cleaved zymogen provides a mechanism to prevent aberrant cross-linking activity, in the absence of an accompanying rise in Ca^{2+} levels (Ahvazi *et al.*, 2003).

Biochemical and crystallographic evidence now exists that TG3 also undergoes GTPase-cycling, but unlike TG2 this enzyme does not target ATP (Ahvazi *et al.*, 2004). It has been demonstrated that substitution of the Ca^{2+} ion at site 3 for Mg^{2+} is required for binding of GTP/GDP accompanied by regional conformational changes producing the movement of the ^{320}DKGSDS^{325} sequence motif. To summarise, this structural alteration targets the same sites involved in the activation of the enzyme and reflects the negative regulatory role of nucleotides.

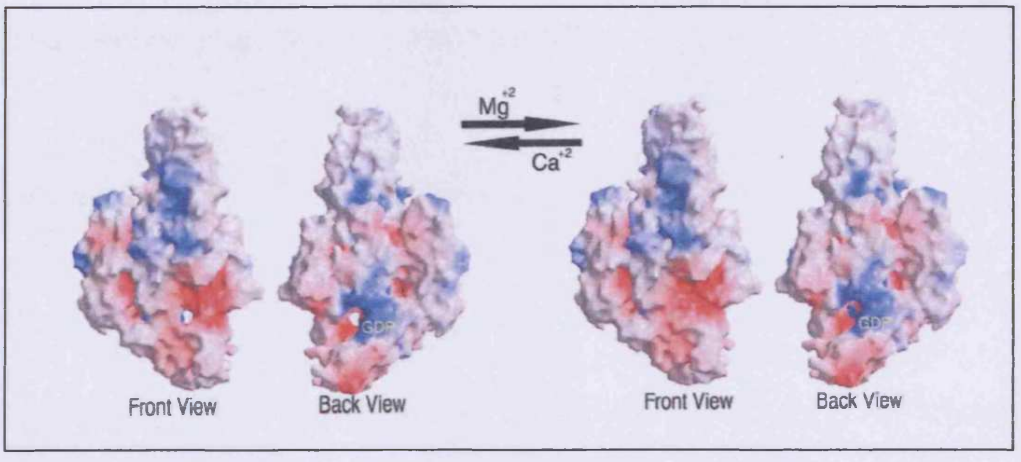

Fig. 8 The electrostatic surface potential comparison of the TG3-GDP complex when bound to Ca^{2+} or Mg^{2+} at site 3: The front and back view represent images rotated 180° with respect to each other. The acid and basic regions are coloured red and blue respectively. An open channel is clearly evident in the Ca^{2+} bound form and is lost following Mg^{2+} substitution (Ahvazi *et al.*, 2004).

TG3 is expressed in brain, forestomach, small intestine, testis, skeletal muscle and skin (Hitomi *et al.*, 2001). As is the case with TG1, the majority of information on this enzyme's physiological role concerns its involvement in terminal differentiation of keratinocytes (Kim *et al.*, 1993) and it is sometimes used as a late stage marker for this process. *In vitro* studies have ascertained its particularly high affinity for loricrin (Candi *et al.*, 1995). However $TG1^{-/-}$ mice illustrate the role of TG3 must be a cooperative one and it cannot compensate for the loss of TG1 activity (Matsuki *et al.*, 1998). No diseases have yet been linked to mutations in the TGM3 gene. It has been suggested that TG3 preferentially forms intramolecular cross-linking, facilitating the incorporation of proteins into the CE structure rather than directly generating macromolecues (Candi *et al.*, 1995).

1.1.8 TG4

The most extensive studies carried out with TG4 to date have included the rat form of the enzyme. It was revealed that this 75 kDa protein (692 amino acids) exists as a homodimer (Wilson and French, 1980) and has been identified as a major secretory product of rat dorsal prostate and coagulating glands (Ho *et al.*, 1992). As has been observed with other secreted TGs, TG4 contains no recognised signal peptide and is N-terminally blocked. Immunogold electron microscopy has detected TG4 in apocrine secretory vesicles, however, its absence from the Golgi apparatus, suggests direct entry from the cytoplasm (Seitz *et al.*, 1990; 1991). Concerning post-translational modifications, TG4 has been demonstrated to be mannosyl-linked and a phosphotidyl anchor has been identified (Seitz *et al.*, 1991).

The best-characterised function of TG4 is its rapid catalysis of polyamines to produce seminal plugs (Williams-Ashman, 1984).

1.1.9 TG5

Ubiquitous low level expression of TG5 is observed in human tissues, with the exception of the lymphatic and central nervous systems (Aeschlimann *et al.*, 1998; Candi *et al.*, 2004). This 720 amino acid (81 kDa) enzyme is expressed in its active form and has been reported to be N-terminal acetylated (Rufini *et al.*, 2004). TG5 mRNA isolated from human keratinocytes has revealed the presence of three alternative splice products in addition to the full-length enzyme, in which exons III, XI or III and XI are absent. *In vitro* studies have ascertained that exon III is required for enzyme activity (Candi *et al.*, 2001). Splice products lacking exon XI produce a frame-shift mutation, resulting in a novel sequence of 25 amino acids followed by premature termination (Candi *et al.*, 2001). Due to its low level expression a number of TG5 studies have utilised keratinocytes transfected to overexpress the protein. Such studies have found this TG isoform is resistant to extraction and retrieval has only been successful by treatment with SDS or urea (Candi *et al.*, 2001). This corresponds closely to the profile of insoluble proteins and cell fractionation studies have demonstrated that TG5 associates with the nuclear matrix and cytoskeleton. Further to this confocal analysis suggests TG colocalises with perinuclear vimentin (Candi *et al.*, 2001).

As has been observed with TG2, TG5 is also capable of binding ATP and GTP (Fig. 8), which have been demonstrated to inhibit the enzymes cross-linking activity (Candi *et al.*, 2004). As a consequence of the limited characterisation of TG5 the cellular function of this GTPase activity is not yet known.

Following the finding that TG5 expression increased several-fold when cultured keratinocytes were induced to differentiate (Aeschlimann *et al.*, 1998), work began to ascertain whether TG5 is involved in CE formation. Recombinant TG5 can utilise classical CE components, including involucrin, loricrin, SPR1 and SPR2 (Candi *et al.*, 1995). When incubated with loricrin, TG5 has demonstrated its ability to use it as a complete substrate, i.e. targeting both Gln and Lys residues. It also produced a combination of intra- and inter-protein cross-links.

1.1.10 TG6

As yet there is virtually no published data concerning this isoform. The full-length enzyme consists of 708 amino acids with a calculated mass of 80 kDa (H. Thomas Thesis, 2004). However, TG6 has been shown to undergo alternative splicing of exon XII, the absence of which produces a frameshift and premature termination within exon XIII. The resulting short form is 626 amino acids in length (70 kDa).

TG6 was first amplified from the small lung carcinoma cell line, H69 (H. Thomas Thesis, 2004) and subsequent Northern blot analysis identified widespread expression at low level in human tissues. High level expression was observed within the central nervous system, leading to speculation that this enzyme might be involved in certain neurodegenerative diseases (H. Thomas Thesis, 2004). In addition to this, murine *in situ* data localised this isoform to the epidermis.

1.1.11 TG7

This most recently discovered member of the TG family was first isolated from a prostate carcinoma cell line. TG7 is expressed as a 710 amino acid protein (80 kDa) and Northern blot analysis has revealed wide spread low level expression in human tissue with the highest levels detected in testis and lung tissue (Grenard *et al.*, 2001). TG7 has also been amplified from a number of cells and cell lines by RT-PCR including, dermal fibroblasts (TJ6F, HCA2), primary keratinocytes and mammary epithelium (Grenard *et al.*, 2001). To date no data concerning the physiological function of this enzyme is available, however the ubiquitous nature of TG7 expression would suggest broad applications.

Over the years, TG studies have identified the involvement of these enzymes with numerous and wide ranging physiological disorders including cataract formation, tissue fibrosis, artherosclerosis, cancer metastasis, celiac disease, rheumatoid arthritis, neurodegenerative diseases and a number of keratinising skin disorders (Selkoe *et al.*, 1982; Weinberg *et al.*, 1991; Bowness *et al.*, 1994; Johnson *et al.*, 1994; 1997; Dietrich *et al.*, 1997; Mirza *et al.*, 1997; Candi *et al.*, 2002; Zemaitaitis *et al.*, 2002). This has produced growing interest in the TG family as therapeutic targets. For the purposes of this study the focus will remain on the role of TGs in skin homeostasis and the consequences of their misregulation therein.

1.2 Skin homeostasis

The skin is considered the largest organ of the body, forming the continuous integument of the body and providing four major functions:

- **Protection:** The skin provides protection against ultraviolet light, mechanical, chemical and thermal insults in addition to protecting against invasion by micro-organisms. As a relatively impermeable surface the skin also has a key function in preventing dehydration.
- **Sensation:** The skin is rich in receptors for touch, pressure, pain and temperature.
- **Thermoregulation:** In man, skin is a major organ of thermoregulation. The presence of hair and subcutaneous adipose tissue insulate against heat loss. Conversely sweat evaporation from the skin surface and vasodilation within the rich vascular network of the dermis facilitates heat loss.
- **Metabolic functions:** Vitamin D is synthesised in the epidermis, supplementing pools derived from dietary sources.

Mammalian skin consists of two tissue layers (Fig. 9a-b), a protective stratified epidermis and an underlying layer of collagen-rich dermis generated by fibroblasts. These tissues are separated by a basement membrane. Skin tissue undergoes regular remodelling and replenishment under careful regulation.

1.2.1 The dermis

The dermal layer of the skin provides a robust base for the epidermis in addition to metabolic support to this avascular tissue. The dermis contains a number of epidermal appendages including, hair follicles and sweat glands, which originate from epithelial tissue during embryological development. Micrographs of this tissue have identified two distinct zones (Fig. 9a). Adjacent to the epidermis is the papillary dermis, comprising of loosely interlacing collagen fibres and is highly vascular. However the main bulk of the dermis is formed by the reticular layer, named after the interlacing arrangement of collagen fibres, which are denser than the papillary zone.

The predominant TG isoenzyme within the dermal compartment is TG2 (De Laurenzi and Melino, 2001), which is expressed in fibroblasts and secreted into the ECM. As discussed previously, TG2 has been linked to cell adhesion, spreading and motility coupled with ECM remodelling and stabilisation. These functions lead to a hypothesised role in wound healing, which have since been confirmed (Haroon *et al.*, 1999). FXIII is also detected within the dermal ECM and has a putative role in wound healing (Cohen *et al.*, 1982; Knox *et al.*, 1986; Mosher *et al.*, 1991; Corbett *et al.*, 1997). The mRNA of other TG isoforms has been amplified from primary fibroblasts or fibroblast cell lines including TG1 (Phillips *et al.*, 1993; Stephens *et al.*, 2004), TG5 (Stephens *et al.*, 2004) and TG7 (Grenard *et al.*, 2001; Stephens *et al.*, 2004). As yet no physiological functions have been characterised for these enzymes in the dermis.

1.2.2 The epidermis

The epidermis is a continuously renewing tissue with a complete cell turnover occurring approximately every 28 days (Roop, 1995). This tissue comprises of four histologically distinct cell layers, the stratum basale, stratum spinosum, stratum granulosum and stratum corneum (Fig. 9b).

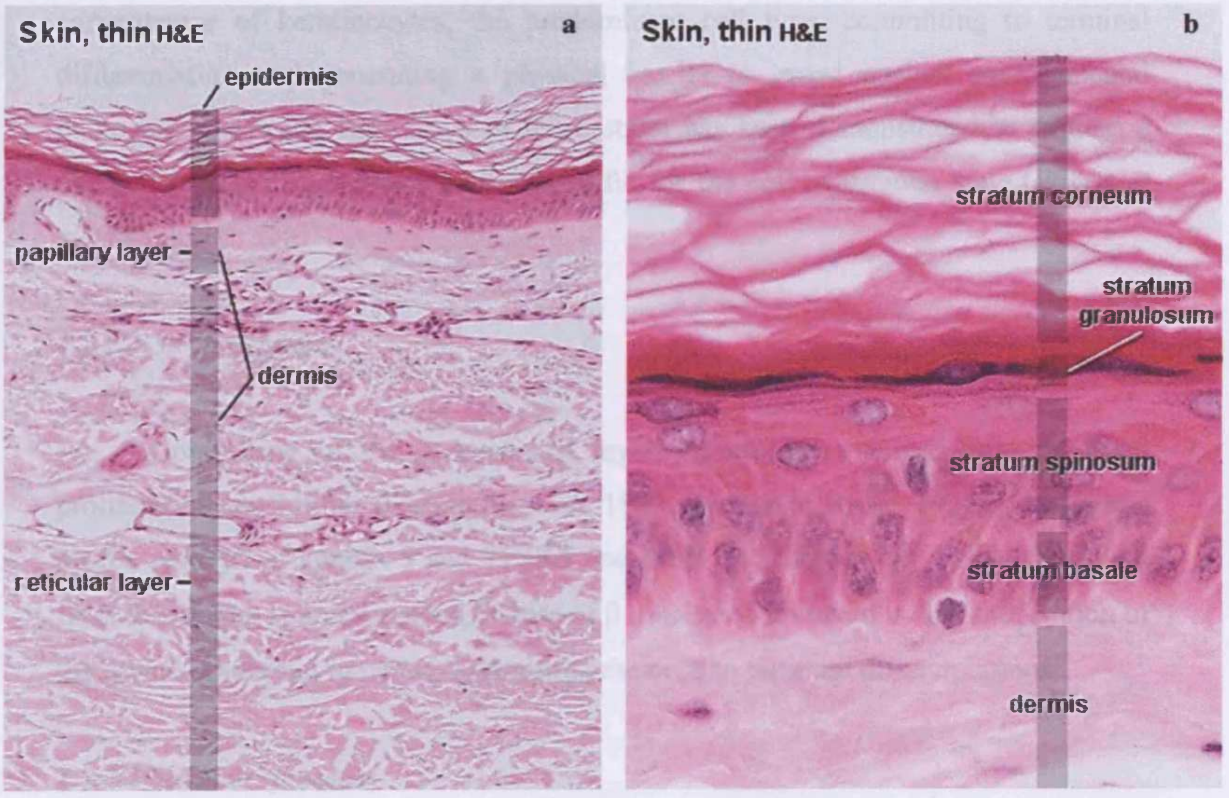

Fig. 9 The tissue architecture of skin: Hematoxylin and eosin (H&E) staining reveals three distinct domains (a) the avascular epidermal tissue formed by keratinocytes committed to terminal differentiation. The dermis can be dissected into the papillary and reticular layers. The former of these layers is immediately adjacent to the epidermis and can be distinguished by the greater density of fibroblasts. This region is relatively thin and formed by a fine network of collagen and elastin fibres. The underlying reticular dermis contains coarse collagen and elastic fibres in addition to the larger blood vessels, which feed into the capillary network of the papillary layer. The epidermis can be divided into a further four morphologically distinct layers as seen in a high magnification picture of a region of thin skin (b). The stratum basale is formed from the deepest layer of keratinocytes and demonstrates a cuboidal or columnar morphology. Several layers of polygonal keratinocytes comprise the stratum spinosum. In the case of thin skin regions, the ketohyalin granule-containing stratum granulosum is apparent as a single layer of dark and flattened cells although this can increase to several layers in regions of thick skin. Finally the outermost layers form the stratum corneum, containing anuclear, flattened cells termed corneocytes.
(http://www.lab.anhb.uwa.edu.au/mb/mb140/CorePages/Integumentary/Integum.html#Epidermis)

The observed morphological changes within the epidermis are the consequence of keratinocytes, the predominant cell type, committing to terminal differentiation and generating a physical barrier to guard against environmental pathogens and water loss. Each of these strata has been demonstrated to express a characteristic set of marker proteins specific for the cell maturation state (Eckert *et al.*, 1989).

1.2.2.1 Stratum basale

Comprising of the deepest cell layer, keratinocytes demonstrate regulated proliferative capabilities (Cotsarelis *et al.*, 1989; Fuchs and Byrne, 1994). The keratin profile consists of keratin 5 and 14 (K5 and K14) (Reichert *et al.*, 1993). Transition from this region is accompanied by loss of β1 integrins involved in the stabilisation of the dermo-epidermal junction, committing the cells to terminal differentiation.

1.2.2.2 Stratum spinosum

This strata accounts for the majority of the epidermal cell layers and is a region containing extensive desmosomes. These cell-cell connections contribute to the strength of the tissue and accounts for the "spikey" appearance of keratinocytes (sometimes referred to as the "prickly layer"). At this stage of differentiation the ability of the cells to proliferate is lost (Fuchs and Byrne, 1994; Eckert *et al.*, 1997) and keratin profile alters, predominantly expressing K1 and K10 (Fuchs and Green, 1980). These keratins are abundant and aggregate to form intermediate filaments with important structural functions. It is in the more superficial layers of the spinous region that components of the cornified envelope (CE) are expressed, including involucrin. The formation of this envelope structure is a key stage in skin barrier formation.

1.2.2.3 Stratum granulosum

Keratinocytes within this stratum are characterised by keratinisation-specific lipid synthesis (Swartendruber *et al.*, 1989; Wertz *et al.*, 1989; Schurer *et al.*, 1991; Elias, 1996). The distinct histology of cells within this region is the consequence of granule-enclosed storage of proteins and lipids (Matoltsy and Matoltsy, 1966; Lavker and Matoltsy, 1971; Holbrook and Odland, 1975; Lavker, 1976; Ishida-Yamamoto *et al.*, 1993). These transient structures contain CE precursors (Steven *et al.*, 1990), including loricrin (Mehrel *et al.*, 1990) and profilaggrin (Steinert and Marekov, 1995), both considered markers of late stage differentiation.

1.2.2.4 Transition Zone

The transition between the granular layer and stratum corneum is marked by extensive remodelling, including the cornification process. This term describes the process of reabsorbing the cell plasma membrane and its replacement with the extensively cross-linked CE. This structure comprises of a protein and lipid component and is discussed in more detail in Section 1.2.3. Occurring concomitantly with this step is the extrusion of lipids into the inter-cellular space (Landmann, 1986), the stabilisation of keratin intermediate filament bundles and the destruction of intracellular organelles by the action of proteases and nucleases. This limits the cell metabolism to catabolic reactions, but often leads to these cells being dismissed as dead (Eckert *et al.*, 2005).

1.2.2.5 Stratum corneum

The thickness of this surface region has been shown to vary considerably with body site, containing between 4-100 layers of cells (Ya-Xian *et al.*, 1999). These differentiated keratinocytes form plate-like structures and are distinguished by the term corneocytes. Similarly the unique cell-cell interactions are termed corneosomes (Allen and Potten, 1975; Chapman and Walsh, 1990) and following the breakdown of these structures, cells are lost by the process of desquamation (Eckert *et al.*, 1997). These cells are embedded in lipid lamellae and although the stratum corneum may be dissected into its separate components, in essence, extensive cross-linking creates a continuous macromolecule, providing the barrier function required of this tissue.

1.2.3 The cornified envelope

The CE comprises of protein and lipid components accounting for 90 and 10 % of the stratum corneum's dry weight respectively (Swartzendruber *et al.*, 1988). The protein element comprises of a 15 nm shell (Matoltsy and Balsamo, 1955; Farbman, 1966; Hashimoto, 1969) that is formed on the cytoplasmic surface of the plasma membrane (PM) eventually replacing it, as the lipid bilayer is broken during cornification. This substitution provides the skin with more mechanically robust properties (Marks *et al.*, 1983). A 5 nm lipid component has been distinguished by electron microscopy as a lucent band (Lavker, 1976) and is located on the cell surface. This has been characterised as a monolayer of ester linked ω-hydroxyceramides known as covalently bound lipids (CBLs) (Wertz and Downing, 1987; Marekov and Steinert, 1998). These lipids are among those extruded into the extracellular space from keratinocytes in the transition zone, the remainder form unique lipid lamellae with a reduced phospholipid content and increased fatty acids, cholesterol and ceramides (Shurer and Elias, 1991; Elias, 1996). The hydrophobic nature of the environment in which corneocytes are embedded distinguishes a role for the CBLs, capable of interdigitating with the surrounding lamellae to enhance the barrier formation (Wertz *et al.*, 1989). The generation of the CE structure begins in the stratum spinosum generating a scaffold in inter-desmosomal regions to which further components are sequestered. The result is a highly insoluble structure, which may be retrieved by boiling in SDS/reducing agent buffers (Sun and Green, 1976; Manabe *et al.*, 1981).

The extensive covalent linkages within the CE has somewhat hindered the identification of its components. Studies of the envelope have involved a number of experimental approaches: 1) Antibodies raised against the isolated CE have been used in identifying envelope precursors (Kubilus *et al.*, 1987; Michel *et al.*, 1987; Nagae *et al.* 1987). 2) Antibodies have been raised against putative CE components and immunohistochemical studies have revealed staining at the cell periphery of corneocytes (Rice and Green, 1979; Lobitz and Buxman, 1982; Zettergren *et al.*, 1984). 3) Sequencing has been carried out on peptides retrieved following extensive proteolysis of the CE (Candi *et al.*, 1995; Steinert and Marekov, 1995). 4) The ability of potential precursors to be cross-linked by TG enzymes has been assessed *in vitro*

(Rice and Green, 1979; Simon and Green, 1984; Candi *et al.*, 1995; 1999; 2001). Although this thesis focuses specifically on epidermal tissue, CEs have been identified in a range of stratified squamous epithelia (e.g. oral epithelia, hair cutical). Further to this, variations in CE composition have been found between epithelial tissue and body site (Steinert *et al.*, 1998). This variation can most likely be accounted for by differing tissue-specific requirements (Steinert and Marekov, 1995; Steinert, 2000). Interestingly the protein-shell is not a homogenous structure (Steinert and Marekov, 1995), suggesting spatial and temporal regulation is involved in its formation.

1.2.4 The role of transglutaminases in cornified envelope formation

Initial studies attributed the cross-links within the CE macromolecule to disulfide bonds (Matoltsy and Matoltsy, 1970), however further studies have identified γ-glutamyl-ε-lysl (Rice and Green, 1977) and γ-glutamyl-polyamine isopeptide bonds within this structure. The latter almost exclusively involve spermidine (Piacentini *et al.*, 1988, Martinet *et al.*, 1990). Immunohistochemical studies have been carried out with antibodies raised against the isopeptide bond structure (Fig. 10). Results clearly indicate the number of cross-links increase as differentiating keratinocytes translocate to the epidermal surface with a rapid increase in staining observed within the in transition zone. This is accompanied by intense staining across dermo-epidermal junction (DEJ). These findings strongly implicated TG enzymes in the formation of the CE.

Of the nine isoforms, six are expressed in the epidermis, TG1, 2, 3, 5, 6 and 7. As yet little data exists concerning physiological functions of the two latter enzymes and the expression of TG2 has been limited to the basal layer of keratinocytes (Aeschlimann *et al.*, 1998; Haroon *et al.*, 1999) having putative role in stabilising the DEJ. In contrast TG1, 3 and 5 have exhibited differentiation specific expression (Kim *et al.*, 1993; 1995a; 1995b; Aeschlimann *et al.*, 1998; Candi *et al.*, 2001) and have demonstrated an ability to cross-link identified CE components *in vitro* with high affinity (Candi *et al.*, 1995; 1999; 2001). Interestingly it has been demonstrated that these enzymes target the same Gln and Lys residues involved with cross-linking *in vivo*, although different isoforms were observed to preferentially cross-link distinct residues within the same substrate. Some of the most compelling evidence for TG involvement in the CE formation is the discovery that TG1 mutations have been linked to lamellar ichthyosis (LI) (Huber *et al.*, 1995; Parmentier *et al.*, 1995; Russell *et al.*, 1995) a heterogeneous group of skin diseases exhibiting defective CE formation and compromised skin barrier formation.

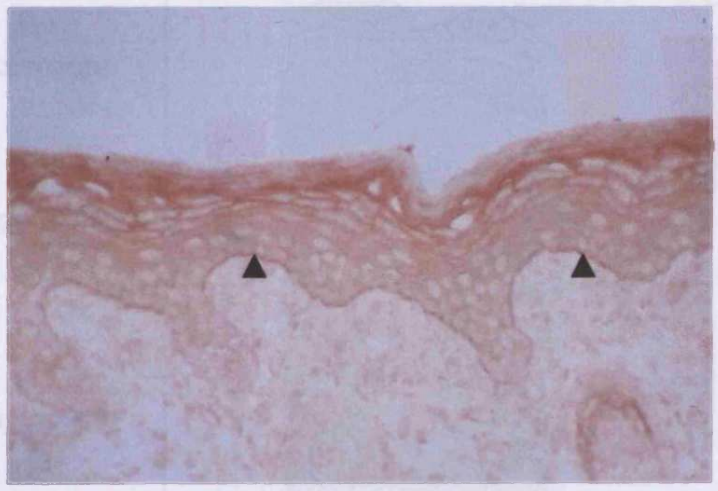

Fig. 10 The extent of γ-glutamyl-ε-lysine cross-linking increases with keratinocyte terminal differentiation: Antibodies elicited against γ-glutamyl-ε-lysine cross-links demonstrate a greater degree of staining in the more superficial layers of the epidermis. Particularly intense staining is observed in the transition zone (Z) of the epidermis and the dermo-epidermal junction (designated by arrowheads). Courtesy of D. Aeschlimann, University of Wales, UK

TG1 is the first isoform to be expressed, low level mRNA has been reported from the basal layer (Steinert *et al.*, 1996a) however a rapid increase is observed in the upper spinous layer, terminating within the transition zone (Yamada *et al.*, 1997). Immunohistochemical studies have observed gradient staining with anti-TG5 decorating the spinous and granular layers (Candi *et al.*, 2002). TG3 is expressed in the later stages and is approximately concomitant with other late stage differentiation markers loricrin and profilaggrin (summarised in Fig. 11).

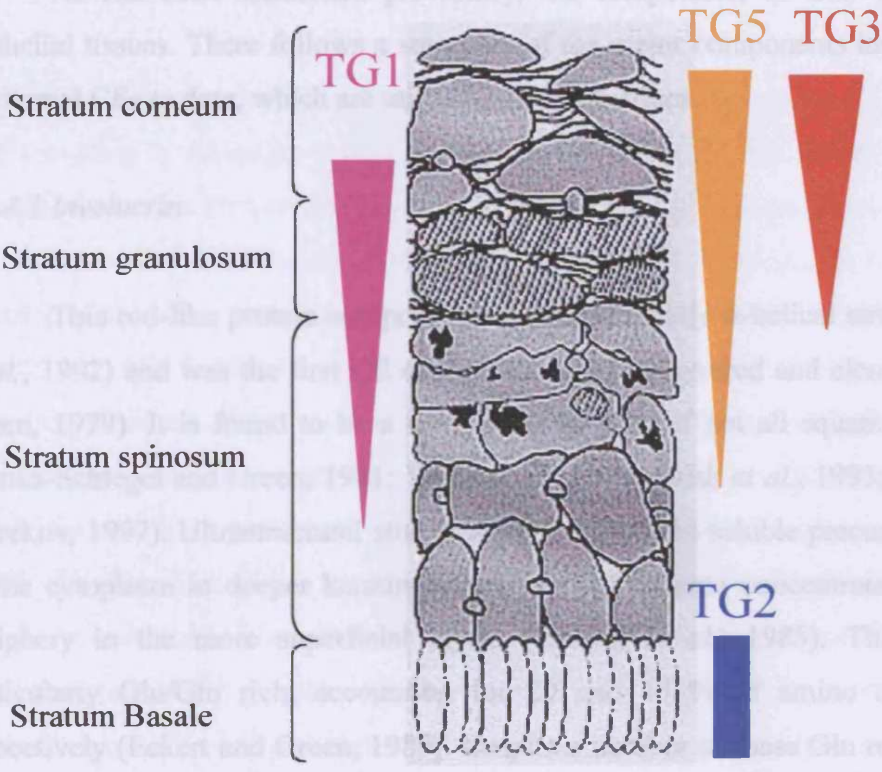

Fig. 11 Schematic representation of transglutaminase distribution in the epidermis: Representation of proteins levels is as follows TG1 (magenta), TG2 (blue), TG3 (red) and TG5 (orange).

As has been mentioned previously, the components of CEs vary between epithelial tissues. There follows a summary of the major components identified from epidermal CEs to date, which are utilised as TG substrates.

1.2.4.1 Involucrin

This rod-like protein comprises of a predominantly α-helical structure (Yaffe *et al.*, 1992) and was the first CE component to be discovered and cloned (Rice and Green, 1979). It is found to be a component of most if not all squamous epithelia (Banks-Schlegel and Green, 1981; Walts *et al.*, 1985; Crish *et al.*, 1993; Steinert and Marekov, 1997). Ultrastructural studies observed that this soluble precursor localised to the cytoplasm in deeper keratinocyte layers but became concentrated at the cell periphery in the more superficial layers (Warhol *et al.*, 1985). This protein is particularly Glu/Gln rich, accounting for 20 and 15 % of amino acid residues respectively (Eckert and Green, 1986). Despite a number of these Gln residues being utilised by TG enzymes (Etoh *et al.*, 1986; LaCelle *et al.*, 1998) it was observed that Gln^{496} was preferentially targeted in labelling experiments (Simon and Green, 1988; Nemes *et al.*, 1999a).

Involucrin has been localised to the external region of the CE (Steinert and Marekov, 1997) and protease cleaved peptides have demonstrated this protein is cross-linked to a wide range of CE components, confirming its involvement in the early stages of CE formation. Recovery of lipopeptide fragments following protease digestion has also identified involucrin as the primary envelope precursor coupled to ceramide lipids. This accounts for ~35 % of CBLs (Marekov and Steinert, 1998).

1.2.4.2 Loricrin

Loricrin accounts for ~75 % of the total protein content of the CE (Hohl *et al.*, 1991) making it the major component and correspondingly the amino acid profiles obtained from this 26 kDa protein are qualitively similar to those from isolated CEs (Reichert *et al.*, 1993). Step-wise digestion of the CE by Proteinase K have localised loricrin to the inner two thirds of the CE at the cytoplasmic face (Steinert and Marekov, 1995). In fact its contribution to the protein content rises to 95 % in the final third demonstrating its late stage recruitment and the extent of its incorporation. Interestingly loricrin, a highly insoluble protein, is detected in granules (L-granules) within the stratum granulosum (Steven *et al.*, 1990; Ishida-Yamamoto *et al.*, 1993, 1996). This insolubility has been partly attributed to disulfide bonds (Mehrel *et al.*, 1990) and it has also been observed that interactions between aromatic amino acids produce a secondary structure (Hohl *et al.*, 1991). The loricrin molecule can be subdivided into Gln-Lys rich terminal regions embedding three adjacent Gly-Ser rich domains divided by two Gln-rich sequences (Hohl *et al.*, 1991). Based on sequence data, it was predicted that up to twenty residues could be targeted by TG enzymes (Holh *et al.*, 1991b). Recovery of peptide fragments following proteolytic digests of CEs revealed at least two Lys residues and four Gln are involved in cross-linking *in vivo*. Incorporation of loricrin occurs within the transition zone, following its release from L-granules. There has been some speculation as to the nature of its translocation and cross-linking into the CE due to its lack of solubility. It has been proposed that coupling to highly soluble small proline-rich proteins may modify solubility of loricrin (Kalinin *et al.*, 2002).

Concerning loricrin as a TG substrate, it can be cross-linked *in vitro* by TG1, 3 and 5. However it has been reported that TG1 predominantly catalyses inter-molecular cross-links, whilst TG3 promotes intra-molecular bonds between favoured Lys and Gln residues and is unable to form the polymers observed with TG1 (Candi *et al.*, 2001). Significantly, loricrin has been reported to accumulate in transgenic $TG1^{-/-}$ mice, perhaps highlighting the role of this enzyme in incorporating this protein into the CE (Matsuki *et al.*, 1998).

1.2.4.3 Small proline rich proteins

The SPR proteins form a 14-member multigene family (Tesfaigizi and Carlson, 1999) comprising of several proline-rich repeats, flanked by N- and C-terminals rich in Pro, Gln and Lys (Gibbs *et al.*, 1993). It is the Gln and Lys within these sequences that participate in cross-linking and it has been proposed these enzymes function as bridges between CE components (Steinert *et al.*, 1998).

Both TG1 and 3 are capable of using SPR1 as a complete substrate *in vitro*, whereas TG2 cross-links SPR1 proteins poorly (Candi *et al.*, 1999). However, different residues are targeted by the isoforms and it would seem that the activity of both enzymes is required for the formation of oligomers.

1.2.4.4 Cystatin and elafin

These precursors contribute as minor components to the CE structure (Takahashi *et al.*, 1994) and there has been some speculation about their physiological role. It has been hypothesised that members of the cystatin family and elafin may regulate protease activity required for envelope maturation (Takahashi *et al.*, 1994). Cystatin A is a protease inhibitor and elafin functions as a potent inhibitor of elastase and proteinase 3. In fact mutations in another cystatin family member, cystatin M/E is associated with disturbed cornification and subsequent impaired barrier formation (Zeeuwen *et al.*, 2004).

1.2.4.5 Filaggrin

Filaggrin is synthesised as profilaggrin, which consists of a number of filaggrin units flanked by the N- and C-terminal domains (Presland *et al.*, 1992, 1997; Pearton *et al.*, 2002). Profilaggrin contains two calcium-binding EF hand motifs (Presland *et al.*, 1992; Markova *et al.*, 1993), which is a characteristic shared by other envelope precursors such as S100 proteins (Donato, 1999). The processed form of filaggrin has been shown not simply to function as a CE component but is also involved in bundling intermediate keratin filaments (Dale *et al.*, 1978; Mack *et al.*, 1993).

1.2.4.6 S100 proteins and annexin 1

From this family of calcium regulated EF hand-containing proteins, S100A10 and S100A11 are found within the CE of normal human keratinocytes (Robinson *et al.*, 1997). However, potential cross-linking sites have been identified in the N-/C-terminals of several other S100 proteins (Robinson and Eckert, 1998; Ruse *et al.*, 2001). It has been observed that S100A11 translocates to the cell periphery following calcium stimulation, this process relies on a tubulin-dependent mechanism (Broome and Eckert, 2004).

S100A11 has been demonstrated to form heterotetramers with annexin 1 including two molecules of each component (Rety *et al.*, 2000). Almost all annexins display calcium channel activity *in vitro* (Chen *et al.*, 1993; Cohen *et al.*, 1995; Benz *et al.*, 1996; Burger *et al.*, 1996; Gerke and Moss, 2002) and although this activity is not evident under normal intracellular conditions, it may be possible under the oxidising conditions and more acidic pH observed in epidermal regions, thereby contributing to calcium flux (Gerke and Moss, 2002).

1.2.4.7 Desmoplakin, envoplakin, perplakin and type II keratins

Keratins are the most abundant proteins within the corneocyte, with the assembled intermediate filaments connecting to the cell periphery within desmosomal regions (Green and Gaudry, 2000). Since the CE scaffold is formed on the cytoplasmic surface of the plasma membrane, it is perhaps not surprising that desmosomal components (such as desmoplakin, envoplakin and periplakin) and keratin bundles become incorporated (Steinert and Marekov, 1995; 1997). A Lys residue within the N-terminus of type II keratins has been found to be crucial in the cross-linking of this protein by TGs (Candi *et al.*, 1998). Envoplakin and perplakin have been identified as sites of CBL linkage, although not to the extent of involucrin (Marekov and Steinert, 1998).

1.2. 5 The epidermal differentiation complex

Genes encoding envelope precursors are often mapped to a 2.5 Mbp cluster located at locus 1q21 (Volz *et al.*, 1993; Mischke *et al.*, 1996), this region has been termed the epidermal differentiation complex. Such precursors include annexin 1, profilaggrin, involucrin, loricrin, SPR and S100 proteins. Many of these proteins share sequence similarities including Gln and Lys-rich tracts often targeted by TG enzymes. It is believed that these genes share a common ancestor and the cluster arose through repeated duplications (Backendorf and Hohl, 1992; Krieg *et al.*, 1997).

1.2.6 Putative mechanism for cornified envelope formation

Slowly a more complete picture is emerging concerning the sequence of events involved in CE formation (Candi *et al.*, 1995; Nemes and Steinert, 1999; Steinert, 2000). It is proposed that an involucrin-enriched scaffold is constructed against the background of membrane-associated proteins (Eckert *et al.*, 1993; Steinert, 1995; Steinert and Marekov, 1997). Nemes *et al.* (1999b) have reported that involucrin spontaneously binds the membrane in a Ca^{2+}-dependent manner. This initial structure produces deposition sites for other envelope precursors. Involucrin becomes cross-linked to envoplakin and periplakin (LaCelle *et al.*, 1998; Marekov and Steinert, 1998) succeeded by the incorporation of SPRs. This amalgen spreads across the cytoplasmic face of the plasma membrane, consequently incorporating desmosomal proteins (Steinert and Marekov, 1995; 1997). Maturation of the scaffold primarily involves the incorporation of loricrin, which accounts for the majority of the protein content (Hohl *et al.*, 1991; Mehrel *et al.*, 1990; Steinert and Marekov, 1995) (summarised in Fig. 12). This proportion increases towards the cytoplasmic face of the envelope, indicating its importance in the later stages of the process (Steinert and Marekov, 1995).

Findings have revealed that TG3 predominantly catalyses intra-molecular cross-links, in contrast with the ability of TG1 to form multimers (Candi *et al.*, 1995). It is possible that the modifications made by TG3 promote loricrin's incorporation by TG1. Alternatively, TG1 cross-links this precursor into the macromolecular structure where it undergoes further modifications by TG3 (Reichert *et al.*, 1993; Eckert *et al.*,

1993; Steinert, 1995). Estimates have been made concerning the comparative involvement of the TG isoforms and it has been calculated that approximately 65 % of loricrin cross-links are the result of TG3 activity whilst only 35 % are due to TG1 (Candi *et al.*, 1995).

Despite the coordinated sequence of events suggested for CE generation, it is evident this system is resilient and flexible. In fact altering the expression of known precursors does not produce an overt phenotype or one that is quickly compensated for (Yoneda and Steinert, 1993; Dijan *et al.*, 2000; Koch *et al.*, 2000). In the case of loricrin ablation in mice the dry and scaly appearance of neonatal skin is lost within a matter of days, however, retention of fragile envelopes is reported. This has lead to the "precursor availability" hypothesis, suggesting the existence of compensatory mechanisms. In fact fibroblasts have demonstrated an ability to form pseudo envelopes following the disregulation of Ca^{2+} (Simon and Green, 1984; Nicholas *et al.*, 2003). But these CE-like structures appear to be disordered and non-specific, not producing any of the discrete bands following proteolysis and peptide resolution, observed with normal CE analysis (Simon and Green, 1984).

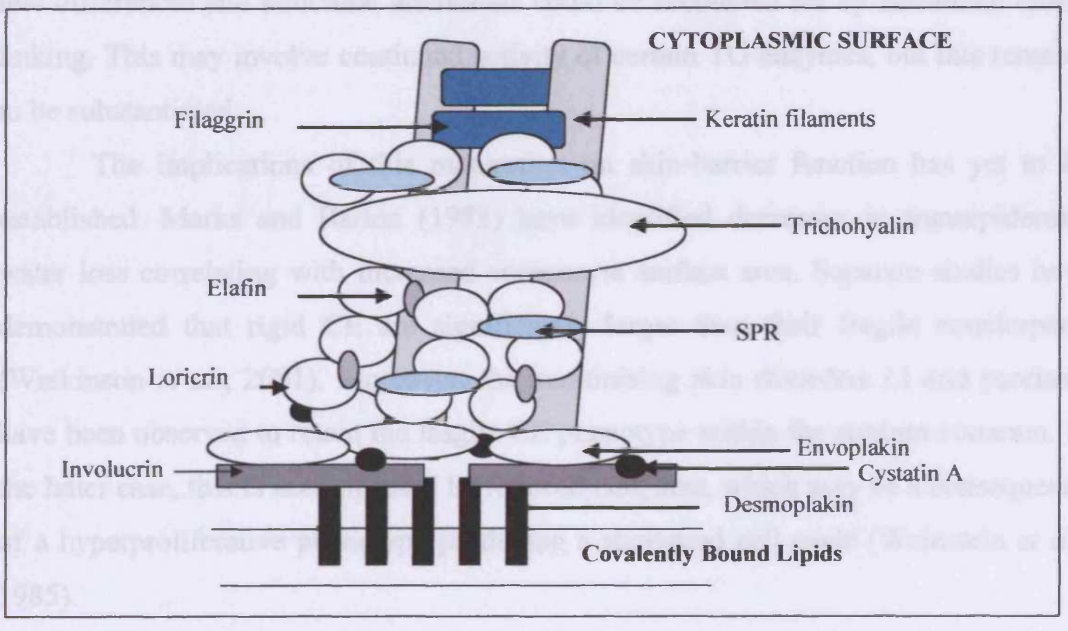

Fig. 12 Schematic diagram demonstrating the heterogenous nature of the cornified envelop: Based on the suggested mechanism for an initial involcrin and cystatin-rich scaffold being laid down on the backdrop of plasma membrane-associated proteins. Precursors continue to be incorporated in a coordinated fashion, with increasing amounts of loricrin. Adapted from (Steinert and Marekov, 1995).

1.2.7 The existence of a mature form of cornified envelope and its possible impact on skin barrier formation

Analysis of CEs, following their isolation from stratum corneum tissue, has revealed two morphologically distinct populations (Fig. 13). The first being irregularly shaped (termed "fragile") whilst the second is larger and polygonal (termed "rigid") (Michel *et al.*, 1988). In normal skin the fragile envelopes are found almost exclusively in the lower layers of the stratum corneum, whereas greater proportions of the rigid envelopes are recovered in the more superficial layers. This distinct spatial distribution would seem to indicate different stages of maturation (Michel *et al.*, 1988). This hypothesis is supported by immunohistochemical studies carried out with antibodies elicited against the C-terminal sequence of loricrin. Staining obtained with these antibodies revealed uniform staining in the stratum granulosum and deeper layers of the stratum corneum, which diminishes in the surface layers (Hohl *et al.*, 1991). This could indicate epitope masking following cross-linking. The amino acid components of the two envelope forms demonstrate few differences and structural alterations could be accounted for by additional cross-linking. This may involve continued activity of certain TG enzymes, but this remains to be substantiated.

The implications of this maturation on skin-barrier function has yet to be established. Marks and Barton (1983) have identified decreases in transepidermal water loss correlating with increased corneocyte surface area. Separate studies have demonstrated that rigid CE are significantly larger than their fragile counterparts (Watkinson *et al.*, 2001). Moreover, the keratinising skin disorders LI and psoriasis have been observed to retain the fragile CE phenotype within the stratum corneum. In the latter case, this is accompanied by reduced cell, size, which may be a consequence of a hyperproliferative phenotype producing a shortened cell cycle (Weinstein *et al.*, 1985).

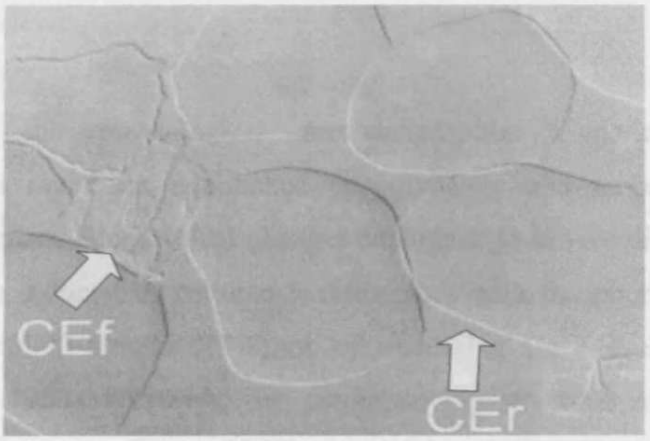

Fig. 13 Normaski phase contrast microscopy of cornified envelopes demonstrating two morphologically distinct phenotypes: Cornified envelopes were isolated by boiling in SDS/β-mercaptoethanol and revealed a combination of irregularly shaped structures with a ruffled appearance (CEf), and putatively more mature polygonal envelopes (CEr) (Watkinson *et al.*, 2001).

1.2.8 Triggers for keratinocyte differentiation and the regulation of transglutaminase genes

To date, the physiological mechanism for triggering keratinocyte differentiation has not been established unequivocally and probably involves a combination of signals. Biochemical changes analogous to *in vivo* differentiation can at least in part be induced in cultured keratinocytes with the phorbol ester, 12-*O*-tetradecanoylphorbol-13-acetate (TPA) or by increasing Ca^{2+} levels in the media (Hennings *et al.*, 1980). However, the accompanying structural changes are only observed in the latter case (Dotto, 2000). A calcium gradient is reported to exist *in vivo*, with a significant increase observed between the mid and upper granular layers (Menon *et al.*, 1992; Forslind *et al.*, 1997). Its impact on the intracellular environment could occur in a number of ways or in combination. Calcium sensitive receptors may be present in the keratinocyte plasma membrane, analogous to those found in parathyroid cells (Herbet and Brown, 1995; Bikie *et al.*, 1996), or possibly raised calcium levels could effect cell-cell and cell-matrix interactions thereby promoting stratification of keratinocytes (Dotto, 2000). It has been proposed that differentiation pathways converge to induce p21 expression, resulting in cell cycle arrest (Dotto, 2000).

TG1, 3 and 5 have each demonstrated differentiation-specific expression, however further analysis has revealed distinct control mechanisms for each isoform. TG1 transcript is negatively regulated by retinoids but upregulated by Ca^{2+} and by TPA (Zhang *et al.*, 1995; Lichti and Yuspa, 1998; Candi *et al.*, 2001). The mRNA encoding the TG3 zymogen is also upregulated by Ca^{2+} but in culture appears to downregulated by TPA and to a lesser extent by retinoic acid (RA) (Candi *et al.*, 2001). TG5 expression undergoes a transient increase when stimulated with Ca^{2+} and TPA, returning to baseline levels within three days (Candi *et al.*, 2001). Treatment with RA does not produce significant changes in TG5 mRNA levels. In contrast TG2, an isoform restricted to undifferentiated basal keratinocytes, is downregulated by Ca^{2+} and TPA but induced by RA (Lichti and Yuspa, 1998).

A number of studies have been carried out on the TGM1 and TGM3 promoter regions. One such study isolated a section of the TGM1 promoter incorporating the 2.5 Kb sequence upstream of the initiation site. This sequence was coupled to a reporter gene in transgenic mice and was found to confer tissue and terminal

differentiation specific expression (Yamada *et al.*, 1997). Within this sequence two Sp1 consensus elements have been identified (Yamada *et al.*, 1997). Later studies have further localised the key distal promoter region to between –1.6 and –1.1 Kb upstream of the transcription start site (Phillips *et al.*, 2004). The two Sp1 elements were found to reside in this region in addition to an identified AP1 consensus sequence, significantly these were largely conserved across four mammalian species. AP1 and Sp1 binding sites are commonly found in keratinocyte-specific genes, with keratinocytes containing unusually high levels of both factors (Saffer *et al.*, 1991; Phillips *et al.*, 2004). It has also been postulated that Sp1 is essential for TPA-responsive gene activation (Yamada *et al.*, 1997). Deletion analysis of the TGM1 promoter region revealed that mutations in all three consensus sequences eliminated nearly all transcriptional activity, contrasting with the relatively small effects observed with single mutations (Phillips *et al.*, 2004). This, in conjunction with mobility shift assay data, led to the proposal that cooperation between these transcription factors and others yet to be identified is necessary for specific expression (Phillips *et al.*, 2004).

Sp1 promoter elements have also been described in the TGM3 gene. The 3.0 Kb sequence 5' upstream of the initiation site contains adjacent Sp1 and ets-like recognition motifs (Lee *et al.*, 1996). It has been proposed that cooperative interactions occur between these consensus sequences for TG3 expression (Lee *et al.*, 1996). Previous studies have reported that ets transcription factors normally function as components of large transcription complexes (Vasylyk *et al.*, 1993) and it has been postulated that they may function in regulating late differentiation genes in the epidermis (Lee *et al.*, 1996). However, the 3.0 Kb section of the promoter sequence produced high-level gene expression in cultured squamous epithelial cells and would seem to require distal regions for differentiation-specificity (Lee *et al.*, 1996).

To date there have been no articles published concerning the TGM5 promoter sequence and studies analysing up to –1.6 kb 5' upstream region of TGM2 did not demonstrate high level expression or retinoic acid inducibility (Lu *et al.*, 1995).

1.2.9 Misregulation of transglutaminases in skin disorders

1.2.9.1 Lamellar Ichthyosis

As has been mentioned previously in this chapter, mutations associating with LI have been identified in the TGM1 gene (Huber *et al.*, 1995; Parmentier *et al.*, 1995; Russell *et al.*, 1995). The term ichthyosis is used to describe a heterogeneous group of diseases and TGM1 is not exclusively involved, mutations have also been mapped to a number of other loci (Bale *et al.*, 1996; Parmentier *et al.*, 1996). LI describes a congenital autosomal condition, effecting the cornification of the epidermis and hair. The clinical phenotype can range from large plate-like scales that are brown in colour, to fine white scales with underlying reddening (erythroderma). The skin appears taut and babies are often born surrounding in a collodion-like membrane (Williams and Elias, 1985) (Fig. 14a), which has been reported to comprise of thickened stratum corneum tissue (Frenck and Mevorah, 1977). The histopathology involves hyperkeratosis accompanied by thickening of the outer skin layers (Traupe *et al.*, 1984; Williams and Elias, 1985; 1993; Williams, 1992).

1.2.9.2 Murine TG1$^{-/-}$ model

An interesting distinction between the different forms of LI is that only individuals carrying a TGM1 mutation demonstrate an absence of the CE structure in their stratum corneum (Jeon *et al.*, 1998). As a consequence of these findings transgenic TG1$^{-/-}$ mice were generated and although they were born at a Mendelian frequency, neonatal death ensued within 5 hours of birth (Matsuki *et al.*, 1998). This lethality has been attributed to dehydration resulting from compromised skin barrier formation. It is evident from these findings that the loss of TG1 activity cannot be compensated for by other isoforms, with analysis of TG2 and TG3, revealing levels comparable to the wild-type control. The skin of these mice is shiny and taught similar to that observed with the human condition, although it is accompanied by retarded skeletal growth which has yet to be accounted for (Matsuki *et al.*, 1998) (Fig. 14b). Due to the lethal nature of this knockout model, studies at later developmental time points have required skin grafting onto athymic nude mice (Inada *et al.*, 2000). Histological analysis of these grafts revealed upregulation of K6α, a marker of a hyperproliferative phenotype. This was accompanied by thickening of the stratum corneum and the virtual absence of CE structures (Matsuki *et al.*, 1998). Wound models utilising these grafts have demonstrated slower healing than grafts obtained from normal neonates, supporting a role for TG1 in re-epithelialisation (Inada *et al.*, 2000).

1.2.9.3 Psoriasis

Psoriasis is a chronic skin disorder, which develops in genetically predisposed individuals (Capon *et al.*, 2000). This condition is characterised by hyperproliferation and altered keratinocyte differentiation, accompanied by cell mediated immunity and inflammation (Barker, 1991). The histopathological features of this psoriasis include skin thickening with the retention of cell nuclei in the stratum corneum and the proliferation of upper dermal layers into the epidermis. This misregulation of differentiation is evident from the detection of K14 in all cell layers including the stratum corneum and the corresponding down-regulation of TG3 has been reported (Candi *et al.*, 2001). Lesions are characterised by a scaly appearance accompanied by erythroderma (Fig. 14c)

1.2.9.4 Dermatitus Herpetiformis

Evidence also exists for TG3 serving as an auto-antigen in gluten sensitivity linked skin disease. Gluten sensitivity typically presents as a chronic small intestine disorder, termed celiac disease (Reif and Lerner, 2004) where TG2 has been identified as the predominant epitope. In certain individuals this gluten sensitivity is associated with a skin disorder termed dermatitis herpetiformis (DH). This condition is characterised by immunoglobulin A (IgA) deposits in the papillary dermis and blistering at the dermo-epidermal junction as a consequence of inflammatory-response (Fig. 14d). Often this is accompanied with mild or complete absence of intestinal disfunction (Fry, 1995). Antibodies isolated from DH patients demonstrate a high avidity for TG3 and this enzyme has been localised to the IgA deposits (Sardy *et al.*, 2002) possibly these complexes are deposited from the circulatory system. Evidence suggests the original IgA autoantigen response is initiated by TG2-gluten complexes, however the reasons for the subsequent epitope spreading and mild enteropathy remain to be elucidated.

As yet TG5 has not been directly implicated in any skin disorders, although it has been upregulated as a secondary effect in a number of conditions and may contribute to the hyperkeratotic phenotype observed with some icthyosis conditions (Candi *et al.*, 2002).

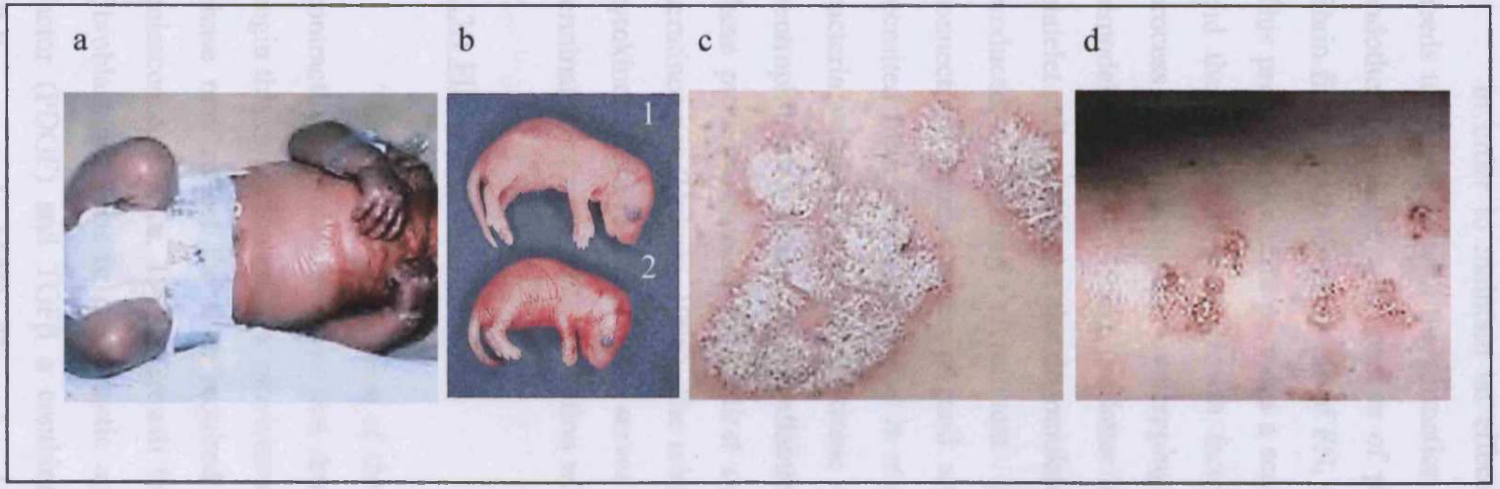

Fig. 14 Skin disorders and transgenic models highlighting a role for TG enzymes in skin homeostasis: (a) Mutations in TGM1 lead to the development of LI. A photograph of a collodion baby is included here. (b) Gross morphology of TG1-/- neonatal mice. TG-/- neonates (b2) were smaller than the control group (b1), with taut skin demonstrating coarse wrinkles (Matsuki *et al.*, 1998). (c) A skin lesion of a psoriasis patient is shown. This disorder is accompanied by misregulation of TG3. (d) Photograph of blisters symptomatic of the autoimmune disease, dermatitis herpetiformis. TG3 has been identified as the primary epitope in this condition. (http://www.emedicine.com)

1.3 Wound healing

In order to maintain an effective barrier, the initial response to wounding needs to be rapid, with the formation of a temporary clot. This clot is initiated by endothelial damage and consists of platelets embedded in a mesh of cross-linked fibrin fibres, with lower levels of FN, vitronectin and thrombospondin (Clark, 1996). This provisional matrix provides a scaffold for cells migrating into the wound space and the sequestering of growth factors. Cutaneous wound healing is a complex process consisting of three overlapping phases termed inflammation, proliferation and remodelling (Clark, 1996), the latter may continue years after the wound event. As platelet cells within the clot degranulate a reservoir of cytokines and growth factors is produced, triggering recruitment of inflammatory cells, re-epithelialisation, connective tissue contraction and angiogenesis. Neutrophils and monocytes are recruited from circulating blood in response to 1) platelet-derived growth factors 2) bacteria within the wound 3) tissue debris (Clark, 1996). Studies have identified neutrophils as a source of pro-inflammatory cytokines and it has been proposed that these provide some of the earliest signals to activate surrounding fibroblasts and keratinocytes (Hubner, 1996). The release of macrophage-derived growth factors and cytokines, from recruited cells, serves to amplify these earlier signals following the termination of neutrophil infiltration within a few days of wounding.

1.3.1 Fibroplasia

The subsequent invasion of the clot by fibroblasts and capillaries produces a contractile granulation tissue that draws the wound margins together. Fibroblasts begin this migration into the provisional matrix 3-4 days following wounding, this lag phase may reflect the time required for these mesenchymal cells to emerge for quiescence (Martin, 1997). Growth factors within the wound site may function as fibroblast mitogens or chemotactic agents, in the cases of platelet-derived growth factor (PDGF) and TGFβ a combination of these functions have been reported (Eriksson *et al.*, 1992). These invading fibroblasts begin to generate new ECM, although this lacks the organised basket-weave meshwork of collagen observed in normal tissue, instead, forming dense parallel bundles classified as scar tissue.

1.3.2 Re-epithelialisation

Keratinocyte migration initiates several hours post-wounding, this lag phase is most likely a consequence of necessary integrin receptor and cytoskeleton remodelling (Grinnell, 1992). The keratinocytes involved in cutaneous re-epithelialisation, do not migrate over the surface of the provisional clot but transect a portion of the clot matrix adjacent to the wound (Gibbins, 1968; Odland and Ross, 1968; Croft *et al.*, 1970). A number of proteases, which may be necessary for this process have been isolated from keratinocyte culture media, including neutral proteases, collagenases and plasminogen activator (Donoff *et al.*, 1971; Woodley *et al.*, 1985; Morioka *et al.*, 1987). These migrating keratinocytes form actin-rich protrusions termed lamellipodia and filopodia, at the cells leading edge. This is succeeded by the disassembly of focal complexes beneath the moving keratinocyte body or their being removed from the substrata as the rear edge of the cell rolls upwards. In contrast focal complexes within flanking regions are not immediately recycled, instead they fuse at the rear of the cell, producing large focal adhesion-like structures (Anderson and Cross, 2000). This is essential in providing lateral tension, required for traction and cell mobility (Lee *et al.*, 1994; Anderson *et al.*, 1996). Keratinocytes residing at the wound-edge are found to be involved in re-epithelialising the denuded surface and a proliferative burst has been observed behind these margin regions, thought to provide a replacement pool of cells (Garlick and Taichman, 1992). If hair follicle remnants are left within the wound these epithelially derived structures are found to contribute heavily in re-epithelialisation (Martin, 1997).

What is yet to be established is which populations of keratinocytes migrate into the denuded space. *In vitro* studies have reported that keratinocytes expressing the differentiation marker involcrin demonstrate a reduced rate of migration (Obedencio *et al.*, 1999). However suprabasal cells at the leading edge have been reported to exhibit an atypical integrin expression normally associated with proliferating basal cells (Hertle *et al.*, 1992). Retrovirus labelling studies have lead to a hypothesised "leapfrogging" of suprabasal cells over basal keratinocytes (Garlick and Taichman, 1992) with keratinocytes becoming immobilised on contact with the wound bed (Winter, 1972).

The epidermal growth factor (EGF) family comprises of a group of growth factors with known promoting effects on keratinocyte migration and hence re-epithelialisation. This family includes EGF itself, transforming growth factor α (TGFα) and more recently heparin bonding epidermal growth factor (HB-EGF), each acting via the EGF receptor. All three of these factors are found in abundance at sites of injury (Clark, 1996; McCarthy *et al.*, 1996; Martin, 1997) and it has been reported that exogenous application of EGF or TGFα in wound models increased the rate of re-epithelialisation (Brown *et al.*, 1986; 1989; Schultz *et al.*, 1987). It is evident that these EGFs are capable of stimulating keratinocyte proliferation in addition to migration (Barrandon and Green 1987). These mechanisms may be due in part to the ability of EGF to activate a small GTPase Rac, which mediates lamellipodial extension and the assembly of focal adhesion complexes (Ridley *et al.*, 1992; 1995). However, separate studies have indicated that keratinocyte migration is at least partly mediated by solid components. It was demonstrated that EGF stimulates the production of FN in keratinocytes and a significant portion of the stimulated motility could be inhibited with FN targeting antibodies (Nicklolff *et al.*, 1988). This was also found to be true of TGFβ, another inducer of keratinocyte motility. FN is not the only solid factor to demonstrate an effect on keratinocyte migration and another component of the provisional clot, thrombospondin, had a similar impact. The upregulation of this protein is also observed with EGF but not TGFβ. Conversely, it was found that the basal lamellae component laminin 5 inhibited keratinocyte migration (Donaldson and Mahan 1984; Nickloff *et al.*, 1988).

1.3.3 Epithelial-mesenchymal interactions

Numerous coculture studies have highlighted the importance of epithelial-mesenchymal interactions for epidermal homeostasis and repair. This includes the identification of cross-talk between the dermal and epidermal compartments necessary for keratinocytes growth and differentiation (Mass-Szabowski *et al.*, 2001). This signalling pathway is initiated by epithelial interleukin-1 (IL-1), which subsequently stimulates the release of granulocyte macrophage-colony stimulating factor (GM-CSF) and keratinocyte growth factor (KGF). Keratinocyte migration models, assessing cell out-growth on collagen gels, found that the extent of migration observed with fibroblast-populated gels could not be recreated following lysing of the mesenchymal cells. However, it was possible to enhance cell migration by a coculture system with fibroblasts contained within Millicell inserts (Tuan *et al.*, 1994). This suggests that mesenchymal cells can activate keratinocyte outgrowth via a soluble factor, although, the study went on to eliminate KGF after the exogenous addition of this factor and its antibody produced no effect (Tuan *et al.*, 1994). Similarly IL-6-deficient transgenic mice demonstrate mesenchymal requirements for keratinocyte migration. It was found that these mice displayed significant delays in cutaneous wound healing, therefore isolated keratinocytes and fibroblasts were cultured for further study (Gallucci *et al.*, 2004). Exogenous IL-6 was found to have little effect on keratinocytes cultured in isolation, however keratinocyte-fibroblast cocultures or conditioned media of IL-6 treated fibroblasts, produced up to a 5-fold increase in migration. Corresponding arrays of known migratory factors did not suggest a likely candidate and the factor involved is yet be identified.

1.3.4 Identified roles of transglutaminases in wound healing

The following information is summarised in Fig. 15.

1.3.4.1 FXIII

It has been demonstrated that epithelial wound healing requires the concerted action of several TG enzymes. FXIII has an established role in the initial clot formation with reports of impaired clot stabilisation accompanied by delayed bleeding arrest in murine knockout models (Lauer *et al.*, 2002; Koseki-Kuno *et al.*, 2003). This isoform has also been implicated in matrix re-organisation of granular tissue following wounding (Cohen *et al.*, 1982; Knox *et al.*, 1986; Mosher *et al.*, 1991; Corbett *et al.*, 1997). In addition to this, FXIII catalyses the sequestering of certain fibrinolysis inhibitors, including plasminogen activator inhibitor-2 and α-antiplasmin (Ritchie *et al.*, 2000). This activity would be expected to further increase the stability of the preliminary clot.

1.3.4.2 TG1

Increased TG1 levels have been observed in the epidermal edges of wounds in murine models (Inada *et al.*, 2000). These raised levels are evident within hours of wounding and continue until re-epithelialisation is complete (Inada *et al.*, 2000). Increased levels of TG1 were also detected in migrating keratinocytes and were reported to colocalise with involcrin (Inada *et al.*, 2000). This has led to speculation that a premature cornified envelope is formed, possible providing mechanical strength to the migrating cells dissecting the clot or protecting against damage from various proteases necessary for dissection. As discussed in Section 1.2.9.2, studies involving skin grafts from $TG1^{-/-}$ mice confirm this enzymes importance in wound healing, with a marked delay in regeneration over an eleven-day period.

1.3.4.3 TG2

TG2, a truly multifunctional enzyme, appears to be involved in a number of key stages of wound healing. Its apparent function in cell adhesion, spreading and migration has been discussed in some detail in Section 1.1.6.2. Models of wound healing, employing punch biopsies in rats, were established in an attempt to elucidate the distribution of TG2 during this process (Haroon *et al.*, 1999). This group have reported an upregulation of TG2, maintained up to nine days postwounding and accompanied by an increase in isopeptide linkages (Haroon *et al.*, 1999). This extended increase in TG2 levels would suggest a role for this enzyme throughout the wound repair process. TG2 mRNA and protein were detected in migrating epithelial cells, sites of neovascularisation and granulation tissue within one day of the wound event (Haroon *et al.*, 1999). Epithelial expression proved to be transient and was observed to return to baseline levels following re-epithelialisation. In contrast TG2 levels remained raised within the DEJ region (Haroon *et al.*, 1999), where clinical studies have implicated this isoform in catalysing the attachment of the epidermis (Raghunath, 1996). TG2 expression was maintained in endothelial cells, macrophages and muscle cells throughout the nine days. To summarise, these results suggest possible TG2 functions in neovascularisation, the stabilisation and remodelling of the provisional clot matrix, re-epithelialisation and the migration of cells into the clot. This investigation supports a number of other studies, which have reported TG2 1) to be upregulated following wounding in rats (Bowness *et al.*, 1988) 2) to bind the ECM after mechanical wounding of fibroblast monolayers (Upchurch *et al.*, 1991) 3) to increase the breaking strength of wound tissue (Dolynchuk *et al.*, 1994) 4) to function in matrix repair and remodelling (Griffin *et al.*, 2002; Stephens *et al.*, 2004; Zang *et al.*, 2004).

The involvement of TG2 in an integrin-independent pathway of cell adhesion has been identified in recent years (Verderio *et al.*, 2003) and has a proposed function in wound healing (Verderio *et al.*, 2005). It was reported that extracellular TG2-FN complexes restored lost cell adhesion following the inhibition of integrin coreceptors with exogenous Arg-Gly-Asp peptides (Verderio *et al.*, 2003). Further investigation by this group revealed transamidating activity of TG2 was not required for this function and the TG2-FN complexes associated with cell surface heparan sulfate (HS). This pathway would be capable of ensuring cell adhesion following damage to

the ECM. Under such conditions, ECM fragments are capable of inhibiting the integrin-dependent pathway (Verderio *et al.*, 2003).

TG2 is also reported to be expressed at sites of inflammation (Greenberg *et al.*, 1991) and significantly, this TG isoform is upregulated by a number of acute phase cytokines. This includes IL-6 (Ikura *et al.*, 1994), TGFβ (Vollberg *et al.*, 1992; Ritter and Davies, 1998) and Tumour neucrosis factor α (TNFα) (Kuncio *et al.*, 1998). As mentioned previously in Section 1.1.6.2, this TG isoform is also capable of modulating the activity of TGFβ.

1.3.4.4 Role of TG2 in tissue fibrosis

Further evidence for the role of TG2 in normal wound healing is the pathological effect of its misregulation. The term fibrosis describes a condition arising from acute tissue repair transmuting to chronic healing. Abundant TG2 cross-linking has been reported in numerous fibrotic diseases including; renal interstitial fibrosis, liver cirrhosis, parasitic liver fibrosis and pulmonary fibrosis (Mirza *et al.*, 1997; Johnson *et al.*, 1997; Kunico *et al.*, 1998; Hattasch *et al.*, 1996). In fact, the TG2 inducer, TGFβ is among the inflammatory mediators linked to this disease (Ziyadeh *et al.*, 2000). The extent to which the impact of TG2 is reliant on its cross-linking activity increasing the ECM's resilience to breakdown, or its activation of TGFβ and the subsequent stimulation of matrix synthesis has yet to be established.

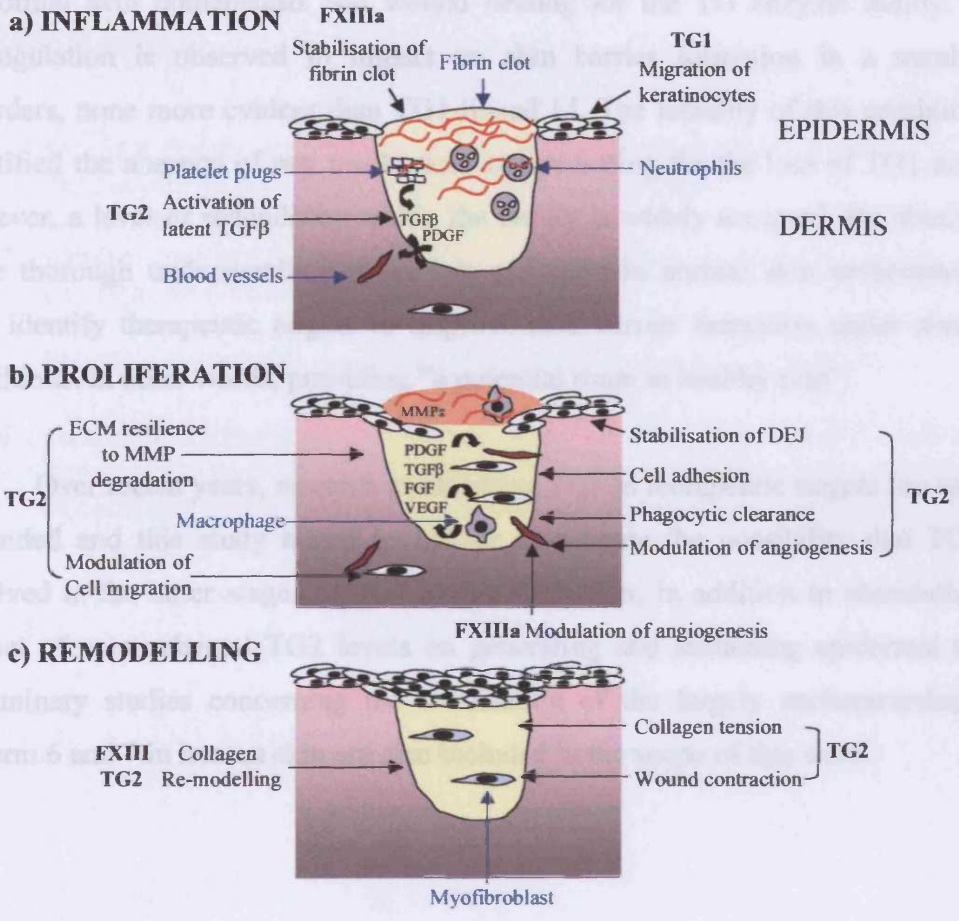

Fig. 15 Shematic representation of the three stages of wound healing in relation to the actions of transglutaminases: (a) Following the initial wound event, a blood clot comprising of cross-linked fibrin is rapidly formed. This is followed by invasion of neutrophils succeeded by monocytes and lymphocytes, thereby triggering the inflammatory phase of wound repair. Various cytokines and growth factors secreted by these cells, aggregated platelets and later macrophages (PDGF, TGFβ, FGF, VEGF) mediate the transition to tissue repair. (b) During re-epithelialisation, keratinocytes undergo extensive alterations, including the dissolution of desmosomes and hemidesmosomal links. This permits cell movement into the wound space, between the collagenase dermis and provisional fibrin matrix. Re-epithelialisation is accompanied by proliferative bursts and migration of dermal fibroblasts from adjacent tissue into the wounded area. These fibroblasts then participate, substituting the temporary matrix with collagenous tissue. MMPs play a key role in matrix remodelling, creating paths for cell migration through their proteolytic activity. Neovascularization occurs to provide oxygen and nutrients required to sustain the proliferation of keratinocytes and fibroblasts and the formation of new tissue. (c) During the transition from granulation to scar tissue, a relatively acellular matrix is generated in which many cells and blood cells are removed by programmed cell death. The multipoint actions of various TG isoforms are indicated. Adapted from (Verderio *et al.*, 2005).

Together the body of work reviewed here establishes wide reaching functions in normal skin homeostasis and wound healing for the TG enzyme family. Their misregulation is observed to impact on skin barrier formation in a number of disorders, none more evident than TG1-linked LI. The lethality of this condition has identified the absence of any mechanism compensating for the loss of TG1 activity, however, a level of redundancy within the family is widely accepted. By obtaining a more thorough understanding of the key pathways in normal skin homeostasis we may identify therapeutic targets to improve skin barrier formation under abnormal conditions. In other words, providing "a potential route to healthy skin".

Over recent years, research establishing TGs as therapeutic targets has steadily expanded and this study aimed to further investigate the possibility that TGs are involved in the latter stages of skin barrier formation, in addition to elucidating the impact of mesenchymal TG2 levels on generating and sustaining epidermal tissue. Preliminary studies concerning the localisation of the largely uncharacterised TG isoform 6 and 7 in human skin are also included in the scope of this work.

1.4 Aims of study:

1. Confirm the expression of the relatively uncharacterised enzymes TG6 and TG7 in skin tissue following generation of antibodies.

2. Identify possible substrates of TG6 and TG7 from keratinocyte and fibroblast cell lines derived from human skin.

3. Identify possible TG candidates involved in corneocyte maturation.

4. Further investigate the involvement of epithelial-mesenchymal interactions in keratinocyte growth, differentiation and migration through the development of coculture models. Alterations in TG2 levels were specifically considered.

Chapter 2:

Materials and Methods

2.1 Gel analysis

2.1.1 Agarose Gel Electrophoresis

Deoxyribonucleic acid (DNA) samples were loaded in 6 x sample buffer [0.05 % w/v bromophenol blue, 6 % v/v glycerol, 12 mM Ethylenediaminetetraacetic acid (EDTA), pH 8]. Fragments were separated through 1-1.2 % agarose (Invitrogen) in 1 x Tris/acetate/ Ethylenediaminetetraacetic acid (TAE) buffer [40 mM Tris acetate, 2 mM Na_2EDTA, pH 8.5] supplemented with 0.1 μg/ml ethidium bromide (Sigma). Electrophoresis was carried out at a constant voltage (100 v) before the DNA was visualised by exposure to an Ultra Violet (UV) light source.

2.1.2 Western Blotting

2.1.2.1 Ethanol Precipitation of protein

Protein solutions were precipitated in 9 volumes of ethanol (24 h, -20°C). Following pelleting (16000 x g, 30 min, 4°C), proteins were resuspended in 8 M urea before analysis by sodium dodecyl sulfate polyacrylamide gel electrophoresis (SDS PAGE) or Western blotting.

2.1.2.2 Sodium dodecyl sulfate Polyacrylamide Gel Electrophoresis

To normalise sample loading, protein concentrations were established by bicinchoninic acid (BCA) protein assay (Pierce Chemical Co.) according to the manufacturer's protocols. A bovine serum albumin (BSA) dilution series was included as a standard.

Each protein sample (2-7.5µl) was mixed with an equal volume of 2 x loading buffer [25 mM Tris, 39 mM EDTA, 4 % w/v SDS, 30 % v/v glycerol, 0.3 % w/v bromophenol blue, 2 % 2- mercaptoethanol] and boiled for 5 min prior to loading onto a pre-cast 4-20% Tris-Glycine gel, 1.5 mm x 15 well (Novex). Both reservoirs contained 25 mM Tris HCl (pH 8.3), 192 mM glycine, 0.1 % w/v SDS. Proteins were resolved over a period of 2 h at a constant voltage (125 V). When appropriate the protein loading was assessed by 0.1 % Coomassie Brilliant Blue R-250 (ICN) in a mixture of 7 % acetic acid and 50 % methanol. Destaining was carried out sequentially in solution I [10 % acetic acid, 25 % isopropanol], solution II [10 % acetic acid, 10 % isopropanol] and solution III [7 % acetic acid].

2.1.2.3 Protein transfer

Protein was electrophoretically transferred to a Protran® nitrocellulose membrane (Schleicher & Schuell) under a current of 125 mA for 2 h in the presence of transfer buffer [25mM Tris, 192 mM glycine, 20% methanol v/v]. Protein transfer was assessed using ponceau S staining [5% acetic acid v/v, 0.1% w/v ponceau S]. Non-specific protein binding sites were blocked by an overnight incubation (4 °C) with 5 % w/v non-fat dry milk powder (Marvel) in Tris Buffered Saline (TBS) [20 mM Tris base, 137 mM NaCl, pH 7].

2.1.2.4 Immunoblotting

All antibodies used to probe Western blots were diluted in TBS with 5 % milk powder (summarised in Table. 1). All secondary antibodies used were horse radish peroxidase (HRP) conjugated. Unless specified otherwise incubations with primary and secondary antibodies were carried out at room temperature (RT) under agitation for 1 h. Each incubation step was followed by three 5 min washes with TBS containing 0.05 % v/v Tween-20 (Sigma). Protein levels were detected by chemi-luminescence produced following 1 min incubation with ECL plus Western blotting detection reagent (Amersham Pharmacia) before exposing to either a Kodak Biomax or a Hyperfilm™ ECL™ film (Amersham Pharmacia) for up to 10 min.

Primary Antibody	Raised In	Dilution/Concentration	Source
TG1	Goat	1:50	Dr P. Steinert (Laboratory of Skin Biology, Niams)
TG2 (CUB7402)	Mouse	1:200-1:1000	Neomarkers
TG3	Rabbit	1:100	Dr N. Smyth (University of Cologne, Germany)
TG4 (TGase 4/84-96)	Rabbit	1:2000	CovalAb
TG5	Rabbit	1:500	GIL
TG6S	Goat	5 µg/ml	GIL
TG6L	Goat	5 µg/ml	GIL
TG7	Goat	5 µg/ml	GIL
Pan Cytokeratins (C 2931)	Mouse	1:2000	Sigma
Actin (A 2066)	Rabbit	1:100	Sigma
Vimentin (V 2258)	Rabbit	1:100	Sigma
Secondary Antibody		Dilution/Concentration	Source
Anti-Goat HRP conjugated (Z 0228)	Rabbit	1:1000	DAKO
Anti-Mouse HRP conjugated (P 0260)	Rabbit	1:1000	DAKO
Anti-Rabbit HRP conjugated (P 0399)	Mouse	1:1000	DAKO

Table. 1 Summary of antibodies utilised in Western blot studies: Monoclonal antibodies are shown in blue. Antibodies generated in our laboratory are designated GIL.

2.1.2.5 Membrane stripping

In order to remove antibodies from membranes for re-probing, the nitrocellulose was incubated in stripping buffer [1 M Tris HCl, 10 % w/v SDS, 0.07 % 2-mercaptoethanol] for 30 min at 50°C under gentle agitation. This was followed by 2 washes with TBS containing 0.05 % v/v Tween-20 and three sequential washes with unsupplemented TBS (5 min each).

2.2 Immunohistochemistry

2.2.1 Cryosections:

8 μm fresh frozen sections of normal human skin were a kind gift from Dr. M. Donavon (Unilever, Colworth).

Sections were air-dried overnight prior to fixing in acetone (10 min). This was followed by three 5 min washes with TBS.

2.2.2 Paraffin sections:

Sections were deparaffinised with 2 x 10 min incubations with xylene and rehydrated in an ethanol gradient (5 min in 90, 70, 60 and 40 % sequentially). Three 5 min washes in TBS ensured all traces of the solvent were removed. To ensure intracellular epitopes were accessible a 5 min incubation step with 0.1% Triton X-100 (Sigma) was included. When suggested in manufacturers protocols epitope retrieval was carried out by heating in a citrate buffer [10 mM citric acid (Sigma), pH 3] for 30 min at 37°C.

2.2.3 Detection of antibody-protein complexes

When employing the 3-amin-9-ethyl-carbozide (AEC) development system, endogenous peroxidase was blocked by two 20 min incubations with 1 % H_2O_2 in methanol followed by three TBS washes. Non-specific binding was blocked overnight at 4°C with 5 % BSA (ICN) in TBS containing 10 % Fetal Bovine Serum (FBS)(Sigma).

All antibodies were diluted with 1 % w/v BSA/TBS (Table. 2) and precipitates removed by centrifugation at 10 000 x g. Sections were incubated with antibody solutions in a humidity chamber for 1 h at RT. Unbound antibodies were removed by three 5 min TBS washes. Secondary antibodies were either Fluorescein (FITC) conjugated or HRP conjugated. In the latter case sites of antibody deposition were

visualised by the addition of freshly prepared substrate containing hydrogen peroxide (H_2O_2) [100 mM NaCl, 10 mM citric acid, 100 mM imidazole, 0.2 % v/v H_2O_2, pH 7] and the chromogen AEC (2 mg/ml). Colour development of the resulting red-brown precipitate was allowed to continue for 10 min before transfer to TBS.

Pictures were taken using an Olympus AX70 camera linked to an Olympus PM-CJSDX microscope. Nikon ACT-1 software (version 2.20) was running on the connected computer.

Primary Antibody	Raised in	Dilution/Concentration	Source
TG2 (CUB7402)	Mouse	1:50	Neomarkers
TG3	Rabbit	1:50	Dr N. Smyth (University of Cologne, Germany)
TG6S	Goat	20 µg/ml	GIL
TG6L	Goat	20 µg/ml	GIL
TG7	Goat	20 µg/ml	GIL
Keratin 10 (CBL 196)	Mouse	1:20	Chemicon® International
Integrin β1 (M-106)	Rabbit	1:50	Santa Cruz Biotechnology, Inc.
Secondary Antibody		**Dilution/Concentration**	**Source**
Anti-Goat FITC conjugate (F 7367)	Rabbit	1:500	Sigma
Anti-Goat HRP conjugated (Z 0228)	Rabbit	1:1000	DAKO
Anti-Mouse HRP conjugated (P 0260)	Rabbit	1:1000	DAKO
Anti-Rabbit HRP conjugated (P 0399)	Mouse	1:1000	DAKO

Table. 2 Summary of antibodies utilised in immunohistochemical studies: Monoclonal antibodies are shown in blue. Antibodies generated in our laboratory are designated GIL.

2.3 Cell culture

2.3.1 Culture conditions

Materials; unless specified otherwise reagents were obtained from Life Technologies, abbreviations are in bold type.

Adenine (Sigma), Antibiotic-Antimycotic (10 000 U/ml penicillin (base), 10 000 μg/ml streptomycin and 25 μg/ml amphotericin B), Cholera Toxin (Sigma), Dulbecco's MEM high glucose **DMEM** 1 x and 10 x (Sigma), dispase II (Boehringer Mannheim), human Epidermal Growth Factor **EGF** (Sigma), Fetal Bovine Serum **FBS**, Geneticin, Hydrocotisone (Sigma), N-2-hydroxyethylpiperazine-N'-2-ethane sulphonic acid monosodium salt **HEPES** (Promega), Insulin (Sigma), Keratinocyte Serum Free Medium **Keratinocyte SFM**, Mitomycin C (Sigma), Penicillin-Streptomycin-Glutamine 100x **PSG** (10 000 U/ml penicillin, 10 000 μg/ml streptomycin (base) and 29.2 mg/ml L-glutamine), 1 x Trypsin/EDTA (0.25% trypsin, 1mM EDTA.4Na).

Cells were cultured at 37°C with 5 % CO_2/95 % air unless otherwise specified. Cells used in experimental set ups were mycoplasma negative and grown to passage 2-7.

2.3.1.1 Mycplasma testing

Cells were sparsely seeded (2 x 10^5) onto glass cover slips within a 24 well plate. Following overnight culture the cells were fixed with two successive methanol washes (500μl each). Hoechst 33258 stain (Sigma) was applied (at a final concentration of 0.05 μg/μl) for a period of 15 min at 37°C. Following extensive washing with dH_2O, fluorescence staining was visualised through a blue filter. This analysis was carried out using a Carl Zeiss Axiocam camera linked to an Axiovert 200M Zeiss microscope.

2.3.1.2 Fibroblast cells

Murine 3T3, untransfected HCA2 and human primary dermal fibroblasts were cultured in DMEM supplemented with 10 % FBS and 1 % v/v PSG.

Primary cells were a kind gift from Dr. Stuart Jones (University of Wales, Cardiff). Cells were derived from normal dermal tissue and had undergone 5 population doublings.

Generating feeder layers:

To generate feeder layers for keratinocyte cultures, murine 3T3 fibroblasts were grown to 70 % confluence. Cells were then washed with PBS and incubated for 6 h with 16.75 μg/ml Mitomycin C in DMEM media in order to arrest the cell cycle in G_0 phase. Following extensive washing with PBS the cells were trypsinised and reseeded at 7.5 x 10^5 cells/T75 flask.

2.3.1.3 HCA2 fibroblast cell culture

Immortalised HCA2 human dermal fibroblasts (transfected with the reverse transcriptase gene hTERT) have been stably transfected with pcDNA3/human TG2 constructs (Bond *et* al. 1999; Stephens *et al.* 2004). Transfection with these constructs produced high-level constitutive expression of TG2 sense RNA, antisense RNA as well as a TG2 mutant RNA. In the latter case the catalytic Cysteine (Cys) residue was replaced by Serine (Ser), generating a cross-linking deficient form of the enzyme. A clone transfected with an empty vector was also produced as a control (mock-transfected).

Cultures were grown in DMEM supplemented with 10 % FBS, 1 % v/v PSG and 400 μg/ml Geneticin to ensure selection of transfected cells. These cells were included in skin equivalent models, Western blot analysis and keratinocyte migration assays.

2.3.1.4 Primary human keratinocyte culture

Normal human skin was obtained following face-lift surgery. The subcutaneous fat was removed and the remaining sample divided into ~5 mm^2 sections. These were incubated overnight at 4°C with a dispase-containing buffer [2 μg/ml dispase II in DMEM, 2mM Ca^{2+}, 20 mM HEPES buffer, 1 % v/v PSG and 5 μg/ml Geneticin] to cleave dermo-epidermal contacts. The epidermis was removed as a sheet and trypsinised (30 min, 37°C) to produce a cell suspension. Keratinocytes were collected by centrifugation (1000 x g, 5 min) and seeded onto feeder layers. Cells were cultured in DMEM, 2 mM Ca^{2+}, 10 % FBS, 400 μg/ml hydrocortisone, 10 μg/ml EGF, 5 mg/ml Insulin and 1 % v/v PSG.

2.3.1.5 Primary mouse keratinocyte culture

Primary mouse keratinocyte cultures were obtained from six C57/BL6 mice between 9 and 12 months. Keratinocytes were isolated from mouse ears by incubation in Keratinocyte SFM supplemented with 0.25% Trypsin/EDTA, 1% v/v Antibiotic-Antimycotic overnight at 4°C. The epidermis was removed as a sheet and desmosomes further digested in Trypsin /EDTA (15 min at 37°C). Basal cells were isolated using a 40 μm cell strainer (BD biosciences) and distributed across 3 x 10 cm dishes. Cells were cultured in Keratinocyte SFM supplemented with 10 ng/ml EGF, 10^{-10} M Cholera Toxin, 1 % v/v PSG before seeding onto dermal gels to form skin equivalents.

2.3.1.6 Ntert/Htert keratinocyte cell culture

The keratinocyte cell lines were derived from normal human keratinocytes transfected with hTERT and deficient in $p16^{INK4a}$ expression (Dickson *et al.*, 2000). Ntert and OKF6 were derived from keratinising (epidermal) and non-keratinising (oral epithelial) cells respectively.

For the purposes of seeding skin equivalents, Ntert cells were cultured on Mitomycin C treated murine 3T3 feeder layers. However, in the case of ribonucleic acid (RNA) extraction and methyl cellulose sphere formation the keratinocytes were cultured in isolation. In both instances the cells were grown in FAD media [65 % v/v DMEM, 22.5 % v/v Ham's F12, 10 % FBS, 400 ng/ml hydrocortisone, 10^{-10} M cholera toxin, 10 ng/ml EGF, 0.089 mM Adenine, 5 ng/ml Insulin and 1 % v/v Antibiotic-Antimycotic].

2.3.2 Metabolic labelling of cells

HCA2 labelling media; DMEM without (w/o) methionine (Met), cysteine (Cys), or glutamine (Glut) (ICN), 580 μg/ml L-Glut (Sigma), 10 % FBS, 1 % v/v PSG, 10 μci/ml ^{35}S Met/Cys Redivue™ Pro-mix™ (Amersham Pharmacia).

Ntert labelling media; DMEM w/o Meth, Cys or Glut, 580 μg/ml L-glutamine, 10 % FBS, adenine (Sigma), insulin (Sigma), 1 % v/v antibiotic/antimitotic, 10 μci/ml Met/Cys Redivue™ Pro-mix™.

HCA2 chase media; DMEM (Gibco), 1 % v/v PSG

Ntert chase media; DMEM, adenine, insulin, 1 % v/v antibiotic/antimitotic

On reaching 80 % confluency cells were incubated for 24 hour in the relevant labelling media, excess ^{35}S Met/Cys was removed prior to extraction by 24 hour chasing in serum free media.

2.3.3 Cell extraction of protein

2.3.3.1 Transglutaminase :

Cells were cultured in 10 cm dishes. Once cells reached 80 % confluency, proteins were extracted in 1 ml of 0.25 M sucrose supplemented with 1 % Triton X-100 (soluble fraction). In order to inhibit protease activity extractions were carried out on ice. Particulate material was cleared by centrifugation (16, 000 x g, 10 min at 4°C) and the resulting pellet homogenised in 20 mM Tris-HCl, pH 8.0, containing 1 % SDS, 100 mM NaCl, 1 mM EDTA, 1 mM dithiothretol (DTT) and 1 mM phenylmethyl sulphonylfluoride (PMSF) (particulate fraction).

2.3.3.2 Signalling molecules:

Cell cultures were extracted in ice cold lysis buffer [20 mM HEPES, 150 mM NaCl, 1 % v/v Triton X-100, 1 % w/v Na deoxycholate, 0.1 % SDS, 10 % glycerol, 1.5 mM MgCl, 1 mM Ethyl glycol-bis(2-aminoethylether)-N,N,N',N'-tetraacetic acid (EGTA), 1 mM Na_3VO_4, 10 mM Na pyrophosphate, 100 mM NaF, 10 μg/ml leupeptin, 100 U aprotinin, 1 mM PMSF, pH 7.4]. The particulate fraction was removed by centrifugation (16, 000 x g for 10 min at 4°C). These cell extracts were utilised in immunoprecipitation experiments and β-barrel binding studies (Section 2.6).

2.3.4 Cell extraction of total RNA

Total RNA was extracted from Ntert keratinocyte and HCA2 fibroblast cultures using TRIzol (Invitrogen). A total of four 10cm dishes of each cell type were lysed and following the addition of 10 % v/v chloroform, RNA was isolated in the aqueous layer using an Eppendorf Phase Lock Gel™ (12000 x g, 30s). RNA within the aqueous fraction was precipitated in an equal volume of isopropanol and following washing with 75 % ethanol, the pellet was resuspended by heating in 500 μl nuclease free water (65°C). Extracts were stored at –80°C.

2.4 Production of a recombinant human transglutaminase 7 protein

2.4.1 Generation of the expression construct

Competent INVαF' and BL21 cells were obtained from Life Technologies.

Luria broth (LB broth); 1 % w/v tryptone, 0.5 % w/v yeast extract and 90 mM NaCl.

Restriction enzymes were obtained from Promega or Biolabs and digests carried out according to recommended protocols.

2.4.1.1 TA Cloning of transglutaminase 7 domains into a PCRII vector

Two hTG7 polymerase chain reaction (PCR) products amplified from cDNA stocks were a kind gift from Mrs. P. Aeschlimann. The first being amplified from the N-terminus of the enzyme using the primers Forward 20 (5' CGACAGGAGAAGGAGGAGATGG 3') and Reverse 15 (5' CAGCGGAACGACGTGGTGTATG 3'). This incorporated the base pairs 2–669 with an additional 14 bp sequence at the 5' end (5' CGACAGGAGAAGGA 3') and was termed the N-fragment. The second PCR product spanned the C-terminal β-barrel domains (1069-2229 bp) including the loop connecting the catalytic domain. This product was termed the C-fragment. This fragment was amplified using the primers Forward 18 (5' AC GGG TGG CAG GTT CTG GAC 3') and Reverse 1 (5' GGC TAT GTC GTC TTG GCT CCA CCT CTG TCC T 3'). The PCR reaction [1x salt buffer, 2 mM $MgCl_2$, 0.2 mM dNTP, 0.5 μM each primer, 0.125 U AmpliTaq gold] was carried out for 35 cycles under the following conditions; 30 s at 94°C, 45 s 60 °C, 45 s 72 °C with the first cycle containing an extended denaturation period (7 min) and the last cycle containing an extended elongation period (7 min).

The N-fragment PCR product was isolated by gel electrophoresis through 1 % agarose (Invitrogen) and extracted using the QIAQUICK^R Gel Extraction Kit (Qiagen). The product was eluted in 50 µl distilled water (dH_2O), heated to 50°C to maximise the yield. In the case of the C-fragment the crude PCR mixture was included in subsequent cloning experiments. Utilising the 3' A-overhang introduced by the Taq polymerase the fragments were TA cloned into a PCRII vector (Invitrogen) and transformed into INVαF' *E.coli* cells. Colonies were allowed to grow overnight (37°C) on agar plates supplemented with kanamycin (100 µg/ml) and coated with 40 µl of 40 mg/ml X-Gal. To confirm successful ligation five "white" bacterial clones, demonstrating an interruption in the vectors β galatosidase encoding gene, were grown overnight at 37°C in 3 ml LB medium supplemented with 50 µg/ml kanamycin (Sigma). The plasmids were isolated using the Wizard^R Plus SV Minipreps DNA Purification System (Promega) following the manufacturers instructions. To optimise plasmid recovery the elution step was carried out with 50 µl distilled water heated to 50°C. Confirmation of successful ligation and insert orientations was carried out by restriction digest analysis (1 h at 37°C). In the case of the N-fragment construct this included digestion with EcoRI and BamHI. The C-fragment construct was analysed by digestion with EcoRI, PstI and SacI (conditions summarised in Table. 3). To identify any mutations introduced to the insert, two clones from each transformation were sequenced using the dRhodamine Terminator Cycle Sequencing Kit (Applied Biosystems) and an ABI 310 automated sequencer (primers summarised in Table. 4). Sequencing with the vector primers T7 and M13 were sufficient to confirm the sequence of the N-fragment. Additional sequencing reactions were required in the case of the C-fragment and TG7 specific primers were included to this purpose (Forward1, 9 and 11) (summarised in Table. 4).

Enzyme	Concentration [U/µl]	Buffer	pH
BamHI	10	6mM Tris-HCl, 6mM $MgCl_2$, 50mM NaCl	7.5
EcoRI	50	90mM Tris-HCl, 10mM $MgCl_2$, 50mM NaCl	7.5
PstI	10	90mM Tris-HCl, 10mM $MgCl_2$, 50mM NaCl	7.5
SacI	10	10mM Tris-HCl, 7mM $MgCl_2$, 50mM KCl	7.5
ScaI	10	6mM Tris-HCl, 6mM $MgCl_2$, 150mM NaCl	7.9
XmnI	5	6mM Tris-HCl, 6mM $MgCl_2$, 50mM NaCl	7.5
EcoRI/BamHI	50/10	6mM Tris-HCl, 6mM $MgCl_2$, 50mM NaCl	7.5
EcoRI/EcoRV	50/10	6mM Tris-HCl, 6mM $MgCl_2$, 150mM NaCl	7.9

Table. 3 A summary of restriction enzymes utilised in this study; including optimised conditions. All restriction digests were carried out for 1 h at 37°C in the presence of BSA (1 µg/µl).

Primer	Target	Sequence (5'→3')
T7	PCRII Vector	ccctatagtgagtcgtatta
M13	PCR II Vector	caggaaacagctatgac
Forward 1	C-fragment	tgggcaaggcgctgagagtccatg
Forward 9	C-fragment	cttagggatcagccagcgcagc
Forward 11	C-fragment	ccagcgccagagcatcaccagc
Reverse 7	C-fragment	ctgcgtatccagagggtgccaga

Table. 4 A summary of sequencing primers.

2.4.1.2 Subcloning of transglutaminase 7 fragments into a pGEX-2T vector

pGEX-2T was selected as a suitable expression vector for recombinant TG7. This vector introduced an N-terminal Glutathione S-transferase (GST) tag with an initiation codon under the direction of an Isopropyl β D-thiogalactoside (IPTG) inducible lac promoter. To generate a fragment that would be expressed in frame an EcoRI digest of the PCRII/N-fragment construct was sufficient, whilst PCRII/C-fragment underwent double digestion with BamHI/EcoRI (Table. 3). In each case the PGEX-2T vector was digested with the same enzymes, which were subsequently inactivated by heating to 65°C for 15 min. In order to prevent religation this step was followed by treatment with 1 U calf intestinal alkaline phosphatase (CIAP) (Biolabs) in the NEB buffer 3 provided (37°C for 30 min). Fragments were gel purified and ligated at an insert:vector ratio of 2:1 estimated following resolution through agarose gel and ethidium bromide detection. To ensure the optimal expression of these fusion proteins, constructs were transformed into the protease deficient BL21 strain of *E.coli*. In-frame ligation of the insert was confirmed by sequencing with the Thermo Sequenase™ Cy™ 5/ Cy 5.5 Dye Terminator sequencing kit (Forward1 and Reverse7, see Table. 4). Reactions were carried out with the Cy 5.5 label only. The resulting sequence was read using an Open Gene System Long Tower reader (Visible Genetics Inc.).

2.4.1.3 Ligation of restriction digests into plasmid vectors

Ligations were carried out overnight at 14.2°C, catalysed by 3 U/μl T4 DNA ligase (Promega).

2.4.2 Expression of recombinant transglutaminase β-barrel domains from transformed *E.coli*

2.4.2.1 Preparation of competent BL21 cells

BL21 *E.coli* were cultured in LB broth (40 ml) until an $OD_{650\ nm}$ of ~0.35 was reached (measured using a DU® 800 spectrophotometer, Beckman Coulter), when the cells were transferred to ice for the remaining steps. Following a 30 min incubation, the *E.coli* were collected by centrifugation (1600 x g for 8 min at 4°C) and the pellet washed with 10 ml sterile $MgCl_2$. Finally the cells were incubated in a 2 ml solution of 100 mM $CaCl_2$ over 16 h. Cells were frozen in 200 µl aliquots in a 25 % glycerol solution and utilised in subsequent heat shock transformations.

2.4.2.2 Transformation of E.coli cells by heat shock method

Competent cells (INVαF or BL21) were incubated with 2-5 µl of ligation mix in the presence of 20 mM β-mercaptoethanol (Invitrogen) for 30 min at 4°C. The cells then underwent rapid heat shock at 42°C (30 s) before recovering cell integrity by culturing for 1 hour at 37°C, 225 rpm with the SOC media provided (Invitrogen). To ensure distinct growth of colonies, a series of volumes from the transformation was plated onto agar plates supplemented with kanamycin (100 µg/ml) for PCRII constructs and ampicillin (50 µg/ml) with pGEX-2T vectors. Transformed *E.coli* were allowed to grow overnight at 37°C and a number of colonies selected for further analysis by restriction digests or sequencing.

2.4.2.3 Sequencing by 2',3'-dideoxy nucleotide termination

ABI Prism® dRhodamine terminator cycle sequencing kit (Applied Biosystems)

250 ng of sample plasmid underwent 25 amplification cycles in the presence of 200 nM forward and reverse primers in 4 µl of the sequencing reaction mix provided (total reaction volume of 10 µl). Each cycle contained a 20 s denaturing step (90°C), a 10 s annealing step (50°) and a 4 min extension step (60°). Reaction products were

purified from excess label by precipitation in 50 µl of 95 % ethanol containing 80 µM sodium acetate, pH 5 (20 min, RT). Precipitated DNA fragments were collected by centrifugation (16 000 x g, 20 min). Following washing with 250 µl of 70 % ethanol the pellet was dried (90°C, 5 min). Finally DNA fragments were resuspended in the template suppression reagent provided (95°C, 2 min) before transferring to ice.

Samples were analysed using an ABI Prism 310 Genetic Analyser.

Thermo Sequence™ Cy™5/Cy 5.5 dye-terminator sequencing kit (Amersham Pharmacia)

Four sequencing reactions with Cy 5.5 labelled ddATP, ddCTP, ddGTP and ddTTP were carried out separately. 500 ng of the DNA plasmid underwent 30 amplification cycles in 12 mM Tris HCl (pH 9.5) containing 3 mM $MgCl_2$, 110 µM deoxy nucleotide (NTP) mix, 2.5 µM of the relevant dideoxy nucleotide (ddNTP), 2 nM of the forward and reverse primer and 0.3 U/µl Thermo Sequence DNA polymerase (final volume of 8 µl). Each cycle contained a 30 s denaturing step (95°C), a 30 s annealing step (60°C) and a 1 min 30 s extension step (72°C). Reaction products were precipitated in chilled 95 % ethanol (30 µl) facilitated by 8 µM ammonium acetate and 10 mg/ml glycogen. Precipitates were pelleted by centrifugation (12 000 x g, 4°C, 30 min) and washed with 200 µl 70 % ethanol. Finally the pellet was resuspended by vortexing in 6 µl formamide and heated to 72°C for 2 min before quenching on ice.

Generated fragments were resolved through 6 % polyacrylamide gel for a period of 4h at constant voltage (1300 V). Buffer chambers were filled with Tris-Borate-EDTA (TBE) buffer [90 mM Tris-Borate, 2mM EDTA, pH 8]. The gel temperature was maintained between 30-50°C. Samples were analysed using an Open Gene System Long Tower reader. A laser power of 50 % was employed with sampling carried out every 0.5 s.

2.4.2.4 Optimising extraction of transglutaminase 7 fusion protein from E. coli

2YA media; 1.6% w/v NZ amine, 1 % w/v Yeast extract, 90 mM NaCl

Osmotic Lysis buffer; 20 mM Tris HCl pH 8, 25 mM EDTA, 5 mM Diothiothretal (DTT), 1 mM N-ethyl malemide (NEM), 1 mM PMSF, 0.1 % Na Deoxycholate

Elution buffer; 100 mM Tris HCl pH8, 20 mM glutathione, 0-0.5 M NaCl, 5 mM DTT, 0.1 % Na deoxycholate

To generate the GST tagged TG7 fusion protein, transformed BL21 cells were cultured in 2YA media until an OD_{600nm} of 0.5 was reached. Expression was induced by the addition of 0.1-10 mM IPTG (Sigma) and allowed to continue up to 24 h under agitation between 20-37°C (discussed in relevant Sections). Cells were pelleted (3000 x g, 30 min at 4°C) and resuspended in Osmotic Lysis buffer (10 ml/L culture). The digestion of the cell wall was facilitated by the addition of 1.5mg/ml lysozyme (Sigma) for 5 min at RT. This was followed by the removal of genomic DNA with 10 µg/ml DnaseI (Amersham Pharmacia) and 15 mM $MgCl_2$ for 15 min at 37°C. Cell lysate was isolated by centrifugation (10000 x g, 10 min at 4°C) in 25 % sucrose (Fisher). For analysis by SDS PAGE or Western blotting the pellet fraction was resuspended in 8M urea (Fisher).

2.4.3 Purification of transglutaminase 7 fusion protein

2.4.3.1 Glutathione affinity purification – batch method

Unpacked Glutathione Sepharose 4B was prepared by washing with Osmotic Lysis buffer and collected by centrifugation (500 x g, 5 min). BL21 lysate supplemented with 25 mM DTT was incubated with Sepharose (5 ml/700 µl matrix) under agitation at RT for 30 min. Unbound proteins were removed by three washing steps with Osmotic Lysis buffer (5 min) before eluting with 500 µl elution buffer (30 min, 37°C whilst rocking). The elution process was repeated up to three times and the aliquots pooled.

2.4.3.2 Glutathione affinity purification – pre packed column

5 ml BL21 soluble extract was loaded onto a 1 ml pre-packed glutathione linked Sepharose column (Amersham Pharmacia) coupled to an AKTA Prime (Amersham Pharmacia). The flow rate was maintained at 0.5 ml/min. Loading buffer was exchanged for elution buffer and following 10 column volume (cv) washes an NaCl gradient was introduced over a further 10 cv (0-500 mM). The eluant was collected in 0.5 ml fractions and those corresponding with the $OD_{280\ nm}$ protein peak were pooled and stored at - 20°C.

2.4.3.3 Attempt to purify GST tagged TG7 beta barrels by ion Exchange Chromatography

For cation exchange chromatography a Mono S column (Pharmacia Biotech) was selected. To ensure the TG7 fusion protein carried a positive charge the protein solution was loaded in 50 mM Sodium acetate pH 5.5 (PI estimated to 7.6, using DNAsis software). Following buffer exchange by dialysis, 5 ml bacterial supernatant was loaded onto the selected ion exchange column coupled to an Akta purifier 10 (Amersham Pharmacia) running Unicorn V4.00.16 software. The flow rate was established at 0.5 ml/min in order to optimise protein binding. Any proteins remaining

bound following 5 cv washes with the loading buffer were eluted in a salt gradient (0-1 M NaCl).

Fractions forming protein peaks were pooled and analysed by SDS PAGE and Western blotting.

2.5 Generation of peptide antibodies against transglutaminase 6 and 7

2.5.1 Peptide design

Suitable sequences for peptide design were identified using ProtScale software (discussed in Section 3.2.3.1). Further analysis by comparative modelling utilised CLUSTALW or 3Djigsaw allowed confirmation of surface accessibility and 3D models were produced using Rasmol software (v 2.6).

Available murine and human sequence data, obtained from the National Center for Biotechnology Information (NCBI) database, were employed in the design of three peptides (work carried out by Dr. K. Becks) referred to as **P6L**, **P6S** and **P7**. These peptide sequences are derived from unspliced TG6, spliced TG6 and TG7 respectively. In the case of the spliced form of TG6 (lacking exon XII) the protein sequence is terminated prematurely to produce a truncated form of the enzyme. However this variant contains a unique sequence at its C-terminus distinguishing it from the unspliced form. Peptides were synthesised at Sigma Genosys, purified by High Performance Liquid Chromatography (HPLC) and identified by mass spectrometry:

P6L CGWRDDLLEPVTKPS

P6S TIRAYPGASGEGLSP

P7 ESGGLRDQPAQLQL

2.5.2 Coupling of peptides to keyhole limpet hemocyanin

Keyhole limpet (KHL) hemocyanin (Sigma) was selected as a suitable carrier protein due to its invertebrate-specific expression. This would limit antibody populations, which may cross-react with human samples.

Conditions for coupling peptide haptens to KHL hemocyanin via amine or thiol linkages were established using mondansyl cadaverine, MDC (Sigma) and coumarin as a control (Pierce) respectively.

2.5.2.1 Primary amine linkage (P6S and P7)

Reaction buffer; dH_2O

KHL hemocyanin was reconstituted to 5 mg/ml and dialysed into dH_2O to remove traces of contaminants. Subsequently, the pH was adjusted to 7.5 by the addition of dilute HCl. 5 mg of KHL hemocyanin or BSA (dialysed against distilled water) was activated by the serial addition of 16 μmol N-hydroxysulfosuccinimide (sulfo-NHS) and 1-ethyl-3-(3-dimethylaminopropyl)-carbiimide (EDC). The resulting reaction with carboxylate groups generated active esters. This mixture was allowed to stand at RT for 5 min before the addition of P6S, P7 or MDC control (12 mg/ml in dH_2O or 3 mg/ml in 10 mM HCl respectively). The coupling reaction was allowed to continue overnight with the pH maintained at 7.5. Following this step, a buffer exchange of the reaction mix with Phosphate buffered saline (PBS) was carried out over a PD_{10} sephadex column (Amersham Pharmacia) removing low molecular weight contaminants from the reaction mixture.

2.5.2.2 Thiol linkage (P6L)

Reaction buffer; 20 mM HEPES, pH 7.4

Work carried out by Helen Thomas.

In the case of P6L, the thiol group of a cysteine residue was utilised in the coupling reaction since the inclusion of primary amines in the Arg side chain made amine linkage unfeasible. Briefly:
Reaction buffer containing 5 mg/ml KHL hemocyanin or BSA was used to bring 6.1 mg (N-[g-Maleimidobutyryloxy]sulfosuccinimide ester) (sulfo-GMBS, a heterobifunctional cross-linking reagent) into solution with stirring at 4°C for 45 min (final concentration of 16 μmol). Unconjugated contaminants were removed over a PD_{10} Sephadex column equilibrated with the reaction buffer and the eluant collected in 0.5 ml fractions. Those containing the activated protein were identified by OD_{280nm} readings and were pooled. P6L or 7-mercapto-4-methyl coumarin was added to these fractions producing a final concentration of 4 μmol. The pH of the solution was adjusted to 6.8 and coupling allowed to continue overnight at 4°C with stirring. The conjugate was separated from low molecular weight contaminants over a PD_{10} column equilibrated with PBS.

2.5.3 Generation of transglutaminase antibodies in goat

The final eluants for P6S, P6L and P7 conjugates were collected in a series of 0.5 ml fractions and OD_{358nm}/OD_{280nm} readings were taken. Those fractions corresponding to a protein peak were pooled and stored at –20°C.

Hemocyanin conjugates were sent to Micropharm and antibodies raised in goat. In week 1, primary immunisation was carried out with 1 mg of the conjugate (mixed with Freund's complete adjuvant) followed by three re-immunisations carried out in week 5, 9 and 13, using 0.5 mg aliquots (mixed with Fruend's incomplete adjuvant). Sera bleeds were collected at week 10 and 14 with a final double bleed at week 16.
BSA conjugates were stored for analysis of the antisera by Enzyme-linked immunosorbent assay (ELISA).

2.5.4 Analysis of peptide antibodies by ELISA

100 µl aliquots of BSA or hemocyanin conjugates for the three peptides (50 µg/ml in TBS, pH 7.4) were plated into a 96 well plate (Fisher), unconjugated BSA and hemocyanin were included as controls. These antigens were allowed to coat the wells overnight at 4°C before unbound proteins were removed by washing with 0.01 % TBS/Tween-20. Residual protein binding sites were blocked with a 2 h incubation with 1 % w/v BSA in TBS. Goat sera for each TG peptide obtained from the first bleed underwent serial dilution with blocking solution of 1/50 to 1/12800 and was incubated with the antigen coated wells for 1 h at RT. Each assay was carried out in duplicate. Further washing steps were followed by incubation with 1/10000 alkaline phosphatase-conjugated anti-goat antibody (DAKO) for 1 h. The chromogenic signal was developed for 10 min by the addition of 0.8 mg/ml 5-amino-2-hydroxy benzoic acid, (pH 6) and 0.0015 % H_2O_2. The reaction was terminated with 1 M NaOH and the extent of the reaction assessed by OD_{490nm} measurements taken by a Microplate Autoreader (BIO-TEK Instruments).

2.5.5 Production of peptide-linked Sepharose columns

2.5.5.1 Primary amine linkage (P6S and P7)

ECH Sepharose 4B (Amersham Pharmacia) was swollen in dH_2O to a final volume of 1 ml. This gel matrix was washed in several bed volumes of the same by repeated centrifugation and resuspension. Carboxylic groups were activated by the addition of 5.6 µmol EDC and sulfo-NHS (5 min, RT) freshly prepared in 1 ml dH_2O. Excess reagents were removed by washing with 1 volume dH_2O before the addition of P6S or P7 (14 µmol). Coupling was allowed to continue overnight at RT with the pH maintained at between 4.5-6.0 for the first hour, thereby promoting acid catalysed condensation. The gel matrix underwent five washing steps with dH_2O and remaining carboxylic groups were blocked by incubation with 0.1 M ethanolamine (1 h, RT). Three cycles of washing was carried out with solutions of high and low pH (0.1 M Tris HCl, pH 8.3 and 0.1 M sodium acetate, pH 4.2 respectively) to ensure residual ligand was removed. Finally the columns were equilibrated with TBS.

2.5.5.2 Thiol linkage (P6L)

0.4 g Thiol Sepharose 4B was rehydrated in dH_2O followed by extensive washing in the same. A final wash was carried out with 20 mM Tris HCl, pH 7.4, supplemented with 150 mM NaCl and 1 mM EDTA. All buffers underwent degassing to prevent oxidation and subsequent formation of disulphides between molecules in solution. P6L was added to a final concentration of 1 μM and coupling continued for 1 h at RT. The formation of disulphides between the matrix groups and ligand was accompanied by a 2-thiopyridone leaving group. This produced a corresponding OD_{343nm} absorbance peak. Finally the matrix was equilibrated with TBS following extensive washing.

Peptide linked Sepharose was transferred into 1 ml Glass Econo-Columns® (Biorad) by pouring in one continuous motion and allowed to settle under gravity. This produced bed volumes of between 0.3-1 ml.

2.5.6 Affinity chromatography of peptide antibodies from goat sera

All solutions were run onto affinity columns under gravity;

1 ml aliquots of goat sera (anti-TG6S, 6L and 7) obtained from the 3rd bleed sera were run onto the appropriate column at 4°C and incubated for a further 30 min. Unbound proteins were removed by 5 cv washes with TBS (with the addition of 0.05 % Tween-20 where specified). Antibodies remaining bound to the column were eluted in 2 cv 3 M potassium thiocyanate (KSCN) or by pH shift (TBS, pH 3). Eluants were immediately dialysed against TBS to prevent irreversible denaturation.
Later protocols included an overnight blocking step with 5 % BSA (4°C) to reduce non-specific binding.

2.6 Binding properties of transglutaminases

Buffer A; 50 mM HEPES pH 7.4, 150 mM NaCl, 1 % Triton X-100, 1 % Na deoxycholate, 0.1 % SDS, 10 % glycerol, 1.5 mM MgCl, 1 mM EGTA, 1 mM Na_3VO_4, 10 mM Na pyrophosphate, 100 mM NaF, 10 µg/ml leupeptin, 100 U aprotinin, 1 mM PMSF

Buffer B; Buffer A – 0.1 % SDS, - 1 % Na deoxycholate

Buffer C; 50 mM HEPES pH 7.4, 150 mM NaCl, 1 % Triton X-100, 10 % glycerol

Metabolically labelled HCA2 mock transfected fibroblasts and Ntert keratinocytes (see Section 2.3.2) were extracted in Buffer A (750 µl /10 cm plate) and further incubated with shaking at 4°C before cell debris were removed by centrifugation (16000 x g, 10min, 4°C).

Normalised protein loading was determined by counts per minute (cpm) measured in the presence of Optiphase 'Hisafe' 3 scintillant (PerkinElmer™) using a Packard TRI-CARB 2100TR liquid scintillation analyser. A volume of 10 µl labelled protein was precipitated in the presence of 50 % trichloroacetic acid (TCA) (1h, -20°C) the collected pellet (16000 x g, 10 min) was resuspended by boiling in a mixture of 2 % SDS/9 M urea followed by the addition of 4 ml scintillant. Counts were measured over a period of 1 min, the upper limit of the programme was set at 156 eV and the lower at 4 eV, background readings were taken from scintillant alone. Volumes demonstrating between 3.5 x 10^6 - 1.05 x 10^7 cpm were used in subsequent experiments. For cold repeats protein loading was calculated by BCA assay.

2.6.1 Immunoprecipitation

Ntert keratinocytes were allowed to grow to 80 % confluence on tissue culture grade plastic prior to extraction.

On reaching confluence HCA2 mock transfected fibroblasts were collected by incubation with trypsin, the action of this enzyme was terminated with the addition of 0.5 mg/ml Soy Bean (T) inhibitor (Sigma) before the cells were pelleted (1000 x g, 5 min). Half the cells were reseeded onto TEC-1™ type I collagen (Organogenesis Inc.) coated plates to adhere and spread for 1 h at 37°C. The remaining cells were incubated in suspension under the same conditions. These cells were then extracted in Buffer A (Section 2.6).

To reduce non-specific binding cell extracts were pre-incubated with Fast G Sepharose (Amersham Pharmacia) at a ratio of 50 µl Sepharose matrix/750 µl extract for 1 h at 4°C under agitation. Unbound proteins were collected (5000 x g, 15 sec) and incubated with 1 µg anti-TG2 CUB7042 (Neomarkers); the non-specific Ig, anti-Goat HRP conjugate (DAKO); anti-pan cytokeratin (Sigma) or one of the peptide antibodies produced by our laboratory (anti-TG6L and anti-TG7). Antibody complexes were allowed to form over night at 4°C, following which 50 µl fast G Sepharose was introduced to each mixture and incubated for a further 2 h. The matrix bound antibody complexes were isolated (5000 x g, 15 sec) and washed once with Buffer B followed by two washes with Buffer C (800 µl/wash). Precipitated proteins were retrieved by boiling in equal volumes of 2 x loading buffer (Section 2.1.2.2) or 8M urea.

2.6.2 Substrate binding of immobilised transglutaminase β-barrels

2YA media; NZ amine, Yeast extract, 90mM NaCl

Osmotic Lysis buffer; 20mM Tris HCl pH 8, 25mM EDTA, 5mM DTT, 1mM NEM, 1mM PMSF, 0.1% Na Deoxycholate

A number of transformed BL21 *E.coli* expressing N-terminal GST-tagged recombinant transglutaminases have been produced in our laboratory. In the case of TG5, 6L and 7 the DNA sequence encoding the C-terminal β-barrels has been ligated into the vector. However in the case of TG2 the full-length enzyme is expressed. To obtain the fusion proteins of interest transformed BL21 cells were cultured in 2YA media until an OD_{600nm} of 0.5 was reached. Expression of each recombinant protein was induced by the addition of 10 mM IPTG (Sigma) and allowed to continue overnight at 28°C under agitation. Cells were extracted in Osmotic Lysis buffer (described in Section 2.4.2.4) and protein concentrations were equalised following BCA assay.

Glutathione-linked Sepharose (Amersham Pharmacia) was used as a scaffold for binding the recombinant TG proteins, 500 μg BL21 extract TG2/5/6L/7 and uncoupled GST were incubated with 50 μl Sepahrose matrix for 1 h RT whilst rocking. TG2 was set up in duplicate, one batch being supplemented with 1mM GTP (Sigma). Unbound extract was removed by washing with Osmotic Lysis buffer followed by Buffer A.

Ntert keratinocytes and HCA2 mock-transfected fibroblasts were grown to confluence on tissue culture grade plastic before extraction in Buffer A (described in Section 2.6). In an effort to reduce background readings in radiolabelling experiments the cell extracts were incubated with Sepharose-linked GST for 1 h rocking at RT. The supernatant collected (5000 x g, 15 sec) was aliquoted across Sepharose linked to recombinant TGs and incubated for a further 1 h. However in later experiments this pre-incubation step was replaced by treating the GST linked matrix as another sample. Unbound proteins were removed by two washes with Buffer A before matrix-bound proteins were retrieved by boiling in equal volumes of 2 x loading buffer or 8M urea.

2.6.3 Detection of radioactive proteins by fluorography

Proteins were separated across a 4-20 % gradient Tris-glycine gel (Invitrogen). To ensure protein resolution, this process was extended from 2 h to 3 h. Three 1 h incubations were carried out with the resulting gel (RT) with, Coomassie Brilliant Blue R-250, followed by TBS and finally 1mM sodium salicylate, pH 5 (Chamberlain, J.P., 1979). The gels were dried for 2 h at 80°C using a Biorad Model 543 Gel Dryer. A Kodak Biomax film was exposed to the fluor signal for 1 week (-80°C) or when using the Typhoon 9400 variable mode imager system (Amersham) Pharmacia) the gel was exposed to phosphor screen for 48 h (Amersham Pharmacia).

2.6.4 Selection of transglutaminase fusion proteins by Sepharose-linked actin

2.6.4.1 Production of a β-actin-linked Sepharose column

Coupling buffer; 0.1 M $NaHCO_3$, 0.5 M NaOH, pH 8.3

0.3 g Cyanogen bromide (CNBr) activated Sepharose was swollen in 1 mM HCl for 15 min at RT, before washing in a further 200 ml of the same solution. 1 mg lyophilised actin from rabbit muscle (Sigma) was dissolved in 1 ml coupling buffer before mixing with 1 ml of the prepared Sepharose overnight at 4°C. The resulting coupling reaction proceeded via the primary amine groups available within the ligand. Excess ligand was removed with washing in the coupling buffer (5 x 5 ml) and any remaining active groups were blocked by incubation with 1 M ethanolamine, pH 8.0 for 2 h at RT. Finally the Sepharose matrix was washed with 3 cycles of alternating pH (5 ml 0.1 M acetate pH 4.0 followed by 0.1 M Tris HCl pH 8.0, each containing 0.5 M NaCl) and transferred to a glass Econo-Column®.

2.6.4.2 Affinity chromatography

Following equilibration with Osmotic Lysis buffer BL21 extracts containing 800 μg TG5, 6 or 7 fusion protein were run onto the column under gravity and incubated for 30 min at 4°C. Following 5 cv washes with the same buffer bound proteins were eluted in 1 cv 3M KSCN and analysed by Western blotting.

2.7 Quantifying epidermal Transglutaminase levels

2.7.1 Reverse transcription polymerase chain reaction

Reverse transcriptions were performed using the Superscript II System (Life Tecnologies). 1 μg total RNA was included in a reaction mix containing, 25 ng oligo dT primer (Invitrogen), 0.5 mM dNTPs, 10 mM DTT and 100 U RNase H⁻ Reverse Transcriptase in supplied buffer [250 mM Tris-HCl, 375 mM KCl, 15 mM $MgCl_2$, pH 8.3]. This reaction was allowed to continue at 42°C for 50 min before the enzyme was inactivated upon heating to 90°C. To ensure a maximum yield of mRNA, a second round of transcription was carried out following the addition of a further 100 U of Reverse Transcriptase. To verify TG expression in fibroblast and keratinocyte cell lines, 1 μl of the resulting cDNA was subjected to PCR with primers specific to TG6 (F6 5' GTGAAGGACTGTGCGTGATG 3', R6 5' CGGGAAGTGAGGGCTTACAAG 3') and TG7 (F7 5' CCTCATCAATGGGCAGATAGC 3', R7 5' CTTGACCTCGTTGCTGA 3') Amplification was carried out in a total reaction volume of 25 μl [1x Taqman buffer A, 2mM $MgCl_2$, 0.2 mM dNTP, 0.125 U Taq DNA polymerase (Promega) and 1 μM of each primer]. The conditions were as follows; 35 cycles of 45 s at 95 °C (denaturation), 1 min at 60 °C (annealing) and 1 min 30 s at 72°C (extension) with the first cycle containing an extra step to activate the polymerase enzyme (95°C for 2 min) and the final cycle containing an extended extension period (72°C for 7 min). Resulting DNA fragments were resolved in a 1.2 % agarose gel.

2.7.2 Quantitative PCR

Primers were synthesised at Invitrogen. Restriction enzyme, Taq DNA polymerase and salt buffer were obtained from Promega.

Taqman PCR core reagent kit was ordered from Applied Biosystems (Roche, New Jersey). Quantitative PCR (QPCR) probes were synthesised at Applied Biosciences, incorporating a 5' 6-carboxyfluorescein (FAM) reporter and 3' 6-carboxytetramethylrhodamine (TAMRA) quencher.

Total RNA extracts from human epidermal tissue were a kind gift from Dr. R. Ginger (Unilever, Colworth). Samples were equalised to include up to 50 ng total RNA, which was subjected to two-cycles of reverse transcription (Section 2.7.1) selecting molecules of messenger RNA (mRNA). The resulting cDNA was analysed in subsequent quantitative PCR (QPCR) assays.

QPCR conditions to assay TG1 and TG2 have been optimised in our laboratory (Table. 5). Reactions were carried out in multiwell plates with plasmid constructs containing the appropriate sequence as standards (50 pg-5 fg). Nuclease free water was included as a negative control for each assay, referred to as "no template controls" (NTCs) and Ribosomal Protein-S26 (RP-S26) was selected as an appropriate housekeeping gene. All assays were carried out in duplicate with a reaction volume of 25µl [1 x Taqman buffer A, 2 mM $MgCl_2$, 0.2 mM dNTP, 0.125 U AmpliTaq gold DNA polymerase]. Primer and probe sequences are summarised in Table. 5 with their optimal concentrations quoted. The conditions were as follows; 40 cycles of 15 s at 95°C (denaturation) and 1 min at 60°C (annealing/extension) with the first cycle containing an extra step to activate the polymerase enzyme (95°C for 10 min). Reactions were carried out in an ABI Prism™ 7000 sequence detection system (Applied Biosystems).

Gene product	Forward primer	Probe	Reverse primer	Concentration [nM] (F, P, R)
TG1	5'ACCGTGTGACCATGCCAGTG	5'TGCTCAATGTCTCAGGCCACGTCAAGG	5'GCTGCTCCCAGTAACGTGAGG	300,125,300
TG2	5'ATGAGAAATACCGTGACTGCCTTAC	5'AGCTACCTGCTGGCTGAGAGGGACCTC	5'CAGCTTGCGTTTCTGCTTGG	300,150,300
RP-S26	5'AGATGCAGCAGATCCGCAT	5'AGGCTGTGGTGCTGATGGGCAAGAAC	5'ATATGAGGCAGCAGTTTCTCCAG	300,100,300

Table. 5 Summary of qPCR assay conditions: Primer sequences for TG1, 2 and RP-S26 are shown with the optimal concentrations of the forward primer (F), probe (P) and reverse primer (R).

2.8 Identifying depth related changes in transglutaminase proteins through the stratum corneum

Tissue specimens were obtained with the approval of Colworth's Research Ethics committee and informed consent from company employees.

2.8.1 *Ex vivo* texas red labelled cadaverine incorporation assays

Labelling mixture; 50 mM Tris-HCl (pH 8), 150 mM NaCl, 9 μM texas red cadaverine in Dimethl sulfoxide (DMSO, Molecular probes) +/- 20 mM cystamine.

Human corneocyte samples were harvested from the inner volar forearm by adhesion to glass slides with cyanoacrylate and subsequent removal of the surface layers. Following incubation with 300 μl labelling mixture, incorporation of the texas red labelled TG substrate cadaverine was allowed to continue for 1 h at 37°C in a humidity chamber. Unbound sample was removed by two 5 min washes in 50 mM Tris-HCl supplemented with 1 % Triton X-100 followed by two 5 min washes in 5 mM DTT 1 % v/v SDS. Samples were then mounted in non-quenching medium (DAKO) and the extent of fluorescence labelling assessed by microscopy.

2.8.2 Generating depth profiles

Successive layers of skin corneocytes were removed within a marked area of the lower volar forearm using Sellotape strips. Previous studies at Unilever (Colworth) carried out by Dr. R. Ginger estimate Sellotape strips remove a single layer of skin with each strip. An area of the epidermis measuring 19 cm^2 was divided into four sectors (tape strips were 10 cm by 1.9 cm in size). Groups of four successive layers were pooled from the four sectors (1-4, 5-8, 9-12 and 13-16). Due to natural variations in stratum corneum depth between individuals, samples were sometimes limited to 12 successive layers. From this point samples were kept on ice.

Sellotape adhesive was dissolved in hexane and corneocytes collected by gravitation. A further 5 washes with 1 ml of solvent ensured removal of all traces of glue. Freezing and lyophilising the samples removed residual solvent. The dried corneocytes were incubated at 60°C for 1 hour in 150 μl extraction buffer [50 mM

Tris HCL (pH8) containing 9 M urea, 2 % w/v SDS, 2.0 mM EDTA, 1.0 mM PMSF, 1.0 mM NEM, 10 mM benzamidine HCL, 100mM 6-aminohexanoic acid]. Insoluble structures were pelleted by centrifugation at 14000 x g, 2 min. Supernatant containing 5 μg protein was subsequently used for Western blot analysis following normalisation by BCA assay. Sucrose/Triton X-100/2 % SDS buffer extracts containing TG2 and TG5 were obtained from HCA2 cells transfected with mRNA sense constructs and included as controls.

In order to identify which pools of solubility contained each TG isoform, a serial extraction was carried out on samples of corneocytes prepared as described above. Cytoplasmic proteins were isolated by a 1 h extraction in 100 mM Tris HCL (pH8) containing 1.0 mM PMSF and 10 mM EDTA carried out at 4°C under agitation. The process was repeated with the addition of 1 % Triton X-100 to the extraction buffer in order to target membrane associated proteins. Finally highly insoluble proteins were extracted by heating in the SDS/urea buffer used for preparation of depth profiles. Large variations in total protein extracts obtained by the three buffers prevented complete equalisation of protein loading, consequently 1.5 μg of Tris extract, 0.5 μg Tris/triton extract and 2 μg SDS/urea extract was included in Western blot analysis.

2.8.3 Investigating possible cross-reactivity of transglutaminase antibodies with keratin using 2D gel electrophoresis

2D gel electrophoresis was carried out using the Zoom® IPGRunner™ System (Invitrogen)

Rehydration Buffer;

8M urea, 2% 3-[(3-Cholamidopropyl)dimethylammonio]propanesulonate (CHAPS), 0.5% (v/v) Zoom® carrier ampholytes (pH 3-10), 0.002% bromophenol blue.

Corneocytes isolated from tape strip samples of human epidermis (described in Section 2.8.2) were extracted by heating to 30°C for 30 min in 100 μl rehydration buffer. This reduction in temperature was necessary to prevent protein carbamylation. Up to 9 μl supernatant was included in a total volume of 155 μl of the same buffer (total of 10 μg). This solution was used to rehydrate an immobilised gel Zoom® strip

with a pH gradient of 3-10 (non linear) or 4-7. This incubation step continued overnight at RT.

Isoelectric focusing (IEF) was carried out in a buffer comprising of a 2:1 ratio of ultra pure and dH_2O. The following step wise gradient was used with a minimal current (< 1 mA); 20 min at 200 V, 15 min at 450 V, 15 min at 750 V and 30 min at 2000 V. However, in an attempt to improve protein resolution the four steps were later extended by 10 min each.

Zoom® strips containing the resolved proteins then underwent preparation for SDS gel electrophoresis with 2 x 15 min step incubations with 5 ml 1 x NuPAGE® LDS sample buffer first supplemented with the reducing agent supplied and finally with 125 mM iodoacetamide alkylating solution. Each Zoom® strip was secured to a Novex® 4-20 % Tris-Glycine Zoom® gel using 0.5 % agarose dissolved in SDS running buffer [25 mM Tris HCl (pH 8.3), 192 mM glycine, 0.1 % w/v SDS] and heated to 60°C. SDS PAGE and Western blotting were carried out as described previously (Section 2.1.2), however the transformation period was shortened to 1.5 h, allowing for the reduced thickness of the pre-cast gels used.

2.9 Generation of *in vitro* skin equivalents

2.9.1 Isolation of type I collagen from rat tail tendons

Tendons from 10 rat-tails were excised and their proteins extracted in 300 ml 0.1 % v/v acetic acid (48 h at 4°C with stirring). The supernatant was isolated by centrifugation (16000 x g for 1h at 4°C) and the collagen component precipitated with a pH shift to 7. The precipitate was pelleted (8000 x g for 20 min at 4°C) and redissolved with 0.1 % acetic acid to produce a stock solution of 4 mg/ml.

2.9.2 Formation of dermal equivalents - Contraction method

Dermal equivalents were prepared with native type I collagen extracted from rat-tail tendons with 0.1 % acetic acid as described above.

2 x 10^6 HCA2 or murine 3T3 cells were suspended in a mixture of 3.5 mg/ml collagen in DMEM, 10 % FBS and 1 % v/v PSG. Aliquots (15 ml) of the fibroblast/collagen mix were allowed to fibrilise and contract in 5 cm non-adherent dishes (Bibby Sterilin). Pre-conditioning continued for one week under culture conditions. The resulting floating lattices were transferred to FAD media and seeded with 1 x 10^6 Ntert, OKF6 or primary keratinocytes. Skin equivalents were raised to the air/liquid interface after three days and cultured for up to four weeks (cocultures containing primary keratinocytes were incubated at 30°C).

2.9.3 Formation of dermal equivalents - Insert method

3 x 10^6 HCA2, murine 3T3 or primary fibroblast cells were suspended in a mixture containing 10 % v/v 10 x DMEM, 3 mg/ml bovine collagen in 10 mM acetic acid and 10 % FBS following neutralisation with 3-4 drops NaOH. 3 ml of this mixture was aliquoted into culture inserts within a BIOCOAT® 12 deep well plate (Becton Dickinson Labware) and allowed to fibrilise for 30 min at 37°C. The resulting dermal equivalents were submerged with 10 ml FAD media and conditioned for up to 1 week prior to seeding 2 x 10^6 keratinocytes. Cells were induced to differentiate by raising to the air/liquid interface 3 days post-seeding. Skin equivalents were cultured for up to 10 days before harvesting for immunohistochemical analysis.

2.9.4 Keratinocyte seeding

Skin equivalents were produced by seeding Ntert, OKF6 or primary keratinocytes onto dermal equivalents (established using the contraction or insert method). With the exception of primary mouse keratinocytes, cells were seeded below the air/liquid interface following selection of basal cells with a 40 μm cell strainer (BD Biosciences).

2.9.5 Harvesting skin equivalents

Skin equivalents were fixed in 4 % paraformaldehyde/PBS (4.5 h at 4°C). Samples were paraffin embedded and 10 μm sections used for immunohistochemical analysis or Hematoxalin/Eosin (H&E) staining.

2.10 Keratinocyte Migration

2.10.1 Generation of keratinocyte spheroids

100 % stock solution of methyl cellulose was produced by dissolving methyl cellulose (Sigma) in a mixture of DMEM:Ham's F12 (2:1) to a final concentration of 12 mg/ml. Precipitates were cleared by centrifugation (5000 x g, 1.5 h).

Confluent monolayers of Ntert were trypsinised and pelleted (1000 x g, 5 min). Cells were resuspended in FAD media containing 20 % methyl cellulose and counted. To generate keratinocyte spheroids of defined size and cell number this suspension was diluted with the 20 % methyl cellulose solution to a final concentration of 12500 cell/ml. Aliquots of 200 µl (2500 cells) were seeded into non-adherent round-bottom 96 well plates (Griener, Frickenhousen, Germany). The prevention of adhesion, by methyl cellulose, resulted in the formation of cell aggregates overnight (37°C, 5 % CO_2) referred to as spheroids.

2.10.2 Calcein AM green labelling of Ntert spheroids

Optimisation of calcein AM green (Molecular Probes) labelling and assessment of toxicity was carried out using Ntert monolayers. 5 x 10^5 keratinocytes were seeded onto 5 x T25 flasks and once cells had adhered they were incubated in FAD media supplemented with 0.1-10 µM Calcein AM green (37°C, 15 min). The extent of fluorescence labelling was monitored over 48 h before a cell count was carried out on cells retrieved by trypsinisation.

The decision was made to label keratinocytes following spheroid formation and cells were incubated with 5 µM Calcein AM green for 15 min prior to seeding.

2.10.3 Analysis of Ntert migration

Calcein AM green-labelled spheroids were seeded in FAD media onto hyperconfluent HCA2 transfectants. Seeded in 24 well plates, these fibroblasts had been grown to three days post confluency in the presence of 50 μg/ml ascorbic acid (Sigma). In subsequent experiments investigating the role of the generated extracellular matrix (ECM) in migration, fibroblasts were treated with a 0.01 % triton/PBS wash. Alternatively fibroblasts underwent three freeze-thaw cycles followed by a 1 % Na deoxycholate wash to remove cellular debris before seeding. To avoid cross-talk between spheroids, a single keratinocyte spheroid was seeded in each well. Keratinocyte adhesion occurred within 2 h at 37°C, following which the first set of pictures were taken. This was repeated after 24 h and 48 h.

Pictures were taken using a Carl Zeiss Axiocam camera linked to an Axiovert 200M Zeiss microscope. Improvision Openlab™ 3.1.7 was running on the connected computer.

In most cases migrating keratinocytes were seen to form an oval body of cells, consequently two measurements were taken at the longest and widest points for each time point. Migration of keratinocytes over mock-transfected HCA2 fibroblasts was established as the control with which data from antisense, sense and serine mutant transfectants were compared.

2.10.3.1 Statistical analyses

All comparisons were performed using unpaired student's t test with $p < 0.05$ considered significant. Results were expressed as mean ± SD.

Chapter 3:

Generation of antibodies against the novel transglutaminase enzymes 6 and 7

3.1 Introduction

To date, 9 members of the TG family have been identified in man with a wide range of physiological functions, including fibrin clot stabilisation (Pisano *et al.*, 1968), semen coagulation (Williams-Ashman, 1984), the formation of cornified envelopes (Steinert and Marekov, 1995; 1997; Candi *et al.*, 1999) and the stabilisation of ECM structures (Aeschlimann and Thomazy, 2000). Each TG has a characteristic tissue distribution, although individual enzymes are present in a number of different tissues and are often in combination with other isoforms. TG2 is recognised as the most ubiquitously expressed member of the TG family. In contrast the expression of other TGs are more specialised, such as band 4.2, which is limited to haematopoietic cells (Grenard *et al.*, 2001).

To date, there is little data available on the recently identified TG6 and TG7. Northern blot data has demonstrated TG7 expression is highest in lung, testis and fetal tissue (Grenard *et al.*, 2001). It has also been amplified from fibroblast cell lines by reverse transcription polymerase chain reaction, RT-PCR (Stephens *et al.*, 2004). Further to this murine *in situ* studies have demonstrated that TG6 is expressed within the epidermal compartment of skin (H. Thomas Thesis, 2004). These findings confirm TG6 and 7 are of particular interest to this project's aims to elucidate the roles of TG enzymes in the physiology of healthy skin. To investigate the protein distribution of TG6 and 7 in human skin, antibodies would provide a powerful tool. Therefore, work was begun to generate polymeric antibodies against a recombinant form of TG7. However, following limited success in purifying this protein, synthetic peptides were produced and used to raise antibodies against TG7 and the two splice variants of TG6 (the full-length enzyme, designated TG6L and a truncated version, referred to as TG6S).

3.2 Results

3.2.1 Generation of a Glutathione S-transferase /hTG7 fusion protein

3.2.1.1 C-fragment

A 1160 base pair (bp) fragment spanning the C-terminal β barrels of TG7 (C-fragment) was amplified from cDNA stocks by PCR (Work performed by Mrs P. Aeschlimann). This sequence incorporated the bp 1069-2229 and contained two silent mutations at 1769 bp (g→c) and 2111 bp (a→c). The 3' A-overhangs generated by the polymerase enzyme were utilised to TA clone this fragment into a PCR II vector (Invitrogen) directly from the PCR mix (described in Section 2.4.1.1). Five colonies produced by subsequent transformation of INVα *E.coli* were selected for restriction digest analysis. This confirmed the required construct had been isolated and established the orientation of the insert (data not shown). Clone 1 produced fragments predicted from orientation 1 (5' base pairs of vector and insert adjacent), in contrast Clone 5 demonstrated the digest pattern expected from orientation 2 (3' insert adjacent to 5' vector base pairs). These clones were sequenced and in addition to the silent mutations already identified, Clone 1 had a further silent mutation at 1856 bp (g→a) and a substitution at 1729 bp (a→g), resulting in the residue lysine 575 (Lys^{575}) being replaced with arginine (Arg). It was, however, confirmed that clone 5 was free from further mutations and suitable for generation of a fusion protein (Appendix 1).

The pGEX-2T expression vector (Amersham Pharmacia) was selected as suitable for generation of a construct. This vector incorporates a 26 kDa N-terminal Glutathione S-transferase (GST) tag, under control of an isopropyl β D-thiogalactoside (IPTG) inducible lac promoter. It was established from sequence data that a double digest of the vector and PCRII/C-fragment construct with EcoRI and BamHI would allow in frame ligation and expression of the β-barrel domains. Accordingly, digests were performed and ligation reactions were established using an estimated insert:vector ratio of 2:1. BL21 *E.coli* were selected for transformation, since this strain is deficient in *lon* and *omp T* proteases and would optimise fusion protein yield. Analysis of the resulting colonies was carried out with restriction

digests and finally, sequencing confirmed the fusion protein had ligated in frame (Appendix 1). This construct produced a fusion protein with a predicted size of 55 kDa, including amino acid residues 452-710 of TG7 (Fig. 1).

MSPILGYWKIKGLVQPTRLLLEYLEEKYEEHLYERDEGDKWRNKKFELGLEFPNLPYYIDGDVKLTQSMAIIRYIA
DKHNMLGGCPKERAEISMLEGAVLDIRYGVSRIAYSKDFETLKVDFLSKLPEMLKMFEDRLCHKTYLNGDHVTHPD
FMLYDALDVVLYMDPMCLDAFPKLVCFKKRIEAIPQIDKYLKSSKYIAWPLQGWQATFGGGDHPPKSDLVPRGSPE
ERAVFMKASRKMLGPQRASLPFLDLLESGGLRDQPAQLQLHLARIPEWGQDLQLLLRIQRVPDSTHPRGPIGLVVR
FCAQALLHGGGTQKPFWRHTVRMNLDFGKETQWPLLLPYSNYRNKLTDEKLIRVSGIAEVEETGRSMLVLKDICLE
PPHLSIEVSERAEVGKALRVHVTLTNTLMVALSSCTMVLEGSGLINGQIAKDLGTLVAGHTLQIQLDLYPTKAGPR
QLQVLISSNEVKEIKGYKDIFVTVAGAPZ

Fig 1. The amino acid sequence of the TG7 fusion protein: The N-terminal GST tag is shown in blue a short sequence from the flexible hinge region is shown in black, β-barrel 1 in green and β-barrel 2 in magenta.

3.2.1.2 N-fragment

In parallel to experiments generating a fusion protein encoding the C-fragment, experiments were performed using a second hTG7 PCR product. A 682 bp fragment (N-fragment), incorporating the N-terminal sandwich and catalytic domains of hTG7 was amplified from human cDNA (Work performed by Mrs. P. Aeschlimann). Although a mutation free PCRII construct was generated (data not shown), the production of a pGEX-2T construct proved unsuccessful, despite increases in the insert:vector ratio at the ligation step. Since a pGEX-2T construct incorporating the complete C-terminal β-barrel domains had been produced, this work terminated here. The C-terminal fragment had the added advantage of including the region of lowest homology between TG enzymes and would reduce the likelihood of cross-reactivity from any antibodies produced.

3.2.1.3 Optimisation of fusion protein expression

To demonstrate the inducible effect of IPTG on transformed BL21 (described in Section 2.4.2.4), Western blots targeting the GST tag were established with equal volumes of soluble and insoluble fractions, collected from cultures before and after the addition of 1 mM IPTG (Fig. 2). The soluble pool of proteins were extracted in 20 mM Tris-HCl buffer (pH 8), containing 2.5 mM EDTA, 5 mM DTT, 1 mM NEM, 1 mM PMSF and 0.1 % sodium deoxycholate. Insoluble proteins were pelleted and resuspended in 8 M urea. It was evident that the majority of the GST-tagged TG7 β-barrel domains were localised to the insoluble pellet fraction (Fig. 2). The reason for this is not apparent, since TG7 has no predicted post-translational modifications that would cause problems for prokaryotic expression. This distribution could be the result of hyprophobic interactions with insoluble proteins as reported with TG5 (Candi *et al.*, 2001). In order to work with the fusion protein and be confident the native conformation was retained, the decision was made to utilise the soluble fraction in future studies and to scale up culture volumes to obtain the required protein levels. This is in preference to attempting to solubilise the protein from the pellet fraction. It was also observed that a 26 kDa protein corresponding to the GST tag was detected in the BL21 extracts, indicating some protein cleavage had occurred despite the use of BL21 *E.coli* (Fig. 2). The TG7 fusion protein construct was retransformed into commercially available BL21 stocks (Life Technologies) but the cleavage product remained evident (data not shown).

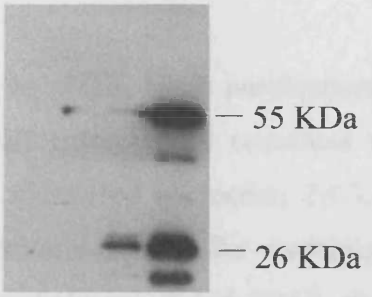

Fig. 2 Induction of transformed BL21 *E.coli* with 1 mM IPTG produces a 55 kDa GST-tagged TG7 fusion protein: Aliquots of transformed BL21 culture were taken before and after 5 h induction with 1 mM IPTG at 37°C. These samples underwent a two-step extraction; the first with 20 mM Tris HCl (pH 8) containing 2.5 mM EDTA, 5 mM DTT, 1 mM NEM, 1 mM PMSF and 0.1 % sodium deoxycholate. The insoluble pellet was collected (10 min, 10000 x g) and underwent a second extraction with an equal volume of 8 M urea. Anti-GST immunoblots revealed the majority of the fusion protein is localised to the urea soluble pellet fraction (P) as opposed to the Tris/EDTA soluble fraction (S). There is also evidence of protein breakdown with the 26 kDa GST tag detected.

Optimal culture conditions of BL21 culture were established by a series of experiments, including culture duration, temperature and the concentration of IPTG. These alterations did not produce large effects on the protein quantity, solubility or the extent of GST tag cleavage (data not shown). To summarise, future cultures were grown at 28°C for 5 h and protein expression was induced by 0.75 mM IPTG.

3.2.2 Purification of hTG7 fusion protein

3.2.2.1 Affinity chromatography

Initial attempts were made to obtain batch purifications of the GST fusion protein, by incubating the bacterial extract with unpacked Glutathione Coupled Sepharose (Amersham Pharmacia) (described in Section 2.4.3.1). Elution of bound proteins was attempted by competition with a buffer containing excess glutathione [100mM Tris-HCl pH8, 20mM glutathione, 0-1M NaCl, 5mM DTT, 0.1% Na deoxycholate]. However, it was evident from the flow through retrieved that the majority of the fusion protein remained unbound and later experiments demonstrated this could not be improved by reducing the temperature to 4°C (data not shown). The fraction of the fusion protein that did associate with the Glutathione Sepharose was found to bind with a high affinity. This interaction was not disrupted by competition with free glutathione and proteins were only retrieved in 8 M urea (data not shown). To address the problem of elution, further experiments included a 0-500 mM salt gradient over 10 column volumes (cv) utilising a 1 ml pre-packed column incorporated to an Akta Prime (Amersham Pharmacia) (described in Section 2.4.3.2). This change in protocol produced an elution peak commencing at a NaCl concentration of 415 mM (Fig. 3a). Once again, a relatively small portion of the fusion protein bound, but the presence of the TG7 fusion protein within this peak was confirmed by anti-GST immunoblotting and Coomassie Brilliant Blue R-250 staining (Fig. 3b and c). It was noted that comparison between anti-GST blots and Coomassie Brilliant Blue detection identified distinct antibody affinities for the fusion protein and GST tag in isolation. This antibody population, raised against the GST tag, demonstrated a significantly lower affinity for the fusion protein. Consequently Western blot analysis alone could produce misleading data concerning the relative concentrations of the two proteins. The Coomassie Brilliant Blue R-250 staining also revealed a 14 kDa protein, which stained negative for a GST tag, providing evidence of non-specific binding to the glutathione-affinity column. The fractions forming the protein peak (fractions 44-51) were pooled, however, this produced a poor yield from the 2 L culture, with a concentration calculated to be 10 μg/ml (Fig. 3d) by bicinchoninic acid (BCA) protein assay (Pierce) (described in Section 2.1.2.2).

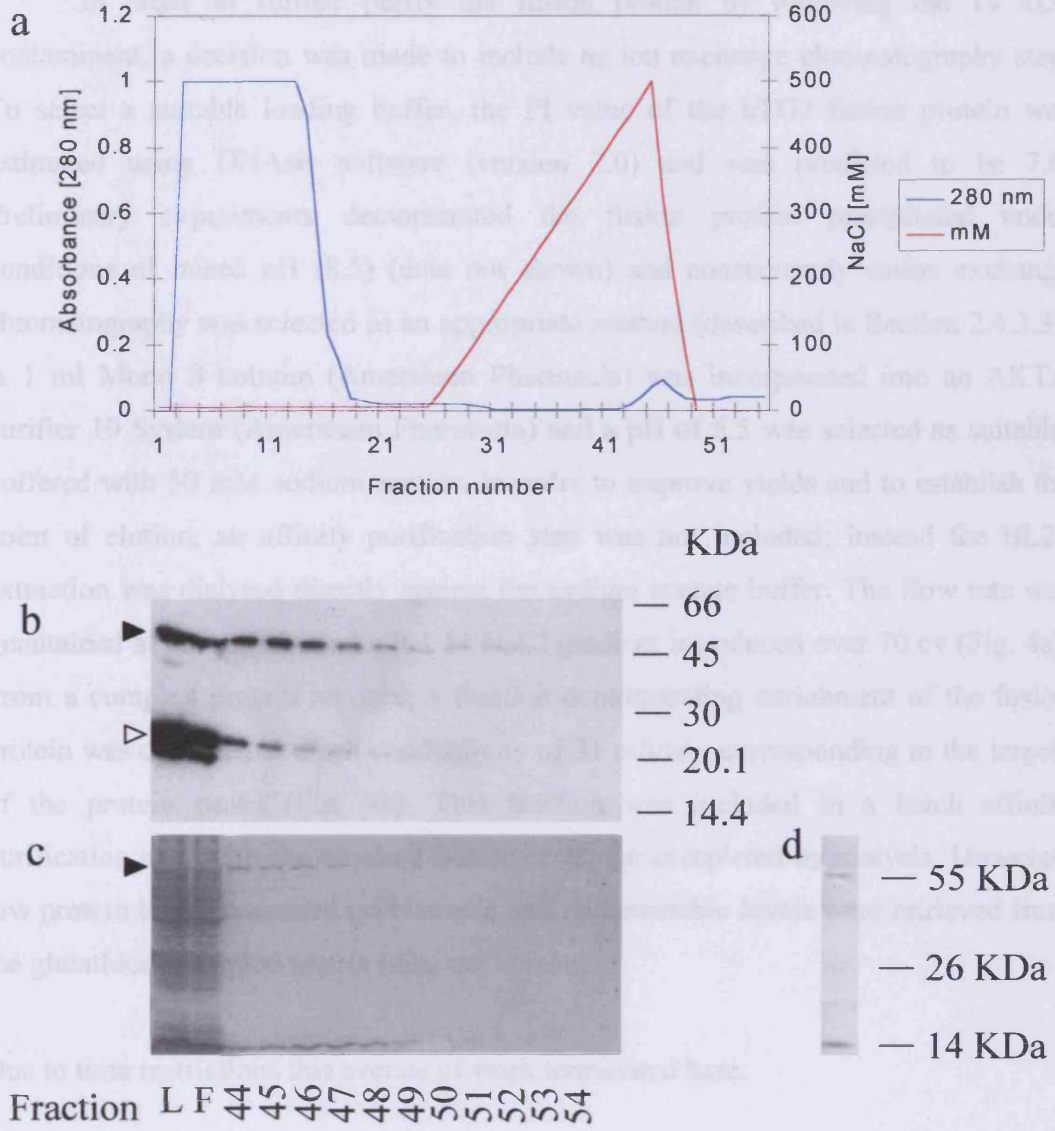

Fig. 3 The TG7 fusion protein elutes from a glutathione-affinity column at a salt concentration of 415 mM but is not completely purified: (a) 5 ml soluble BL21 extract from a 2 L culture was loaded onto a pre-packed glutathione-linked column (1 ml). A 500 mM NaCl gradient was introduced over 10 cv and 0.5 ml fractions collected (fraction number indicated on x-axis). (b) Fractions forming the elution peak (44-54) underwent anti-GST blotting, and (c) Coomassie Brilliant Blue R-250 staining. The 55 kDa full-length fusion protein (solid arrowhead) and 26 kDa GST tag (hollow arrowhead) were present within the fractions. Samples of the extract loaded (L) and unbound proteins retrieved in the flow through (F) were included to ascertain the efficiency of the system. (d) Fractions 44-51 were pooled and analysed using Coomassie staining. This revealed a poor protein yield estimated to be 10 µg/ml (4 ml aliquot). In addition to proteins corresponding to the full-length fusion protein and GST tag, a 14 kDa band was observed. Since this stained negative with the Anti-GST blot it would suggest non-specific binding to the affinity column.

3.2.2.2 Cation exchange chromatography

In order to further purify the fusion protein by removing the 14 kDa contaminant, a decision was made to include an ion exchange chromatography step. To select a suitable loading buffer, the PI value of the hTG7 fusion protein was estimated using DNAsis software (version 2.0) and was predicted to be 7.6. Preliminary experiments demonstrated the fusion protein precipitated under conditions of raised pH (8.5) (data not shown) and consequently cation exchange chromatography was selected as an appropriate method (described in Section 2.4.3.3). A 1 ml Mono S column (Amersham Pharmacia) was incorporated into an AKTA purifier 10 System (Amersham Pharmacia) and a pH of 5.5 was selected as suitable, buffered with 50 mM sodium acetate. In order to improve yields and to establish the point of elution, an affinity purification step was not included; instead the BL21 extraction was dialysed directly against the sodium acetate buffer. The flow rate was maintained at 0.5 ml/min and a 0-1 M NaCl gradient introduced over 70 cv (Fig. 4a). From a complex protein mixture, a fraction demonstrating enrichment of the fusion protein was collected at a salt conductivity of 31 mS/cm, corresponding to the largest of the protein peaks (Fig. 4b). This fraction was included in a batch affinity purification step with the required buffer exchange completed by dialysis. However, low protein levels remained problematic and no detectable levels were retrieved from the glutathione-coupled matrix (data not shown).

Due to time restrictions this avenue of work terminated here.

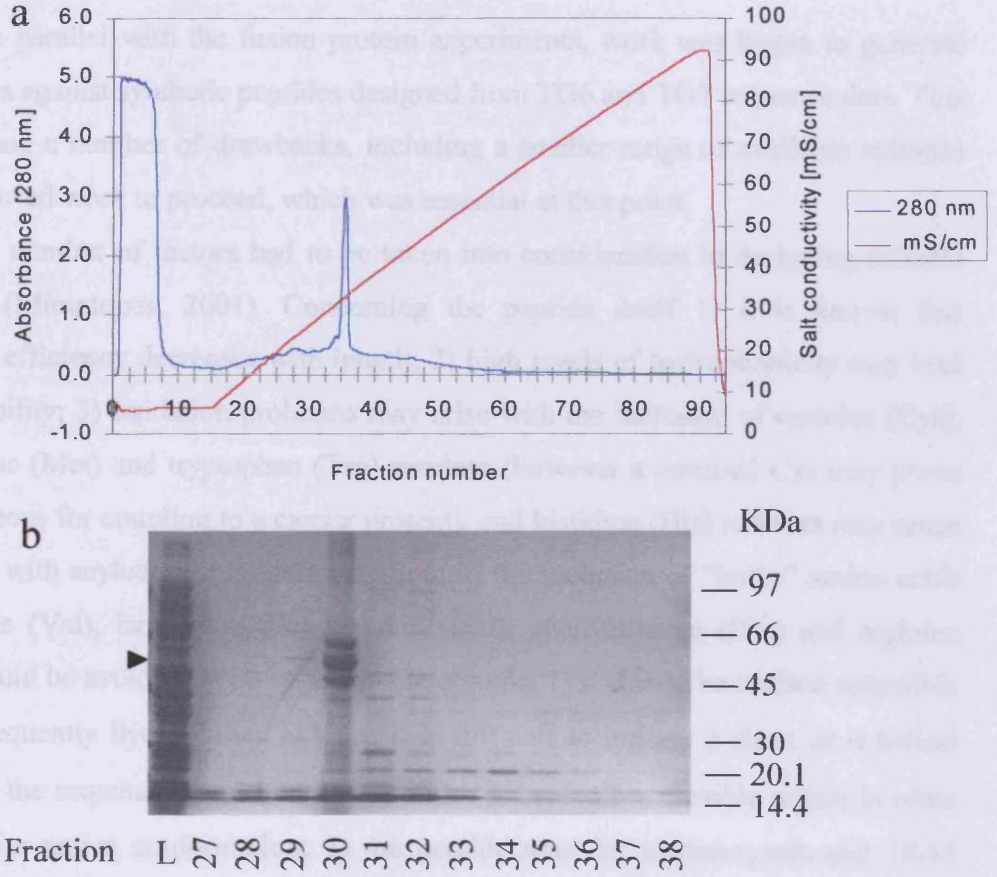

Fig. 4 Cation exchange chromatography of crude BL21 extract over a 1ml Mono S column produced a fraction enriched with the TG7 fusion protein: (a) The BL21 extract was dialysed against sodium acetate, pH 5.5 and loaded at a flow rate of 0.5 ml/min before a 1 M NaCl gradient was introduced over 70 cv. A number of unresolved peaks were observed between 3 – 68 mS/cm the largest being around 32 mS/cm. (b) Fractions between 27 and 38 were analysed by Coomassie Brilliant Blue R-250 staining and it was observed that the fraction corresponding to the greatest protein peak was enriched for the 55 kDa fusion protein (indicated by solid arrowhead) when compared to the loaded sample (L).

3.2.3 Generation of antibodies against TG6 and TG7 peptides

3.2.3.1 Peptide Design

In parallel with the fusion protein experiments, work was begun to generate antibodies against synthetic peptides designed from TG6 and TG7 sequence data. This method had a number of drawbacks, including a smaller range of available epitopes but it allowed work to proceed, which was essential at this point.

A number of factors had to be taken into consideration in designing suitable peptides (Mimotopes, 2001). Concerning the peptide itself 1) it is known that synthesis efficiency decreases with length; 2) high levels of hydrophobicity may lead to insolubility; 3) oxidation problems may arise with the inclusion of cysteine (Cys), methionine (Met) and tryptophan (Trp) residues (however a terminal Cys may prove advantageous for coupling to a carrier protein), and histidine (His) residues may cause problems with acylation or enantimerisation; 4) the inclusion of "bulky" amino acids e.g. valine (Val), isoleucine (Ile), leucine (Leu), phenylalanine (Phe) and arginine (Arg) should be avoided. With regard to the epitope; 1) it should be surface accessible and consequently hydrophilic; 2) since it is difficult to imitate β-sheet or α-helical structures the sequence should be derived from β-turn/coil or flexible region in order to adopt its native conformation; 3) the peptide must be immunogenic and 10-15 residues is considered the optimum length; 4) the epitope should not be post-translationally modified.

Three peptides, corresponding to TG7 and the two splice alternatives of TG6; TG6L (full-length) and TG6S (truncated short form) were designed using ProtScale (work carried out by Dr. K. Beck). This software allows the prediction of sequence structure with regard to flexibility, surface accessibility, hydrophobicity, turns, β-strands and α-helices. If all these parameters are designated a probability greater than 0.5, the sequence can be considered to have no clear secondary structure.

To confirm the suitability of the epitopes selected, comparative modelling, based on other resolved TG structures (FXIII, Yee *et al.*, 1994; TG2, Shenping *et al.*, 2002; and TG3, Ahvazi *et al.*, 2002), was carried out using the CLUSTALW computer programme (Higgins *et al.*, 1994) or 3Djigsaw. The predicted three-dimensional configurations allowed epitopes residing in a surface accessible region to be selected for synthesis (Fig. 6). Sequences were selected from the flexible hinge

region connecting the enzymes' catalytic domain and the first of the C-terminal β-barrel domains. The three peptides were designated P6L (TG6L - **CGWRDDLLEPVTKPS**), P6S (TG6S - **TIRAYPGASGEGLSP**) and P7 (TG7 - **ESGGLRDQPAQLQL**). In the case of P6L and P6S, two points should be noted. Firstly, the alternative splicing of exon XII in TG6S produces a frame shift in the sequence, generating a short unique protein segment within this isoform prior to its premature termination (Appendix 1). It is this region of amino acids on which the peptide P6S is based. Secondly, a combination of human and murine sequence data was included in the final design of P6L and P6S in order to produce antibodies suitable for broad-based studies (Fig. 5). The design of these peptides has already been discussed at length in previous work (H. Thomas Thesis, 2004). In contrast the peptide P7 was derived solely from human sequence data. Peptide synthesis was carried out by Sigma Genosys, as was the subsequent purification by high HPLC and characterisation by mass spectrometry (Appendix 1).

```
human TG6L  462  FGVEASGRRIWIRRAGGRCLWRDDLLEPATKPSIAGKFKVLEPPMLGHDLRLALCLA
mouse TG6L  462  LSVEAWGRRRRIRRASVRGVWRDDLLEPVTKPSITGKFKVLEPPVLGQDLKLALCLT
       P6L                          CGWRDDLLEPVTKPS

human TG6S  566  YSKYKEDLTEDKKILLAAMCLVTKGEKLLVEKDITLEDFITIKRAYPGASGEGLSPV
mouse TG6S  566  YSQYKGDLTEDKKILLAAMCLVSKGEKLLVEKDITLEDFITIKRAYPGASGEGLSPV
       P6S                                                TIRAYPGASGEGLSP
```

Fig. 5 Comparison of peptides with native human and mouse TG6 sequences: Peptide sequences are shown in blue. The C-terminal residue in the peptides was the carboxamide. A cysteine residue added to P6L, for conjugation to a carrier protein, is highlighted in red.

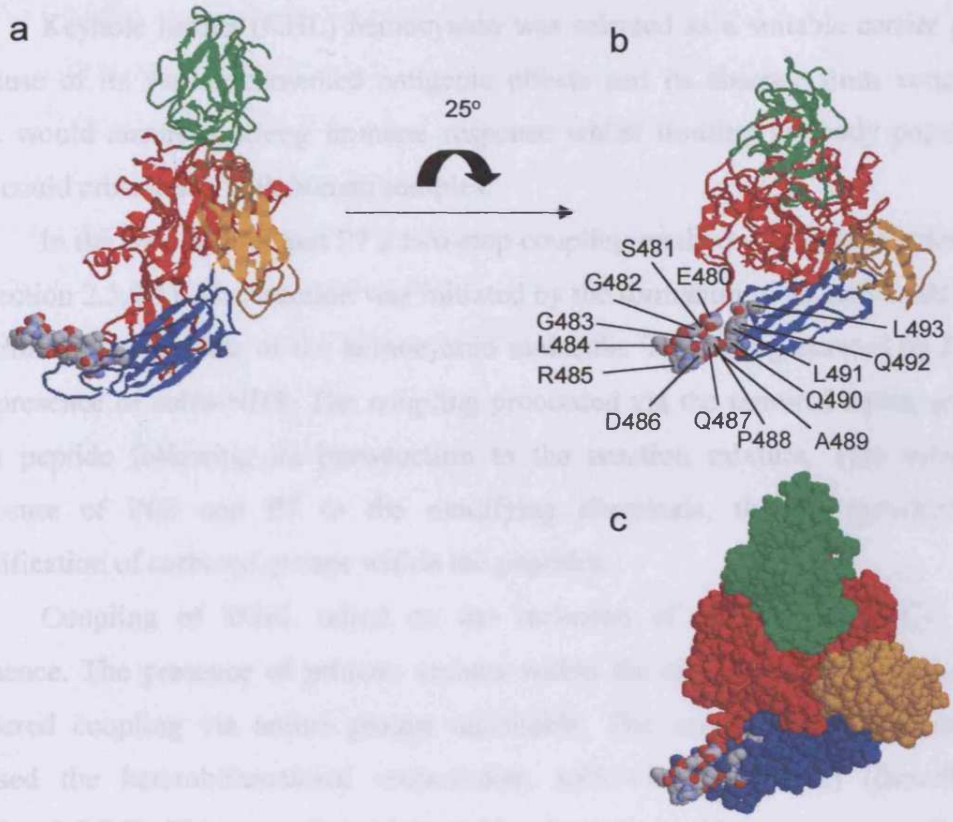

Fig. 6 The P7 epitope resides within a flexible hinge region and is surface accessible: (a-b) Ribbon image of the structure of TG7 as determined by comparative modelling, with 3Djigsaw software. The four domains are designated the N-terminal β-sandwich (green), the catalytic core (red), β-barrel 1 (blue) and β-barrel 2 (orange). Residues in the P7 peptide are located in a connecting loop between the catalytic core and β-barrel 1 domain (represented in the CPK style). (b) The space-filled representation of the model confirms the P7 epitope is surface accessible.

3.2.3.2 Peptide Coupling

Keyhole limpet (KHL) hemocyanin was selected as a suitable carrier protein because of its well-documented antigenic effects and its absence from vertebrates. This would ensure a strong immune response whilst limiting antibody populations that could cross-react with human samples.

In the case of P6S and P7 a two-step coupling method was selected (described in Section 2.5.2.1). The reaction was initiated by the formation of an active ester at the C-terminus carboxylate of the hemocyanin molecule. This was generated by EDC in the presence of sulfo-NHS. The coupling proceeded via the terminal amine group of each peptide following its introduction to the reaction mixture. This avoids the exposure of P6S and P7 to the modifying chemicals, thereby preventing the modification of carboxyl groups within the peptides.

Coupling of TG6L relied on the inclusion of an N-terminal Cys in its sequence. The presence of primary amines within the side chain of its Arg residue rendered coupling via amine groups unsuitable. The selected coupling procedure utilised the heterobifunctional cross-linker, sulfo-GMBS (Pierce) (described in Section 2.5.2.2). This cross-linker is capable of reacting with amino groups (Lys side chains) on the surface of the carrier protein, adding maleimido groups. The sulfhydryl of the peptide is capable of reacting with these active groups to form stable thioester bonds (work carried out by H. Thomas). This is one of the most widely used methods of coupling peptides to a carrier protein via a specific amino acid residue since it conserves peptide antigenicity (Lee *et al.*, 1985).

To establish effective coupling conditions by the two methods suitable controls were required. For the EDC mediated coupling, monodansyl cadaverine (MDC) was included as a control (Sigma), whilst coumarin (Pierce) was selected for sulfo-GMBS catalysed coupling. These controls are known to produce fluorescence with corresponding absorbance at OD_{335nm} and OD_{358nm} respectively. This had the advantage of distinguishing the hapten from the carrier protein OD_{280nm} peak.

For each method the conjugates were isolated from low molecular weight contaminants by passing the mixture over a PD_{10} column (Amersham Pharmacia) and elution profiles were established from the collected fractions. Although the MDC control produced an OD_{280nm} peak between 5-8 ml of the eluant (Fig. 7a), absorbance

at OD_{335nm} was insufficient to produce a distinct peak. Consequently, the collected fractions were transferred to a UV transilluminator and the presence of MDC was verified by the resulting fluorescence (Fig. 7b). The coumarin control produced an OD_{358nm} absorbance peak between 2-4.5 ml of the eluant (Fig 7c).

Following the establishment of successful conditions, coupling reactions were performed with the three TG peptides (P6L, P6S and P7) and their protein elution peaks overlaid with that of the relevant control (Fig 7a and c). The decision was made to pool 4.5-7.5 ml of the eluant retrieved following P6S and P7 conjugation (amine linkage) with 2-4 ml pooled in the case of P6L (thiol linkage).

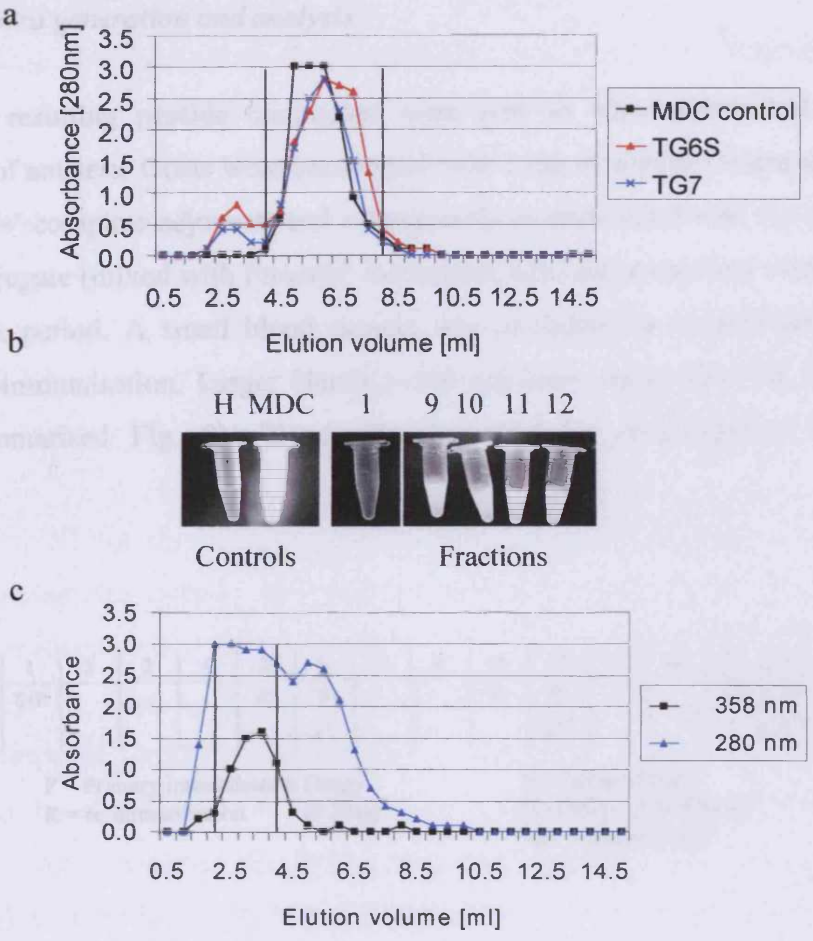

Fig. 7 Elution peaks of hemocyanin conjugated peptides following coupling reactions: (a) 12 mg/ml P6S and P7 were coupled to 5 mg KHL hemocyanin following activation with 16 µmol sulfo-NHS and EDC. Conjugates were separated from low molecular weight contaminants by elution over a PD10 column and collected in 0.5 ml fractions. A control experiment was carried out with 3 mg/ml monodansyl cadaverine and identified the conjugate peak within fractions 4.5 –7.5 ml (indicated by vertical lines). These fractions were subsequently pooled. No corresponding OD_{335nm} peak was observed for the monodansyl control. (b) Sample fluorescence of eluted fractions was produced with a UV transilluminator and confirmed the presence of mondansyl cadaverine. Hemocyanin (H) and uncoupled monodansyl cadaverine (MDC) were included as respective negative and positive controls. The initial 0.5 ml fraction sample collected prior to the elution peak (1) produced no fluorescence, in contrast to fractions forming the peak (9-12). (c) The success of coupling via sulfyl groups (P6L) was assessed using a coumarin control with corresponding absorbance at OD_{358nm} (work carried out by H.Thomas). OD_{280nm} was plotted to produce the elution profile of P6L. Fractions 2-4 ml were pooled (indicated by vertical lines).

3.2.3.3 Antisera generation and analysis

The resulting peptide conjugates were sent to Micropharm Ltd. for the production of antisera. Goats were immunised with 1 mg of peptide-conjugate (mixed with Freunds' complete adjuvant) and subsequently re-immunised with 0.5 mg of the peptide-conjugate (mixed with Freunds' incomplete aduvant) every four weeks over a twelve-week period. A small blood sample was provided pre-immunisation and 6 weeks post-immunisation. Larger bleeds (~300 ml) were taken after 10, 14 and 16 weeks (summarised Fig. 8). Blood was harvested by centrifugation following coagulation.

Week	1	2	3	4	5	6	7	8	9	10	11	12	13	14	16
	S/P				R	S 1st			R	B 2nd			R	B 3rd	DB 4th

P = Primary immunisation (1mg)
R = re-immunisation (0.5mg)

S = Sample (4ml)
B = Bleed (200-400ml)
DB = Double bleed

Fig. 8 Timeline of peptide antibody generation: Antibodies against P6L, P6S and P7 were raised in goat with an initial immunisation (1 mg) and 3 subsequent re-immunisations (0.5 mg) (work carried out by MicroPharm). Bleeds were taken at week 6, 10, 14 and 16.

In order to analyse the resulting sera, bovine serum albumin (BSA) conjugates of the three peptides were generated and isolated using the same method as the hemocyanin coupling (data not shown). On receiving the 1st bleed samples, ELISAs were performed (described in Section 2.5.4) with a serial dilution (1/50-1/12800) using the hemocyanin and BSA conjugates as antigens (50 μg/ml) and the unconjugated proteins included as controls (Fig. 9a-c). In the case of the anti-TG6S sera (Fig. 9b), the hemocyanin and BSA peptide conjugate curves almost overlay with a steady decrease in signal observed only following a sera dilution of 1/3200. In contrast, a clear sigmoidal curve is seen with the unconjugated hemocyanin antigen, decreasing from a 1/400 dilution. It was anticipated that antibody populations would be generated against hemocyanin epitopes, but the fact that OD_{490nm} readings

decreased at a higher concentration than its conjugate demonstrates that antibody populations directed against the P6S peptide are present in the serum. For the BSA control, OD_{490nm} readings above the background levels were only observed at high sera concentrations (1/50-1/200) and are most likely the result of non-specific binding. In the case of anti-TG6L and anti-TG7 (Fig. 9a and c respectively), the conjugated and unconjugated forms of hemocyanin produced similar curves with very little decrease in signal observed with sera dilution. This demonstrates a high titre of antibodies specific to the carrier protein, hemocyanin. However, the BSA conjugates of P6L and P7 produced higher readings when compared with the unconjugated control, providing evidence of a population of antibodies specific for the peptide hapten.

Further ELISA experiments were established to confirm antibodies had been generated against the peptide sequence and not as a consequence of the linkage introduced or alterations in protein structure produced by cross-linking. To achieve this, P6S and P7 BSA conjugates were utilised, since these peptides were both coupled via an amine linkage (in comparison to the thiol linkage in the case of P6L). A serial dilution of anti-TG6S and TG7 sera was included, using each BSA-peptide conjugate as an antigen (Fig. 10). Both sera produced greater signals when incubated with conjugates containing the target antigen. This confirmed specific interactions between the sera and corresponding antigen sequence. Some signal was observed at high sera concentrations (1/100-1/200) with the putative negative control, providing evidence of a possible antibody population raised against the cross-link structure. However this signal does not exceed that observed with unconjugated BSA controls in the previous set of ELISA experiments.

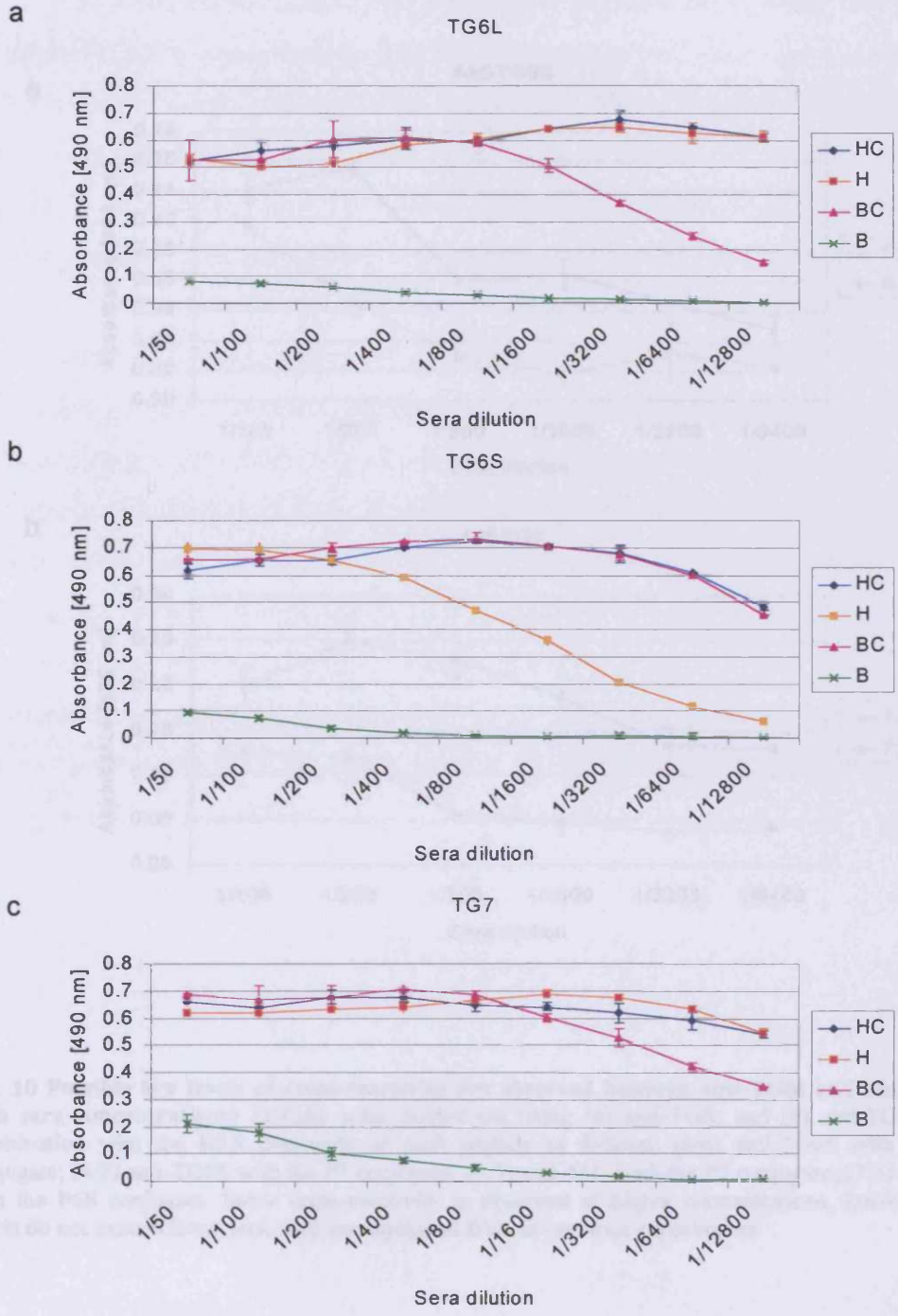

Fig. 9 Analysis of TG peptide antibodies by ELISA: specificity of 1st bleed sera of (a) anti-TG6L (b) anti-TG6S (c) anti-TG7 was assessed by its ability to bind wells coated with 50 µg/ml of the corresponding hemocyanin/BSA conjugates (HC and BC), unconjugated proteins were included as controls (H and B). Serial dilutions ranging from 1/50-1/12800 were included for each sera. Antibody binding was detected with a HRP conjugated secondary antibody and chromatic signal developed using 5-amino-2-hydroxy benzoic acid as a substrate. Each assay was carried out in duplicate and SD is expressed as error bars.

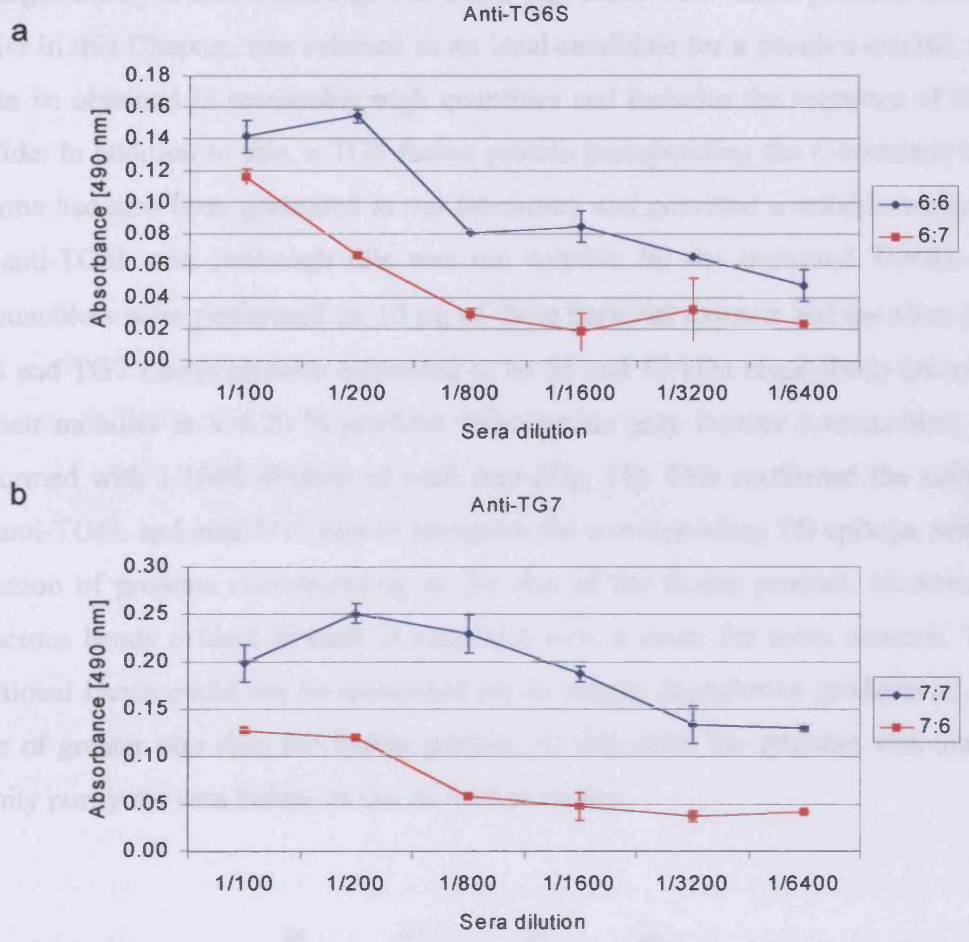

Fig. 10 Possible low levels of cross-reactivity are observed between anti-TG6s and anti-TG7 at high sera concentrations: ELISAs were carried out using (a) anti-TG6s and (b) anti-TG7 sera in combination with the BSA conjugate of each peptide as follows: (6:6) anti-TG6S with the P6S conjugate; (6:7) anti-TG6S with the P7 conjugate; (7:7) anti-TG7 with the P7 conjugate; (7:6) anti-TG7 with the P6S conjugate. Some cross-reactivity is observed at higher concentrations, however these levels do not exceed those seen with unconjugated BSA in previous experiments.

The next step in analysing the sera was to demonstrate its ability to recognise its target TG by Western blotting. The BL21 expressed TG7 fusion protein, discussed earlier in this Chapter, was selected as an ideal candidate for a positive control, since it can be obtained in reasonably high quantities and includes the sequence of the P7 peptide. In addition to this, a TG6 fusion protein incorporating the C-terminus of the enzyme had also been generated in our laboratory and provided a suitable antigen for the anti-TG6L sera (although this was not suitable for the truncated TG6S). GST immunoblots were performed on 10 μg of these bacterial extracts and the sizes of the TG6 and TG7 fusion proteins estimated to be 55 and 53 kDa respectively (according to their mobility in a 4-20 % gradient Tris-Glycine gel). Further immunoblots were performed with 1/1000 dilution of each sera (Fig. 11). This confirmed the ability of the anti-TG6L and anti-TG7 sera to recognise the corresponding TG epitope, with the detection of proteins corresponding to the size of the fusion product. However the numerous bands evident in each immunoblot were a cause for some concern. These additional bands could not be accounted for as simple degradation products as some were of greater size than the fusion protein. At this point the decision was made to affinity purify the sera before its use in further studies.

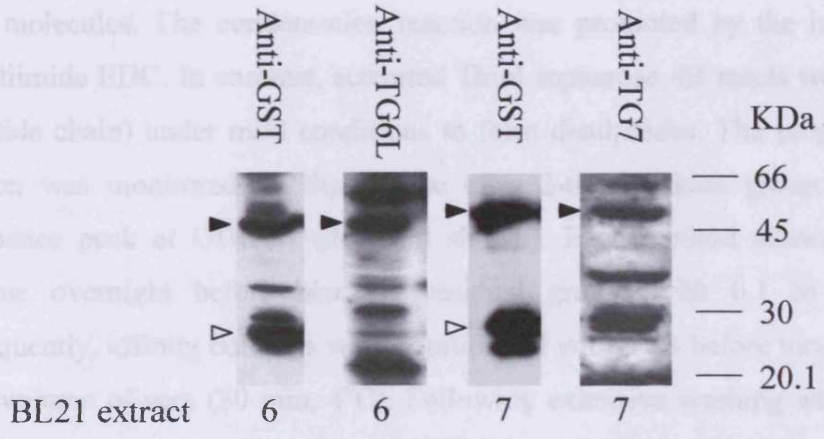

Fig. 11 Peptide generated antibodies are capable of detecting TG fusion proteins: Immunoblotting was carried out on 10 μg BL21 extract containing TG7 (7) and TG6 (6) fusion proteins with anti-GST, anti-TG6L and anti-TG7. The full-length fusion proteins are marked with a solid arrowhead (TG7 – 55 kDa, TG6 – 53 kDa) the cleaved GST tag is identified by a hollow arrowhead (26 kDa).

Prior to affinity purification, selection of a sera batch was necessary, since a total of three bleeds were obtained from the P7 immunisation and four from P6L. In order to make this decision a series of immunoblots were established using the BL21 extracts, containing the TG6 and TG7 fusion proteins. This provided positive and negative controls in each case (Fig 12a). Although multiple bands were observed in each lane, bands corresponding to the expected size were detected in the positive controls and absent from the negative controls for each sera. It was also established that no variability was observed between bleeds and comparable staining profiles were obtained. Taking this into consideration, in conjunction with the available bleed volumes, the 3rd bleeds were selected for affinity purification in each case.

3.2.3.4 Affinity purification of transglutaminase antibodies

Following the selection of the 3rd bleed sera for purification, the three peptides were used to produce 1 ml affinity columns by coupling to ECH Sepharose 4B (P6S and P7) or Thiol sepharose 4B (P6L) (described in Section 2.5.5). The former relied on linkages between the primary amine groups of the peptide ligand and the free carboxyl groups situated at the end of 9-atom spacer arms. The inclusion of this long hydrophilic spacer arm makes this matrix particularly suitable for immobilisation of small molecules. The condensation reaction was promoted by the inclusion of the carbodiimide EDC. In contrast, activated Thiol sepharose 4B reacts with thiol groups (Cys side chain) under mild conditions to form disulphides. The progression of this reaction was monitored by the release of a 2-thiopyridone group, producing an absorbance peak at OD_{343nm} (data not shown). Each method allowed coupling to continue overnight before blocking residual groups with 0.1 M ethanolamine. Subsequently, affinity columns were equilibrated with TBS before incubation with an equal volume of sera (30 min, 4°C). Following extensive washing with TBS (5 cv), bound antibodies were retrieved in 3 M KSCN and immediately dialysed against TBS, to prevent denaturation (described in Section 2.5.6). Purified aliquots were diluted to 5 μg/ml in 5 % milk solutions and new immunoblots performed on the BL21 extracts. This confirmed purification of the sera with a single band observed in each case corresponding to the full-length fusion protein (Fig. 12b).

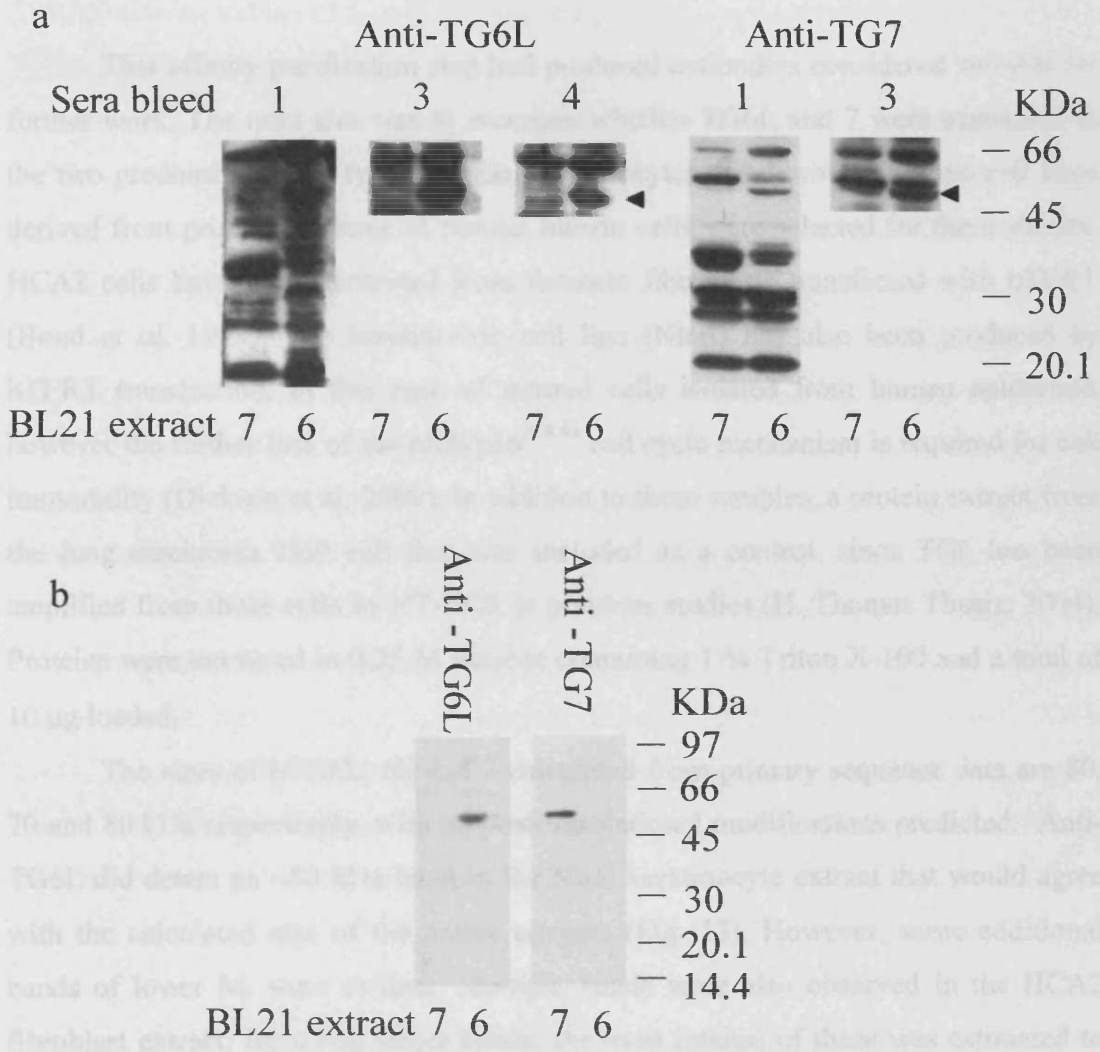

Fig. 12 Selection of sera batch for affinity purification: (a) Normalised loading of BL21 extracts containing TG6 and TG7 were probed with each of the sera bleeds received, 1 (1st bleed), 3 (3rd bleed) and 4 (4th bleed). A dilution of 1/1000 was used in each case. This produced numerous bands in each case; bands corresponding to the relevant fusion protein are marked with a solid arrowhead. There were concerns that there was a misidentification between the 2nd sample bleeds and consequently these samples were excluded. Taking this into consideration in conjunction with available sera volumes the 3rd bleed was selected for each enzyme. (b) 3rd bleed Goat sera was incubated with an equal volume of Sepharose-linked peptide (P6L, 6S and 7) for 30 min at 4°C before extensive TBS washing (10 cv) and elution in 3 M KSCN. Samples were immediately dialysed against TBS to prevent denaturation. Blotting with the affinity purified antibodies (5 µg/ml) produced a single band in each case corresponding to the size of the fusion protein (TG7 designated 7 and TG6 designated 6).

This affinity purification step had produced antibodies considered suitable for further work. The next aim was to ascertain whether TG6L and 7 were expressed in the two predominant cell types in skin, keratinocytes and fibroblasts. Two cell lines derived from primary cultures of normal human cells were selected for these studies. HCA2 cells have been generated from foreskin fibroblasts transfected with hTERT (Bond *et al.* 1999). The keratinocyte cell line (Ntert) has also been produced by hTERT transfection, in this case of normal cells isolated from human epidermis, however the further loss of the pRB/p16^{INK4a} cell cycle mechanism is required for cell immortality (Dickson et al, 2000). In addition to these samples, a protein extract from the lung carcinoma H69 cell line was included as a control, since TG6 has been amplified from these cells by RT-PCR in previous studies (H. Thomas Thesis, 2004). Proteins were extracted in 0.25 M sucrose containing 1 % Triton X-100 and a total of 10 μg loaded.

The sizes of hTG6L, 6S and 7 calculated from primary sequence data are 80, 70 and 80 kDa respectively, with no post-translational modifications predicted. Anti-TG6L did detect an ~80 kDa band in the Ntert keratinocyte extract that would agree with the calculated size of the native enzyme (Fig. 13). However, some additional bands of lower M_r were evident. Multiple bands were also observed in the HCA2 fibroblast extract, including larger bands, the most intense of these was estimated to be ~90 kDa in size. In H69 cells, no distinct bands of the predicted size were observed. Instead a ~90 kDa protein produced the most intense band and it is possible that the cross-linking activity of these enzymes may produce protein complexes as has been reported for other TG isoforms (Barsigian *et al.*, 1991; Candi *et al.*, 2001). No bands corresponding to the full-length native TG7 were observed, however, intense bands at ~40 kDa were detected in HCA2 and H69 extracts, in addition to a faint 97 kDa band present in all samples. The former of these may be a fragment of the enzyme and would correspond to the active site domain (calculated to be 39 kDa).

Since the cell extracts included in the Western blots had undergone a freeze-thaw cycle and were not supplemented with protease inhibitors, the proteins of interest may have become degraded. Subsequent blots were performed using fresh cell extracts and a two-step extraction procedure to establish where the majority of the enzymes were localised. Soluble proteins from Ntert keratinocytes and HCA2

fibroblasts were extracted in a 0.25 M sucrose buffer, supplemented with 1 % Triton X-100, the insoluble pellet was collected by centrifugation (10 min at 16000 x g), before undergoing further extraction in a 20 mM Tris-HCl buffer (pH 8) containing 1 % SDS, 1 mM PMSF, 100 mM NaCl, 2.5 mM EDTA and 1 mM DTT (described in Section 2.3.3.1). 20 μg of soluble extract and 10 μg of each pellet fraction were included in immunoblots with affinity purified anti-TG6L, 6S and 7 (Fig. 14). This removed the multiple bands, confirming that protein degradation had occurred. In the case of the TG6L blot, 80 kDa bands were observed in the soluble extract of the Ntert keratinocytes and HCA2 fibroblasts. TG7 detection also produced an 80 kDa band in the soluble fibroblast extract, a faint band of the same size was also observed in the pellet extract from the keratinocyte cell line. The antibody raised against TG6S detected a single protein in the soluble Ntert extract calculated to be ~40 kDa in size (corresponding to the calculated size of the active domain). The presence of a 55 kDa protein doublet was evident in the keratinocyte pellet fraction for both the anti-TG6L and TG7 blots. This raised some concerns that keratin antibodies may be present despite the affinity purification step and experiments were performed to investigate this hypothesis.

Fig. 13

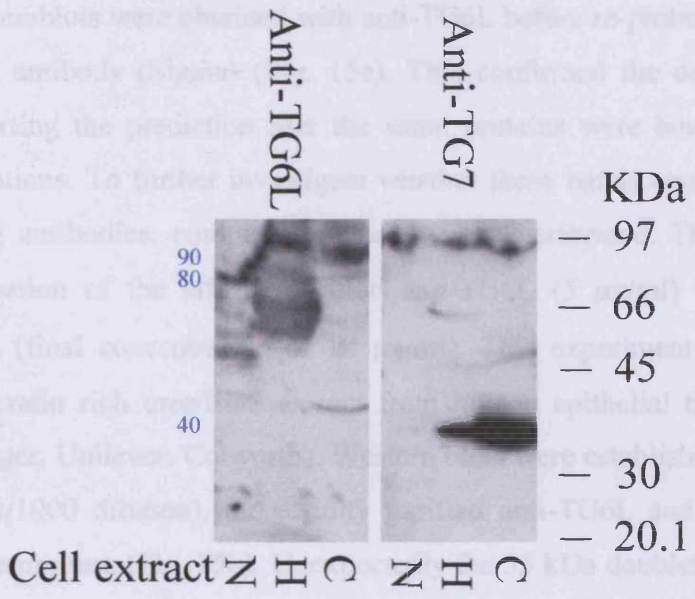

Fig. 14

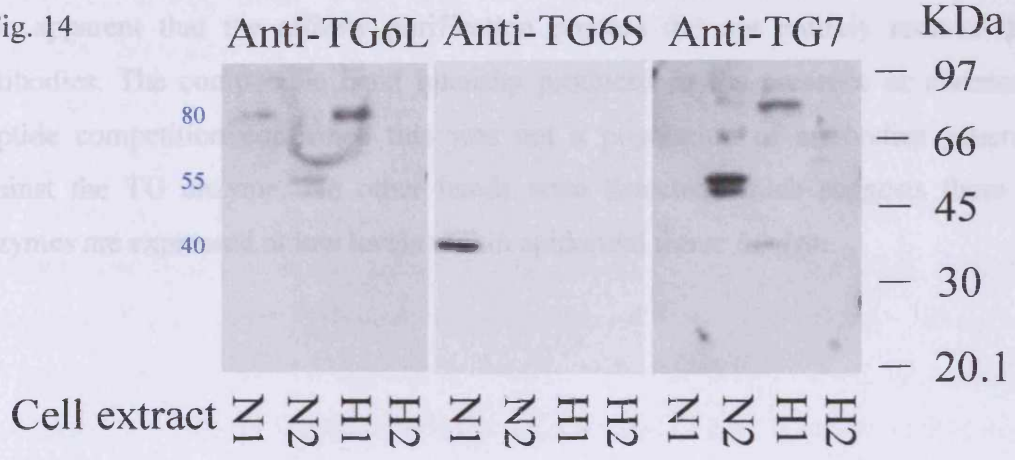

Fig. 13 Identifying cell types expressing TG6L and TG7 using frozen extracts: Immunoblotting was carried out with three cell extracts (Ntert keratinocytes – N, HCA2 fibroblasts – H and the H69 carcinoma cell line – C). Cells were extracted into 0.25 M sucrose containing 1 % Triton X-100, 10 µg of each extract was loaded. Proteins smaller than the predicted size (80 kDa TG6L and 7) were evident in each case, suggesting degradation.

Fig. 14 Identifying expression pools of TG solubility in fresh cell extracts: A two step extraction was carried out on Ntert keratinocytes (N) and HCA2 fibroblasts (H) with a 0.25 M sucrose buffer containing 1 % v/v/ Triton X-100 (1) followed by Tris buffer containing 1 % w/v SDS (2). 20 µg and 10 µg of proteins were loaded for the respective buffers. Detection with the three affinity purified TG antibodies were carried out (5 µg/ml).

Calculated masses of predominant bands are shown in blue.

The first of the experiments to investigate this possible population of keratin antibodies utilised keratin-rich extracts of human corneocytes in 8 M urea containing 1 % SDS. Immunoblots were obtained with anti-TG6L before re-probing with an anti-pan cytokeratin antibody (Sigma) (Fig. 15a). This confirmed the detected proteins overlaid, supporting the prediction that the same proteins were bound by the two antibody populations. To further investigate whether these bands could be attributed to TG targeting antibodies, competition studies were performed. This included an overnight incubation of the affinity-purified anti-TG6L (5 μg/ml) with the BSA-conjugated P6L (final concentration of 10 μg/ml). This experiment utilised 10 μg aliquots of a keratin rich urea/SDS extract from human epithelial tissue (kind gift from Dr. R. Ginger, Unilever, Colworth). Western blots were established with the pre-immune sera (1/1000 dilution), the affinity purified anti-TG6L and the competing antibody-peptide mixture (Fig. 15b). Unexpectedly the 55 kDa doublet was evident in the pre-immune sera; it was predicted the generation of keratin antibodies would most likely have resulted from contamination of the antigen used for immunisation. It was also apparent that the affinity purification process did not entirely remove these antibodies. The comparable band intensity produced in the presence or absence of peptide competition confirmed this was not a population of antibodies generated against the TG enzyme. No other bands were detected which suggests these TG enzymes are expressed at low levels within epidermal tissue *in vivo*.

3.2.3.5 Removal of the contaminating antibody population

It was evident the affinity purification protocol required some alteration, particularly if these antibodies were to be employed in immunohistochemical studies. A number of different approaches were assessed, the first being an adaptation in the elution step. Affinity purification of TG6L antibodies was performed using a pH shift of 7 to 3, followed by the 3 M KSCN elution, as described in the previous section. Results were assessed by Western blotting, including the keratin-rich epithelial extract to identify the presence of contaminating antibodies and BL21 extracts containing the TG fusion protein as a positive control. The pH shift was unsuccessful in removing the contaminating antibodies and produced a poor yield of the TG specific antibodies (data not shown). In parallel, a set of experiments were carried out to establish the effect of 1) including detergent in the wash buffer 2) incorporating a pre-incubation step of sera with Sepharose and 3) including a column blocking step with 5 % milk/TBS. The adjustment to the wash buffer was made with the addition of 0.05 % Tween-20. Immunoblots included samples of the collected column wash (5 cv) and the subsequent 3 M KSCN elution. Antibodies capable of recognising a doublet ~55 kDa were present in the column wash, in the absence of the TG specific antibodies (Fig. 16a). However, 5 cv washes proved insufficient to completely remove the contaminations. Neither of the latter experiments (2 and 3) was entirely successful and although incubation with uncoupled Sepharose improved the ratio between the TG specific and the putative keratin antibodies, the yield of the former decreased and the latter contaminants were still evident (Fig. 16a). Finally, attempts were made to block the affinity column with 5 % BSA overnight (4°C) and the results with anti-TG6L and TG7 proved successful (Fig. 16b). The effectiveness of this method was unexpected, since the sera applied to the column would contain serum albumin levels far in excess of those used in the blocking step. However, this improved protocol was now adopted and performed on the sera raised against TG6S.

Fig. 15

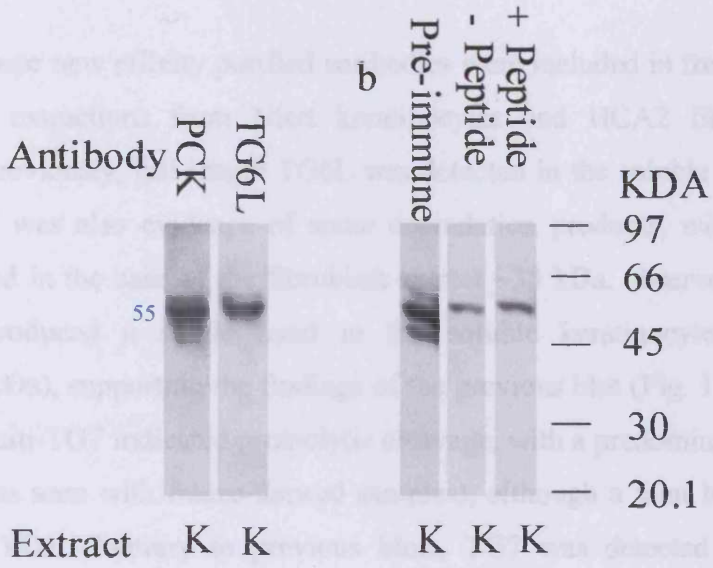

Fig. 16

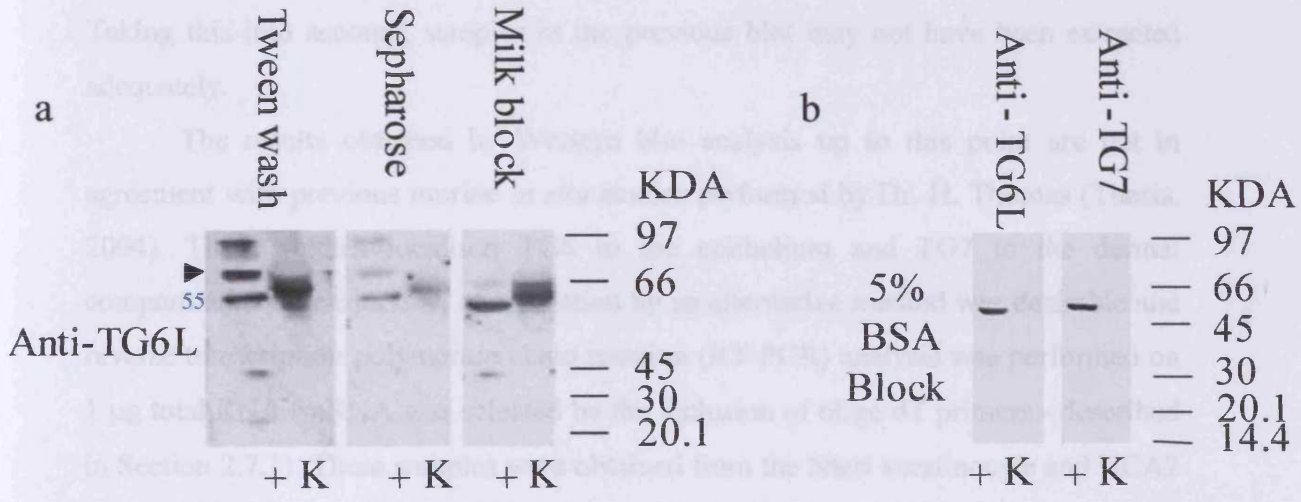

Fig. 15 Evidence of contaminating keratin antibodies: (a) Comparison of anti-pan cytokeratin (PCK) and anti-TG6L immunoblots established with keratin-rich corneocyte extracts (K) demonstrated corresponding doublets around 55 kDa in size (marked 55). (b) Peptide competition experiments were established using keratin rich SDS/Urea extracts of epidermal skin abrasion samples (K). Blotting was carried out with pre-immune sera, 1/1000 (pre-immune); affinity purified TG6L, 2 µg/ml (- Peptide) and affinity purified TG6L following incubation with 1.5 µg/ml of its BSA conjugate (+ Peptide).

Fig. 16 Blocking affinity column with 5 % BSA proves successful in removing contaminating antibodies: (a) Initial attempts to remove the contaminating population of antibodies included; 5 cv washes with 0.05% Tween/TBS (Tween wash), pre-incubating affinity purified antibodies with an equal volume of Sepharose (Sepharose) and the inclusion of a 5 % milk powder blocking step of the peptide-linked column prior to serum incubation (Milk block). Blots were probed with 5 µg/ml of the retrieved antibodies. BL21 expressed TG fusion proteins (marked with a solid arrowhead) are included as positive controls (+) and skin abrasion samples provided a keratin rich control (K) (marked 55). (b) An overnight blocking step with 5 % BSA at 4°C was included. Both anti-TG6L and TG7 purified by this method detect the positive control (+) without any evidence of the 55 kDa doublet in the keratin rich skin abrasion sample (K).

3.2.4 Western blot analysis of keratinocyte and fibroblast cell extracts for TG6 and 7

Aliquots of these new affinity purified antibodies were included in fresh blots, containing two-step extractions from Ntert keratinocytes and HCA2 fibroblasts (Fig. 17a). As seen previously, full-length TG6L was detected in the soluble pools of each cell type, there was also evidence of some degradation products, with lower bands of ~40 kDa and in the case of the fibroblast extract ~35 kDa, observed. Once again, anti-TG6S produced a single band in the soluble keratinocyte extract (calculated to be 35 kDa), supporting the findings of the previous blot (Fig. 17b). The result obtained with anti-TG7 indicated proteolytic cleavage, with a predominant band of ~35 kDa in size (as seen with freeze-thawed samples), although a faint band was also detected at 80 kDa. Contrary to previous blots, TG7 was detected in both keratinocyte and fibroblast soluble extracts and this was the case for all future blots. Taking this into account, samples in the previous blot may not have been extracted adequately.

The results obtained by Western blot analysis up to this point are not in agreement with previous murine *in situ* studies performed by Dr. H. Thomas (Thesis, 2004). These studies localised TG6 to the epithelium and TG7 to the dermal compartment. Consequently, confirmation by an alternative method was desirable and reverse transcription polymerase chain reaction (RT-PCR) analysis was performed on 1 μg total RNA (mRNA was selected by the inclusion of oligo dT primers - described in Section 2.7.1). These samples were obtained from the Ntert keratinocyte and HCA2 fibroblasts cell lines, using TG6 and 7 specific primers. mRNA from the two TG enzymes was indeed amplified from both cell lines (Fig. 17c), although TG6 was expressed in greater quantities from keratinocytes and TG7 from the dermal fibroblasts. This disparity with proteomic data would seem to suggest translational controls are involved with these isoforms and have already been proposed for TG2 (Clark *et al.*, 1959; Aeschlimann *et al.*, 1994).

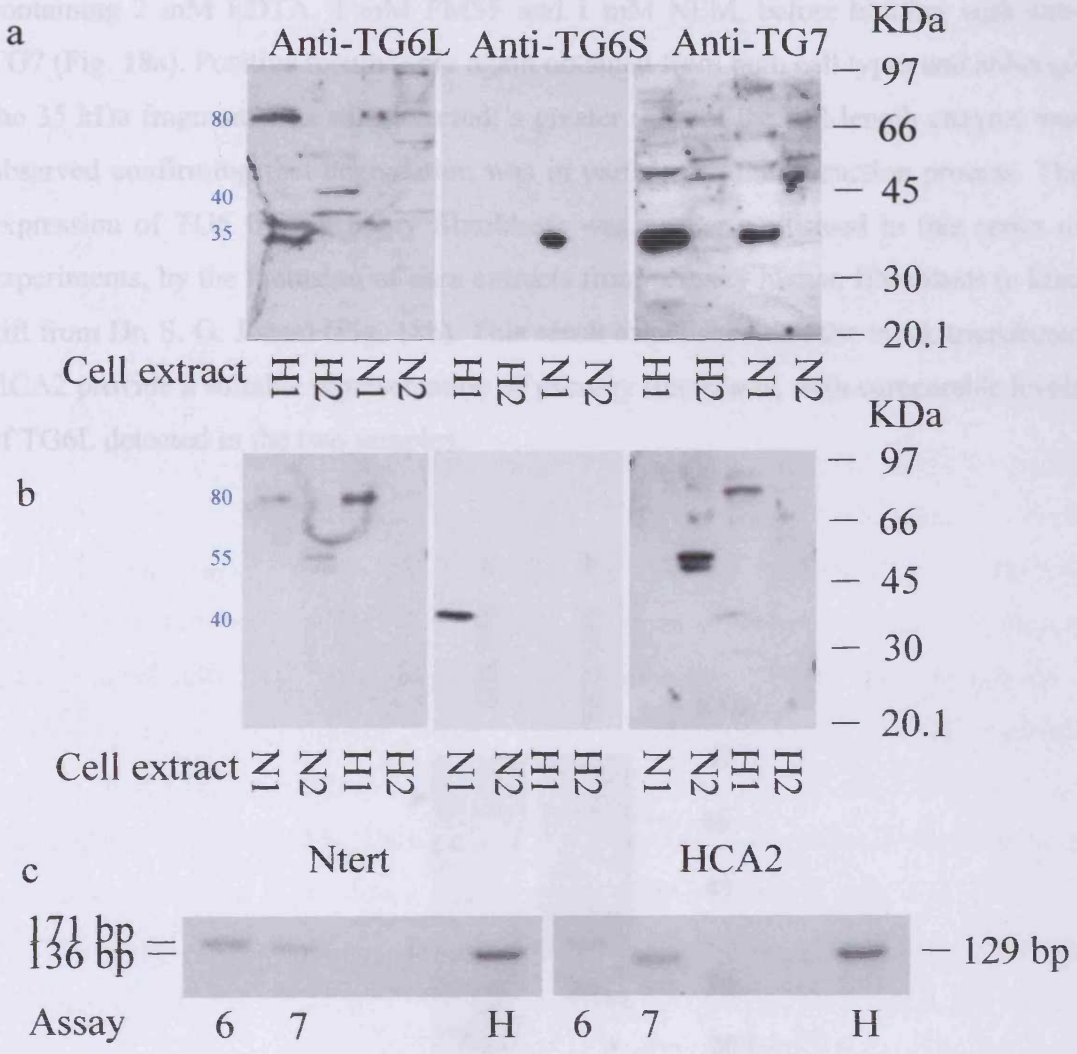

Fig. 17 Repeat of TG detection from keratinocyte and fibroblast cell lines following the removal of contaminating antibodies: (a) Protein extractions were carried out on Ntert keratinocytes (N) and HCA2 fibroblasts (H). 20 µg proteins extracted in 0.25 M sucrose containing 1 % v/v/ Triton X-100 (1) and 10 µg from the subsequent extraction in Tris buffer containing 1 % w/v SDS (2) were blotted with anti-TG6L. TG6S and TG7 purified on a 5% BSA blocked affinity column. (b) Previous immunoblots established using fresh keratinocyte and fibroblast extracts are included here as a comparison. Estimated protein masses are shown in blue. (c) RT PCR analysis of TG expression from keratinocytes and fibroblasts confirm TG6L and TG7 are expressed in both cell lines. 1µg total RNA underwent 2 cycles of reverse transcription before PCR amplification of TG6 (6) and TG7 (7). RP-S26 (H) was included as a housekeeping gene.

To address the issue of protein degradation, cells were extracted in 8 M urea containing 2 mM EDTA, 1 mM PMSF and 1 mM NEM, before blotting with anti-TG7 (Fig. 18a). Positive results were again obtained from both cell types and although the 35 kDa fragment was still detected, a greater ratio of the full-length enzyme was observed confirming that degradation was in part due to the extraction process. The expression of TG6 from primary fibroblasts was further confirmed in this series of experiments, by the inclusion of urea extracts from primary human fibroblasts (a kind gift from Dr. S. G. Jones) (Fig. 18b). This result established that the mock-transfected HCA2 provide a suitable representation of primary fibroblasts, with comparable levels of TG6L detected in the two samples.

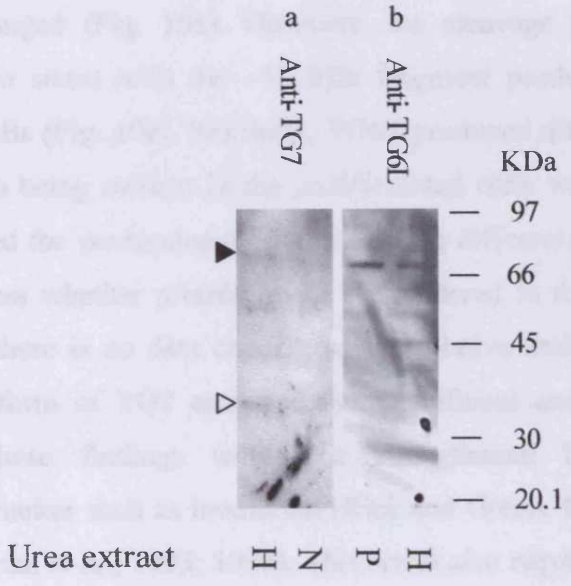

Fig. 18 Urea extractions of cellular proteins reduce the extent of TG7 degradation and confirm the expression of TG6L in primary human fibroblasts: (a) Proteins from HCA2 fibroblasts (H) and Ntert keratinocytes (N) were extracted in 8 M urea containing 2 mM EDTA, 1 mM PMSF and 1 mM NEM. 20 μg were incorporated in blots with anti-TG7. Although the 35 kDa fragment observed in previous work is still evident (hollow arrowhead) a higher proportion of the full-length protein is seen (solid arrowhead). (b) 20 μg 8 M urea extracts from human primary dermal fibroblasts (P) and mock transfected HCA2 fibroblasts (H) were immunoblotted with 5 μg/ml anti-TG6L. Proteins with a calculated size of ~80 kDa were detected in both cell types.

3.2.4.1 Alterations in transglutaminase cleavage with keratinocyte differentiation

Other TG enzymes expressed in mammalian epidermis (TG1, 3 and 5) have established roles in the formation of the cornified envelope and have been demonstrated to alter their expression with keratinocyte differentiation (Kim *et al.*, 1993; 1995a; 1995b; Aechlimann *et al.*, 1998; Candi *et al.*, 2001). Experiments were established to determine whether the expression of TG6 and 7 demonstrate similar differentiation-specific regulation. To analyse this, Ntert keratinocytes were sub-cultured and half the cells induced to differentiate by growing to confluency (Fig. 19a). Both RNA and protein extractions were performed for parallel RT-PCR and Western blotting studies. It was apparent that mRNA levels of both enzymes remain comparable following differentiation (Fig. 19b). Similarly TG6L protein levels remained unchanged (Fig. 19c). However, the cleavage pattern of TG7 differed between the two states with the ~35 kDa fragment producing intense staining in differentiated cells (Fig. 19c). Similarly, TG6S produced different sized fragments, a ~40 kDa protein being evident in the undifferented cells whilst a ~35 kDa cleavage product produced the predominant band following differentiation (Fig. 19c). It is not practical to assess whether protein levels have altered in the cases of the two latter enzymes since there is no data concerning the relative antibody affinities, however, the full-length form of TG7 extracted from confluent and sub-confluent cells are comparable. These findings would be strengthened by the inclusion of a differentiation marker such as involucrin (Rice and Green, 1979; Banks-Schlegel and Green, 1981; Crish *et al.*, 1993; 1998). This result also requires reassessment of some earlier blots, examining the fragment sizes produced in Fig 17, it seems likely that the Ntert keratinocyte cultures extracted for the later blot (Fig. 17a) had been grown to confluency in an attempt to produce high protein concentrations and consequently, the cells had undergone differentiation.

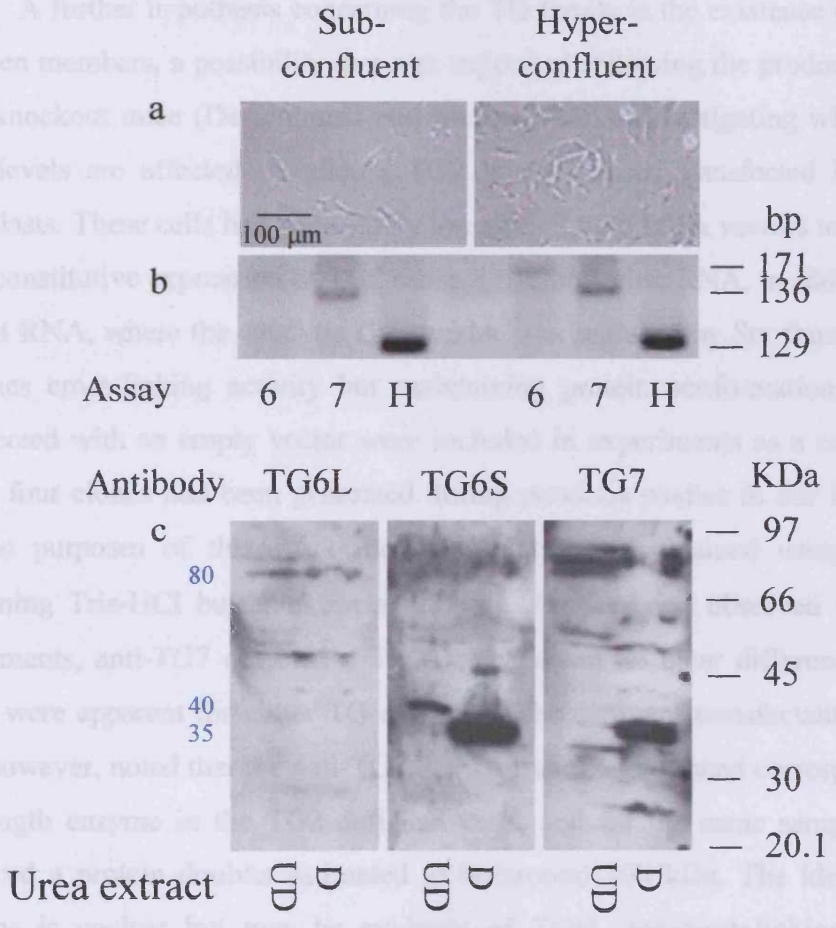

Fig. 19 Although TG6 and TG7 mRNA levels do not alter with keratinocyte differentiation, distinct protein fragments of TG6S and 7 are observed: Ntert keratinocytes were sub cultured (a) and either maintained in the undifferentiated state (Sub-confluent) or induced to differentiate by growing to past confluence (Hyper-confluent). (b) RT-PCR analysis from 1 µg total RNA obtained from undifferentiated and differentiated keratinocyte cultures demonstrate TG6L (6) and TG7 (7) mRNA levels do not alter. RP-S26 (H) was included as a housekeeping gene. (c) Immunoblots were carried out with anti-TG6L, TG6S and TG7 on 20 µg urea extracts from the undifferentiated (UD) and differentiated keratinocytes (D). No alterations with differentiation state were demonstrated in the TG6L protein. In contrast TG6S and TG7 both show a difference in protein cleavage with a predominant 35 kDa fragment observed in the differentiated cells. Estimated protein masses are shown in blue.

3.2.4.2 Possible compensatory mechanisms for altered transglutaminase 2 expression

A further hypothesis concerning the TG family is the existence of redundancy between members, a possibility that was supported following the production of viable TG2 knockout mice (De Laurenzi and Melino, 2001). Investigating whether TG6 or TG7 levels are affected by altered TG2 levels utilised transfected HCA2 human fibroblasts. These cells had been stably transfected with DNA vectors to produce high level constitutive expression of TG2 sense RNA, antisense RNA, in addition to a TG2 mutant RNA, where the catalytic Cys residue was replaced by Ser thus removing the enzymes cross-linking activity but maintaining protein conformation. HCA2 cells transfected with an empty vector were included in experiments as a control (mock). These four clones had been generated during previous studies in our laboratory and for the purposes of this work duplicate blots were obtained using the sucrose containing Tris-HCl buffer extracts (20 μg). As has been observed with previous experiments, anti-TG7 detected a 35 kDa, band but no clear differences in protein levels were apparent for either TG enzyme in the different transfectants (Fig. 20). It was, however, noted that the anti-TG7 demonstrated a faint band corresponding to the full-length enzyme in the TG2 deficient cells, and for the same sample anti-TG6L produced a protein doublet estimated to be around 100 kDa. The identity of these proteins is unclear but may be evidence of TG6L autocross-linking activity. To confirm the fibroblastic phenotypes remained unaltered and loading had been normalised, re-probing with monoclonal CUB7402 anti-TG2 (Neomarkers) and Coomassie Brilliant Blue R-250 staining was included (Fig. 20).

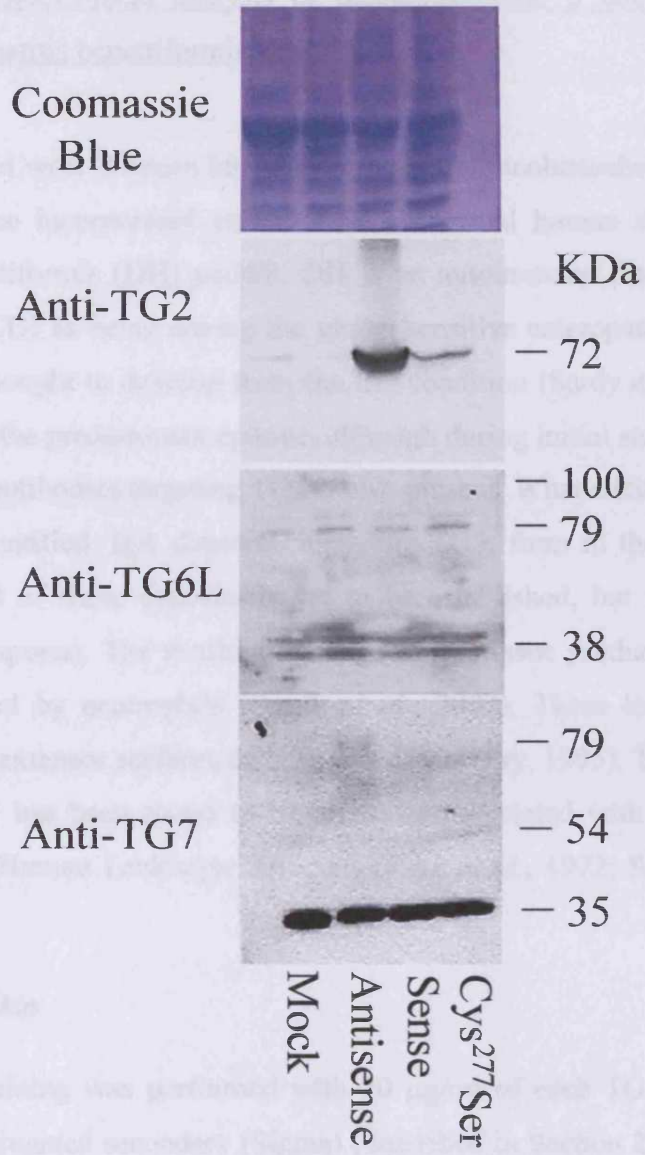

Fig. 20 TG6L and TG7 are not upregulated in TG2 deficient fibroblasts: Blotting with anti-TG6L and TG7 was carried out on stable HCA2 transfectants underexpressing TG2 (AS) as well as overexpressing the cross-linking active (S) and inactive ($Cys^{277}Ser$) form of the enzyme. Proteins were extracted in 0.25 M sucrose containing 1 % v/v Triton X-100 and 20 µg was included in SDS PAGE analysis. To demonstrate the fibroblast phenotype blots were re-probed with anti-TG2 (CUB7402) and normalised loading was established by Coomassie Brilliant Blue R-250 staining. Protein levels were not seen to compensate for TG2 although higher levels of the full length TG7 were seen in the TG2 deficient fibroblasts. As has been observed previously with this extraction process, TG7 underwent extensive breakdown.

3.2.5 Immunohistochemical analysis of transglutaminase 6 and 7 localisation in normal and dermatitis hepertiformis skin.

In parallel with Western blotting analysis, immunohistochemical studies were performed. These incorporated cryosections of normal human skin and skin of a dermatitis herpetiformis (DH) patient. DH is an autoimmune disorder classed with celiac disease (CD) as being among the gluten sensitive enteropathy (GSE) diseases. In fact, DH is thought to develop from the CD condition (Sardy *et al.*, 2002). In DH patients, TG3 is the predominant epitope, although during initial stages of the disorder a population of antibodies targeting TG2 is also present. What elicits this epitope-shift has not been identified. IgA deposits, including TG3, form in the papillary dermis. The exact effect of these deposits is yet to be established, but they may elicit an inflammatory response. The resulting damage to the tissue produces basal blistering heavily populated by neutrophils (Smith *et al.*, 2002). These lesions are typically located over the extensor surfaces of the major joints (Fry, 1995). The molecular basis for CD and DH has been found to be primarily associated with the HLA Class II genes encoding Human Leukocyte Antigens (Katz *et al.*, 1972; Sollid, 2000; Sardy, 2002).

3.2.5.1 Normal skin

Initial staining was performed with 20 μg/ml of each TG antibody detected with a FITC conjugated secondary (Sigma) (described in Section 2.2.1). As would be expected from Western blot studies, TG6L and TG7 produced staining within the dermis and throughout the epithelium, from the basal layer to the stratum corneum, including the epithelially derived hair follicles (Fig. 21a, c, d, e, g and h). In comparison, TG6S produced virtually undetectable staining (Fig. 21b) when compared to the negative controls (incubated with the secondary antibody only – Fig. 21f). This is contrary to Western blotting data within this study, which has identified TG6S expression in keratinocytes (confluent and sub-confluent). The reasons for this are unclear, possibly the fixation process was detrimental to the TG6S epitope.

Because of the inherent background fluorescence produced by skin, these experiments were repeated using HRP conjugated secondary antibodies in conjunction with the chromogen, 3-amin-9-ethyl-carbozide (AEC) (described in Section 2.2.3). These results largely concurred with the fluorescence staining and Western blot data. Both keratinocytes and fibroblasts stained positive with anti-TG6L and TG7 (Fig.22 a, c, d and e). In addition to this, anti-TG7 staining produced a gradient, with increased staining observed in suprabasal keratinocytes. Possibly this is due to the presence of the 35 kDa fragment which produced intense staining with this antibody in Western blotting analysis. Observations of dermal structures revealed sebaceous glands also stained positive for TG6L and TG7 (Fig. 22f and h), previous work involving rat skin has also identified the presence of TG2 within these glands (Haroon *et al.*, 1999). Anti-TG6S produced a positive result with this method. Staining was evident from the granular region of the epidermis to the stratum corneum surface, with the majority localised to the stratum corneum (Fig. 22b). Despite this antibody producing positive results from undifferentiated keratinocyte extracts in Western blots, the spinous region and basal cells stained negative. This would suggest that in its native conformation, this epitope may be unavailable, possibly due to protein interactions and, following differentiation, cleavage of this protein unmasks the site.

3.2.5.2 Dermatitis herpertiformis skin

Experiments utilising fluorescence detection of the FITC conjugated secondary antibody demonstrated the distribution of the TG7 isoform remained unchanged in this condition. However, comparatively intense staining was evident throughout the epidermis, suggesting upregulation of the enzyme (Fig. 21k). This is an interesting result, suggesting a possible secondary role for TG7 in this disease. It is unlikely to be providing a compensatory function since it has been observed that TG3 expression within the epidermis of DH patients remains unaltered (Sardy *et al.*, 2002). The staining pattern produced with anti-TG6L was diffuse in comparison with the normal skin sections and may be slightly downregulated (Fig. 21i). A function for this in the DH condition remains to be ascertained.

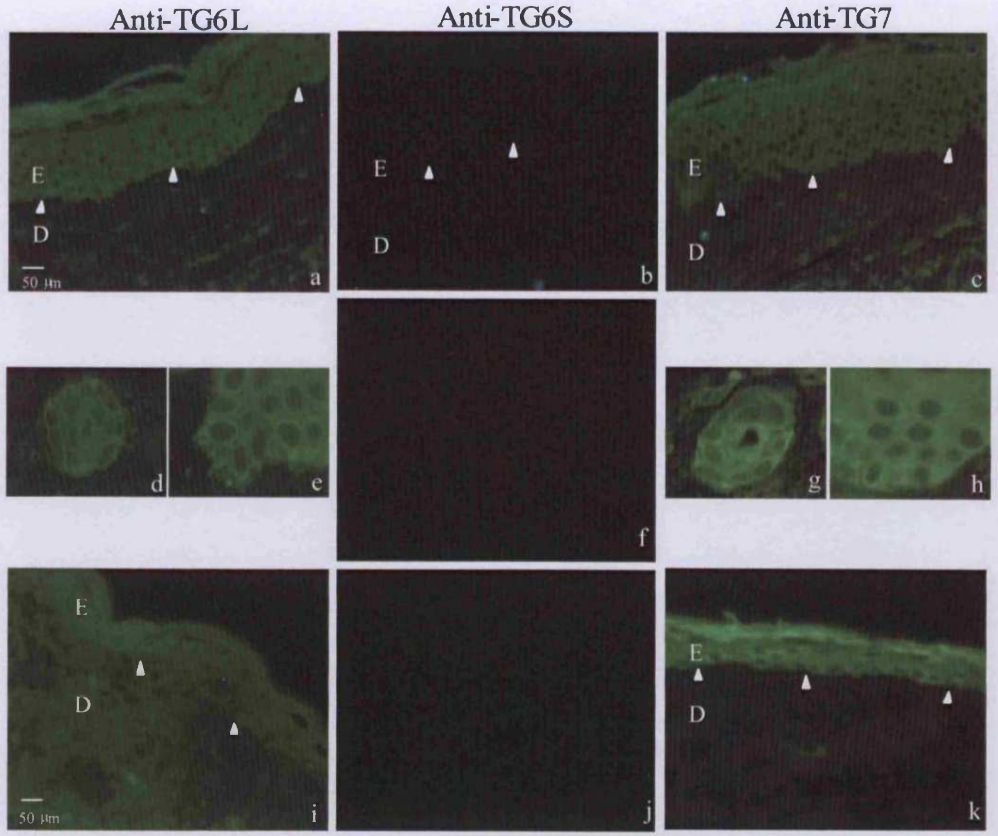

Fig. 21 Immunohistochemical analysis of TG expression in normal skin and that of a dermatitis herpetiformis (DH) patient (Fluorescence): 8 µm frozen sections of human skin (normal and DH patient) were probed with 20 µg/ml of each anti-TG (6L, 6S and 7). Bound antibody was detected with FITC conjugated anti-goat. The epidermal region is designated E and the dermal compartment D; the basement membrane is identified by arrowheads. Virtually no fluorescence was observed with anti-TG6S. In contrast anti-TG6L and anti-TG7 produced staining in both the dermal and epidermal compartments. In the case of TG7 staining within the epidermis was increased in the DH sample suggesting a possible secondary role in this disorder. (a) Normal skin anti-TG6L (b) Normal skin anti-TG6S (c) Normal skin anti-TG7 (d) Normal skin, high magnification hair follicle anti-TG6L (e) Normal skin, high magnification epidermis anti-TG6L (f) Normal skin control (secondary antibody only) (g) Normal skin, high magnification hair follicle anti-TG7 (h) Normal skin, high magnification epidermis anti-TG7 (i) DH anti-TG6L (j) DH TG6S (k) DH anti-TG7.

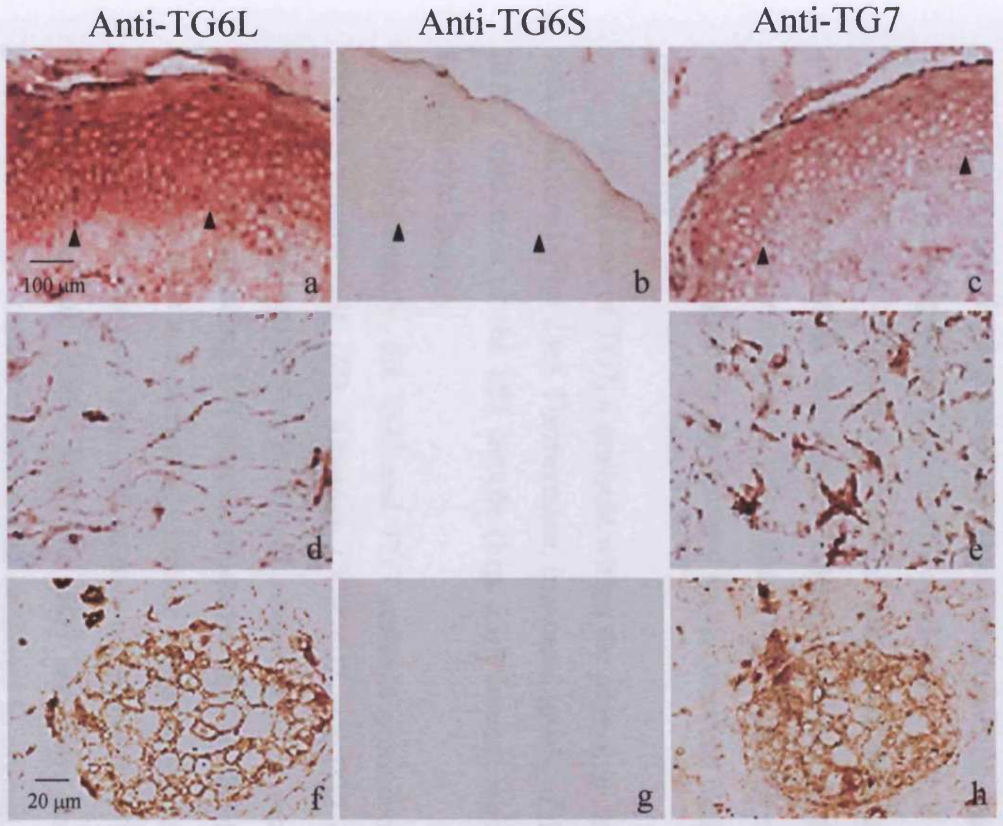

Fig. 22 Immunohistochemical analysis of TG expression in normal skin (AEC): 8 μm frozen sections of normal human skin were probed with 20 μg/ml of each anti-TG (6L, 6S and 7). Bound antibody was detected with horse radish peroxidase (HRP) conjugated anti goat and detected using AEC colour development. The basement membrane region is denoted by arrowheads. Results largely agreed with previous immunohistochemical studies, anti-TG6S produced staining from the granular region of the epidermis. anti-TG6l and TG7 produced staining throughout the epidermis and also produced positive results from the dermal fibroblasts. (a) Normal epidermis anti-TG6L (b) Normal epidermis anti-TG6S (c) Normal epidermis TG7 (d) Normal dermis anti-TG6L (e) Normal dermis anti-TG7 (f) High magnification sebaceous gland anti-TG6L (g) Negative control (h) High magnification sebaceous gland anti-TG7.

Finally, an experiment was performed to confirm the observations made with the DH samples, including TG2 and TG3 controls (Fig. 23). The staining produced in initial experiments with TG6L, 6S and 7 was successfully repeated (Fig. 23c,d, e, h, i and j).

TG6L was expressed throughout the dermis and epidermis in native and DH samples. But once again the DH sample exhibited a more diffuse staining pattern, appearing to stain the dermal ECM. These results would also seem to confirm a slight reduction in staining levels with the DH condition.

TG6S was detected in the late stages of differentiation in normal skin, predominantly staining the stratum corneum. However, the negative control also produces some staining within this region (Fig. 23p). The corresponding DH sample produced no staining above background levels observed in the control (Fig. 23h and q respectively).

In the case of TG7, a gradient within the phenotypically normal skin epidermis was confirmed (Fig. 23e). Furthermore, increased levels of this isoform were detected in the epidermis of the DH sample (Fig. 23j). Intense staining was observed in all keratinocyte layers.

Unfortunately, the TG2 and TG3 controls produced results in opposition to previous studies (Fig. 24). Although CUB7402 anti-TG2 (1:50) produced staining within the basal keratinocytes in normal human skin, the section quality is poor (Fig. 23a). The corresponding DH sample produced high levels of staining, which was not localised to the cells and particularly intense colour development was observed at the dermo-epidermal junction (Fig. 23f) as may be expected of TG2 (Aeschlimann *et al.*, 1998; Haroon *et al.*, 1999). With the TG3 antibody, staining from the stratum granulosum to the stratum corneum was observed in normal skin, as is characteristic of this isoform (Fig. 23b). However the intensity of the staining was faint and no staining was evident with this antibody in the DH sample (Fig. 23g). This may suggest a problem with the antibody aliquot used.

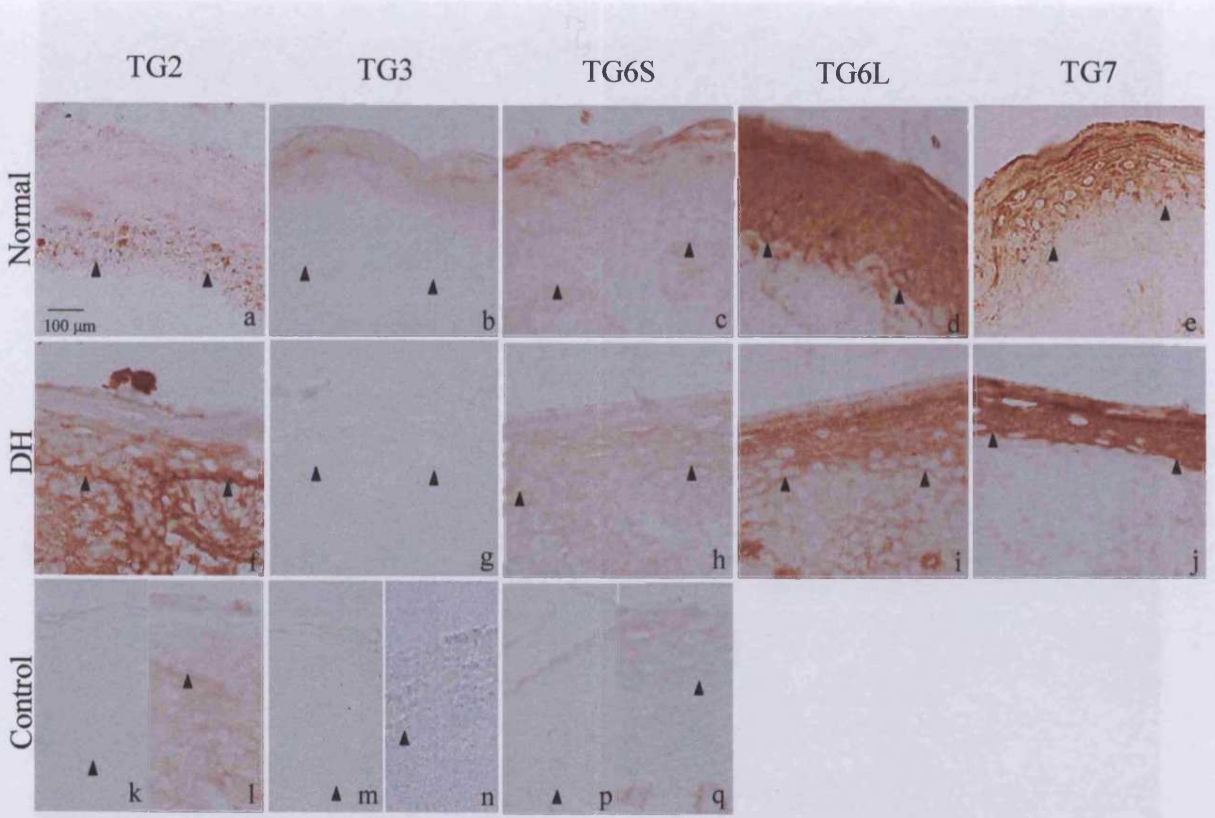

Fig. 23 Immunohistochemical analysis of TG expression in normal skin and that of a dermatitis herpetiformis (DH) patient (AEC): 8 µm frozen sections of human skin (normal and DH patient) were probed with 20 µg/ml of each anti-TG (6L, 6S and 7) with anti-TG2 and TG3 included as controls. Bound antibody was detected with HRP conjugated secondary antibodies and colour developed using the AEC system, the basement membrane region is denoted by arrowheads. Secondary antibodies alone were included as negative controls. (a) Normal skin, anti-TG2 (b) Normal skin, anti-TG3 (c) Normal skin, anti-TG6S (d) Normal skin, anti-TG6L (e) Normal skin, anti-TG7 (f) DH patient, anti-TG (g) DH patient, anti-TG3 (h) DH patient, anti-TG6S (i) DH patient, anti-TG6L (j) DH patient, anti-TG7 (k) Normal skin control, anti mouse (TG2) (l) DH patient control, anti mouse (TG2) (m) Normal skin control, anti rabbit (TG3) (n) DH patient control, anti rabbit (TG3) (p) Normal skin control, anti goat (TG6S, 6L and 7) (q) DH patient control, anti goat (TG6S, 6L and 7).

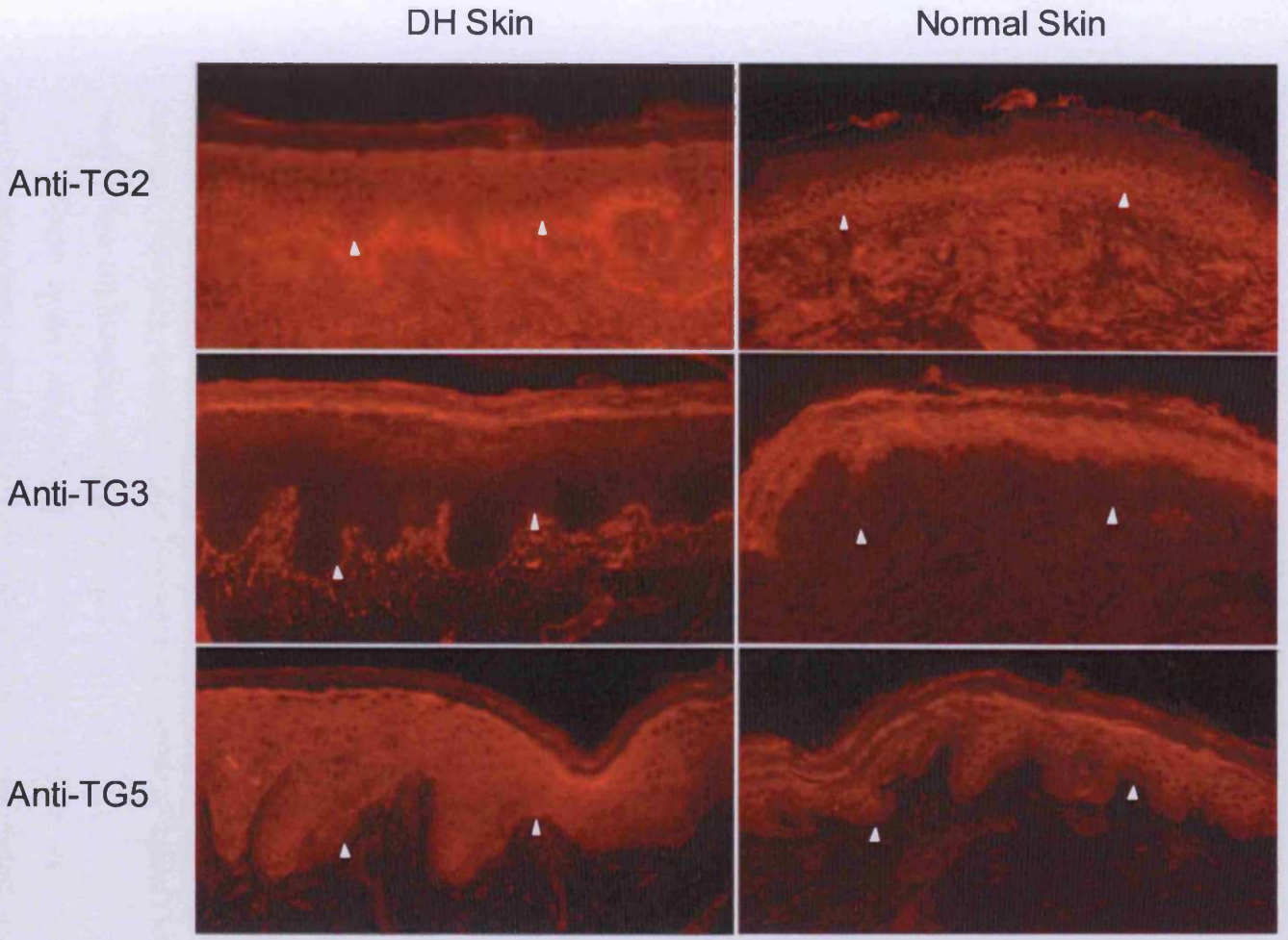

Fig. 24 Comparison of TG2, 3 and 5 expression in normal and DH skin: Immunohistochemical analysis of TG2, 3 and 5 proteins, detected with Texas Red conjugated secondary antibodies (Images provided by Prof. D. Aeschlimann, University of Wales, Cardiff). The dermo-epidermal junction is denoted by arrowheads. TG3 aggregates are evident in the papillary dermis of the DH patient.

3.3 Conclusions and future work

In the course of these studies antibodies were successfully raised against peptides designed from TG6 and TG7 sequence data, following unsuccessful attempts to isolate a recombinant form of the TG7 enzyme.

Western blotting studies required relatively high quantities of protein loading to obtain detectable levels of these TGs (20 μg). TG6L and TG7 were found to be expressed in both keratinocytes and fibroblasts, an observation confirmed by RT-PCR and immunohistochemical studies. It was also noted that TG7 is highly susceptible to degradation, particularly when extracted from fibroblasts. Although this degradation can be reduced by extraction with a chaotropic agent, such as urea, it is not completely removed and may be present *in vivo*. Whether such a fragment is active is not dealt with in these studies. The fragment size does correspond to the catalytic core of TG7 and the epitope the anti-TG7 serum was raised against is adjacent to this domain. Literature regarding the cleavage of TG enzymes reports differing effects on cross-linking activity. The cleavage of TG1 and TG3 within this flexible loop region has demonstrated significantly increased activity (Steinert *et al.*, 1996a; Kim *et al.*, 1990; Kim *et al.*, 1993). In contrast, a loss of activity has been reported in FXIII and TG2 following cleavage or deletion of the β-barrels (Takahashi *et al.*, 1986; Lai *et al.*, 1996). Conclusive evidence would require isolation of this fragment for TG activity assay with conventional substrates such as putrescine or casein. Moreover, resolving cell extracts containing such TG fragments under non-reducing conditions would identify whether or not these fragments remain associated, as is the case following cleavage of TG1 and TG3 *in vivo*.

The predicted full-length form of TG6S (70 kDa) was not detected in any of these studies, instead a 35-40 kDa protein was observed. This is most likely a cleaved form of the enzyme (corresponding to the calculated size of this enzymes catalytic domain). However, retrieval of the fragment by a column-linked form of the antibody would allow confirmation by sequencing.

These studies also aimed to address the possible role of these enzymes in family redundancy and keratinocyte differentiation. The results produced no strong evidence that TG6L or TG7 provide compensation for loss of TG2 expression. However there was evidence of altered TG6S and TG7 cleavage with keratinocyte

differentiation. Whether these fragments also demonstrate altered activity or binding properties would require further investigation, as discussed above.

Finally, immunohistochemical experiments have detected the TG6L and TG7 proteins within dermal and epidermal compartments. TG6S was not consistently detected within normal human epidermis and never in the basal cells or stratum spinosum, despite contradictory data obtained by Western blotting. Furthermore, immunohistochemical analysis utilised relatively high concentrations of primary antibodies (20 μg/ml) and may be indicative of low antibody affinities for TG6L, TG6S and TG7 in their native conformations. Expansion of these immunohistochemical studies consistently suggested TG7 is upregulated within the epidermis of this DH patient. In contrast TG6L and TG6S could be downregulated to a lesser extent. To confirm whether this altered expression is truly a feature of DH pathology, studies should be extended to include further samples. If this were the case it would provide an interesting avenue for further work, providing some insight into the pathological pathways of this condition and possible therapeutic targets.

Chapter 4:
Identifying potential transglutaminase substrates

4.1 Introduction

Despite their high sequence homology, transglutaminases (TGs) demonstrate exquisite substrate specificities, particularly concerning acyl donors. It has been reported that isoforms cross-linking the same protein can target different glutamine residues (Candi *et al.*, 1995, 1999; Tarcsa *et al.*, 1998; Steinert *et al.*, 1999) and demonstrate distinct affinities (Gorman *et al.*, 1981; 1984; Candi *et al.*, 1995). In contrast, acyl acceptors are derived from a wider pool of substrates, including polyamines, such as spermidine (Folk *et al.*, 1980; Martinet *et al.*, 1990). It has been suggested that these acyl acceptors approach the enzyme from the direction of the active site, whilst acyl donors may approach from the C-terminal β-barrels (Lorand and Graham, 2003). It is well documented that the N-and C-terminal regions demonstrate the lowest levels of sequence homology throughout the enzyme family and may account for differences in target substrates between the isoforms (Greenberg *et al.*, 1991; Reichert *et al.*, 1993; Kim *et al.*, 1995a).

Over recent years, numerous TG2 substrates have been identified both *in vitro* (Summarised in Table. 1) and to a lesser extent *in vivo* (Nemes *et al.*, 1997; Orru *et al.*, 2003). In contrast, there is little data available regarding TG6 and TG7 substrates. Therefore, this chapter of work was established to identify fibroblast and keratinocyte proteins with the potential to bind these isoforms. This study incorporated two experimental approaches. The first being immunoprecipitation, utilising the peptide antibodies characterised in Chapter 3. The second more specifically addressed the role of β-barrel domains in protein interactions, using recombinant TG proteins (comprising of GST tagged C-terminal domains) to select proteins from cellular extracts.

Protein substrate	Reference
Actin	(Safer *et al.*, 1997)
Aldolase	(Lee *et al.*, 1992)
Amyloid βA4	(Rasmussen *et al.*, 1994; Jensen *et al.*, 1995)
BHMT	(Ichikawa *et al.*, 2004)
BiP protein	(Orru *et al.*, 2003)
C1 inhibitor	(Hauert *et al.*, 2000)
C-CAM	(Hunter *et al.*, 1998)
Cementoin	(Nara *et al.*, 1994)
Chaperonin subunit 3	(Orru *et al.*, 2003)
Clathrin heavy chain	(Orru *et al.*, 2003)
Collagen III, V, XI	(Bowness *et al.*, 1987; Kleman *et al.*, 1995)
Crystallin βA3	(Berbers *et al.*, 1984; Groenen *et al.*, 1994)
Cytochrome *c*	(Butler and Landon, 1981)
Dihydropyrimidinase-2	(Orru *et al.*, 2003)
DNase γ	(Orru *et al.*, 2003)
Elongation factor 1α	(Orru *et al.*, 2003)
Elongation factor 1γ	(Orru *et al.*, 2003)
EMP b3	(Murthy *et al.*, 1994)
β-Endorphin	(Pucci *et al.*, 1988)
ERM	(Orru *et al.*, 2003)
Fatty acid synthase	(Orru *et al.*, 2003)
F-box only protein	(Orru *et al.*, 2003)
Fibrinogen A	(Ritchie *et al.*, 2000)
Galectin-3	(Mahoney *et al.*, 2000)
GAPDH	(Ruoppolo *et al.*, 2003)
Glucagon	(Folk and Cole, 1965)
α_2HS-glycoprotein	(Kaartinen and McKee, 2002)
Heat shock 60 kDa	(Orru *et al.*, 2003)
Heat shock 70 kDa	(Orru *et al.*, 2003)
Heat shock 70/90	(Orru *et al.*, 2003)
Heat shock 90 kDa	(Orru *et al.*, 2003)
Huntingtin	(Kahlem *et al.*, 1998)
Histone H1	(Ballestar *et al.*, 1996; Cooper *et al.*, 2000)
IGFBP-1	(Sakai *et al.*, 2001)
Importin β1 subunit	(Orru *et al.*, 2003)
Insulin A chain	(Folk and Cole, 1965)
KGDHC	(Cooper *et al.*, 1997)
Lipocortin I	(Ando *et al.*, 1991)
MAGP-1	(Trask *et al.*, 2001)
MBP	(Selkoe *et al.*, 1982)
Midkine	(Kojima *et al.*, 1997)
Myosin	(Orru *et al.*, 2003)
Nidogen	(Aeschlimann *et al.*, 1992)
NSB	(Orru *et al.*, 2003)
Osteonectin	(Hohenadl *et al.*, 1995)
Osteopontin	(Sorensen *et al.*, 1994)
Periplakin	(Aho, 2004)
PGD	(Orru *et al.*, 2003)
Phosphorylation kinase	(Nadeau *et al.*, 1998)
PLA_2	(Cordell-Miele *et al.*, 1990)
PSA	(Quash *et al.*, 2000)
RAP	(Rasmussen *et al.*, 1999)
RhoA	(Schmidt *et al.*, 1998)
40 S Ribosomal SA	(Orru *et al.*, 2003)
ROCK-2	(Orru *et al.*, 2003)
Sialoprotein	(Kaartinen and McKee, 2002)
Spectrin α	(Orru *et al.*, 2003)

Statherin	(Yao *et al.*, 2000)
Substance P	(Porta *et al.*, 1988)
Synapsin	(Facchiano *et al.*, 1993)
α-Synuclein	(Jensen *et al.*, 1995)
Tau	(Murthy *et al.*, 1998)
T-complex protein	(Orru *et al.*, 2003)
Thymosin β_4	(Safer *et al.*, 1997; Huff *et al.*, 1999)
Thyroglobulin	(Saber-Lichtenberg *et al.*, 2000)
β-Tubulin	(Maccioni and Arechaga, 1986)
Tumour rejection ag-1	(Orru *et al.*, 2003)
Uteroglobin	(Mukherjee *et al.*, 1988)
UV RAD23	(Orru *et al.*, 2003)
Valosin	(Orru *et al.*, 2003)
Vigilin	(Orru *et al.*, 2003)
Vimentin	(Clement *et al.*, 1998)
VIP	(Esposito *et al.*, 1999)

Table. 1 *In vitro* TG2 protein substrates identified by structural proteomics: BHMT, bentaine-homocysteine S-methyltransferase; EMP b-3, erythrocyte membrane protein band 3; ERM, ezrin-radixin-moesin binding phosphoprotein 50; KGDH; α-ketoglutarate dehydrogenase; IGFBP-1, insulin-like growth factor-binding protein 1; MAGP-1, microfibril associated glycoprotein-1; MBP, myelin basic protein; NSB, nuclease sensitive element binding protein-1; PGD, phosphoglycerate dehydrogenase; PLA_2, phospholipase A_2; Pro-CpU, procarboxypeptidase U; PSA, prostate-specific antigen; RAP, receptor-associated protein; ROCK-2, Rho-associated coiled-coil-containing protein kinase 2; UV RAD23, UV excision repair protein RAD23; VIP, vasoactive intestinal peptide. Adapted from (Esposito and Caputo, 2004).

4.2 Results

4.2.1 Immunoprecipitation of transglutaminase-protein complexes from fibroblast and keratinocyte extracts

To ensure a broad based approach in identifying potential TG substrates, mock-transfected HCA2 fibroblasts and Ntert keratinocyte cells cultured in the absence of feeder cells were metabolically labelled with 10 μCi/ml ^{35}S-Cys/Met (Redivue™ Pro-mix™, Amersham Pharmacia, described in Section 2.3.2). This labelling step was allowed to continue for a period of 24 h followed by a further 24 h chasing. In the case of HCA2 cells, the culture was subsequently divided, half the cells underwent 1 h culturing in suspension whilst the remainder were allowed to spread on type I collagen-coated plates for the same period of time. This aimed to identify potential interactions produced upon cytoskeleton remodelling.^{35}S-labelled proteins were extracted in a detergent containing Buffer A [20 mM N-2-hydroxyethlpiperazine-N'-2-ethane sulphonic acid monosodium salt (HEPES), 150 mM NaCl, 1% v/v Triton X-100, 1% w/v Sodium deoxycholate, 0.1% Sodium dodecyl sulfate, (SDS), 10% glycerol, 1.5mM MgCl, 1 mM Ethyl glycol-bis(2-aminoethylether)-N,N,N',N'-tetraacetic acid (EGTA), 1 mM Na_3VO_4, 10 mM Na pyrophosphate, 100mM NaF, 10 μg/ml leupeptin, 100 U aprotinin, 1 mM Phenylmethyl sulphonylfluoride (PMSF), pH 7.4]. For analysis of cell extracts, equal amounts of labelled protein were included based on cpm measurements. In an attempt to reduce non-specific binding cell extracts were pre-adsorbed with G Sepharose (Amersham Pharmacia) (described in Section 2.6.1).

The recovered supernatants were divided into four aliquots, which underwent immunoprecipitation (IP) with 1 μg of anti-TG6L, anti-TG7 and anti-TG2 (CUB7402, Neomarkers) antibodies. In addition, an anti-pan cytokeratin (Sigma) was included with the Ntert extract as a positive control and finally a non-specific immunoglobulin (Ig) was incubated with both suspended and adherent fibroblast cultures as a negative control. Ig complexes were precipitated by incubation with G-Sepharose and retrieved by boiling in a loading buffer containing sodium dodecyl sulfate (SDS). Proteins were separated by SDS-polyacrlyamide gel electrophoresis (PAGE) and analysed using fluorography (described in Section 2.6.3).

Results clearly indicated that protein levels were insufficient for detection (data not shown). A faint band of ~ 45 kDa was visible in the anti-TG7 precipitate from Ntert keratinocyte extract. However, there was no additional band corresponding to the intact TG7 enzyme. Unexpectedly, there were also no results obtained with either the anti-pan cytokeratin or the anti-TG2 antibodies.

Since this method had been used previously in our laboratory to precipitate TG2 from HCA2 extracts this negative result raised some concerns regarding the experiment. A cold repeat of the TG2 IP from spread fibroblasts (seeded onto type I collagen) was carried out (Fig. 1). Immunoblotting (described in Section 2.1.2) revealed that this IP method successfully precipitated the TG2 enzyme. Three bands were detected, including an ~80 kDa protein corresponding to the full-length enzyme with additional bands corresponding to the heavy and light chains of the antibody employed for precipitation.

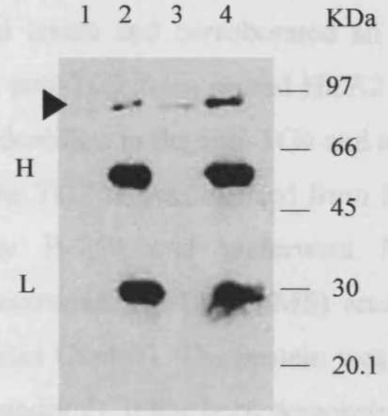

Fig. 1 Assessment of immunoprecipitation methodology: Because of restrictions within the designated radioactivity area an alteration to the original protocol was necessary. The mechanical mixing of the antibody with cell extract over night at 4°C was not possible. Consequently a cold repeat using 1 µg monoclonal anti-TG2 and 500 µg HCA2 extract was set up with these two methods with the exclusion or inclusion of mechanical mixing (lanes 1-2 and 3-4 respectively). Samples included the unbound supernatant proteins (lanes 1 and 3) and bound proteins retrieved by boiling in loading buffer (lanes 2 and 4). Immunodetection was carried out with the same monoclonal TG2 antibody and a HRP conjugated anti-mouse secondary. Full-length TG2 is indicated with an arrowhead, antibody chains are designated H (heavy) and L (light).

4.2.1.1 Anti-transglutaminase 2 precipitates greater quantities of vimentin from HCA2 fibroblasts that have undergone spreading

Since the protein precipitation method was found to be satisfactory, the step was taken to increase the amount of labelled protein included in repeat experiments by 3-fold, (i.e. 1.05 x 10^6 cpm/IP). Despite pre-adsorption with G Sepharose, this produced high background levels (Fig. 2a). Although TG IPs from the HCA2 fibroblasts cultured in suspension produced more intense bands than the non-specific Ig control, the film was overexposed, making it difficult to discern differences between samples. It was observed that a protein calculated to be ~60 kDa in size produced a band of greater intensity in the TG2 IP from spread HCA2 cells, compared to other IPs from the same extract or the TG2 IP from the other two cell extracts.

To confirm this, the gel was exposed to a phosphor screen (Amersham Pharmacia) for 48 h at room temperature (RT) before analysis using the Typhoon 9400 variable mode imager system (Amersham Pharmacia). This shortened exposure successfully reduced background levels and corroborated an increased level of the 60 kDa protein precipitated with anti-TG2 from spread HCA2 fibroblast extract (Fig. 2b). No specific bands could be identified in the anti-TG6 and anti-TG7 precipitates.

The 60 kDa band from the TG2 IP was excised from SDS-PAGE gel stained with Coomassie Brilliant Blue R-250 and underwent Matrix-Assisted Laser Desorption Ionisation/ Mass Spectrometry (MALDI/MS) analysis (work performed by M. Morton, University of Wales Cardiff). The protein was identified as vimentin with a Mowse score of 228 (Appendix 2). It has been demonstrated in primary murine fibroblasts that TG2 binds an antigen within with intermediate filaments that colocalises with vimentin (Trejo-Skalli *et al.*, 1995). This is also true of TG5 in transfected NHEK keratinocytes (Candi *et al.*, 2001). *In vitro* experiments have confirmed the suitability of vimentin as a TG2 substrate (Clement *et al.*, 1998). This does, however, raise the question of how the alteration in culture conditions would affect the binding of TG2. The 'catch-all' approach of the extraction buffer excludes protein translocalisation and the 1 h incubation makes significant protein upregulation unlikely. This would suggest a possible role for the removal of a competing substrate or post-translational modification, since it has been observed that the TG-reactive sites of vimentin fall within regions prone to phosphorylation (Clement *et al.*, 1998).

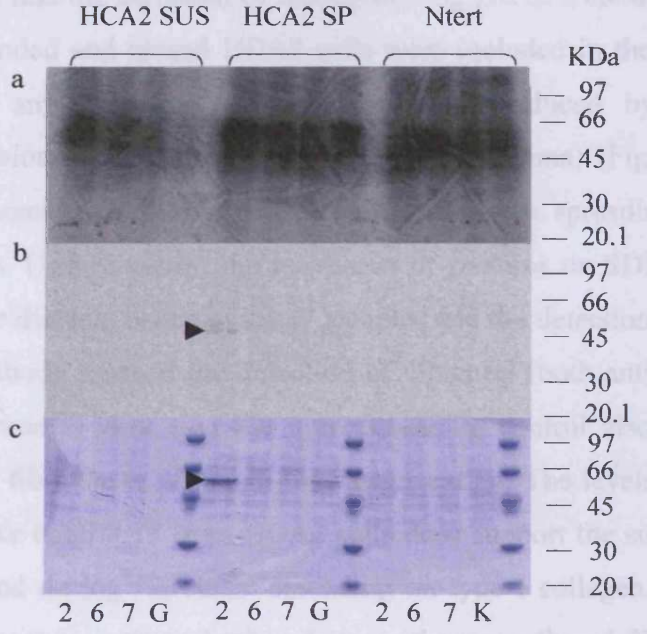

Fig. 2 Immunoprecipitations of TG-protein complexes from fibroblast and keratinocyte cell lines: HCA2 fibroblasts and Ntert keratinocytes were metabolically labelled over a period of 24 h in the presence of 10 µci/ml Redivue pro-mix. This was followed by 24 h chasing in serum-free culture conditions. Subsequently fibroblasts were subcultured, half undergoing 1 h culture in suspension (SUS) and the remainder allowed to adhere and spread on type I collagen-coated plates (SP). ^{35}S labelled proteins were extracted in Buffer A and cell extracts producing 1.05 x 10^7 cpm were immunoprecipitated with 1 µg monoclonal anti-TG2 (2), anti-TG6L (6) or anti-TG7 (7). Anti-pan cytokeratin (K) and HRP conjugated anti-goat (non-specific Ig) (G) were included as controls. Antibody-protein complexes were bound by 50 µl G Sepharose. Following retrieval by boiling in an equal volume of SDS-containing loading buffer 15 µl aliquots were resolved across 4-20% Tris-Glycine gels.
(a) Exposure to Kodak film following treatment with the chemical fluor sodium salicylate (1 week, -80°C) (b) Exposure to Kodak phosphor screen (48 h RT) (c) Coomassie Brilliant Blue R-250 detection of proteins. The protein band excised from the gel and identified by MALDI/MS analysis as vimentin is marked by an arrowhead.

The TG2 IP from the two HCA2 cultures were repeated with 800 μg unlabelled cell extract and the inclusion of non-specific Ig IPs as a control. Untreated cell extracts of suspended and spread HCA2 cells were included in the SDS-PAGE analysis to identify any alteration of vimentin levels induced by cell-matrix interactions. Immunoblotting with anti-vimentin antibody (Sigma) (Fig. 3) revealed there was a slight increase in vimentin levels following 1 h spreading on type I collagen-coated plates. Unfortunately, the resolution of proteins on SDS PAGE was insufficient to produce discrete bands in the IP samples and the detection of the heavy chain of the TG2 antibody masked the detection of vimentin (both antibodies being raised in mouse). It was evident that the non-specific Ig control also precipitated vimentin from HCA2 fibroblasts, although to a lesser extent. The levels of vimentin detected in the negative control IP from HCA2 cells does support the suggestion that vimentin is upregulated during fibroblast spreading on type I collagen. Conversely, this structural protein may be actively broken down in the non-adhered fibroblasts.

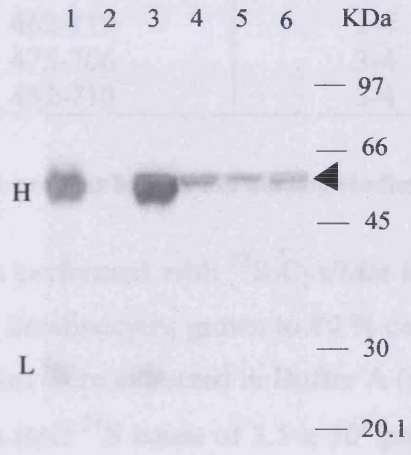

Fig. 3 Vimentin levels increase during fibroblast spreading: 800 μg extractions of HCA2 fibroblasts cultured in suspension (lane 1 and 2) and on type I collagen coated plates (lane 3 and 4) were immunoprecipitated with 1 μg monoclonal anti-TG2 (lane 1 and 3) or HRP conjugated anti-mouse as a non-specific Ig (lane 2 and 4). Precipitated proteins were detected by immunoblotting with anti-vimentin. The band corresponding to vimentin is marked with an arrowhead, antibody chains are designated H (heavy) and L (light). 10 μg untreated cell extracts of fibroblasts cultured in suspension and on type I collagen coated plates were included to detect alterations in vimentin levels with culture conditions (lane 5 and 6).

4.2.2 Protein binding of transglutaminase C-terminal β-barrel domains

The following experiments utilised stocks of recombinant TGs expressed from BL21 *E.coli* with an N-terminal GST tag incorporated (Table. 2). In the case of TG5, 6 (long form) and 7, these proteins included the two C-terminal β-barrels domains and start in the loop connecting these domains to the catalytic core. In the case of TG2, the full-length enzyme was expressed. These recombinant proteins were immobilised onto unpacked glutathione-linked Sepharose via the N-terminal GST tag using a batch purification method (described in Section 2.6.2). This experimental approach had the advantage of specifically analysing the role of the β-barrel domains in protein interactions and also allowed the use of TG concentrations far in excess of those *in vivo*.

TG	Amino acids incorporated	Complete domains spanned	Size of fusion protein / kDa
2	1-686	1-4	103
5	462-719	3-4	55
6	475-706	3-4	53
7	452-710	3-4	55

Table 2. Summary of TG fusion proteins included in binding studies.

An initial study was performed with ^{35}S-Cys/Met labelled cell extracts from HCA2 fibroblasts and Ntert keratinocytes grown to 80 % confluency on tissue culture grade plastic. Cellular proteins were extracted in Buffer A (described in section 4.2.1) and normalised to include a total ^{35}S count of 3.5 x 10^6 per minute, with each 50 µl aliquot of TG coupled Sepharose. To reduce non-specific binding, cell extracts were pre-incubated with Sepharose-immobilised GST alone (described in Section 2.6.2). For each cell extract duplicate samples of the full-length TG2-Sepharose was set up in the presence or absence of 1 mM guanosine triphosphate (GTP). This nucleotide is known to negatively regulate the cross-linking activity of TG2 (Shenping *et al.*, 2001) by inducing a conformational change that burries the active site residues. Proteins retrieved from the TG-Sepharose matrices were resolved by SDS-PAGE analysis and subjected to fluorography as described previously (Fig. 4).

Examination of crude HCA2 extract and its supernatant following incubation with the GST tag-Sepharose matrix, demonstrated the success of protein labelling and the low levels of non-specific binding. With regards to protein-retrieval by the TG fusion proteins, a predominant band calculated to be ~40 kDa was observed in HCA2 fibroblast samples (Fig. 4). It was present in the greatest quantity in the eluant from the TG7 column and absent from that of TG6. In fact, immobilised TG6 did not bind any proteins at detectable levels. It was also noted that the presence of 1 mM GTP did not alter the binding of this unidentified protein to the TG2 column, suggesting the conformation conferring cross-linking activity is not required for this interaction. Protein-capture from the Ntert extract produced two bands, the first estimated to be 55 kDa and the second 45 kDa (fig. 4). Again TG6 demonstrated much lower levels of binding and the inclusion of GTP with TG2 had no effect. The levels of proteins retrieved from the TG7 column were comparable to those from the TG5 column. Significantly TG5 is the isoform that shares the highest level of homology with TG7.

It was observed that the four different TG enzymes did not produce significantly different profiles of protein binding, as might be expected if the β-barrel domains are involved in substrate selection.

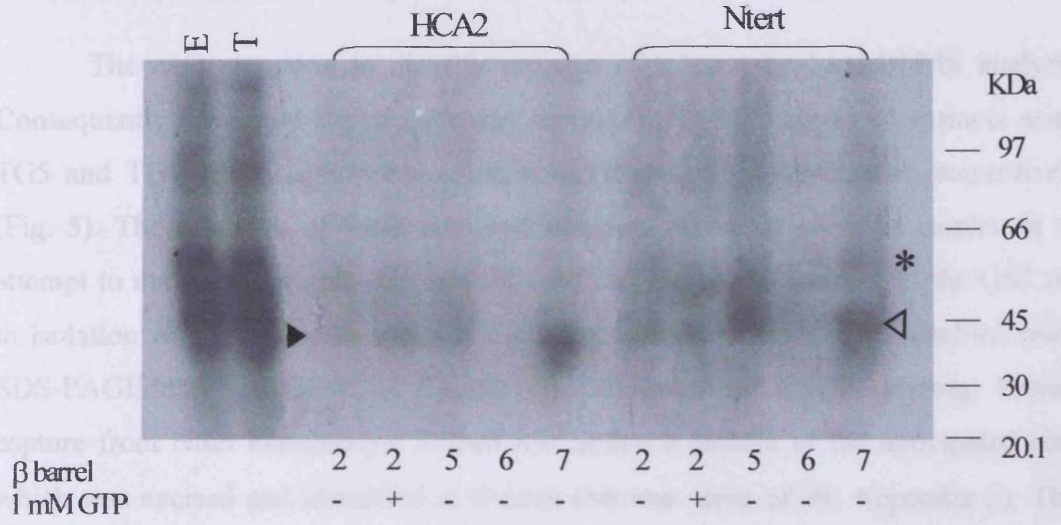

Fig. 4 Selection of TG-binding proteins from ^{35}S labelled cell extracts by recombinant TG β-barrels: 500 μg BL21 extracts containing TG β- barrel domains of TG5, 6 and 7 (5, 6 and 7) or full-length enzyme TG2 (2) were immobilised on 50 μl glutathione-linked Sepharose. TG2 was set up in duplicate to test the effect of GTP binding.
HCA2 fibroblast and Ntert keratinocytes were metabolically labelled over a period of 24 h in the presence of 10 μCi/ml Redivue pro-mix. This was followed by 24 h chasing in serum-free culture conditions. Protein solutions producing 3.5 x 10^6 cpm were incubated with each 50 μl aliquot of TG-conjugated Sepharose. Following extensive washing, proteins were retrieved by boiling in an equal volume of loading buffer and 15 μl resolved across 4-20% Tris-Glycine gels. Proteins were detected by exposure to a Kodak Biomax film 1 week at –80°C following incubation with 1 M sodium salicylate fluor. A sample of crude HCA2 extract (E) and the supernatant retrieved following incubation with Sepharose coupled to the GST tag only (T) were included as a measure of binding specificity.
Two predominant proteins were detected; a 42 kDa from HCA2 extract (solid arrowhead) and a 45 kDa band from Ntert samples (hollow arrowhead). In addition to this a 55 kDa protein was also retrieved from keratinocyte extracts (*).

4.2.2.1 Identifying β-actin as a possible transglutaminase-binding protein

The next step was to identify proteins of interest by MALDI/MS analysis. Consequently the initial experiment was repeated with unlabelled cell extracts using TG5 and TG7 columns in conjunction with Ntert and HCA2 extracts respectively (Fig. 5). The selection of these combinations was based on previous results, in an attempt to maximise protein-capture. In each case a column coupled to the GST tag in isolation was included as a negative control. Eluted proteins were resolved using SDS-PAGE and visualised by Coomassie Brilliant Blue R-250 staining. Protein capture from Ntert keratinocyte extract did isolate a protein of the anticipated size, which was excised and identified as β-actin (Mowse score of 94, Appendix 2). This structural protein has a mass of 42 kDa, which is consistent with the estimate from SDS-PAGE analysis. There is prior evidence that actin can act as a glutamyl substrate for TG2 in leukaemia cells undergoing apoptosis (Nemes *et al.*, 1997). It is therefore plausible that it could interact with other TG isoforms. Since the 55 kDa protein detected in the initial experiment resolved within the same region of the gel as the TG fusion proteins it was not possible to isolate it by this method.

Binding of proteins from HCA2 extract met with limited success, although, a band of 42 kDa was excised, MALDI/MS analysis indicated that a mixture of proteins had been retrieved. Due to time constraints, work now focused on confirming or disproving the interactions of TGs with actin.

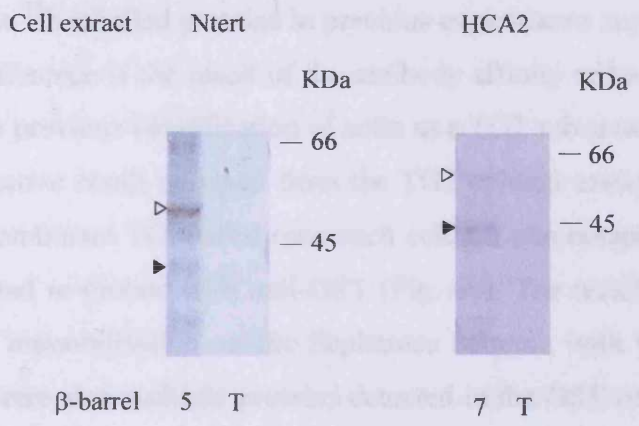

Fig. 5 Isolation of TG β barrel-binding proteins for identification by mass spectroscopy: 1.5 mg unlabelled Ntert/HCA2 protein extract was incubated with 50 µl Sepharose bound recombinant TG5 (5) or TG7 (7) respectively. Each cell extract was also incubated with Sepharose bound GST tag as a negative control (T). Bound protein was retrieved by boiling in 8 M urea. Samples were concentrated by ethanol precipitation prior to resolution through a 4-20% Tris-Glycine gel. Proteins were visualised with Coomassie Brilliant Blue R-250 staining and the bands excised for MALDI/MS analysis are marked by solid arrowheads. The GST tagged TG beta barrels are marked by hollow arrowheads.
The protein isolated from Ntert extract incubated with Sepharose bound TG5 was identified as actin.

Protein-capture from all four TG linked columns (TG2, 5, 6 and 7) was now carried out using unlabelled HCA2 and Ntert extracts. The "GST only" column was included as a separate sample instead of a pre-incubation step. Captured proteins were immunoblotted with anti-actin (Sigma, raised against a C-terminal peptide sequence). Positive results were obtained with the TG5 and 7 fusion proteins following incubation with fibroblast or keratinocyte extracts (Fig. 6a). In each case three bands were evident, of which, one was estimated to be 45 kDa in size identifying it as full-length β-actin. However, the identity of the two additional proteins is unclear. The larger 65 kDa band is most likely a cross-linked form of actin. The lower band has a M_r of ~36 kDa and may be a cleaved form of actin termed fractin. This fragment is thought to be present in cells undergoing apoptosis (Yang *et al.*, 1998).

It is interesting to note that the full-length form of actin produced the weakest signal in this experiment. Neither the Coomassie Brilliant Blue R-250 staining, nor detection of the ^{35}S labelled proteins in previous experiments support this ratio. It may be that this difference is the result of the antibody affinity rather than relative protein quantities. The previous identification of actin as a TG2 substrate (Nemes *et al.*, 1997) render the negative result obtained from the TG2 column unexpected. To ensure the amount of recombinant TG loaded onto each column was comparable the HCA2 blot was stripped and re-probed with anti-GST (Fig. 6b). The results revealed a problem with the TG2 immobilisation on the Sepharose column, with virtually undetectable levels. There were also multiple proteins detected in the GST control between 50 and 66 kDa in size, which did not produce distinct bands. The reason for this is unclear, but this blot did confirm that levels of recombinant TG5, 6 and 7 immobilised on the Sepharose matrix were equal.

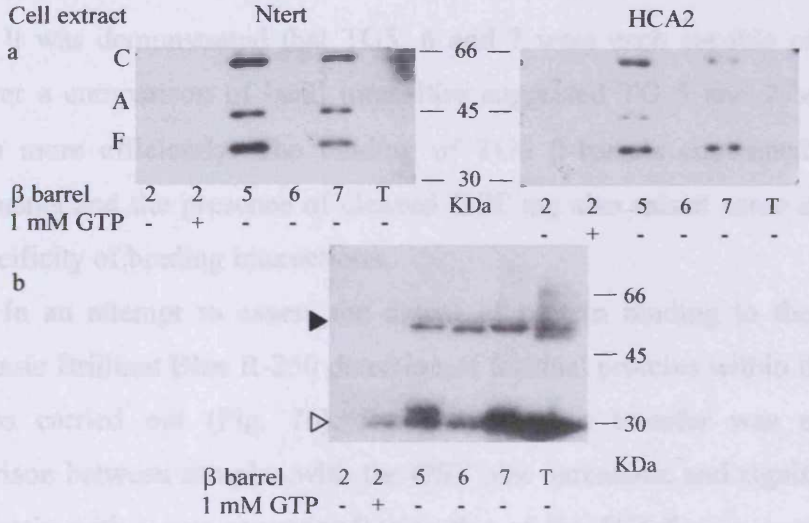

Fig. 6 Sepharose-bound TG5 and TG7 β-barrel domains are capable of binding endogenous actin: Immobilised recombinant TG proteins (2, 5, 6 and 7) were incubated with 500 μg cell extracts, TG2 was set up in duplicate to assess the affect of GTP binding and Sepharose bound GST tag was included as a control (T). Recovered proteins underwent immunoblotting with anti-actin (a). Three bands were detected, a 45 kDa protein thought to correspond with full-length actin (A), a 37 kDa fragment which may be the cleaved form of actin known as fractin (F). In addition a larger 65 kDa band was detected which may represent a cross-linked form of actin (C). (b) To ensure loading of recombinant TGs were equal, the blot including samples isolated from HCA2 cells was re-probed with anti-GST. Fusion proteins and the GST tag are indicated as solid and hollow arrowheads respectively.

To confirm the interaction of the TG enzymes with actin is direct and not the result of a protein complex, the step was taken to reverse the solid and liquid phases of previous experiments. High sequence conservation of actin is apparent between species and its three isoforms, α (skeletal, cardiac, smooth), β (non-muscle) and γ (smooth muscle and non-muscle). Since actin isolated from rabbit skeletal muscle (Sigma) shares 93% sequence homology with human β-actin, it was deemed acceptable to include this protein in further studies. 1 mg of actin was coupled to a 1 ml column of CNBr-activated Sepharose (described in Section 2.6.4.1). Due to concerns over low TG concentrations in cell extracts, the recombinant TG enzymes 5 and 7 were loaded onto the affinity column (800 μg). Bound proteins were eluted in 3 M KSCN following extensive washing and analysed by Western blotting. GST tagged TG6 was included as a negative control, since actin had not bound this isoform in previous experiments. In order to establish a level of quantification, immunoblotting of protein elutions from the column were performed with anti-GST (Fig. 7a).

It was demonstrated that TG5, 6 and 7 were each capable of binding actin. However a comparison of band intensities suggested TG 5 and 7 bound the actin-column more efficiently. The binding of TG6 β-barrels contrasted with previous experiments and the presence of cleaved GST tag also raised some uncertainty over the specificity of binding interactions.

In an attempt to assess the extent of protein binding to the actin column, Coomassie Brilliant Blue R-250 detection of residual proteins within the Tris-Glycine gel was carried out (Fig. 7b). Evidently protein transfer was uneven making comparison between samples with the GST blot unrealistic and significant quantities of a protein with a size corresponding to that of the TG6 fusion protein remained in the gel. It was also apparent that the cleaved GST tag was virtually undetectable with Coomassie Brilliant Blue R-250 detection. This would suggest a higher transfer efficiency than the fusion protein may be accountable for the comparatively high levels detected or reflects the previous finding (Chapter 3) that the anti-GST antibody has a higher affinity for the unfused tag. However if the ratios of protein remaining in the gel is representative of that transferred, the TG fusion proteins are the predominant protein bound to the column.

As a consequence of the TG6 sample producing a positive result, this experiment lacked an adequate negative control. Ideally an unconjugated and blocked Sepharose column should have been included to ascertain whether this binding was the result of interaction with actin or due to non-specific adsorption. It is possible that the immobilisation of TG6 to Sepharose produced conformational changes or steric hindrance that affected the actin binding in previous experiments.

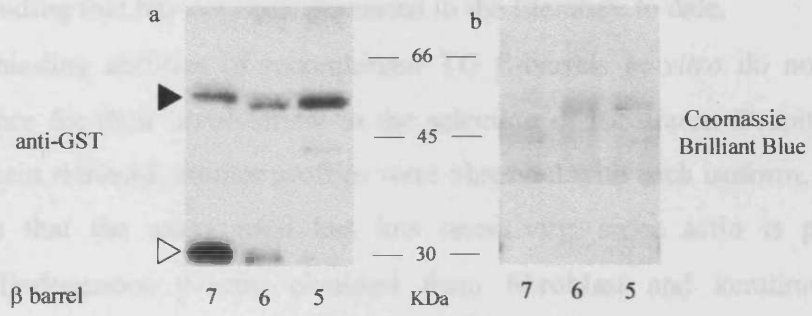

Fig. 7 Sepharose-coupled actin binds TG5, 6 and 7 fusion proteins: 1 mg actin sourced from rabbit muscle, was covalently linked to CNBr activated Sepharose and used to select TG5, 6 and 7 from BL21 extracts. TG6 was included as a negative control in agreement with previous experiments. To establish a level of quantification immunoblotting was carried out with anti-GST (a). The fusion protein and GST tag are designated solid and hollow arrowheads respectively. Untransferred proteins remaining in the gel following blotting were detected by Coomassie Brilliant Blue R-250 staining (b).

4.3 Conclusions and future work

Previous work has identified vimentin as a substrate of TG2 (Clement *et al.*, 1998) and initial IP experiments would seem to confirm this. However, non-specific binding identified from negative controls has restricted the reliability of this data. What has become evident is that the levels of vimentin, an intermediate filament component, increase in the 1 h period following fibroblast spreading on type I collagen, a finding that has not been discussed in the literature to date.

The binding abilities of recombinant TG β-barrels *in vitro* do not provide strong evidence for their involvement in the selection of substrates. Despite varying levels of protein retrieval, similar profiles were observed with each isoform. This may also indicate that the assay used has low sensitivity, since actin is present in abundance. Endogenous β-actin obtained from fibroblast and keratinocyte cell extracts was shown to bind Sepharose-immobilised TG5 and TG7 fusion proteins. However, it was then demonstrated that Sepharose-linked actin, obtained from rabbit muscle, was capable of binding TG 5, 6 and 7 fusion proteins.

It should be noted that data obtained using this experimental approach are limited to the protein interactions of the TG β-barrels. Although these experiments allowed the involvement of these domains in protein selection to be assessed, any interactions relying on residues outside this region would not have been detected. These interactions may provide a good indication of potential substrates, but confirmation would require further analysis. Another point to consider is that, although, the GST-tagged β-barrels would be expected to assume their native conformations, it has not been possible to confirm this prior to these studies.

Future studies should aim to work with TG enzymes in their native conformation. One avenue of investigation would be to generate high-level constitutive expression of TGs from mammalian cells by transfection. Extracts of such cells could be included in further IP studies, targeting either TG or actin, dependent on the efficacy of available antibody stocks. There would also be value in establishing colocalisation studies of actin and the various TG isoforms. Although this would not provide direct evidence of binding it may substantiate associations *in vivo*. To further elucidate the possible function of any such protein interactions it would be pertinent to establish whether these TG isoforms are capable of cross-linking actin.

Although, there is increasing evidence for structural roles of TGs (Lorand and Conrad, 1984; Akimov *et al.*, 2000; Balklava *et al.*, 2002), TG2 has been reported to cross-link actin in the later stages of apoptosis (Nemes *et al.*, 1997). The exact function of this activity is unclear, but it may provide a stabilising effect and prevent "leaking" of cellular components into the surrounding matrix. To date, TG2 is the only isoform with an established function in apoptosis.

Chapter 5:

Identifying a possible role for transglutaminase enzymes in corneocyte maturation

5.1 Introduction

The destruction of organelles observed to accompany keratinocyte terminal differentiation has often led to the resulting corneocytes being viewed as "dead cells". Despite cell metabolism apparently being restricted to catabolic activity, research over the last decade has indicated that following transition to the stratum corneum, corneocytes continue to mature. This produces two morphologically distinct populations. The first of these are irregularly shaped with a ruffled surface whilst the second are significantly larger (Watkinson *et al.*, 2001) demonstrating a more uniform, polygonal shape with a smooth surface (Michel *et al.*, 1988). Based on these observations these envelopes were termed fragile (CEf) and rigid (CEr) respectively. Later micromanipulation studies confirmed this was no misnomer, with CEr resisting maximal compression forces 6-fold greater than CEf (Watkinson *et al.*, 2001).

Previous studies have developed depth profiles of human stratum corneum, generated by successive tape stripping. This method allows adhered corneocytes to be harvested in discrete layers. Analysis of such profiles has established that the ratio of rigid to fragile CE increases towards the skins surface prior to desquamation (Michel *et al.*, 1988; Watkinson *et al.*, 2001). It was also observed that the number of desmosomes in corneocyte structures is reduced in the rigid envelopes (Long and Rogers, 1996). It has been hypothesised that CEr represents a more mature form of corneocyte and the ratio of CEr:CEf may impact on the efficacy of the skin barrier through effects on inherent mechanical strength, desquamation and the alignment of lipid lamellae via covalently bound lipids (CBLs). Marks and Barton (1983) have reported that increases in corneocyte surface area, is accompanied by a reduction in transepidermal water loss. Indeed, defective CE maturation is evident in certain hyperkeratic skin disorders including lamella ichthyosis (LI) and psorasis (Michel and Juhlin, 1990). Studies have reported the retention of the CEf morphology and in the

latter case a corresponding reduction in cell size (Marks and Barton, 1983). It has been observed that the percentage of CEr also alters with body site, those residing in environmentally exposed regions (e.g. hand and cheek) demonstrate lower numbers of CEr correlating with an increased rate of proliferation (Watkinson *et al.*, 2001). The extent to which exposure is accountable for these differences has not been established since the CE composition also varies between body sites (Reichert *et al.*, 1993).

Comparison of the molecular composition of fragile and rigid CEs following cyanogen bromide cleavage and resolution by SDS-PAGE has reported no striking differences (Michel *et al.*, 1988). Therefore it is possible that additional cross-links could account for the morphological change and increased mechanical strength. The predominant cross-links found within the CE are γ-glutamyl-ε-lysine (Rice and Green, 1977) and γ-glutamyl-polyamine isopeptide bonds (Piacentini *et al.*, 1988; Martinet *et al.*, 1990). The formation of both these cross-links is known to be catalysed by TG enzymes. To date TG 1, 3 and 5 have identified functions in CE formation and envelope precursors, such as loricrin, have been demonstrated to provide an efficient substrate to these enzymes *in vitro* (Candi *et al.*, 1995; 2001). It is therefore, reasonable to hypothesise that the action of these enzymes could continue within the stratum corneum. Depth profiles analysing the degree of γ-glutamyl-ε-lysine cross-linking transversing the stratum corneum were established from extensive protease digests and subsequent separation of fragments using high performance liquid chromatography (Watkinson *et al.*, 2001). These studies reported an increased number of isopeptide bonds towards the surface layers, correlating with the morphological changes. Using this method of tape stripping, reduced TG activity has also been linked to defective CE maturation observed with soap-induced "dry" skin. In these studies, three pools of TG activity (buffer soluble, detergent soluble and particulate) were analysed and found to decrease in conjunction with a reduced percentage of CEr upon soap treatment of skin (Long and Rogers, 1996). The greatest change as compared to the control sample was produced in the detergent-soluble pool, predicted to associate with the CBLs and speculated to be TG1.

Together these results strongly support the hypothesis that TGs are involved in corneocyte maturation within the stratum corneum and therefore impact on the integrity of the skin barrier. Interestingly the skin conditions psoriasis and LI, which have demonstrated reduced CEr numbers or complete absence of the CE structure, are accompanied by alterations in TG expression. In the case of psorasis, a chronic inflammatory dermatosis that develops in genetically predisposed individuals, a downregulation of TG3 has been reported (Candi *et al.*, 2002). In contrast LI, an autosomal recessive congenital disorder of keratinisation, can be accompanied by the loss of TG1 expression (Huber *et al.*, 1995; Parmentier *et al.*, 1995; Russell *et al.*, 1995; Candi *et al.*, 2002). If the enzyme or group of enzymes involved with CE maturation can be identified it would provide a target for future therapeutic intervention, attempting to improve skin barrier formation. This chapter discusses experiments carried out to identify candidate TG enzymes for this function by analysis of transcriptional or translational variations during CE maturation in human skin.

5.2 Results

5.2.1 Quantitative analysis of TG1 and 2 expression in human epidermis

A powerful tool for producing quantitative data on gene expression is real-time polymerase chain reaction (PCR). An established TG assay would elucidate comparative enzyme expression occurring within the population and alteration with abnormal skin homeostasis. Work has already been carried out in our laboratory to design primers and corresponding probes for TG1 and 2, including optimisation of relative concentrations (work carried out by Mrs. P. Aeschlimann, University of Wales, Cardiff). Attempts were made to quantify the expression of these enzymes from five individuals (described in Section 2.7.2). The method of sample collection employed has been termed "skin abrasion" and was developed at Unilever, Colworth. It allows the full-depth of epidermal tissue to be harvested without contamination by dermal tissue (unpublished data) and is less invasive than punch-biopsy. Total RNA extractions from five individuals were provided by Dr. R. Ginger (Unilever, Colworth) and it was decided that normalisation would be carried out prior to reverse transcription. Total RNA concentrations of up to 50 ng (pooled from 10 abrasion samples) underwent two cycles of reverse transcription with oligo dT primers and 1 µl of the cDNA generated was included in subsequent assays. Nuclease free water provided a negative control for each assay (no template control, NTC) and plasmid constructs containing the target sequences were serial diluted to generate a standard curve (5 fg- 50 pg). Ribosomal protein S26 (RP-S26) was selected as an appropriate housekeeping gene (Wagener *et al.*, 2001).

Signals detected from the sample groups in both the TG1 and TG2 assay were found to be outside the lower range of the corresponding standard curve (Appendix 3). It was concluded it would be impractical to obtain sufficient RNA levels using this method.

In parallel to these studies, experiments to analyse alterations in TG protein levels within human stratum corneum were also established. This was considered advantageous since upregulation of TG expression may not be substantiated at the protein level. A proteomic approach would also provide more data concerning potential TG activity. A number of the TG enzymes demonstrate regulation of activity with cleavage and this would not be encompassed with molecular analysis.

5.2.2 Corneocytes from the surface layers of the stratum corneum demonstrate a more uniform incorporation of cadaverine.

Tissue specimens were obtained with the approval of Colworth's Research Ethics committee and informed consent from company employees.

The following experiments were set up to confirm increased TG activity in the surface layers of the stratum corneum by incorporation of the texas red conjugated cadaverine, a TG substrate containing primary amine groups (described in Section 2.8.1). Samples were acquired by adhesion of a glass slide to the lower region of the volar (inner) forearm with cyanoacrylate and subsequent removal of the glass slide. This led to the retention of the top layers of corneocytes for analysis. This process was succeeded by a series of 8 tape strips prior to harvesting a second sample. Work carried out by Dr R. Ginger (Unilever, Colworth) has estimated ~ 1 layer of corneocytes is removed with each tape strip (unpublished data). This would localise the second corneocyte sample to approximately half the depth of the stratum corneum. Attempts were made to take a full depth sample following a further 8 tape strips, however, the sample quality obtained was poor and was not included in the experiment. Corneocyte samples were incubated with a reaction mixture comprising of, 50 mM Tris-HCl (pH 8), 150 mM NaCl and 9 μM texas red labelled cadaverine. Cadaverine incorporation was allowed to continue in a humidity chamber for 1 h at 37°C before sample analysis by microscopy. Analysis of the surface corneocyte layers demonstrated a uniform staining pattern (Fig. 1a). In contrast analysis of the half-depth sample revealed the majority of the staining localised to the corneocyte periphery (Fig. 1b). Previous studies have demonstrated an increased number of γ-glutamyl-ε-lysine isopeptide bonds in the more superficial layers of the stratum corneum (Watkinson *et al.*, 2001). A second sample of surface corneocytes was incubated with a labelling mixture supplemented with 20 mM cystamine. The resulting reduction in the fluorescence levels confirmed the enzyme activity responsible for cross-linking the cadaverine substrate relied on the availability of a thiol group, as is the case for TGs (Fig. 1c).

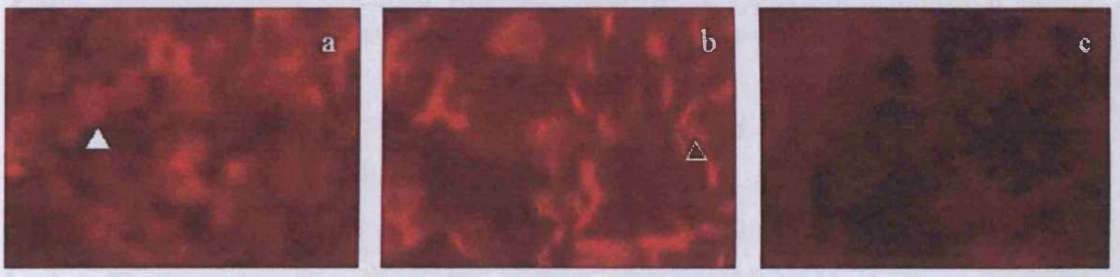

Fig. 1. Incorporation of the TG substrate cadaverine (texas red labelled) into human cornified envelopes is increased in the surface layers of the stratum corneum and is inhibited by cystamine: *Ex vivo* samples of human stratum corneum were harvested on glass slides from the surface layers (a) and at half depth (b). Samples were incubated in a humidity chamber for 1 h at 37°C in a reaction mixture containing texas red labelled cadaverine (9 μM). Following extensive washing, the extent of cadaverine incorporation was assessed by fluorescence microscopy. A second sample of surface corneocytes included 20 mM cystamine in the reaction mixture (c). The reduction in staining indicates the activity of the enzyme responsible for catalysing substrate cross-linking is dependent on a thiol group.

5.2.3 Generation of human stratum corneum depth profile

Tissue specimens were obtained with the approval of Colworth's Research Ethics committee and informed consent from company employees.

Corneocytes were removed (~ 1 cell layer) using strips of Sellotape within four marked regions of the lower volar forearm (Fig. 2a). A series of four successive layers were pooled as follows 1-4 (surface layers), 5-8, 9-12 and 16-20 (deepest layers). The latter group could not be obtained from some individuals due to a natural variation in stratum corneum depth, which ranges from 12-20 layers. Once collected by dissolving the adhesive in hexane, corneocytes were dried and protein extraction carried out in 50 mM Tris-HCl (pH 8) containing 9 M urea, 2 % SDS, 2 mM EDTA and supplemented with protease inhibitors (described in Section 2.8.2). These conditions aimed to retrieve any soluble proteins from the highly cross-linked CE and were carried out for 1 h at 60°C. The insoluble protein fraction of the CE was cleared by centrifugation (14000 x g, 5 min), which proved to be a key step in achieving equal loading (5 μg) of samples in a reproducible manner. Proteins were separated by SDS-PAGE, transferred to nitrocellulose membranes and subjected to immunolabelling with various TG-specific antibodies (described in Section 2.1.2). Confirmation of comparative protein levels was established by immunolabelling with anti-pan cytokeratin (anti-Pck) antibodies (Sigma, targets keratins 4-6, 8, 10, 13 and 18). For control purposes, Western blots included 5 μg extracts from HCA2 fibroblasts stably transfected with sense RNA of TG2 (as discussed in Chapter 3) or TG5 (also generated in our laboratory). Dermal fibroblasts have also been demonstrated to express TG1 but not TG3 (Stephens *et al.*, 2004). To ensure the extraction of TG5, which has proven highly insoluble (Candi *et al.*, 2001) 2 % SDS was included in the fibroblast extraction buffer.

The small volumes of cell extracts obtained from corneocytes provided limited sample. The fact that the TG antibodies included in this study were largely raised in different animals allowed the stripping and re-probing of these immunoblots (TG1, 6 and 7 – goat; TG2, pan cytokeratin – mouse and TG3, 4 and 5 – rabbit) (described in Section 2.1.2.5). In the cases of those TGs detected with the same secondary antibody differences in protein size and cleavage would allow identification of any carry over resulting from incomplete stripping.

5.2.3.1 Transglutaminase profiles across human stratum corneum

Detection with anti-TG4 (CovalAb), 6 and 7 (characterised in Chapter 3) produced no positive results. Expression of the former has not been reported in skin tissue, however TG6 and TG7 expression has been demonstrated in keratinocytes within this thesis. Whether these results are the consequence of the absence of these enzymes from the stratum corneum or their incorporation into the CE structure cannot be determined from these experiments in isolation.

Proteins were detected with anti-TG1, 2, 3 and 5 antibodies (Fig. 2b). The native sizes of these enzymes are as follows; full-length TG1 is estimated to be 92 kDa, although, a 106 kDa protein has been detected with polyclonal antibodies raised against a truncated form of the recombinant enzyme (Kim *et al.*, 1995b). The disparity in size is thought to be due to as yet unidentified protein modifications, and it was these antibodies that were included in this study (a kind gift from Dr P.M. Steinert, Laboratory of Skin Biology, Niams). Further to this TG1 undergoes cleavage to produce 67 kDa (containing the catalytic domain), 33 kDa (C-terminal β-barrels) and 10 kDa (N-terminal extension) fragments; these demonstrate increased activity (Kim *et al.*, 1995a). TG3 is also expressed as a virtually inactive proenzyme (77 kDa), which undergoes cleavage within the flexible hinge connecting the catalytic core and the first of the enzymes β-barrel domains. This generates a 50 kDa (containing the N-terminus and active site) and 27 kDa (C-terminal β-barrels) fragment. This 50 kDa fragment retains some cross-linking activity, however the two cleavage products remain non-covalently associated (Kim *et al.*, 1990). The resulting conformational change in conjunction with the binding of two additional Ca^{2+} ions renders the active site accessible to substrates (Ahvazi *et al.*, 2002, 2003). TG5 is expressed as an active 80 kDa protein and the TG2 enzyme is ~ 80 kDa.

Anti-TG1 detection in the fibroblast extract (positive control) produced bands estimated to be 116, 65, 42 and 32 kDa in size (calculated by their relative mobility in comparison to marker proteins), with the 65 kDa band producing a comparatively intense band (Fig. 2b). No 10 kDa cleavage product was detected, supporting previous observations that this fragment is not recognised with these antibodies (Kim *et al.*, 1995a). Extracts forming the depth profile revealed bands corresponding to full-length TG1 and the 67 kDa cleavage product with additional bands at 60 and 42 kDa.

Whether the two smaller fragments are the result of cleavage at additional sites is not discernable from this data. Steinert *et al.* (1996) have reported the immunoprecipitation of a number of minor TG1 cleavage products from cell culture, also the unstable nature of the TG1 protein has been documented by groups attempting to purify the enzyme (Thacher, 1989). No 33 kDa cleavage product was observed in any of the depth profile samples and no change in TG1 protein levels was evident. It has been established that the 67 kDa fragment of TG1 demonstrates a specific activity 5-fold greater than that of the full-length enzyme but half of that produced by the 67, 33 kDa complex (Kim *et al.*, 1995a). The expression of this TG isoform is thought to account for the majority of TG protein levels throughout the epidermis, but its expression has been reported to terminate in the transition zone between the granular layer and stratum corneum (Yamada *et al.*, 1997).

The monoclonal anti-TG2 antibody (CUB 7402, Neomarkers) also detected multiple proteins (primarily 55 and 50 kDa in size), contrary to the expected 80 kDa band, which was observed in the fibroblast extract (Fig. 2b). Previous studies have demonstrated that the expression of this enzyme is limited to the basal cells of the epidermis. Immunohistochemical staining with the monoclonal CUB 7402 is not reported to produce staining within the stratum corneum (Haroon *et al.*, 1999). It is unlikely this well characterised monoclonal antibody would produce cross-reactivity. This would suggest that TG2 is cleaved and becomes incorporated into the cornified envelope where the epitope may be masked. Despite the fact CUB 7402 recognises a sequence spanning part of the catalytic domain and the loop connecting the first β-barrel domain, it is unlikely that this form would have transamidating activity. The size of the fragment detected correlates with a combination of the enzymes catalytic core and the first β-barrel domain. Deletion studies have identified that premature termination in the latter virtually inactivates the transamidating activity of the enzyme (Lai *et al.*, 1996). However, this has not been established unambiguously, Hwang *et al.* (1995) have reported that partial deletion of the C-terminal domain is not accompanied by a reduction in cross-linking activity.

TG2 fragments have also been observed *in vivo*, but once again reports of the activity of these cleavage products are contradictory. A 48 kDa TG2 fragment has been retrieved from intestinal mucosa and lymphoid cells undergoing apoptosis. In the latter case the fragment was produced by caspase-3 cleavage and was inactive (Fabbi

et al., 1999). It was proposed that this was a protective mechanism to prevent the intact enzyme being released into the surrounding tissues where high Ca^{2+} levels would convert it into a highly active conformation. In the former case the fragment retained its transamidating activity, which proved to be Ca^{2+}-independent (Tsai *et al.*, 1998). This fragment also demonstrated a 10-fold increase in its affinity for putrescine and may selectively cross-link polyamines (putrescine, spermidine and spermine are all present in the epidermis). Finally, this monoclonal antibody has been used to elucidate changes in TG2 during wound healing in rats (Haroon *et al.*, 1999). Western blot analysis identified 55 and 50 kDa fragments, which were predicted to be inactive.

In the case of TG5, polyclonal antibodies generated against the enzymes β-barrels were employed in depth profile analysis. As with TG2 no full-length form of the enzyme was observed with the exception of the positive control (Fig. 2b, 79 and 72 kDa). Samples forming the depth profile produced multiple bands between 70 and 40 kDa.

What is apparent from the results discussed so far is that no significant alterations in TG protein levels (normalised with keratin control) or molecular forms were demonstrated across the stratum corneum. This provided no strong candidates for catalysing the cross-linking reaction involved in the final stage of corneocyte maturation. However, an interesting result was obtained with the TG3 polyclonal antibodies, raised against a recombinant form of the enzyme (a kind gift from Dr. N. Smyth, University of Cologne). These immunblots detected three bands calculated to be 72, 65 and 27 kDa in size (Fig. 2b). Whether the band with an apparent molecular mass of 65 kDa corresponds to the 50 kDa cleavage product is not easy to establish without a positive control. Purified TG3 was not available and TG3 is not expressed at significant levels in cultured keratinocyte cell lines (Hitomi *et al.*, 2001). This immunoblot did, however, produce some evidence of continued zymogen breakdown with corneocyte progression through the stratum corneum and increased levels of the 27 kDa fragment were observed in the more superficial pools (Fig. 2b).

Concerns were raised over the comparative staining patterns of TG1, 2 and 5 immunoblots with that of the cytokeratin control (Fig. 2b). In each case multiple bands were observed within the range of 70-40 kDa. Despite the antibody distinction with regard to the fibroblast control, cross-reactivity with keratins cannot be ruled out, and with such keratin-rich samples it would be particularly evident.

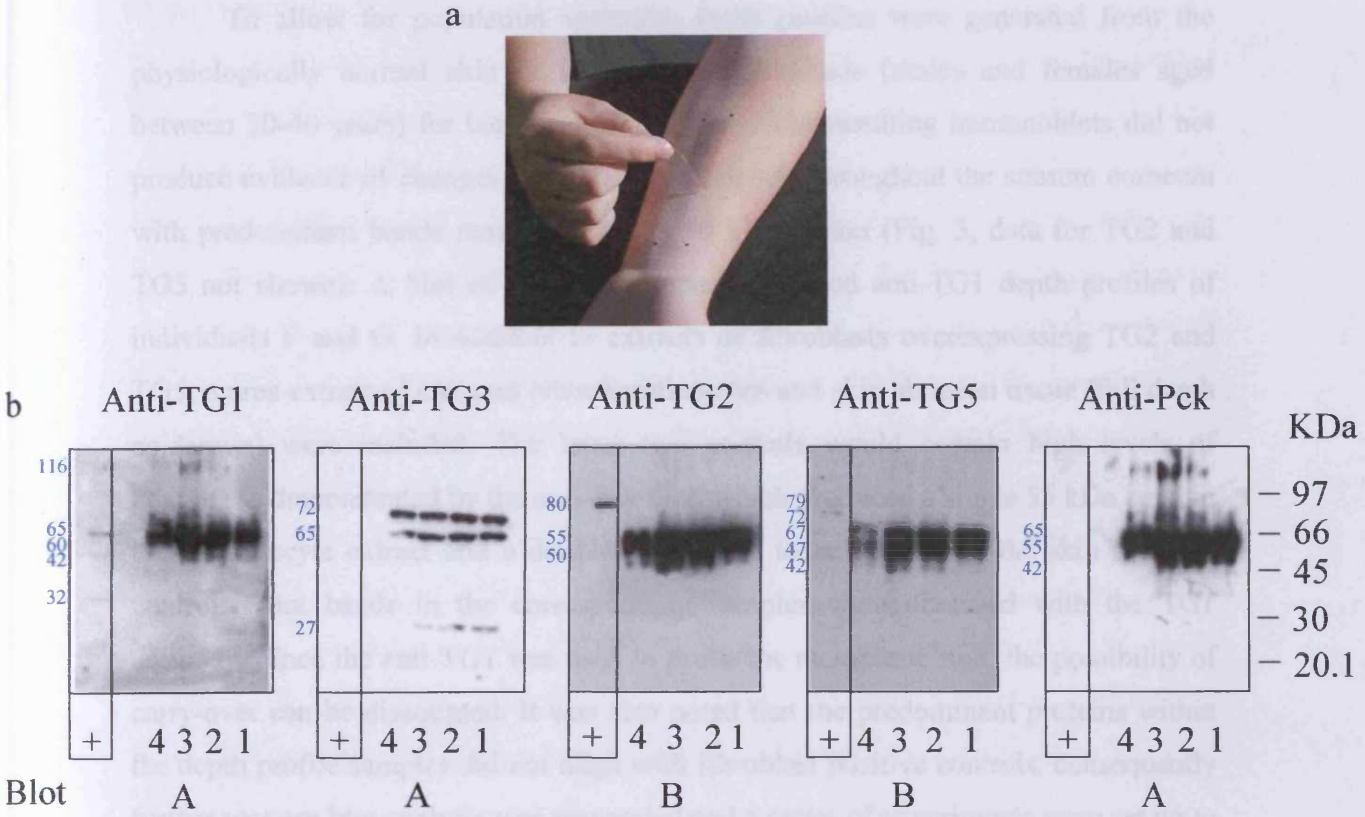

Fig. 2 Sellotape stripping can be utilised to generate depth profiles of human stratum corneum and identifies an increase in the 27 kDa proteolytic fragment of TG3 in surface corneocytes: (a) Photograph demonstrating the tape stripping method. A single marked area (10 cm by 1.9 cm) is shown. (b) Samples harvested from individual A were extracted in SDS/urea containing buffer and utilised to generate two identical blots (A and B). The tape strips were pooled into four groups, layers 1-4 (lane 1), 5-8 (2), 9-12 (3) and 13-16 (4). A mixture of 5 µg fibroblast extracts from HCA2 cells overexpressing TG2 or 5 were included as a control (+). Blots underwent a series of probing and stripping with anti-TG1, 2, 3 and 5 with an anti-Pck included to assess protein loading. Immunoblots are included in the order they were carried out (left to right). The molecular masses of proteins were estimated by relative mobility and are indicated in blue type.

To allow for population variation, depth profiles were generated from the physiologically normal skin of a further 6 individuals (males and females aged between 20-40 years) for inclusion in this study. The resulting immunoblots did not produce evidence of changes in TG1, 2 and 5 levels throughout the stratum corneum with predominant bands remaining in the 50 kDa region (Fig. 3, data for TG2 and TG5 not shown). A blot of particular interest involved anti-TG1 depth profiles of individuals F and G. In addition to extracts of fibroblasts overexpressing TG2 and TG5, a urea extract of cultured Ntert keratinocytes and skin abrasion tissue (full depth epidermis) were included. The latter two controls would contain high levels of keratins as demonstrated by the anti-Pck blot, which produced a single 55 kDa band in the keratinocyte extract and a doublet calculated to be 58 kDa in the skin abrasion control. Faint bands in the corresponding samples were observed with the TG1 antibody. Since the anti-TG1 was used to probe the membrane first, the possibility of carry-over can be discounted. It was also noted that the predominant proteins within the depth profile samples did not align with fibroblast positive controls, consequently further western blot analysis was suspended and a series of experiments were set up to identify potential cross-reactivity (discussed in Sections 5.2.3.2-3).

The group of anti-TG3 blots (Fig. 3) produced more varied results, (summarised in Table. 1). The individuals designated B and E demonstrated an increase in zymogen breakdown in the more superficial corneocyte layers. In contrast individuals C, F and G produced an increase in all protein bands. This would seem to contradict findings that organelles required for anabolic reactions are destroyed in the terminally differentiating cells. Previously individual A had demonstrated a relatively small change in zymogen levels but increased levels of the 27 kDa fragment were evident in the surface layers (Fig. 2b), suggesting the full-length enzyme must be replenished. It was observed that there was significant variation in TG3 levels and its temporal increase between individuals. For example comparatively high levels were evident in all layers of sample F, whilst sample G detected low levels of TG3 in layers 12-5 accompanied by a rapid increase in the four surface layers (1-4). There was also an indication that the putative increased activation of TG3 is not essential for the normal skin phenotype since individual D did not demonstrate any detectable alterations in TG3 levels or the extent of zymogen cleavage. However, it should be noted that no corresponding counts of CEf:CEr ratios were taken for these samples.

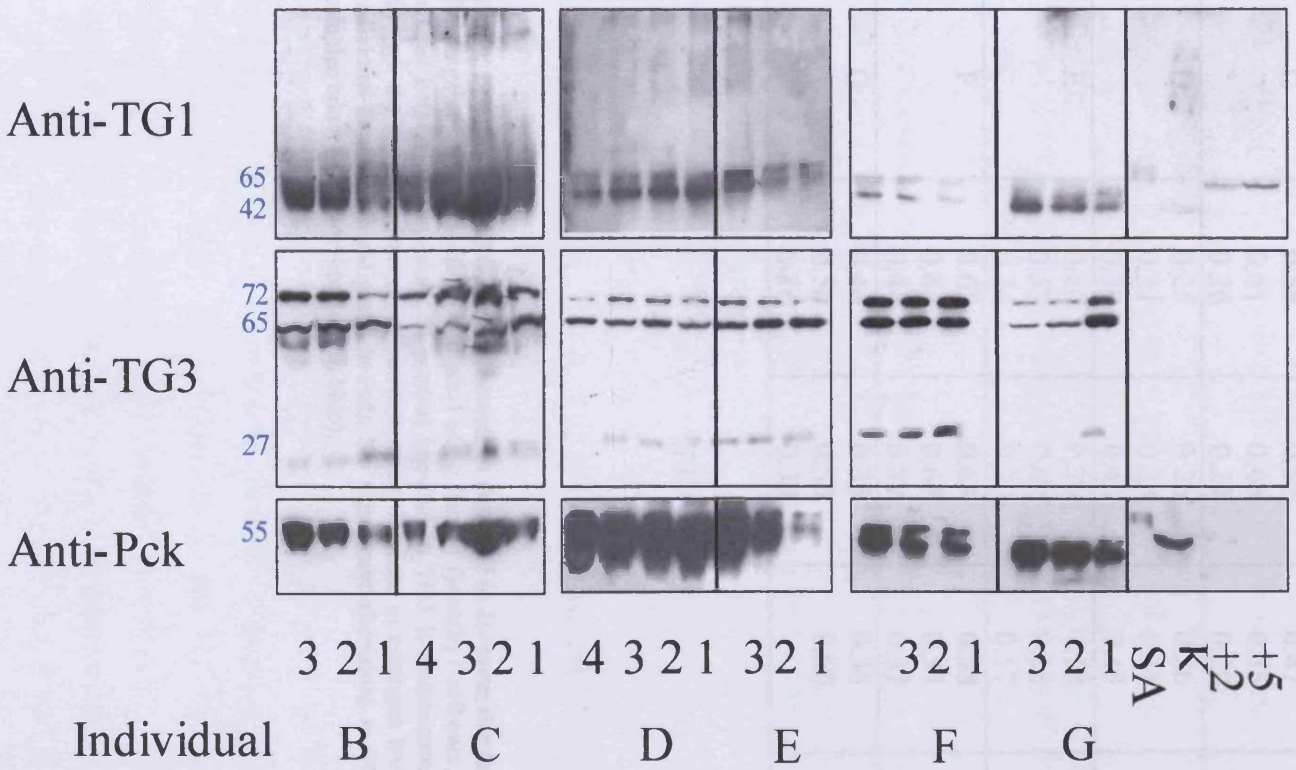

Fig. 3 Alterations in TG3 cleavage in the surface corneocyte layers are confirmed in 5 out of 6 individuals: Anti-TG blots of human stratum corneum depth profiles were expanded to incorporate a minimum sample group of six individuals. These studies included male and female subjects aged between 20-40 years of age. Tape strips were pooled into 3-4 groups depending on the thickness of the stratum corneum, layers 1-4 (lane 1), 5-8 (2), 9-12 (3) and 13-16 (4). 5 µg extracts from HCA2 fibroblasts overexpressing TG2 (+2) or TG5 (+5) were included as controls. In addition to this, 8 M urea extracts of cultured Ntert keratinocytes (K) and epidermal skin abrasions (SA) were included in some blots. Only anti-TG3 blots produced a detectable alteration in protein levels through the stratum corneum (with the exception of individual D) and once again the 27 kDa fragment of the zymogen produces more intense staining in the surface layers of human skin. This is accompanied by decreased zymogen levels in the case of individuals B and E. Estimated molecular masses are shown in blue.

Individual	Band Intensity				Fragment [kDa]
	Layers 1-4	Layers 5-8	Layers 9-12	Layers 13-16	
A	0.42	0.38	0.37	0.38	72
	0.38	0.37	0.36	0.32	65
	0.19	0.17	0.12		27
B	0.44	0.62	0.62		72
	0.62	0.61	0.54		65
	0.38	0.28	0.29		27
C	0.58	0.52	0.47	0.38	72
	0.61	0.46	0.35	0.37	65
	0.26	0.24	0.20	0.20	27
D	0.25	0.26	0.26	0.25	72
	0.31	0.33	0.31	0.35	65
	0.39	0.43	0.43		27
E	0.20	0.20	0.18		72
	0.57	0.42	0.38		65
	0.24	0.20	0.17		27
F	0.65	0.63	0.58		72
	0.64	0.63	0.57		65
	0.44	0.37	0.32		27
G	0.44	0.35	0.35		72
	0.56	0.50	0.50		65
	0.36	0.30			27

Table. 1 Summary of TG3 band intensities detected in forearm depth profiles of individuals A-G: Readings of band intensities (estimated using Biorad Quantity1 software, v 4.3.1) are shown as a ratio against keratin immunoblots. A general increase in TG3 is demonstrated with corneocyte transition through the stratum corneum. A corresponding decrease in zymogen levels (72 kDa) is observed with individual B and E (highlighted in red). No significant alterations in TG3 levels were observed with samples taken from individual D (in blue).

The apparent involvement of TG3 in the later stages of CE formation is supported by a number of findings by previous groups. This includes its downregulation in psoriatic skin (Candi *et al.*, 2002) and absence from cultured keratinocytes, which retain the CEf morphology (Rice and Green, 1979; Reichert *et al.*, 1993). TG3 efficiently catalyses the cross-linking of loricrin *in vitro* (Candi *et al.*, 1995), and it is this protein that constitutes ~ 75 % of the CE recruiting in the later stages of envelope formation (Hohl *et al.*, 1991; Steinert and Marekov, 1995). A proposed mechanism for CE formation, hypothesises the activity of TG1 incorporates precursors into the envelope structure where the activity of TG3 further modifies proteins (Candi *et al.*, 1995). It would therefore be a logical progression that this enzyme would continue to be involved in the process of maturation in normal skin.

5.2.3.2 Identifying pools of transglutaminase solubility

Up to this point the protein extraction process had been exhaustive, aiming to solubilise any protein not covalently linked to the CE. The step was now taken to include a stepwise extraction (described in Section 2.8.2), 1) including a Tris-HCl (pH 7) extraction containing protease inhibitors and 2) the same buffer supplemented with 1 % v/v Triton X-100. This method has the advantage of establishing pools of enzyme solubility and removing the majority of keratins from the protein extract, thereby negating any cross-reactivity with antibodies used. Samples from individuals B and C were included in these Western blot studies. Corneocyte proteins were extracted in each buffer under rotation for 1 h at 4°C to ensure exhaustive extraction. Equal protein loading was established with 1.5 μg and 0.5 μg from the Tris and Tris/Triton X-100 buffers respectively. Detection with antibodies targeting TG1 and TG5 produced no bands. Previous studies have demonstrated that TG5 is highly insoluble, a property attributed to its association with vimentin (Candi *et al.*, 2001). In the case of TG1, myristylation and palmitation within the N-terminal extension, ensures this enzyme is largely membrane-associated prior to cornification (Phillips *et al.*, 1993; Steinert *et al.*, 1996a). The results of this thesis would suggest that no cytosolic or membrane pools of TG1 and TG5 are present within the stratum corneum. However, it is

possible the highly cross-linked CE structure may have rendered the extraction process less efficient.

In contrast, TG3 was retrieved from both fractions (Fig. 4), and taking into consideration the difference in protein loading the greatest concentration was obtained from the Triton X-100 supplemented extract. A pattern of zymogen breakdown, similar to that observed previously, was produced for both individuals. This was particularly pronounced in the case of individual B, with virtually no detectable zymogen observed in the uppermost layers. This supports previous findings that detergent soluble protein pools demonstrate a greater increase in TG activity with cell progression through the stratum corneum compared to physiological salt extracts and insoluble fractions (Watkinson *et al.*, 2001). While this has previously been attributed to TG1, these results suggest that TG3 may significantly contribute to the detergent soluble pool of TG activity in the stratum corneum. It was noted that the two larger proteins (72 and 65 kDa) detected with the TG3 antibody demonstrated mirroring changes in intensity. If indeed the smaller band represented a stable activation product the band intensity would be expected to increase with zymogen cleavage. Interestingly a protein fragment calculated to be 48 kDa produced a faint signal in the two most superficial Tris extract pools (layers 1-4 and 5-8) of individual C. This may correspond to the 50 kDa fragment, which contains the active site of the TG3 enzyme, supporting the proposal that enzyme activation increases with progression through the stratum corneum. Why this fragment was not observed in urea-containing extracts is unclear, it may be the result of diluting effects of other proteins during loading. If this is the correct identification of TG3 cleavage products it raises the question of which TG3 domains form the 65 kDa protein. The absence of a molecular weight fragments corresponding to further cleavage of the β-barrel domains (predicted sizes of ~20 kDa and 7kDa) would suggest that cleavage of the zymogen may first occur within the N-terminus to produce the 65 kDa fragment. If this were the case the resulting 7 kDa fragment would not be expected to be recognised by this antibody (Kim *et al.*, 1995a).

Concerning the putative TG2 fragments within the stratum corneum, a new forearm depth profile was established for individual A. This included serial extraction in Tris and Tris/Triton X-100 buffers, followed by further extraction with the SDS/urea buffer used previously (2 μg loaded). The native enzyme is predominantly localised to the cytosol (~ 80 %), although to a varying degree TG2 is also directed to

the membrane, nucleus and is even externalised by an unknown mechanism. Detection with the TG2 monoclonal antibody only identified 55 and 50kDa fragments in the insoluble protein pool. Bands of similar molecular mass were detected with the anti-Pck antibodies in this fraction, lending credence to the suggestion of keratin cross-reactivity (Fig. 5). The decision was made to carry out 2D gel electrophoresis for a more definitive result on whether cross-reacting antibodies were present in the anti-TG1, anti-TG2 and anti-TG5 sera or if indeed distinct fragments are present in the insoluble fraction of corneocytes.

Fig. 4

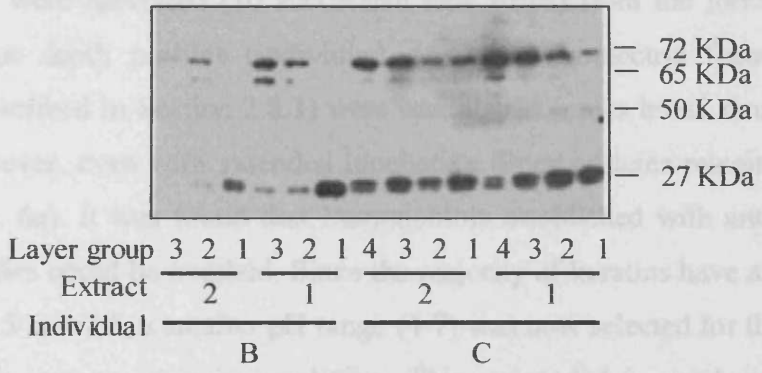

Fig. 5

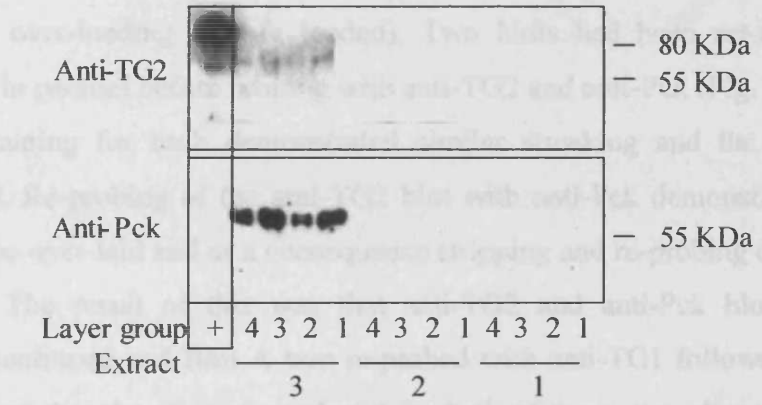

Fig. 4 Depth profiles generated from serial corneocyte extraction demonstrate soluble fractions of TG3 with zymogen cleavage accompanying transition through the stratum corneum: Corneocytes harvested from individuals B and C underwent serial extraction to identify pools of TG activity. Initial extraction of soluble proteins was carried out in Tris-HCl (pH 7) (Extract 1). Lipid-associated proteins were isolated by further extraction in Tris-HCl supplemented with 1% v/v Triton X-100 (Extract 2). Increases in the 27 kDa cleavage product is accompanied by a decrease in TG3 zymogen in all samples.

Fig. 5 Immunoblots of corneocyte extracts with anti-TG2 monoclonal antibody following serial extraction strongly correlates with the keratin control: (a) A depth profile was generated from individual A to include serial extraction in Tris-HCl (Extract 1), Tris HCl containing 1 % v/v Triton X-100 (Extract 2) and finally SDS/urea buffer (Extract 3). 10 µg fibroblast extract was included from HCA2 cells overexpressing TG2 as a control (+). In the case of each antibody, staining was limited to Extract 3 and no alterations in putative TG2 levels were distinguished from deepest corneocytes (4) to the surface layers (1).

5.2.3.3 Identification of keratin cross-reactivity by 2D analysis of anti-transglutaminase 1, 2 and 5

Samples were harvested (10 successive tape strips) from the forearm region used in previous depth profiles (individual A). Initial isoelectric focusing (IEF) experiments (described in Section 2.8.3) were established across broad range pH gels (pH 3-10). However, even with extended incubation times proteins remained largely unresolved (Fig. 6a). It was found that immunoblots established with anti-TG2 and anti-Pck antibodies could be overlaid. Since the majority of keratins have a calculated PI of between 5.5 and 7.5, a smaller pH range (4-7) was now selected for the IEF step in an attempt to improve protein resolution. This succeeded in producing sharper bands (Fig. 6b, Coomassie Brilliant Blue R-250), however the streaking effect may suggest protein over-loading (10 μg loaded). Two blots had been set-up by this method and run in parallel before probing with anti-TG2 and anti-Pck (Fig. 6b, Blot A and B). The staining for each demonstrated similar streaking and the two blots partially aligned. Re-probing of the anti-TG2 blot with anti-Pck demonstrated these blots could not be over-laid and as a consequence stripping and re-probing of the blots was necessary. The result of this was that anti-TG2 and anti-Pck blots directly aligned. Work continued and Blot A was re-probed with anti-TG1 followed by anti-TG5. It was found that the staining produced for both of these also aligned with the anti-Pck blot, although discrete dots were produced. There were some concerns that the anti-TG5 blot was the consequence of incomplete stripping, however the signals produced with anti-TG5 were actually detected at a lower exposure than that of TG1. No additional proteins were detected corresponding to the TG enzymes (the 67 kDa of TG1 has a predicted PI value of 5.2). These results seem to confirm cross-reactivity of the three TG antibodies with keratins. This is particularly problematic for TG1 analysis, since the multiple bands obscure the region in which the active enzyme fragment (67 kDa) resolves.

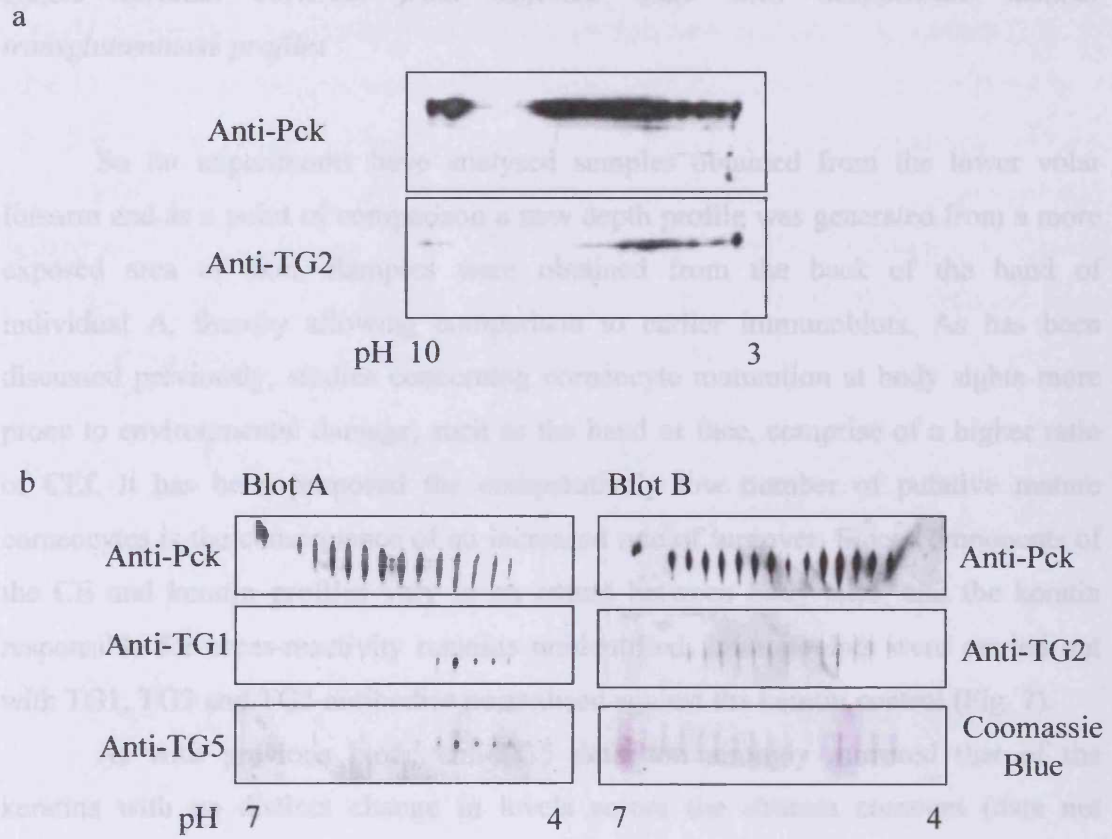

Fig. 6 2D gel analysis supports keratin cross-reactivity with anti-TG1, 2 and 5 antibodies: (a) 2D gel electrophoresis was carried out on 10 µg of human corneocyte extracts (individual A) in 8M urea, 2 % CHAPS, 0.5 % v/v ZOOM® carrier ampholytes and 0.002 % bromophenol blue. A broad-range IEF step (pH 3-10) was incorporated. Poor protein resolution was achieved and TG2 immunoblots (Anti-TG2) aligned with the keratin control (Anti-Pck). (b) Reduction of the IEF range (pH 4-7) produced better resolution with discrete bands detected. However some streaking was observed (Coomassie Blue), possibly a consequence of protein overloading. Two blots were generated (Blot A and B) and probed with anti-TG1, 2 and 5 in conjunction with a keratin control. In all cases the staining pattern produced aligned with that of the keratin control.

5.2.3.3 Stratum corneum from different body sites demonstrate distinct transglutaminase profiles

So far experiments have analysed samples obtained from the lower volar forearm and as a point of comparison a new depth profile was generated from a more exposed area of skin. Samples were obtained from the back of the hand of individual A, thereby allowing comparison to earlier immunoblots. As has been discussed previously, studies concerning corneocyte maturation at body sights more prone to environmental damage, such as the hand or face, comprise of a higher ratio of CEf. It has been proposed the comparatively low number of putative mature corneocytes is the consequence of an increased rate of turnover. Since components of the CE and keratin profiles vary to an extent between body sites, and the keratin responsible for cross-reactivity remains unidentified, immunoblots were carried out with TG1, TG3 and TG5 antibodies normalised against the keratin control (Fig. 7).

As with previous blots, anti-TG5 detection strongly mirrored that of the keratins with no distinct change in levels across the stratum corneum (data not shown). In the case of TG1 the multiple bands observed with samples obtained from the forearm were no longer evident. Instead two distinct bands of 95 and 66 kDa are recognised, the former most likely produced following the cleavage of the 10 kDa membrane-associated region at the N-terminus of the enzyme. Previous studies have observed up to a 10-fold increase in specific activity of TG1 with cleavage into three fragments, as well as the propensity of the full-length enzyme to reduce the activity of these products (Kim *et al.*, 1995a). No distinct alteration in protein levels was observed and a putative role for TG1 in CE maturation largely depends on whether 1) the 67 kDa fragment is present in the forearm stratum corneum but is masked by keratin cross-reactivity and 2) if its activity is modulated by the 95 kDa fragment. If TG1 is indeed absent from stratum corneum regions that demonstrate higher proportions of mature corneocytes it is unlikely to have a role in the maturation process. Conversely if the active 67 kDa fragment is present in forearm stratum corneum as the predominant form it may yet have a function in CE maturation.

So far these studies have focused on the possible role of TG3 in corneocyte maturation and once again this depth profile produced interesting results. In this case,

although the levels of the 72 and 65 kDa proteins remain comparable, the highest levels of the 27 kDa cleavage product were observed in the deepest layers of the stratum corneum and a steady decrease was evident towards the skins surface (Fig. 7, Blot A). This is in direct contrast with forearm depth profiles and was confirmed by a repeat experiment (Fig. 7, Blot B). It may be that the 27 kDa cleavage product plays a key role in the activity of TG3 through its interactions with the 50 kDa fragment and subsequent augmentation of its activity. Samples from the hand epidermis of further individuals would be required for confirmation of these TG profiles obtained from hand epidermis and are not encompassed by these studies.

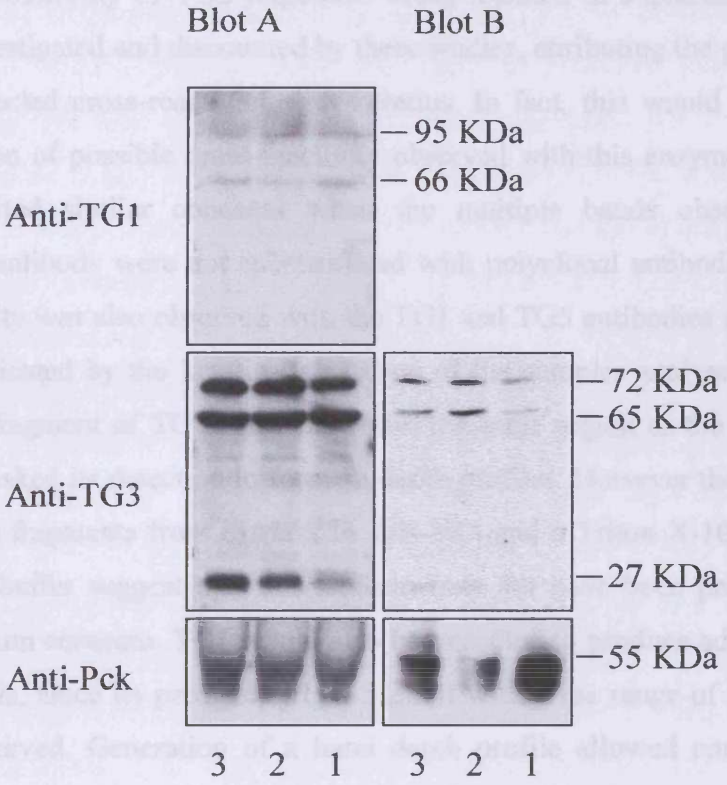

Fig. 7 Depth profile obtained from exposed hand (non palmer) stratum corneum demonstrates decreased levels of TG3 cleavage products and discrete TG1 detection: A depth profile was generated from the back of the hand of individual A and extracted in SDS/urea buffer. Tape strips were pooled as layers 1-4 (1), 5-8 (2) and 9-12 (3) and used to generate two blots (A and B). Detection with anti-TG1, 3 and 5 was carried out with corresponding keratin controls (Anti-Pck). No staining in the 50 kDa region was observed with the TG1 antibody and the anti-TG3 blots demonstrate a decrease in the 27 kDa fragment in surface corneocytes contrasting with forearm profiles.

5.3 Conclusions and Future work

The possibility of TG2 fragments being retained in suprabasal keratinocytes has been investigated and discounted by these studies, attributing the protein detection to an unexpected cross-reactivity with keratins. In fact, this would not be the first documentation of possible cross-reactivity observed with this enzyme. Nanada *et al.* (2001) reported similar concerns when the multiple bands observed with this monoclonal antibody were not substantiated with polyclonal antibodies. This keratin cross-reactivity was also observed with the TG1 and TG5 antibodies employed in this study, complicated by the keratin-rich nature of the samples analysed. The fact that the 67 kDa fragment of TG1 resolves within the same region as the keratin proteins may have masked its detection in forearm depth profiles. However the absence of any TG1 positive fragments from extracts in Tris-HCl and a Triton X-100 supplemented form of the buffer suggest that this isoform may not have been present within the forearm stratum corneum. TG1 would also be expected to produce additional staining in 2D analysis, since its predicted PI of 5.2 fell within the range of the IEF gel, but was not observed. Generation of a hand depth profile allowed comparison of the forearm samples to a stratum corneum known to retain immature CEf in greater numbers. The resulting anti-TG1 blot did not produce evidence of keratin-related bands, instead two discrete bands were observed at 95 kDa (possibly a fragment produced by N-terminal cleavage of the anchor region) and 67 kDa. The latter of these represents a more active form of the enzyme but may be modulated by the presence of the 95 kDa fragment. It does however, need to be taken into consideration that the hand profile blots are yet to be confirmed by expansion of the sample group.

These studies have implicated TG3 in CE maturation in normal skin, with increased zymogen cleavage products evident in the more superficial layers, sometimes accompanied by an increase in the full-length enzyme. In addition to this the extent of the increase varied with individuals, in the case of individual G a comparatively large increase was observed between layers 5-8 and 1-5. This may be partly due to the imprecise nature of tape stripping but a companion study of the CEf:CEr ratios may provide an interesting comparison. This alteration was not observed in all TG3 profiles with 1 out of 7 individuals showing no change in protein levels. However, this does not discount accumulative effects of the enzyme activity.

In contrast with the forearm profiles, this pattern of zymogen cleavage appears to be reversed in stratum corneum obtained from hand epidermal tissue. A reduction in the 27 kDa fragment was evident in the more superficial layers, but awaits confirmation by expanding the sample group. If this profile is verified it raises the question as to whether this is purely the result of increased degradation of the fragment or if the loss of an activating protease prevents the replenishment of intracellular pools. It may be that TG1 levels are increased in the stratum corneum of this body site to compensate for the lower TG3 activity, but this is conjecture.

TG3 was the only TG in this study to be extracted in Tris-HCl and detergent soluble pools. Previously studies have localised TG3 to the cytosol of cells and no membrane-associated fractions have been reported. The presence of such a pool of TG3 activity is certainly intriguing since no post-translational modifications have been reported, possibly the enzyme is non-covalently associated with other components in this fraction. It would be interesting to see if this pool of TG3 is retrieved from keratinocytes in earlier stages of differentiation or if it localises here specifically in the later stages, perhaps modulating its function. Zymogen breakdown in the surface layer corneocytes is well defined in these Tris extracts and for the first time a band estimated to be ~50 kDa active fragment was observed. Whether this is due to low antibody affinity or low protein levels is unclear and would ideally be established with a positive control. Indeed, ascertaining the presence of the active fragment is important for strengthening the hypothesised role of TG3 in CE maturation. Concerning the 65 kDa fragment observed, care was taken in these studies to prevent protein degradation by including a range of protease inhibitors and aliquoting the samples to avoid exposing samples to repeated freeze-thawing. This 65 kDa protein produces a discrete band that is consistently present in extracts and it is possible that it is a physiological fragment. The fact that levels of this fragment are seen in greater quantities in the SDS/urea extraction suggest it may be associated with the CE and is possibly inactive, although this can not be verified without further study.

To summarise these findings, it would seem that only TG3 is retrieved from the human forearm stratum corneum in detectable quantities by this method. Further to this it demonstrates increased protein levels, sometimes combined with increased zymogen cleavage with transition through the surface corneocyte layers. This would suggest a corresponding increase in activity and it could be that the 27 kDa C-terminal

fragment plays an important role in regulating the TG3 activity. This pattern of zymogen activation is not observed in stratum corneum obtained from the hand, a body site reported to retain fragile envelopes, and is accompanied by low levels of TG1 protein.

Together these findings identify TG3 as a candidate for CE maturation and would concur with the prediction that TG3 continues to modify envelope precursors following their incorporation by TG1.

Chapter 6:
The effects of mesenchymal TG2 on keratinocyte migration, morphology and differentiation

6.1 Introduction

6.1.1 Mesenchymal control of keratinocyte proliferation and differentiation

In order to gain a more complete understanding of skin homeostasis, specific interactions between the predominant epithelial and mesenchymal cells types need to be understood. To this purpose previous studies have developed *in vitro* skin models employing keratinocyte-fibroblast cocultures. These models often comprise of keratinocytes seeded onto collagen-embedded fibroblasts (the prevalent cell type found within the dermis) and are referred to as skin equivalents (SE). The mesenchymal influence on the generation and maintenance of a differentiated epidermis was clearly established in a study populating collagen gels with a range of fibroblast numbers (Ghalbzouri *et al.*, 2002). It was observed that in the absence of fibroblasts the epidermis formed contained only three or four viable cell layers, with a complete cessation of keratinocyte proliferation observed within two weeks. In contrast the calculated proliferation index of keratinocytes cultured on fibroblast-populated collagen gels was observed to increase in correlation with the number of fibroblasts incorporated. These growth-promoting effects credited to fibroblasts are supported by other studies (Bell *et al.*, 1981a; 1981b; Prunieras *et al.*, 1983; Asselineau *et al.*, 1986) More particularly it has been demonstrated that keratinocyte derived IL-1 stimulates the release of KGF from dermal cells, thus stimulating keratinocyte proliferation (Smola *et al.*, 1993; Mass-Szabowski *et al.*, 2000).

Concerning the effect of fibroblasts on keratinocyte differentiation, the expression of the early differentiation marker, keratin 10 (K10) remained unaffected by fibroblast numbers within coculture. However the expression of K6, 16 and 17 was clearly downregulated by epithelial-mesenchymal interactions (Ghalbzouri *et al.*, 2002). These keratins are associated with keratinocyte activation and have a putative role in reorganisation of cytoplasmic filaments, an event thought to precede the onset of keratinocyte migration into wound sites. It was also demonstrated that these fibroblast-mediated effects were more pronounced following one week preculturing of the fibroblast populated gels.

6.1.2 Mesenchymal control of keratinocyte migration

Previous studies investigating keratinocyte migration have reported regulation via matrix proteins (O'Keefe *et al.*, 1985; Nickoloff *et al.*, 1988; Guo *et al.*, 1990) and soluble factors (summarised Table 1). In fact the two are not mutually exclusive and it has been observed that TGFβ and EGF induce the production of fibronectin (FN) (Nickoloff *et al.*, 1988) accompanied by enhanced keratinocyte motility (O'Keefe *et al.*, 1985; Nickoloff *et al.*, 1988). Moreover, the increased rates of keratinocyte migration observed in the presence of these growth factors were largely inhibited following the addition of FN-specific antibodies (Nickoloff *et al.*, 1988). Separate *in vitro* studies have reported that, following wounding, keratinocytes exhibit an increased ability to bind FN (Takashima and Grinnell, 1985; Toda and Grinnell, 1987). Nickoloff *et al.* (1988) surmised that substrates found within the wound matrix such as fibronection and thrombospondin produce increased keratinocyte migration from agarose drop explants. In contrast, the basement membrane component laminin, proved to inhibit migration.

The action of soluble factors is by no means limited to the regulation of ECM protein expression. They may also impact on regulation of ECM receptors or secretion of proteolytic enzymes and their inhibitors (Grinnell *et al.* 1981; Clark *et al.*, 1982; Barrandon and Green, 1987; Hebda, 1988; Nickloff *et al.*, 1988; Kaur and Carter, 1992). Clearly dermal fibroblasts may be expected to play an important role in keratinocyte migration, the challenge being to delineate the pathways through which they act. One such study utilised *in vitro* SEs to establish two wound models (Ghalbzouri *et al.*, 2004). The first of these were superficial incisions, whilst the second were described as "full-thickness" wounds. The latter group was produced by localised freezing with liquid nitrogen, which removed viable fibroblasts from the underlying dermal compartment. Analysis of subsequent re-epithelialisation identified slower 'healing' in the full-thickness wound group, which could only be partially counteracted by EGF and to a lesser extent KGF. The discrepancy remaining between the two wound groups lead to a hypothesised role for other soluble factors such as TGFα, TGFβ, granulocyte macrophage colony stimulating factor (GM-CSF), hepatocyte growth factor (HGF), IL-6 and IL-1 (Ghalbzouri *et al.*, 2004).

Factor	References
Transforming growth factor β	Sarret *et al.* (1992), Zambruno *et al.* (1995), Santibanez *et al.* (2000)
Epidermal growth factor	Sarret *et al.* (1992), Chen *et al.* (1993), McCawley *et al.* (1998),
Fibroblast growth factor 7	Tsuboi *et al.* (1992)
Fibroblast growth factor 10	Matsumoto *et al.* (1991), Tsuboi *et al.* (1992, 1993), Sato *et al.* (1995), Cha *et al.* (1996), Gibbs *et al.* (2000)
Hepatocyte growth factor	Tsuboi *et al.* (1992), Sato *et al.* (1995), McCawley *et al.* (1998), Putnins *et al.* (1999), Gibbs *et al.* (2000)
Transforming growth factor α	Cha *et al.* (1996), Jimenez and Rampy (1999)
Insulin-like growth factor 1	Tsuboi *et al.* (1992), Sato *et al.* (1995), Dunsmore *et al.* (1996), McCawley *et al.* (1998)
Granulocyte macrophage colony stimulating factor	Barrandon and Green (1987), Tsuboi *et al.* (1992), Jiang *et al.* (1993), Aragane *et al.* (1996), Cha *et al.* (1996), Ghahary *et al.* (1998)
Interleukin-1	Tsuboi *et al.* (1992), Chen (1995)

Table. 1 Common soluble keratinocyte migratory factors

6.1.3 TG2 in skin

TG2 is one of five TG isoforms known to be expressed in human skin. It has been shown that within the epidermis TG2 expression is limited to basal keratinocytes (Aeschlimann *et al.*, 1998; Haroon *et al.*, 1999). This is in contrast with other TG isoforms demonstrating keratinocyte differentiation-specific expression (Kim *et al.*, 1993; 1995a; 1995b; Aeschlimann *et al.*, 1998; Candi *et al.*, 2001).

TG2 is also expressed in fibroblasts, the predominant dermal cell type (Aeschlimann *et al.*, 1998). It has been demonstrated that TG2 localises to the nucleus (5 %), cytoplasm (80 %), membrane (15 %), and is externalised from the cell. The mechanism of secretion is yet to be established, however it has been demonstrated that TG2 requires cross-linking activity for this process (Balklava *et al.*, 2002). In conjunction with its localisation to the ECM, TG2 has well established functions in ECM remodelling (Aeschlimann and Thomazy, 2000; Stephens *et al.*, 2004). It has also been demonstrated to function independent of its cross-linking activity as an integrin-associated coreceptor, promoting FN fibrilisation in the pericellular matrix and facilitating cell adhesion, spreading and motility (Akimov and Belkin, 2001; Balklava *et al.*, 2002). With regard to the dermo-epidermal junction (DEJ), several basement membrane components have been shown to be TG2 substrates including nidogen/entactin (Aeschlimann *et al.*, 1991; 1992), osteonectin/BM-40/SPARC (Hohenadl *et al.*, 1995), FN (Martinez *et al.*, 1994) and collagen VII (Raghunath *et al.*, 1996). In conjunction with these findings the detection of γ-glutamyl-ε-lysine isopeptide cross links within the basement membrane region have lead to a hypothesised role for TG2 in stabilisation of the DEJ (Aeschlimann *et al.*, 1995). Indeed, these suggestions were confirmed by clinical studies of human skin grafts, which demonstrated that key dermo-epidermal structures, including anchoring fibrils, are cross-linked by transglutaminase (Raghunath *et al.*, 1996). The physical properties imparted by these cross-links were observed to provide stability at this tissue interface.

Concerning the role of TG2 in the repair of wounded skin, a multifaceted approach has been observed. This TG enzyme is upregulated by acute phase injury cytokines, including IL-6 (Ikura *et al.*, 1994), TGFβ (Vollberg *et al.*, 1992) and TNFα (Kuncio *et al.*, 1998). Analysis of rat skin punch biopsies has revealed its upregulation

at sites of neovascularisation and provisional fibrin matrix within 24 h of the initial wound event (Haroon *et al.*, 1999). Endothelial cells, macrophages and skeletal muscle cells were observed to express TG2 throughout the healing process. This study proposed roles for TG2 in angiogensis, production of a scaffold facilitating the migration of endothelial and inflammatory cells and/or remodelling of the granulation tissue. Interestingly transient expression of TG2 in the epithelial layer also suggested a role in re-epithelialisation (Haroon *et al.*, 1999).

This chapter focuses on investigating the effects of altered mesenchymal TG2 levels on the migration, morphology and differentiation of epidermal keratinocytes. This work utilised HCA2 human fibroblasts stably transfected with DNA vectors to produce high level constitutive expression of TG2 sense RNA, antisense RNA as well as a TG2 mutant RNA containing a Ser substitution of the active Cys residue, thus removing the enzymes crosslinking activity but maintaining protein conformation (Baek *et al.*, 2001). HCA2 cells transfected with an empty vector were included in experiments as a control (mock).

6.2 Results

6.2.1 Establishing an *in vitro* skin equivalent model to investigate the effects of altered dermal TG2 levels on keratinocyte morphology and differentiation

In order to better understand the role of epithelial-mesenchymal interactions in normal skin physiology, the development of SE cocultures has provided a useful tool. One such model has been developed by Dr. W. Parish (Unilever, Colworth) incorporating primary human keratinocytes harvested from normal skin in combination with collagen embedded murine fibroblasts (3T3 cell line). Dermal equivalents generated by this method incorporated a one-week preconditioning phase to produce a floating lattice, prior to keratinocyte seeding (referred to as the contraction method) (described in Section 2.9.2). Since lattices are allowed to contract, fibroblasts are not exposed to tensile forces and consequently this method may be considered a model for normal skin. In contrast, dermal equivalents generated under "stressed" conditions (resisting contraction) have been shown to produce growth and growth factors comparable to scar tissue (Nakagawa *et al.*, 1989). Once formed, lattices were transferred to a mesh platform and basal keratinocytes seeded at the air-liquid (A/L) interface followed by up to four weeks culture at 30°C. Following one weeks culture a tissue architecture similar to that of native skin is recognisable (Fig. 1), with columnar basal cells, spinous region and a thin stratum corneum, although no distinct granular layer is apparent. There was also a clear boundary established between dermal and epidermal layers. Swirling cell formations were observed in some regions of the spinous layers, this might be attributed to partially differentiated cells being seeded onto the dermal equivalent.

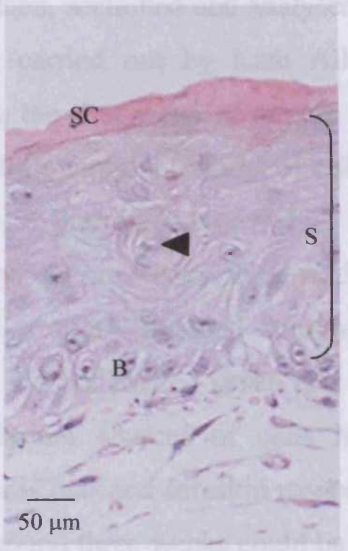

Fig. 1 Hematoxylin and eosin staining of primary human keratinocyte-murine 3T3 coculture following 1 week culture at the air-liquid (A/L) interface: 1 x 10^6 primary human keratinocytes were seeded at the air-liquid interface of a collagen gel containing 2 x 10^6 murine 3T3 fibroblasts. H & E staining of 10 µm sections revealed keratinocytes differentiated to produce morphologically distinct layers as seen *in vivo* including; the basal layer (B), spinous region (S) and the stratum corneum (SC). No granular layer was distinguished within this sample. A swirling cell formation is evident within the spinous layers and is indicated by an arrowhead. This is probably the result of partially differentiated keratinocytes being seeded onto the dermal gel despite attempts to select basal cells with a 40 µm cell strainer.

To evaluate the effects of dermal TG2 levels on keratinocyte morphology and differentiation this method was adapted to incorporate stable transfectants of HCA2 fibroblasts deficient in this enzyme (antisense) in parallel with cells overexpressing the normal (sense) or cross-linking inactive ($Cys^{277}Ser$) form. A mock transfectant was included as a control and was selected to assess the success of a SE model. Previous studies have demonstrated these transfectants have comparable rates of proliferation and over adequate time periods are capable of contracting collagen lattices to the same extent (Stephens *et al.*, 2004). These characteristics are important for maintaining relative cell densities. Unfortunately no regular source of primary keratinocytes was available, so the selection of an appropriate alternative was required. The following experiments investigated the possibility of employing primary mouse keratinocytes or a human derived cell line.

Using the contraction method (Fig. 2), primary mouse keratinocytes isolated from C57/BL6 mice were seeded at the A/L interface of dermal equivalents populated with 2 x 10^6 mock-transfected HCA2 fibroblasts. These lattices had been preconditioned for one week. SEs were cultured up to four weeks with duplicate samples harvested each week (Fig. 3). Following fixing in 4 % paraformaldehyde

tissues were paraffin embedded, sectioned and analysed by hematoxylin and eosin (H & E) staining (processing carried out by Kath Allsop, Cardiff Dental School). Samples obtained following the first week of culture had no established epidermis. Tissue architecture peaked following two weeks of culture, with more rounded basal cells and flattening evident in the upper layers (Fig. 3b). However deterioration in tissue architecture was apparent in weeks three and four (Fig. 3c and d), when keratinocytes demonstrated a more rounded morphology and an irregularity of epidermal thickness, which did not exceed seven cell layers. It should be noted that both the epidermal and dermal sources of cells have origins in body regions demonstrating a thin epidermis (ear and foreskin respectively) (Ya-Xian *et al.*, 1999). Ideally a culture period of around three weeks could be included in the model in order to allow the formation of basement membrane structures as reported by Hinterhuber *et al.* (1998).

Fig. 2

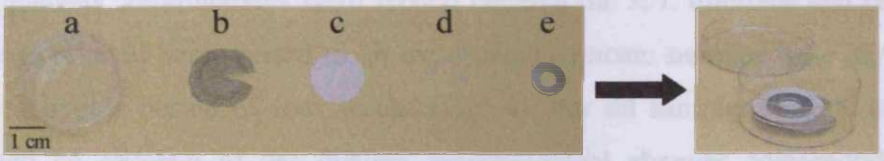

Fig. 3

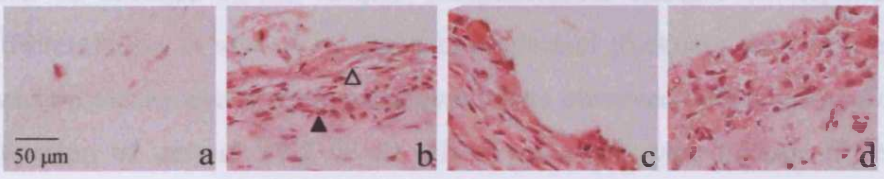

Fig. 2. Experimental set up for the contraction method of keratinocyte-fibroblast coculture: Floating collagen lattices were transferred using a sheet of nylon (d) to a stainless steel mesh stage (b) within a deep culture dish (a). The inclusion of filter paper (c) between the stage and nylon ensured adequate transfer of media to the skin equivalent once raised to the A/L interface. When cells were seeded at this interface a well was created by the inclusion of a 5 mm stainless steel washer (e)

Fig. 3 Tissue architecture of primary mouse keratinocyte-mock HCA2 cocultures: Using the contraction method, 1 x 10^6 keratinocytes isolated from C57/BL6 mice were seeded at the air-liquid interface on collagen lattices containing 2 x 10^6 mock-transfected HCA2 fibroblasts (a, b, c, d). Skin equivalents were cultured for up to four weeks before harvesting and analysis with H&E staining (a) 1 week coculture (b) 2 weeks (c) 3 weeks (d) 4 weeks. Tissue morphology was observed to peak following 2 weeks of culture, when rounded keratinocytes were observed in the deeper layers (solid arrowhead) compared to a more flattened morphology in the surface layers (hollow arrowhead).

Previous studies have utilised a spontaneously immortalised human keratinocyte line, HACAT, to generate SEs, but have demonstrated abnormal keratinocyte differentiation with irregular expression of K1 and K10 (Boelsma *et al.*, 1999). An alternative cell line derived from normal human epidermal keratinocytes, has been established and termed Ntert (discussed in Chapter 3). These cells have demonstrated normal suprabasal expression of involucrin and K10 in stratified colonies (Dickson *et al.*, 2000). This cell line has also been used successfully to generate SEs (Dickson *et al.*, 2000). Studies of the tissue architecture in such cocultures have revealed a model of orthokeratinising differentiation, with an observed granular layer and multilayered stratum corneum. Including this cell line in the skin cocultures forming this study had the advantages of producing a human model and removing batch-batch variation.

Dermal equivalents containing the four HCA2 transfectants (mock, antisense, sense and $Cys^{277}Ser$) were generated using the contraction method; untransfected HCA2 fibroblasts were included as an additional control to confirm that transfection had produced no phenotypical alterations to the fibroblasts. To achieve a more uniform epidermis, keratinocytes were seeded beneath the A/L interface and cultured for three days prior to being raised to air exposure. Duplicate samples were harvested once a week over a period of four weeks (Fig. 4). For all samples H & E staining demonstrated an absence of the distinct morphological changes corresponding to terminal differentiation *in vivo*. Variations in epidermal thickness were still evident and there was no clear increase in keratinocyte layers observed with increased culture time or alteration of dermal TG2 levels. However, there were notable differences observed between the tissue architecture and keratinocyte morphology of the four Ntert-HCA2 transfectant cocultures. In the case of cocultures incorporating the TG2 antisense-expressing fibroblasts, there appeared to be a looser tissue architecture and keratinocytes did not lie in close contact (Fig. 4u), possibly due to a reduction in cell-cell interactions. Keratinocytes cocultured with serine mutant transfectants demonstrated a more rounded morphology and an apparent propensity for invading the dermal gel (Fig. 4v).

To confirm these apparent effects the experiment was repeated, this time with an earlier passage of HCA2 fibroblasts (1-2 passages following transfection with the TG2 constructs) (Fig. 5). The variations observed with the original experiment were

not evident, highlighting problems with reproducibility using this coculture method. However, in some cases within the repeat experiment, the epidermis generated by coculture with the TG2 antisense fibroblasts was observed to have detached from the dermal gel completely. This may demonstrate deficiencies in the DEJ (Fig. 5 h). An improved architecture was observed for SEs including the serine mutant transfectant within the repeat experiment. Some flattening of keratinocytes is apparent in the upper cell layers (Fig. 5u).

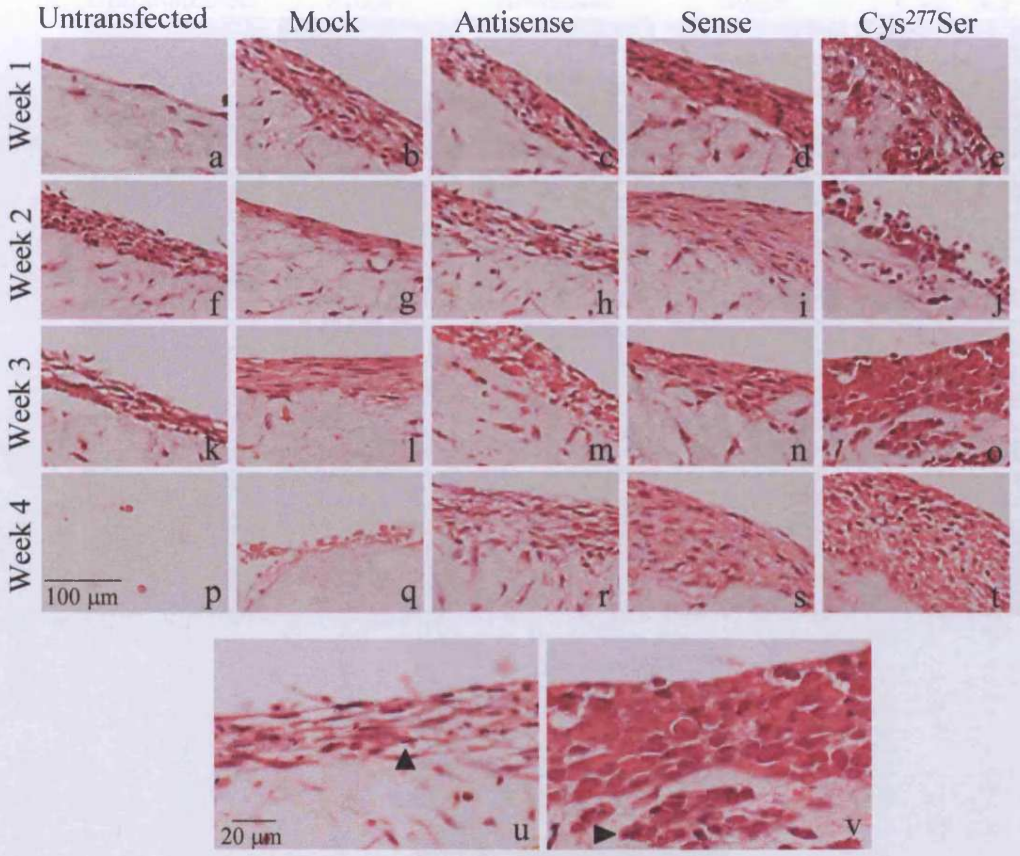

Fig. 4 H & E stained sections demonstrating tissue architecture in organotypic Ntert-HCA2 cocultures (Batch 1): 1 x 10^6 keratinocytes were seeded onto collagen lattices containing 2 x 10^6 HCA2 fibroblasts transfected to produce high level constitutive expression of TG2 antisense RNA (c, h, m, r), sense RNA (d, i, n, s), as well as a TG2 mutant RNA containing a Cys to Ser substitution within the active site domain (e, j, o, t). Controls of untransfected HCA2 fibroblasts (a, f, k, p) and cells transfected with an empty vector, mock (b, g, l, q) were included. Samples were processed for histology following 1-4 weeks of culture and sections stained with H & E.
Pictures u-v are magnified to highlight morphological features of interest. (u) Week 2, Ntert-antisense coculture, keratinocytes demonstrate a loose architecture with numerous gaps between cell layers (arrowhead). (v) Week 3, Ntert-Cys^{277}Ser coculture, Keratinocytes have a distinctly rounded morphology and clusters of keratinocytes are observed within the dermal compartment (identified by arrowhead).

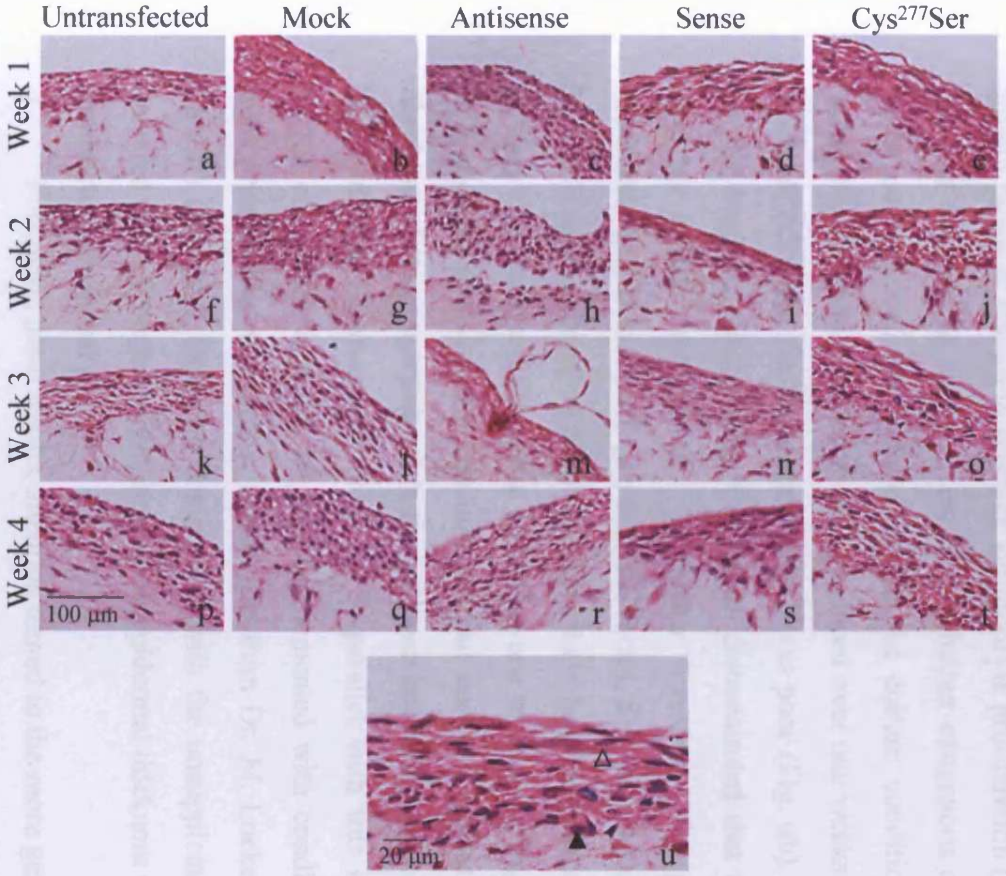

Fig. 5 H & E stained sections showing tissue architecture in repeat organotypic Ntert-HCA2 cocultures (Batch 2): To ensure the phenotype of fibroblasts within collagen lattices had not altered with passaging, cocultures were established using a low passage (1-2) of each transfectant; antisense (c, h, m, r) sense (d, i, n, s), Cys^{277}Ser (e, j, o, t), untransfected (a, f, k, p) and mock-transfected (b, g, l, q). Skin equivalents were cultured at the air-liquid interface for up to four weeks (1 week a-e), (2 weeks f-j), (3 weeks k-o), (4 weeks p-t). (u) Magnified picture of Ntert-Cys^{277}Ser coculture following 3 weeks at the A/L interface, demonstrating increasingly flattened cell morphology in the more superficial layers A rounded basal cell and a disc-like keratinocyte in the surface layer are marked with a solid and hollow arrowhead respectively.

6.2.1.1 Optimisation of coculture conditions

In order to identify the effects of mesenchymal TG2 levels, a baseline closer to native skin was needed and attempts were made to optimise the culture conditions used. Taking into account the thin epidermis generated in initial experiments, the first step taken was to supplement the FAD media with 10 ng/ml KGF (Fig. 6). This growth factor is known to promote keratinocyte proliferation (Andreadis *et al.*, 2001) and this experiment aimed to establish whether exogenous addition of this growth factor compensated for deficiencies in the culture conditions. Although a slight increase in epidermal thickness was produced over one weeks coculture of Ntert with mock HCA2 cells, the tissue architecture was poor (Fig. 6b). This was also the case for the negative control (Fig. 6a), which demonstrated that the contraction method was not highly reproducible. To further investigate the possibility that HCA2 fibroblasts may be deficient in a required factor, SEs were set up incorporating murine 3T3 cells as an alternative fibroblast since these had been successfully cocultured with primary keratinocytes. However, following one week culturing at the A/L interface H & E staining revealed the keratinocytes had become apoptotic and despite 2 x 10^6 fibroblasts being incorporated in the collagen lattice few fibroblasts were discernable in the dermal compartment (Fig. 7). In parallel with this experiment Ntert-mock HCA2 cocultures were set up and supplemented with conditioned media obtained from primary oral fibroblasts, a kind gift from Dr. M. Locke (University of Wales, Cardiff) (Fig. 8b). However comparison with the unsupplemented control (Fig. 8a) revealed that although a slight increase in epidermal thickness was observed the tissue architecture remained poor.

Following these results, attention turned to the more general culture conditions and the step taken was to increase the collagen concentration within the dermal equivalent. The contraction model used had been developed with murine fibroblasts, known to generate lower levels of collagenases when compared with cells from human lineage (Dr. W. Parish, Unilever, unpublished data). It was hypothesised that the higher quantities of collagenases expressed by the human fibroblasts may be compromising the dermal gels and in order to counteract this effect, the collagen concentrations were raised by 10 % (3.5 increased to 3.9 mg/ml). At this stage cholera toxin was removed from the media for all subsequent experiments. Although it was

observed both Ntert keratinocytes and HCA2 fibroblasts could be cultured in its presence there were some concerns it may be having a detrimental effect. Previous studies have observed that cholera toxin induces keratinocyte proliferation (Rahman and Tsuyama, 1993), growth (Brunette, 1984) and their outgrowth form partial thickness wounds (Regauer and Compton, 1990). Although its inclusion in coculture media is commonly documented it does not appear to be a necessary component for SE generation. Ntert-mock HCA2 cocultures were established under these newly adopted conditions and despite the tissue architecture demonstrating polygonal cells in the deeper layers and a flattened morphology towards the surface, results were comparable with the control (Fig. 9a and b respectively).

Fig. 6

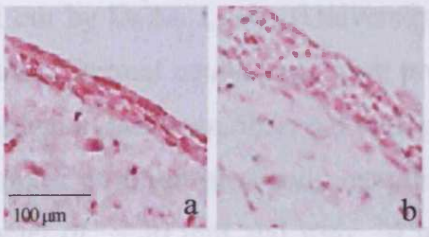

- KGF + KGF

Fig. 7

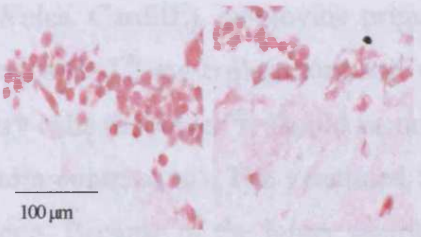

3T3 3T3

Fig. 8

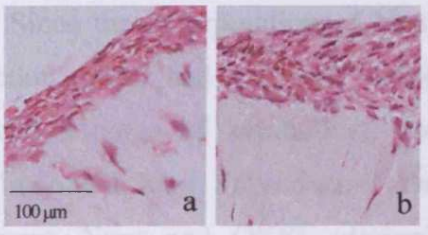

Unconditioned media Conditioned media

Fig. 9

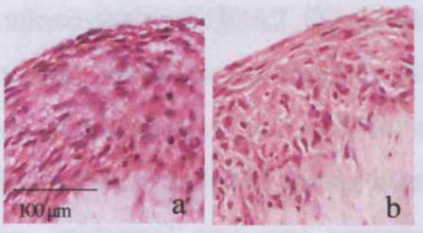

3.5 mg/ml collagen 3.9 mg/ml collagen

Fig. 6 Epithelial tissue formation is not improved by addition of KGF: Epidermal morphology (H & E staining) of 7-day organotypic cocultures containing Ntert keratinocytes and mock-transfected HCA2 fibroblasts in FAD medium as a control (a) or supplemented with 10 ng/ml KGF following seeding (b).

Fig. 7 Ntert-murine 3T3 cocultures resulted in apoptotic keratinocytes: H & E staining of cocultures following 7 days culture at the A/L interface. Keratinocytes were seen to be apoptotic and it was noted that no fibroblasts were detected within the collagen lattice despite the inclusion of 2 x 10^6 cells.

Fig. 8 Conditioned media from primary fibroblasts does not improve epidermis generation: Conditioned media from primary fibroblast dermal equivalents was used to grow Ntert-mock-transfected HCA2 cocultures (b). Unsupplemented FAD medium was used as a control (a). Although there may have been a slight increase in epidermal thickness, tissue architecture was not improved, suggesting the soluble factors alone were inadequate to produce an epidermis comparable to native skin.

Fig. 9 Epithelial tissue formation is not improved by increased collagen concentration: (a) Ntert-mock-transfected HCA2 cocultures were established in the absence of cholera toxin and incorporating a 10 % increase in collagen concentration (3.9 mg/ml). However tissue architecture was not improved when compared to the control (3.5 mg/ml) (b).

6.2.1.2 Adoption of the insert method of coculture

At this point a decision was made to employ a different method of coculture (referred to as the insert method, Fig. 10). Previous work with this method has been carried out by Dr M. Locke (University of Wales, Cardiff.), employing primary oral fibroblasts. Dermal equivalents were produced with 2.2 mg collagen/ml and virtually no contraction had been observed with primary cells (however, it should be noted that the samples were not physically restrained from contracting). The generated SEs had a diameter of ~ 30 mm and were ~4 mm deep. Because of the larger sample size a greater number of cells were incorporated in this model (3 x 10^6 fibroblasts and 2 x 10^6 keratinocytes) (described in Section 2.9.3).

Since the incorporation of Ntert keratinocytes and HCA2 fibroblasts in the contraction model had met with limited success, initial experiments in this study integrated a range of keratinocyte-fibroblast combinations, in order to establish suitability of cell lines. Subsequently, two cell lines were included for the keratinocyte constituent, Ntert and OKF6 (derived from epidermal and oral mucosal tissue respectively). As is the case for the Ntert cell line OKF6 keratinocytes have been transfected with hTERT and emerged as rapidly dividing cells from slow growth phase culture following a mutation in the gene encoding $p16^{INK4\alpha}$ (Dickson *et al.*, 2000). However, in contrast to the Ntert cell line, these keratinocytes demonstrate non-keratinising differentiation when incorporated into SE models, expressing K13 in suprabasal cells (Dickson *et al.*, 2000). For the purposes of this experiment the dermal gel incorporated one of three different fibroblasts; primary oral, murine 3T3 and mock-transfected HCA2. This selection aimed to provide controls for this model, allowing the assessment of the HCA2 fibroblasts ability to support epidermal generation. For these cocultures the source of collagen was changed to bovine stocks in case the preparation from rats' tails had been in part responsible for previous problems. As with the contraction method these collagen embedded fibroblasts were precultured for one week prior to keratinocyte seeding beneath the A/L interface. After three days the media levels were lowered and the keratinocytes cultured for a further week before harvesting and analysis of tissue architecture by H & E staining (Fig. 11). SEs including the OKF6 cells were not successfully cultured with any of the three fibroblast types and were completely absent from cocultures with oral and

HCA2 fibroblasts (Fig. 11d and f). Residual cell debris was apparent with the 3T3-supported coculture (Fig. 11e) indicating cell death had occurred. The inclusion of Ntert keratinocytes met with greater success, however, tissue architecture was poor and in all cases the epidermis had detached from the dermal gel, evidence of a sufficient DEJ being absent. The greatest number of keratinocyte cell layers was observed with 3T3 cocultures (5 layers). Only two cell layers were established on HCA2 populated gels, suggesting these fibroblasts may not be capable of supporting a thicker epidermis with this method. It was also noted that despite counts to equalise cell numbers, HCA2 fibroblasts appeared at a higher density within the dermal gel (Fig 11f).

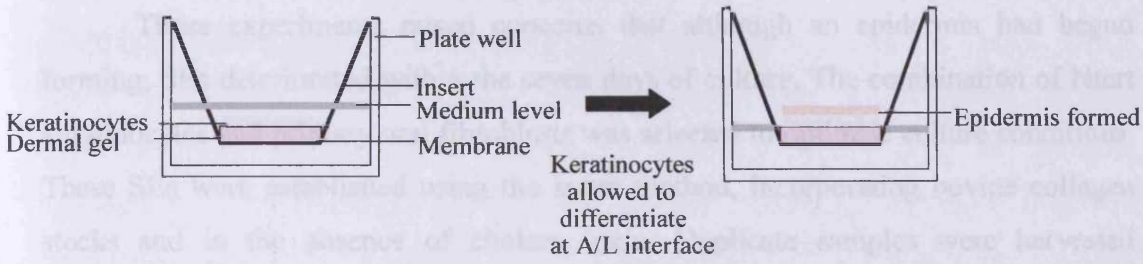

Fig. 11

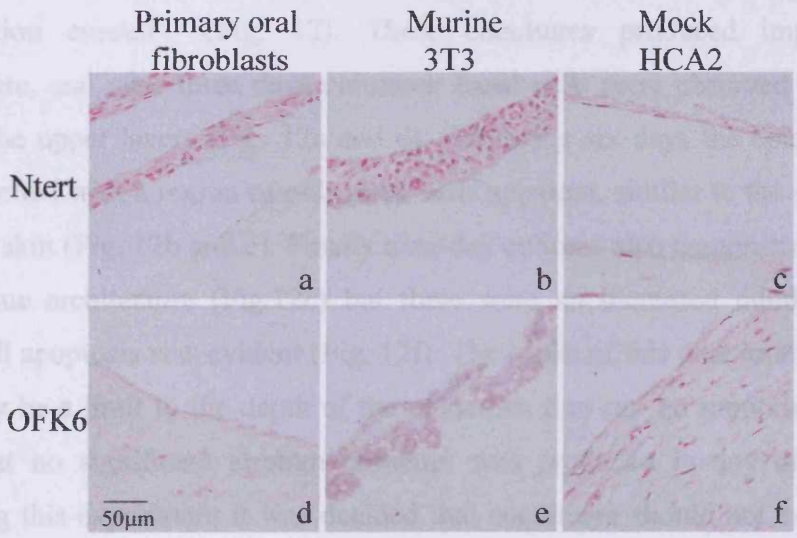

Fig. 10 Apparatus set up used to generate cocultures by the insert method: Dermal gels containing 3 x 10^6 fibroblasts were allowed to fibrilise within culture inserts before submersion in FAD medium and seeding of 2 x 10^6 keratinocytes (Ntert). Differentiation of keratinocytes was induced by altering media levels to expose the dermal gel surface to the A/L interface.

Fig. 11 Ability of HCA fibroblasts to support epidermal growth compared to that of primary fibroblasts and murine 3T3 cells. Skin equivalents were set up using the insert method (2 x 10^6 keratinocytes and 3 x 10^6 fibroblasts) and a variety of keratinocyte-fibroblast combinations. These included keratinising Ntert (a-c) and non-keratinising OFK6 (d-f) cell lines with primary oral fibroblasts (a, d), murine 3T3 (b, e) and mock-transfected HCA2 (c, f). H & E staining revealed attempts to establish an epidermis with Htert cells were unsuccessful. Although skin equivalents including Ntert cells all demonstrated poor tissue architecture it is apparent the HCA fibroblasts produced a thinner epidermis (c) when compared with the primary fibroblasts and murine 3T3 cells (a and b).

These experiments raised concerns that although an epidermis had begun forming, SEs deteriorated within the seven days of culture. The combination of Ntert keratinocytes and primary oral fibroblasts was selected to optimise culture conditions. These SEs were established using the insert method, incorporating bovine collagen stocks and in the absence of cholera toxin. Duplicate samples were harvested following three, six and nine days culture in order to ascertain when tissue deterioration ensued (Fig. 12). These cocultures produced improved tissue architecture, and after three days columnar basal cells were observed with flattened cells in the upper layers (Fig. 12a and d). Following six days the epidermis formed had thickened with a region of polygonal cells apparent, similar to the spinous region of native skin (Fig. 12b and e). Finally nine-day cultures also demonstrated regions of good tissue architecture (Fig.12c) but there were an increased number of regions where cell apoptosis was evident (Fig. 12f). The cause of this deterioration is unclear; there may be a limit to the depth of the epidermis that can be supported. It was also noted that no significant stratum corneum was produced in any of the cultures. Following this experiment it was decided that cocultures should not exceed six days and repeats of the keratinocyte-fibroblast SEs were set up with the primary oral, 3T3 and HCA2 fibroblasts with Ntert keratinocytes. It was apparent that the same level of tissue architecture had not been produced by the oral fibroblast control in this experiment (Fig. 13a), highlighting the difficulties in reproducibility. A comparable number of keratinocyte cell layers were generated by murine 3T3 cells (Fig. 13b), but again the epidermis produced by HCA2 fibroblasts did not exceed two layers and produced no distinct morphology (Fig.13c). This result seems to support the hypothesis that HCA2 cells are not able to support an epidermis comparable to that of native skin.

A final attempt was made to produce a working model incorporating HCA2 fibroblasts. Although it is evident that HCA2 fibroblasts do not generate a differentiated epidermis it is not clear whether these cells are deficient in necessary factors or if there is a toxic affect. To address this, dermal equivalents were set up using oral fibroblasts and the four HCA2 transfectants (mock, antisense, sense and $Cys^{277}Ser$). These were seeded with Ntert keratinocytes on the same day, eliminating the week-long preconditioning step. Following six days culture at the A/L interface, tissue morphology was assessed by H & E staining (Fig. 14). Under these conditions

the HCA2 fibroblasts produced an epidermis of comparable thickness to that of oral fibroblasts, however the abundant presence of apoptotic cells lead to compromised tissue architecture. These results would suggest that the removal of the preconditioning step improves keratinocyte proliferation but does not produce satisfactory tissue architecture. Pictures of SEs following six days coculture demonstrate that HCA2 cells are able to more extensively re-organise the collagen matrix when compared with oral fibroblasts (Fig. 14g and f). Variability in lattice contraction by different transfectants was also observed using this method (Fig. 14f-j). This agrees with previous observations that TG2 cross-linking activity correlates with the rate of ECM re-organisation (Stephens *et al.*, 2004).

Fig. 12

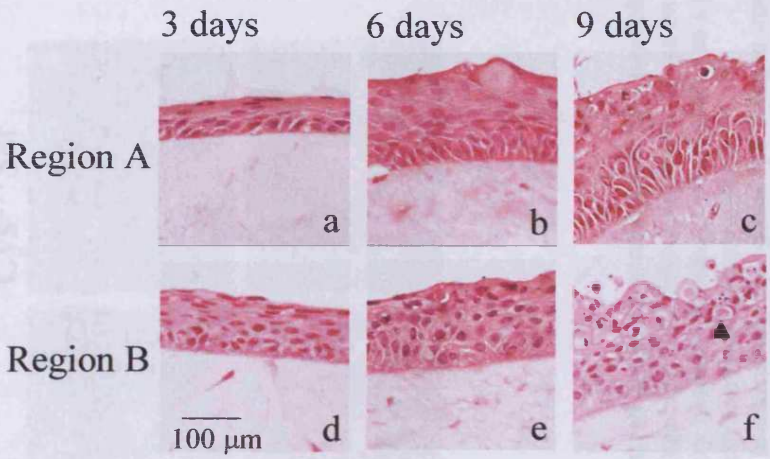

Fig. 13

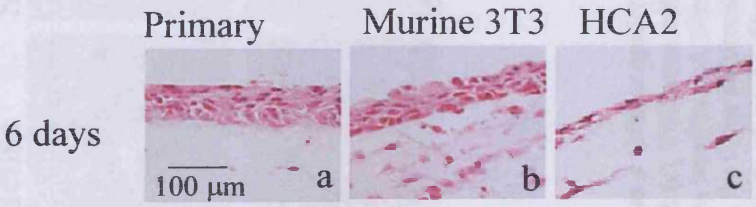

Fig. 12 Optimising culture duration: A series of Ntert-primary oral fibroblast cocultures were set up using the insert method and harvested over a period of nine days after raising to the air-liquid interface; 3 days, (a, d), 6 days (b, e) and 9 days (c, f). A solid arrowhead indicates an example of an apoptotic body. Taking into account epidermal thickness and tissue architecture, 6-day coculture was considered optimum.

Fig. 13 Growth of Ntert cocultures supported by primary oral (a), murine 3T3 (b) and HCA2 (c) fibroblasts using optimised conditions: Skin equivalents were cultured for 6 days at the air-liquid interface before harvesting and H & E staining. It is evident from the positive control (a) that good tissue structure from the optimisation experiment had not been reproduced. However, the epidermis supported by HCA2 fibroblasts is considerably thinner.

Fig. 14

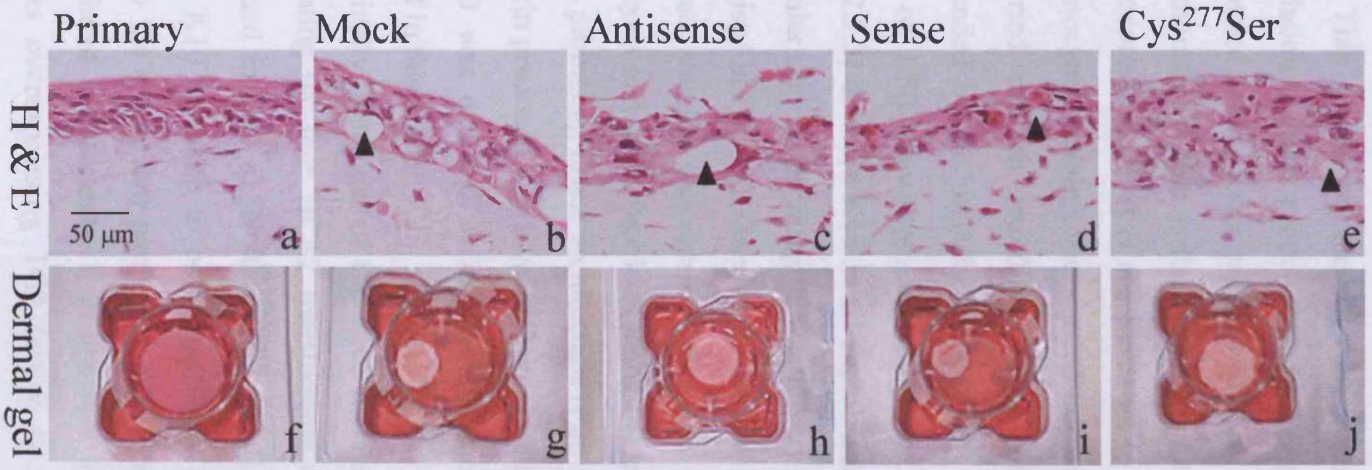

Fig. 14 Seeding keratinocytes onto unconditioned dermal equivalents produces a thicker epidermis but cell apoptosis is abundant: Skin equivalents populated with the four HCA2 transfectants including; mock-transfected (b), TG2 antisense mRNA (c), TG2 sense mRNA, (d) and Cys^{277}Ser mRNA (e) were cultured for six days at the A/L interface following the seeding of keratinocytes on the same day dermal equivalents were formed. Ntert-primary fibroblast cocultures were included as a positive control (a). Although a thicker epidermis is formed, keratinocytes become apoptotic, disrupting the tissue architecture (examples marked with arrowheads).
Pictures of the cocultures following 6 d at the A/L interface demonstrate the ability of HCA2 fibroblasts to extensively re-organise the collagen matrix compared with primary oral fibroblasts (g and f respectively). It was also noted that there was some variation in dermal contraction between the transfectants (mock, g, antisense, h, sense, i and Cys^{277}Ser, j). This agrees with previous findings that TG2 cross-linking activity is involved with the rate of ECM reorganisation.

6.2.1.3 Immunohistochemical analysis of skin equivalents

Although the tissue architecture produced by the two SE models was not analogous with that of native human skin, comparisons of SEs produced with the four HCA2 transfectants were still possible and were included in immunohistochemical studies. This aimed to identify any alterations in the expression keratinocyte differentiation markers produced with changes in dermal TG2 levels. K10 and TG3 were selected as respective markers of early and late stage differentiation. It has also been demonstrated that cells committing to terminal differentiation downregulate integrin expression (Watt *et al.*, 1993) so, to further establish the differentiation state of keratinocytes, staining was carried out with anti-β1 integrin (β1). Initial staining was carried out on paraffin sections of native human skin using dilutions recommended by the manufacturers (K10, 1/20 and β1, 1/50) TG3 was used at a dilution of 1/50. Development using the AEC chromogen system (described in Section 2.2.3) detected K10 in all suprabasal layers whereas TG3 was detected from the granular region. β1 integrin was largely restricted to undifferentiated basal cells (summarised in Fig. 15). Once conditions for immunohistochemical analysis had been established, staining was carried out on the six-day cocultures generated with Ntert keratinocytes and oral fibroblasts using the insert method. This sample had produced the most promising tissue architecture (Fig. 12), however TG3 was not detected and β1 integrin produced low level staining in the lower two layers of the epidermis (Fig. 15). K10 was detected in all layers demonstrating normal differentiation is not produced in this model.

Finally, detection of the three markers was carried out on 7-day cocultures, incorporating the four HCA2 transfectants using the contraction method (Batch 1, summarised in Fig. 4). Neither TG3 nor β1 integrin were detected in any of the samples. K10 appeared to be misregulated and all cells stained positive (Fig. 16). Although the expression pattern of K10 remains the same in SEs supported by the four different transfectants, it is apparent that Ntert keratinocytes cocultured with fibroblasts overexpressing TG2 (active or inactive form) demonstrated increased levels of the protein. However detection of K10 in Batch 2 samples (H&E staining summarised in Fig. 5) incorporating an earlier cell passage did not produce any cell specific staining (data not shown). This may have been the result of tissue processing and prevented the confirmation of these observed differences.

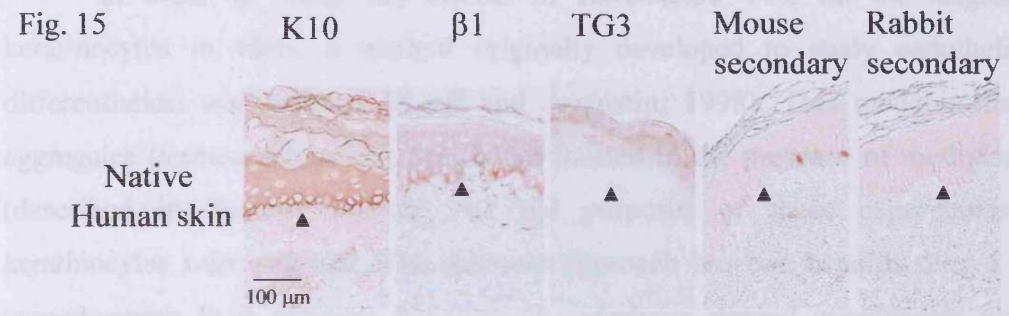

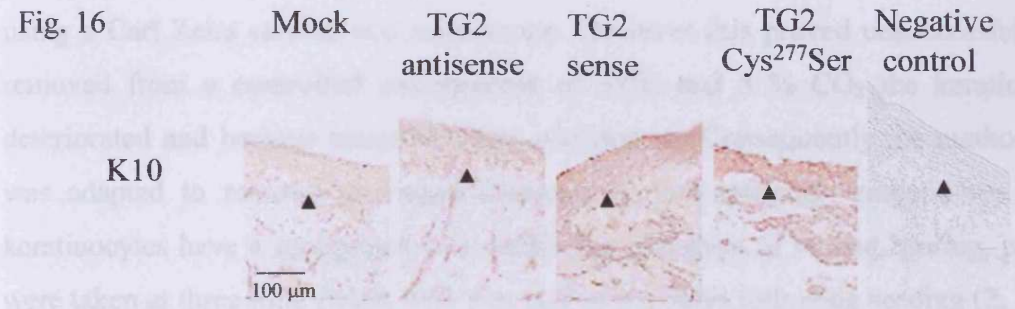

Fig. 15 Skin equivalents incorporating primary oral fibroblasts do not demonstrate expression of differentiation markers observed in native skin: Sections of native human skin and 6-day Ntert-oral fibroblast cocultures were stained with anti-keratin 10 (K10) and anti-TG3 (TG3) as respective markers of early and late differentiation. Distinction between basal keratinocytes and those committed to terminal differentiation were further assessed by anti-β1 integrin staining (β1). Signal development utilised the AEC chromogen system. Incubation with the secondary antibodies alone was included as negative controls (mouse and rabbit secondary), anti-K10 being raised in mouse whilst TG3 and β1 were raised in rabbit. The DEJ is indicated with arrowheads.

Fig. 16 K10 is expressed in all keratinocyte cell layers in Ntert-HCA2 7-day cocultures: Anti-K10 detection in Batch 1 transfectant cocultures (contraction method, Fig. 4) produced positive staining in all cells, with comparatively high levels observed in cocultures including HCA2 fibroblasts over-expressing TG2 (sense and $Cys^{277}Ser$). All negative controls stained negative with the TG2 mock cocultures pictured above (negative control). The DEJ is indicated with arrowheads.

6.2.2 Establishing a migration model

In order to study the effects of fibroblastic TG2 on the migration of keratinocytes *in vitro*, a method originally developed to study endothelial cell differentiation was adapted (Korff and Augustin, 1998). This model utilises cell aggregates (termed spheroids), which are formed in the presence of methylcellulose (described in Section 2.10.1). For the purposes of these experiments Ntert keratinocytes were selected. The spheroid approach has two benefits over a scratch wound assay; 1) it prevents removal of underlying dermal components and 2) it creates a more reproducible model with spheroids of defined size and cell number (2500 cells/spheroid). An initial attempt to employ time-lapse analysis of this migration model was made following seeding of an Ntert spheroid onto the collagen coated well of a 24 well plate. Phase contrast pictures were taken at 30 min intervals using a Carl Zeiss camera and microscope. However this proved unsuccessful, once removed from a controlled environment of 37°C and 5 % CO_2 the keratinocytes deteriorated and became apoptotic (data not shown). Consequently the methodology was adapted to remove prolonged exposure to sub-optimum temperatures. Since keratinocytes have a recognised role within the first days of wound healing, pictures were taken at three time points over a period of two days following seeding (2, 24 and 48 h). Initial experiments were carried out by seeding Ntert spheroids onto hyperconfluent HCA2 fibroblasts (mock, antisense, sense and $Cys^{277}Ser$) induced to generate ECM components by the presence of 50 μg/ml ascorbic acid in the growth media. This has been demonstrated to stimulate FN and procollagen expression (Furcht *et al.*, 1980; Franceschi *et al.*, 1994). An alternative method would have been to produce fibroblast-populated collagen lattices, which would have produced a more homogenous scaffold. However the method selected ensured an ECM produced entirely by the mesenchymal source.

6.2.2.1 Optimisation of Calcein AM green labelling

In order to track the movement of keratinocytes over fibroblast cells the spheroids were labelled with Calcein AM green. This chemical dye produced a fluorescent signal reliant on the inherent esterase activity of live cells. Optimisation of labelling was carried out on Ntert monolayers (50 x 10^4 cells seeded), Calcein AM green was diluted in FAD media to a final concentration of 0.1, 1 and 10 μM. Cells were labelled for 15 min under culture conditions. Pictures were taken at 2, 24 and 48 h before cells were recovered by trypsinisation and counted (Fig. 17a and b). Cell numbers demonstrated the levels of Calcein AM green used were non-toxic (0.1 μM; 70 x 10^4, 1 μM; 61 x 10^4, 10 μM; 64 x 10^4 compared to the negative control; 65 x 10^4). For the purpose of these experiments it was apparent that a concentration of 1 μM produced insufficient signal for the proposed time points, however 10 μM produced high background. Since the intention was to label the keratinocytes following spheroid formation, a further pilot experiment was set up. Spheroids were seeded onto mock-transfected HCA2 fibroblasts grown to three days post-confluence in the presence of 50 μg/ml ascorbic acid. These results ascertained that a final Calcein AM green concentration of 5 μM produced adequate labelling (Fig. 18). It was also observed that when migrating over hyperconfluent HCA2 transfectants the spheroids formed an ovoid body that aligned with the underlying fibroblast strata.

Fig. 17

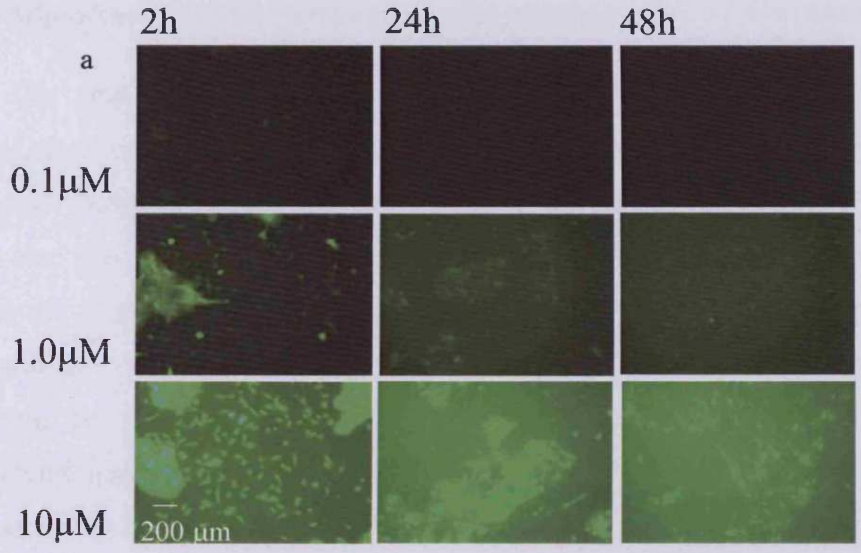

b

Calcein AM green concentration/μM	10^4 cells/ml counted following 48 h labelling
0	65
0.1	70
1	61
10	64

Fig. 18

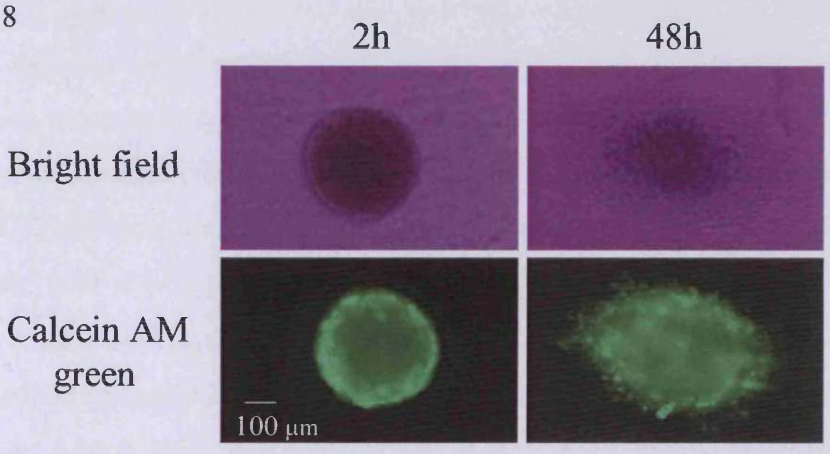

Fig. 17 Optimisation of Calcein AM green labelling: (a) Monolayers of Ntert keratinocytes ($50x10^4$ cells seeded) were labelled with four concentrations of Calcein AM green (0, 0.1, 1.0 and 10μM). Images were taken at three time points (2, 24 and 48 h) to establish the concentration required to maintain adequate levels of fluorescence. (b) After 48 h cells were retrieved by trypsinisation and counted, these numbers ascertained the concentrations used were not toxic.

Fig. 18 Ntert spheroids form ovoid bodies following seeding onto hyperconfluent fibroblasts, which align with the underlying strata: Ntert spheroids were labelled with a final concentration of 5 μM Calcein AM green for 15 min prior to seeding. When migrating over hyperconfluent HCA2 transfectants Ntert spheroids were observed to form oval bodies (pictured with mock transfectants after 48 h). Observations with bright field microscopy revealed keratinocytes aligned with the underlying strata.

6.2.2.2 Migration of Ntert keratinocytes in the presence of HCA2 fibroblasts

The first experiment carried out over hyperconfluent HCA2 fibroblasts included six sample repeats for each transfectant. A repeat experiment was also established, however, in an attempt to reduce the impact of group variability the sample size was increased from six to ten. As was observed in the pilot experiment, keratinocyte migration resulted in the formation of oval bodies (Fig. 19). The extent of migration over the four transfectants clearly varied with an apparent increase correlating to TG2 downregulation and slowed migration accompanying TG2 overexpression independent of cross-linking activity. Measurements were taken along the longest and widest axes and converted into area measurements (mm^2), expressed as a mean ± SD (Fig 20a-d). In addition statistical analysis was carried out using unpaired student's t test ($p<0.05$ considered significant). Migration of keratinocytes over mock-transfected cells was taken as the control with which data from antisense, sense and $Cys^{277}Ser$ cells were compared.

Measurements taken at the first time point (2 h) demonstrated the generation of Ntert aggregates in the presence of methyl cellulose produce spheroids of uniform size, however when comparing the repeat experiments neither absolute values nor the relative increase in spheroid area was comparable, consequently each experiment was analysed separately looking for parallel trends. In the first experiment migration over the TG2 deficient fibroblasts resulted in an increased rate of migration at both the 24 h (mock; 0.20 ± 0.02 mm^2, antisense; 0.28 ± 0.04 mm^2) and 48 h time points (mock; 0.30 ± 0.04 mm^2, antisense; 0.40 ± 0.08 mm^2). In contrast the overexpression of the cross-linking inactive form resulted in a reduced rate of migration within the first 24 h (mock; 0.20 ± 0.02 mm^2, $Cys^{277}Ser$; 0.11 ± 0.01 mm^2). However there were no significant differences apparent between the mock transfectants and fibroblasts overexpressing the active form of TG2 (sense). This would seem to contradict the data concerning the $Cys^{277}Ser$ mutant, however the repeat experiment demonstrated reduced migration rates in both the sense and $Cys^{277}Ser$ transfectants (24 h mock; 0.29 ± 0.02 mm^2, sense; 0.26 ± 0.01 mm^2, $Cys^{277}Ser$; 0.22 ± 0.02 mm^2 48h mock; 0.42 ± 0.04 mm^2, sense; 0.37 ± 0.02 mm^2, $Cys^{277}Ser$; 0.30 ± 0.03 mm^2). Interestingly the data from the two experiments would suggest that the greatest reduction in migration is observed in the presence of the $Cys^{277}Ser$ mutant. Previous studies involving

Western blot analysis of these HCA2 transfectants have demonstrated that higher levels of the TG2 enzyme are actually observed in the sense cells compared to the $Cys^{277}Ser$ (Stephens *et al.*, 2004). This discrepancy in conjunction with the conflicting results of the two migration experiments may suggest the catalytic activity of TG2 and its binding abilities have opposing effects on keratinocyte migration, participating in separate pathways. The repeat experiment did confirm an increase in the rate of keratinocyte migration over TG2 deficient cells (24 h mock; 0.29 ± 0.02 mm^2, antisense; 0.33 ± 0.01 mm^2, 48h mock; 0.42 ± 0.04 mm^2, antisense; 0.58 ± 0.04 mm^2).

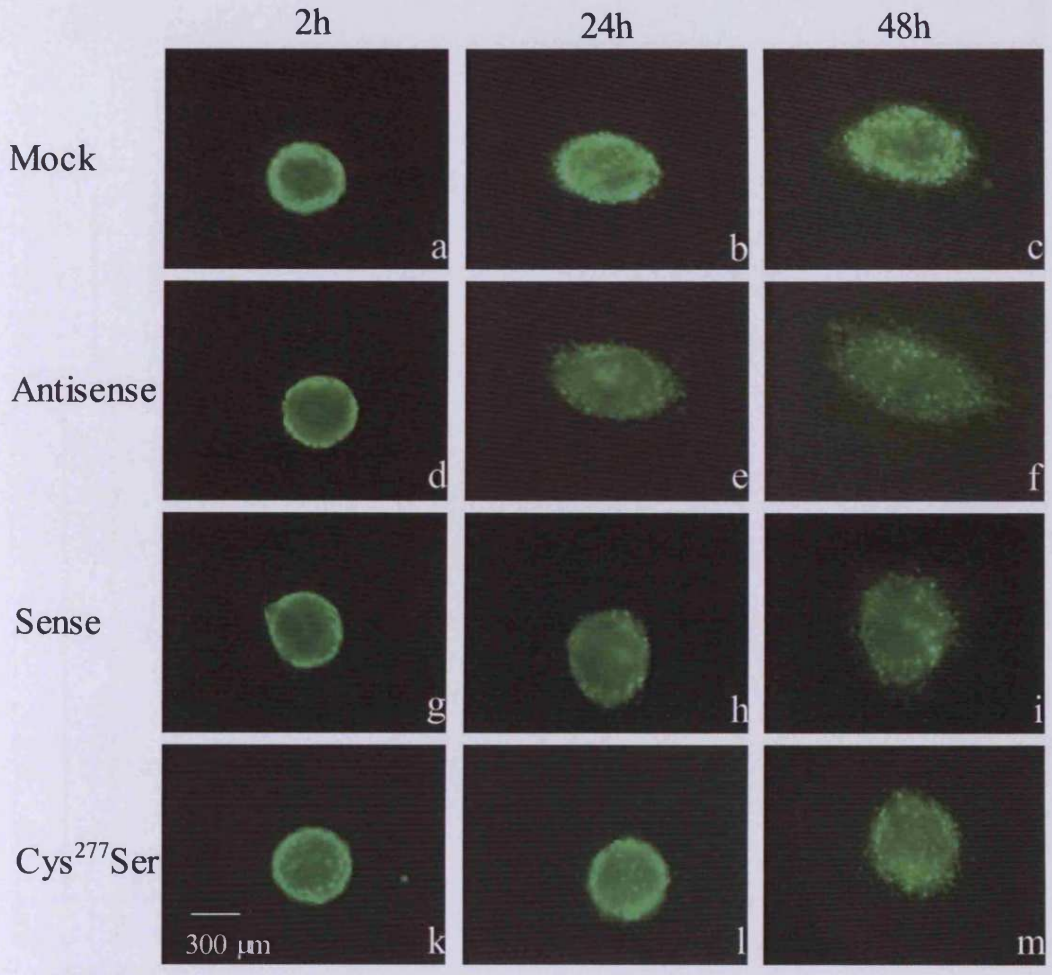

Fig. 19 Migration of Ntert spheroids over hyperconfluent HCA2 transfectants: mock-transfected (a-c), TG2 antisense (d-f), TG2 sense (g-i) and $Cys^{277}Ser$ (k-m) transfectants were included. Pictures selected are representative of mean measurements (experiment 2) taken at three time points, 2h (a, d, g, k), 24 h (b, e, h, l) and 48 h (c, f, I, m)

a

	Time elapsed following seeding/h		
	2h	24h	48h
	Area/mm^2 ± SD	Area/mm^2 ± SD	Area/mm^2 ± SD
Mock	0.07 ± 0.00	0.20 ± 0.02	0.30 ± 0.04
Antisense	0.07 ± 0.00	0.28 ± 0.04	0.40 ± 0.08
	0.53	0.01	0.02
Sense	0.07 ± 0.00	0.19 ± 0.02	0.32 ± 0.02
	0.39	0.88	0.15
Cys^{277}Ser	0.07 ± 0.00	0.11 ± 0.01	0.26 ± 0.05
	0.42	0.00	0.26

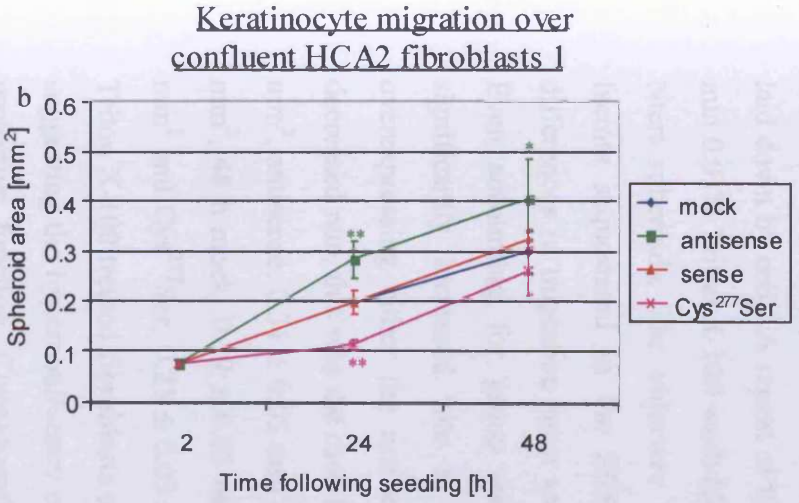

c

	Time elapsed following seeding/h		
	2h	24h	48h
	Area/mm^2 ± SD	Area/mm^2 ± SD	Area/mm^2 ± SD
Mock	0.19 ± 0.01	0.29 ± 0.02	0.42 ± 0.04
Antisense	0.18 ± 0.01	0.33 ± 0.01	0.58 ± 0.04
	0.36	0.01	0.00
Sense	0.17 ± 0.02	0.26 ± 0.01	0.37 ± 0.02
	0.23	0.03	0.01
Cys^{277}Ser	0.18 ± 0.01	0.22 ± 0.02	0.30 ± 0.03
	0.60	0.00	0.00

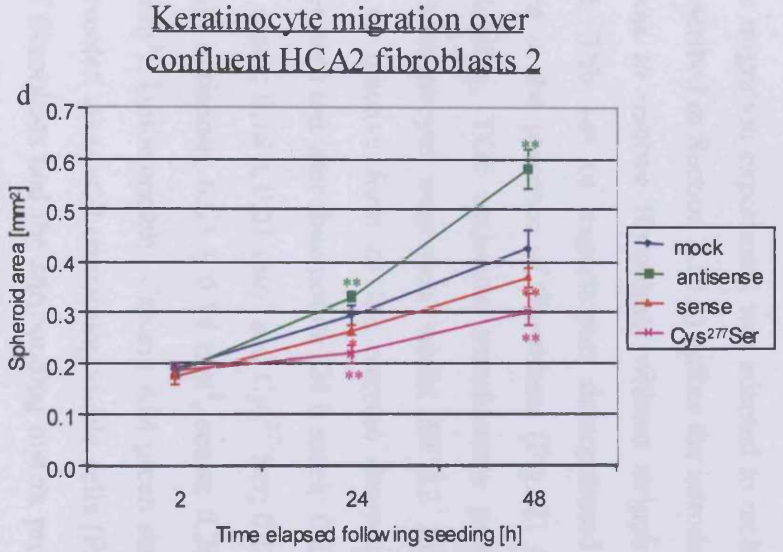

Fig. 20 Ntert spheroid migration over hyperconfluent HCA2 transfectants: Spheroid areas were calculated at three time points (2, 24 and 48h) over two experiments; Experiment 1 (a & b), Experiment 2 (c & d). Data for the four transfectants are shown as mean values ± standard deviation (SD) with p-values shown in blue (a & c), or the mean values are plotted within a graph (b & d) with the SD expressed as error bars. $p<0.05$ * $p<0.01$**

6.2.2.3 Delineating the effects of fibroblast cells from their generated ECM and soluble factors

The next aim of this study was to establish whether these results were dependent on the presence of fibroblasts or could be attributed to differences in ECM laid down by cells. A repeat of the migration experiment was adapted to include a 10 min 0.01% Triton X-100 wash (described in Section 2.10.3) before the introduction of Ntert spheroids. The objective was to remove fibroblasts without stripping away factors sequestered in the ECM. This set of experiments demonstrated similar differences in migration rates seen in the presence of fibroblasts (Fig. 21 and 22). Even accounting for group variability, TG2 antisense transfectants produced a significantly increased rate of keratinocyte migration whilst HCA2 fibroblasts overexpressing either the active or inactive form of the enzyme demonstrated a decreased rate, this was the case for both the later time points (24 h mock; 0.25 ± 0.07 mm^2, antisense; 0.31 ± 0.05 mm^2, sense; 0.18 ± 0.01 mm^2 and $Cys^{277}Ser$; 0.16 ± 0.01 mm^2, 48 h mock; 0.39 ± 0.03 mm^2, antisense; 0.63 ± 0.14 mm^2, sense; 0.26 ± 0.02 mm^2 and $Cys^{277}Ser$; 0.21 ± 0.03 mm^2). Unfortunately, Calcein AM green staining of Triton X-100 treated fibroblasts revealed areas still containing viable cells (Fig. 23b), suggesting the hyperconfluency of fibroblasts and the surrounding matrix produced a protective function. Consequently, cellular effects and the production of soluble factors cannot be disregarded in this experiment.

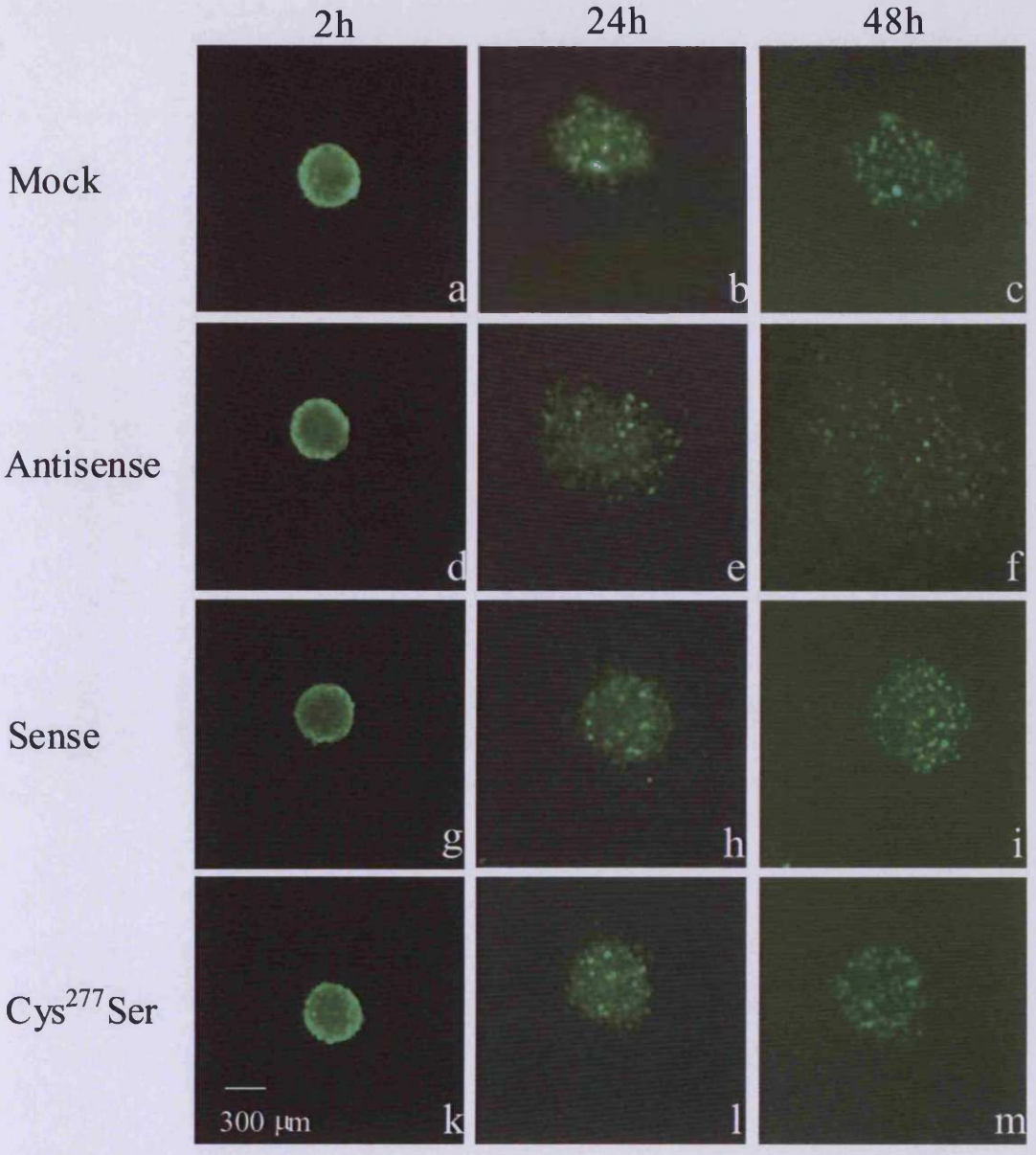

Fig. 21 Migration of Ntert spheroids over Triton X-100 treated HCA2 transfectants: mock-transfected (a-c), TG2 antisense (d-f), TG2 sense (g-i) and $Cys^{277}Ser$ (k-m) transfectants were included. Pictures selected are representative of mean measurements and were taken at three time points, 2h (a, d, g, k), 24 h (b, e, h, l) and 48 h (c, f, I, m).

a

	Time elapsed following seeding/h		
	2h	24h	48h
	Area/mm^2 ± SD	Area/mm^2 ± SD	Area/mm^2 ± SD
Mock	0.09 ± 0.01	0.25 ± 0.07	0.39 ± 0.03
Antisense	0.09 ± 0.02	0.31 ± 0.05	0.63 ± 0.14
	0.74	0.24	0.01
Sense	0.09 ± 0.01	0.18 ± 0.01	0.26 ± 0.02
	1.00	0.45	0.00
Cys^{277}Ser	0.08 ± 0.02	0.16 ± 0.01	0.21 ± 0.03
	0.22	0.03	0.00

b

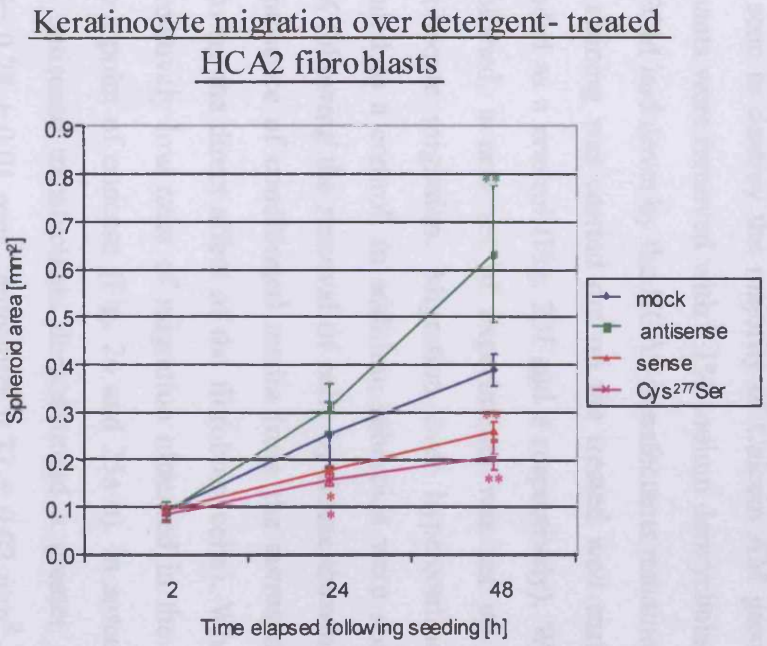

Fig. 22 Ntert spheroid migration over Triton X-100 treated HCA2 transfectants: Fibroblasts were grown to hyperconfluency in the presence of 50 µg/ml ascorbic acid. Prior to spheroid seeding HCA2 cells were washed with 0.01% Triton X-100. Spheroid areas were calculated at three time points (2, 24 and 48h). Data for the 4 transfectants are shown as mean values ± standard deviation (SD) with p-values shown in blue (a & c), or the mean values are plotted within a graph (b & d) with the SD expressed as error bars. $p<0.05$ * $p<0.01$ **

A different approach was now taken to eliminate viable fibroblasts (described in Section 2.10.3), three cycles of freeze-thawing in phosphate buffered saline (PBS) was seen to destroy the majority of Calcein AM green positive cells (Fig. 23c) the remnants were removed with a 1% sodium deoxycholate wash (Fig. 23d). To confirm the ECM laid down by the HCA2 transfectants remained, Coomassie Brilliant Blue R-250 staining was carried out on the treated well surfaces with tissue grade plastic included as a control (Fig. 23f and e respectively). With the success of this method established, a new set of experiments was set up to delineate factors effecting keratinocyte migration. Migration over hyperconfluent HCA2 transfectants were included as a control, in addition, spheroids were seeded onto; 1) HCA2-generated ECM following the removal of cells by freeze-thawing 2) HCA2-generated ECM in the presence of conditioned media from the corresponding transfectant (in essence removing the direct affect of the fibroblast cells). When analysing the resulting data the relatively low rates of migration observed in the presence of HCA2 fibroblasts were a point of concern (Fig. 24 and 25a-b). In agreement with earlier experiments TG2 antisense transfectants demonstrated a greater rate of Ntert migration (24 h mock; 0.28 ± 0.01 mm^2, antisense; 0.32 ± 0.02 mm^2, 48 h mock; 0.33 ± 0.01 mm^2, antisense; 0.37 ± 0.03 mm^2). For the first time the sense transfectant produced migration rates calculated to be significantly greater than the mock control following 24 h (mock; 0.28 ± 0.01 mm^2, sense; 0.32 ± 0.01 mm^2), however measurements taken at the 48 h time point demonstrated no significant differences between the two samples. Despite statistical analysis suggesting significant differences between the $Cys^{277}Ser$ mutant and mock control at both the later time points the population variation does produce overlapping results (24 h, mock; 0.28 ± 0.01 mm^2, $Cys^{277}Ser$; 0.30 ± 0.01 mm^2, 48 h, 48 h mock; 0.33 ± 0.01 mm^2, $Cys^{277}Ser$; 0.30 ± 0.02 mm^2).

Assessment of the ECM contribution by removal of HCA2 fibroblasts revealed an alteration in relative migration rates (Fig. 25c and d) and it was observed that the mock control demonstrated virtually no migration. Although TG2 deficient fibroblasts again produced significantly larger spheroids this was also true of HCA2 cells overexpressing the active or inactive form of the enzyme at both the later time points (24 h mock; 0.25 ± 0.04 mm^2, antisense; 0.30 ± 0.03 mm^2, sense; 0.31 ± 0.06 mm^2, $Cys^{277}Ser$; 0.33 ± 0.05 mm^2, 48 h mock; 0.24 ± 0.02 mm^2, antisense; 0.31 ± 0.04 mm^2, sense; 0.41 ± 0.09 mm^2, $Cys^{277}Ser$; 0.44 ± 0.15 mm^2). In fact the

transfectants overexpressing TG2 produced the greatest rates of migration of the transfectants.

Finally the migration of spheroids over HCA2 derived ECM in the presence of the conditioned media was assessed (Fig. 25 e and f). This allowed two key comparisons to be made. 1) Analysis of this data in conjunction with that obtained in the presence of fibroblasts allowed the direct effect of the mesenchymal cells to be determined. 2) Comparison between migration over fibroblast-generated ECM achieved in the presence or absence of conditioned media allowed the effect of soluble factors to be ascertained.

In the case of the antisense samples the removal of fibroblast cells or their soluble factors demonstrated little impact on the rate of migration, apparently uncoupling the keratinocytes from mesenchymal influences. In contrast the presence of fibroblasts overexpressing the active form of TG2 were observed to reduce the rate of keratinocyte migration (+Cells; 24h, 0.32 ± 0.01 mm^2, 48 h, 0.33 ± 0.02 mm^2. – Cells; 24 h, 0.48 ± 0.12 mm^2, 48 h, 1.30 ± 0.55 mm^2). This raises the interesting possibility that fibroblasts are capable of inhibiting keratinocyte migration, although whether this is a direct effect of TG2 is not clear. It should be noted that this group of experiments do not confirm a similar inhibitory effect in the presence of the $Cys^{277}Ser$ transfected fibroblasts, suggesting the cell effect may rely on cross-linking activity or externalisation of TG2. However, the consistent reduction in keratinocyte migration over hyperconfluent $Cys^{277}Ser$ fibroblasts observed with previous experiments should be considered. It may perhaps be prudent to carry out experimental repeats before further speculating on this point.

From this group of experiments the greatest impact on migration was observed with the conditioned media obtained from sense transfected fibroblasts included in the absence of HCA2 fibroblasts. This produced large increases in spheroid area (Fig. 25e and f). When this data is compared with the corresponding migration over fibroblast-generated ECM in the absence of conditioned media, it supports a role for a soluble mesenchymal factor (-Media 24h, 0.31 ± 0.06 mm^2, 48 h, 0.41 ± 0.09 mm^2. +Media 24 h, 0.48 ± 0.12, 48 h, 1.30 ± 0.55 mm^2). Analysis of mock HCA2 data would seem to support this suggestion since the absence of keratinocyte migration observed over fibroblast-generated ECM is restored following the addition of conditioned media

(-Media 24 h, 0.25 ± 0.04 mm^2, 48 h 0.24 ± 0.02 mm^2. +Media 24 h, 0.28 ± 0.04, 48 h 0.30 ± 0.02 mm^2). Migration rates of the antisense and cross-linking deficient $Cys^{277}Ser$ samples were not significantly altered by the addition of conditioned media. Interestingly TG2 has not been detected in the media obtained from the cultures of either of these transfectants. Despite the expression of cross-linking deficient TG2 and its localisation to the cell surface in the $Cys^{277}Ser$ transfectants, this protein is not externalised to the matrix. Previous studies have demonstrated that the confirmation of the active site is vital for this process (Balklava *et al.*, 2002). This raises the question of whether TG2 has a direct effect on keratinocyte migration or if it functions via another soluble factor.

Fig. 23

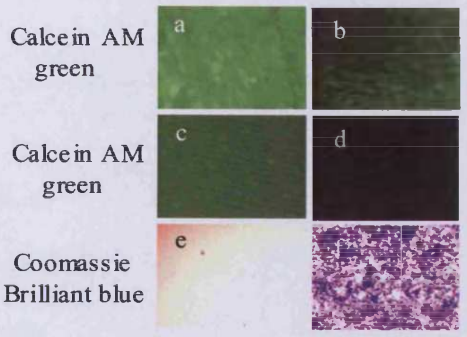

Fig. 24

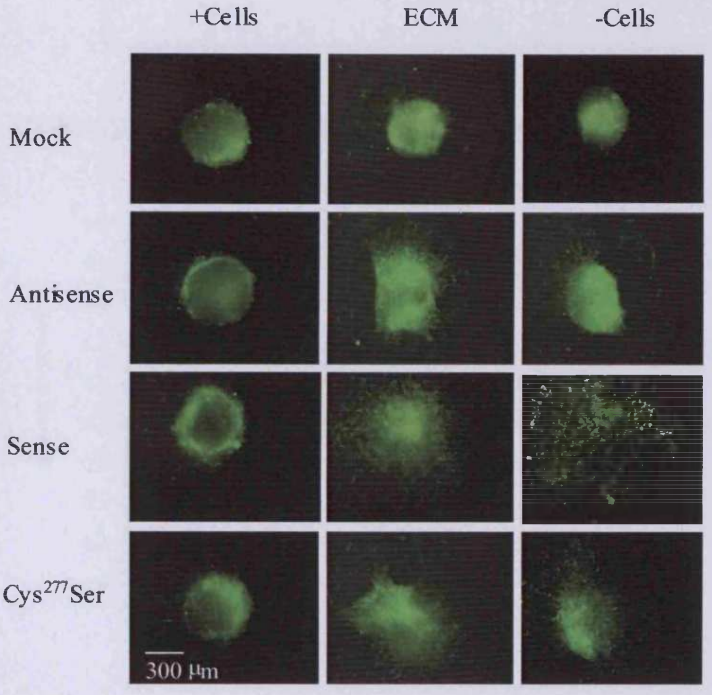

Fig. 23 Establishing a method to remove viable fibroblasts and retain fibroblast-derived ECM: (a-b) 0.01% Triton X-100 treatment of HCA2 fibroblasts is not sufficient to remove all viable cells. Hyperconfluent HCA2 cells were labelled with 5 µM Calcein AM green in duplicate. One set of cells was incubated with 0.01% Triton X-100 for 10 min followed by extensive washing with PBS (b), the second set remained untreated as a control (a). Pictures were taken 48 h after treatment to detect any residual viable cells. (c-f) Freeze-thaw cycles used in combination with 1% sodium deoxycholate washing removed all viable HCA2 cells whilst retaining ECM deposits. Three cycles of freeze-thawing in PBS removes the majority of viable fibroblasts (c) the remainder of which are eradicated with a 1% sodium deoxycholate wash (d). In conjunction, Coomassie Brilliant Blue detection demonstrated that the ECM depositions are retained (f), untreated tissue culture plastic was included as a control (e).

Fig. 24 Migration of Ntert spheroids following 48 h incubation +/- HCA2 transfectants and conditioned media: Spheroids seeded onto hyperconfluent transfectants were included as a control (+Cells) however the oval bodies observed in previous experiments were no longer evident. The removal of HCA2 cells by freeze-thaw cycling determined the contribution of ECM and sequestered factors in migration rates (ECM). In parallel with these experiments spheroids were allowed to migrate over the HCA2 produced ECM in the presence of conditioned media from the corresponding transfectant, in essence knocking out the direct affect of fibroblasts (-Cells). All pictures are representative of the calculated mean.

Fig. 25

a

	Time elapsed following seeding/h		
	2h	24h	48h
	Area/mm^2 ± SD	Area/mm^2 ± SD	Area/mm^2 ± SD
Mock	0.26 ± 0.01	0.28 ± 0.01	0.33 ± 0.01
Antisense	0.26 ± 0.01	0.32 ± 0.02	0.37 ± 0.03
	1.00	0.05	0.03
Sense	0.26 ± 0.01	0.32 ± 0.01	0.33 ± 0.02
	0.86	0.02	0.86
Cys^{277}Ser	0.26 ± 0.01	0.30 ± 0.01	0.30 ± 0.02
	0.24	0.04	0.03

b Keratinocyte migration over hyper - confluent HCA2 fibroblasts

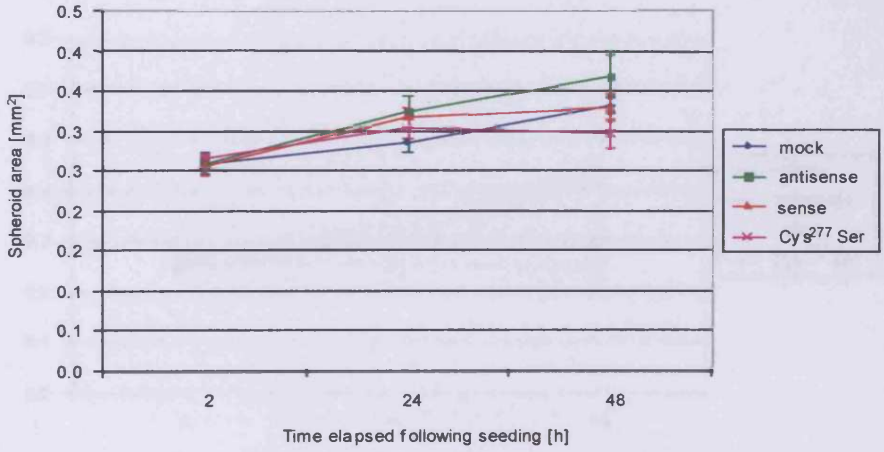

c

	Time elapsed following seeding/h		
	2h	24h	48h
	Area/mm^2 ± SD	Area/mm^2 ± SD	Area/mm^2 ± SD
Mock	0.25 ± 0.01	0.25 ± 0.04	0.24 ± 0.02
Antisense	0.24 ± 0.02	0.30 ± 0.03	0.31 ± 0.04
	0.34	0.06	0.08
Sense	0.26 ± 0.01	0.31 ± 0.06	0.41 ± 0.09
	0.19	0.03	0.04
Cys^{277}Ser	0.27 ± 0.02	0.33 ± 0.05	0.44 ± 0.15
	0.30	0.12	0.09

d

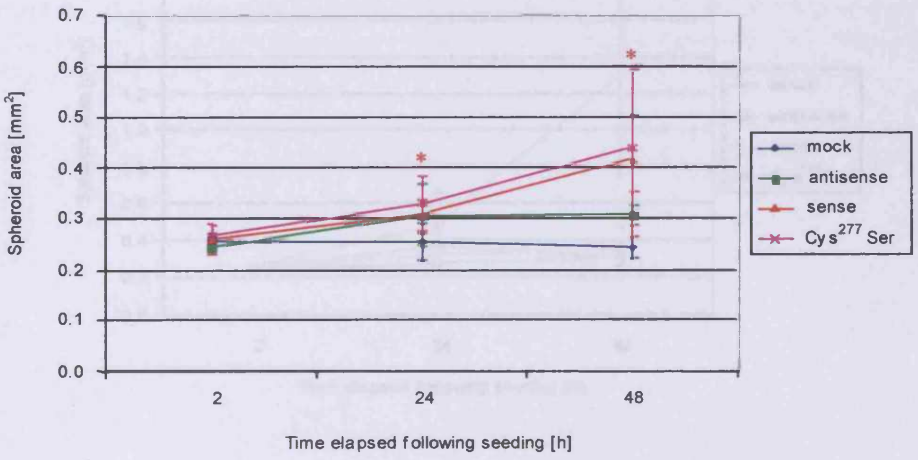

e

	Time elapsed following seeding/h		
	2h	24h	48h
	Area/mm^2 ± SD	Area/mm^2 ± SD	Area/mm^2 ± SD
Mock	0.24 ± 0.01	0.28 ± 0.04	0.30 ± 0.02
Antisense	0.24 ± 0.01	0.37 ± 0.06	0.31 ± 0.05
	0.73	0.06	0.09
Sense	0.26 ± 0.03	0.48 ± 0.12	1.30 ± 0.55
	0.66	0.01	0.01
Cys^{277}Ser	0.26 ± 0.03	0.31 ± 0.04	0.36 ± 0.05
	0.21	0.28	0.03

Keratinocyte migration over HCA2 generated ECM in conditioned media

f

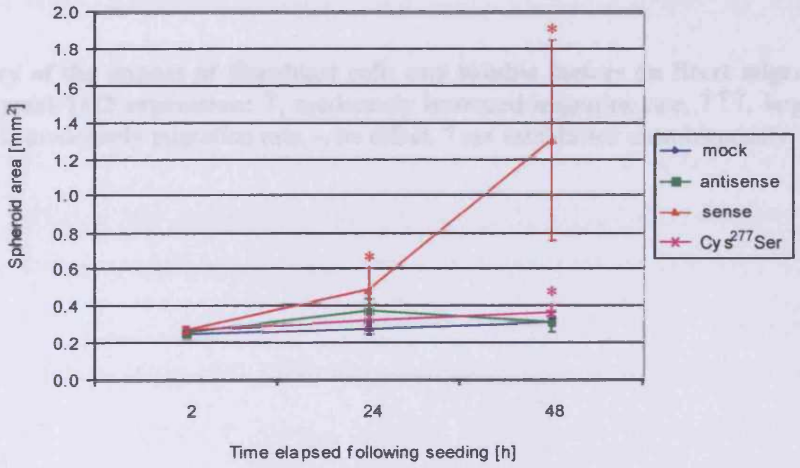

Fig. 25 Establishing factors involved in keratinocyte migration rate with alteration of mesenchymal TG2 levels: Migration over hyperconfluent HCA2 transfectants was included as a control (a-b). In additional migration over the fibroblast generated ECM was studied following removal of viable HCA2 cells by freeze-thaw cycling (c-d). Finally spheroid migration was assessed over HCA2 produced ECM with the addition of conditioned FAD media derived from the corresponding transfectant (e-f).

Data for the 4 transfectants are shown as mean values ± standard deviation (SD) with p-values shown in blue (a & c), or the mean values are plotted within a graph (b & d) with the SD expressed as error bars. $p<0.05$ * $p<0.01$ **

	Cell effect	Soluble factor effect
Mock	-	↑
Antisense	-	-
Sense	↓	↑↑↑
$Cys^{277}Ser$	?	-

Table. 2 Summary of the impact of fibroblast cells and soluble factors on Ntert migration with varying mesenchymal TG2 expression: ↑, moderately increased migration rate, ↑↑↑, large increase in migration rate, ↓, moderately migration rate, -, no effect, ? not established unambiguously.

6.3 Conclusions and future work

Work to develop an *in vitro* SE model met with limited success. The contraction method failed to establish tissue architecture comparable with that of native skin with either primary mouse keratinocytes or the human-derived Ntert cell line. Although some cell flattening was observed in upper layers of keratinocytes, immunohistochemical analysis did not provide evidence of differentiation and may have been the result of cell drying. Although Batch 1 SEs coculturing the four HCA2 transfectants with Ntert cells suggested a possible role for mesenchymal TG2 in morphology, invasive ability and cell-cell interactions, a repeat of this experiment with a lower passage of cells did not confirm these observations. This may indicate a phenotypic alteration acquired through passaging of the transfected fibroblasts. However TG2 antisense cocultures of Batch 2 samples did demonstrate a higher incidence of detachment within the epidermis and from the dermal gel.

The insert method produced improved tissue architecture, although this was only achieved using primary oral fibroblasts and was not consistently reproducible. Despite this improved epidermal morphology, detection of differentiation markers was still at variance with that observed in native skin. Concerns were also raised about the ability of HCA2 fibroblasts to support a differentiated epidermis, this prohibited expansion of these studies to investigate a wound healing model. The decision was made to move into a different avenue of research investigating the role of TG2 on keratinocyte migration.

It is apparent from this study that mesenchymal TG2 expression impacts upon keratinocyte migration. Ntert keratinocytes seeded onto TG2 deficient fibroblasts and their ECM demonstrate a consistently increased rate of migration. The data obtained from fibroblasts overexpressing the active or inactive form of this enzyme suggest a more complicated regulation with the fibroblast cells directly inhibiting keratinocyte migration and conversely the secreted active form of TG2 enhancing Ntert migration (summarised Table 2). These control mechanisms will be considered separately in the following paragraphs.

Concerning the cell effect, it is interesting to note that the formation of oval spheroid bodies was only observed in the presence of an underlying fibroblast substrata, which seem to impose some directional constraints on keratinocyte migration. Whether TG2 is directly involved in this inhibitory regulation cannot be

ascertained from these results in isolation. It is certainly possible that TG2/integrin coreceptors residing on the external surface of the fibroblasts may be involved in cell-cell interactions. Stephens *et al.* (2004) have reported a 3- and 2-fold increase in membrane associated TG2 within sense and $Cys^{277}Ser$ transfectants respectively. Significantly, *in vitro* studies have also been established to investigate the effect of exogenous TG2 on keratinocyte adhesion (Taenaka *et al.*, 2003). This group demonstrated that TG2 produced a dose-dependent increase in keratinocyte adhesion on a FN substrata, this effect was inhibited by arginine-glycine-aspartate (RGD) peptides. Therefore, TG2 coreceptors may retard the rate of migration as a consequence of promoting keratinocyte adhesion.

With regard to the soluble factor effect, it remains to be resolved whether transamidation activity is essential, since TG2 is only externalised to the surrounding matrix from sense transfectants. Whether this increased migration is the direct affect of the externalised enzyme is a suitable avenue of future studies, with sources of this enzyme available commercially. This could be carried out in parallel with experiments evaluating the effect of conditioned media obtained from TG2 sense cells on keratinocyte migration over ECM derived from the other transfectants. A study carried out on IL-6-deficient transgenic mice has identified a significant delay in cutaneous wound healing which could be counteracted by an as yet unidentified soluble factor from fibroblastic culture (Gallucci *et al.,* 2004). Interestingly this cytokine is known to upregulate TG2 (Ikura *et al.*, 1994) and similar delays in wound healing have been observed in $TG2^{-/-}$ mice (Mearns *et al.*, 2002). Gene array studies of IL-$6^{-/-}$ fibroblasts following treatment with the cytokine did not reveal any significant upregulation in a range of soluble factors known to stimulate keratinocyte migration; TGFα, TGFβ, EGF, fibroblast growth factor (FGF) 7, FGF 10, hepatocyte growth factor (HGF), insulin-like growth factor 1 (IGF-1), GM-CSF and IL-β (Gallucci *et al.*, 2004). However these studies did not take into consideration protein modifications and their impact on factor activity. TG2 cross-linking activity has been linked to TGFβ activation from its latent form (Nunes *et al.*, 1997), and may upregulate keratinocyte migration as a consequence of altered expression of ECM components or possibly via integrin remodelling in keratinocytes (Gailit *et al.*, 1994). If such remodelling is involved it may explain the lag phase observed in the sense-

conditioned medium experiment before the rapid increase in spheroid area between 24 and 48 h.

It would also be pertinent to expand studies to assess any mitotic effects on keratinocytes within this model, which due to time restrictions, were not included within the scope of these experiments. Reports exist in the literature for a TG2-linked anti-proliferative effect (Wu *et al.*, 2000).

Chapter 7:
General Discussion

As with any study there are limited time and resources available. This Chapter is included to discuss further opportunities for extending the research incorporated in this body of work.

7.1 Generation of antibodies against the novel transglutaminase enzymes 6 and 7

Work to generate antibodies against a truncated form of human TG7 (hTG7) met with limited success. Sequence spanning the C-terminal β-barrel domains of this isoform was cloned into a construct, incorporating an N-terminal, Glutathione S-transferase (GST) tag. This fusion protein was expressed from *E.coli* cells. Work was terminated following exhaustive attempts to isolate this GST tagged protein to purity failed. This process was largely complicated by the apparently insoluble nature of the fusion protein. Although studies were allowed to progress following the generation of antibodies against synthetic peptides, there would be significant benefits if a method to isolate this recombinant protein could be developed. The inclusion of a wider range of epitopes from domains in their native confirmation could 1) provide more information on apparent TG fragments identified in Western blotting analysis and 2) may prove more opportune in immunoprecipitation studies. Publications, including the generation of recombinant TG3 and TG5, have also encountered problems with protein solubility (Candi *et al.* 2001; Hitomi *et al.* 2003). These have been resolved by alterations in the expression system, it was found that both isoforms demonstrated higher solubility when expressed from insect cell systems. Although TG7 has no reported post-translational modifications this may be an approach worth taking. An alternative tag may also be considered. GST is ~ 26 kDa in size and could sterically inhibit the native folding of domain regions, which may effect soluble properties. GST has also been identified as a substrate of TG2 (Ikura *et al.*, 1998). Members of the TG family share numerous substrates, raising the potential for protein interactions with TG7 domains, even though this truncated form lacks a catalytic core domain. This may impact upon fusion protein solubility if non-covalently associated aggregates are formed. The significantly shorter hexahistidine-tag provides just one alternative.

Western blot studies involving the peptide antibodies (anti-TG6S, anti-TG6L and anti-TG7) produced positive results for the full-length form of TG6 (TG6L) and TG7 from the Ntert keratinocyte and HCA2 fibroblast cell lines. In contrast the TG6S protein was localised to the keratinocyte cell line extract only. All three TG isoforms were isolated from the soluble (cytoplasmic) fraction, this was accompanied by evidence of protein cleavage. The expected 70 kDa protein corresponding to the short form of TG6 (TG6S, exon XII alternatively spliced) was not detected in the series of experiments and instead the predominant protein was estimated to be ~ 35 kDa in size. Similarly detection with TG7 antibodies also revealed 40-30 kDa fragments. Attempts to remove these fragments by modifying the extraction process were only partially successful and raised the possibility that these are in fact physiological fragments. As has been mentioned previously, the restricted epitope range produced from the peptide antigens does limit our understanding of the exact nature of the protein cleavage. Reports have been published, identifying the activation of TG1, TG3 and FXIII proenzymes through protease cleavage (Kim *et al.*, 1990; 1995a). Further to this the sites of protease cleavage were found to be conserved between isoforms (Kim *et al.*, 1995a). Since the cleaved products of TG1 and TG3 are reported to remain associated by non-covalent interactions (Kim *et al.*, 1995a; Steinert *et al.*, 1996a), one method to produce further information concerning the TG6S and TG7 fragments would be to repeat these immunblots under non-denaturing conditions. In order to establish the physiological significance of these results it would be useful to obtain activity data for the enzyme fragments. Unfortunately immunoprecipitations carried out with these antibodies did not prove suited to retrieving the endogenous enzyme or its cleavage products.

Immunohistochemical studies carried out with the peptide antibodies largely concurred with Western blot studies. Both TG6L and TG7 were detected within dermal fibroblasts. In addition to this TG6L demonstrated consistent staining throughout the epidermal layers. In contrast TG7 antibodies produced a gradient across the epidermis with relatively low staining within the basal cells. Whether this is a consequence of increased protein levels or a higher antibody affinity for the cleaved products generated is yet to be determined. The TG6S protein localised to the granular layers and stratum corneum, similar to the profile observed with TG3. Significantly TG6 demonstrates the greatest level of sequence homology with this isoform but this differentiation-specific staining pattern is not consistent with Western blot data.

Expansion of immunohistochemical studies included samples obtained from a dermatitis herpetiformis patient. TG3 has been identified as the predominant antigen in this autoimmune disease, with TG3 containing IgA aggregates deposited in the papillary dermis (Sardy *et al.*, 2002). However it should be noted that TG3 expression within the epidermis remains unaltered (Sardy *et al.*, 2002). Analysis of a single patient revealed an evident increase in TG7 protein levels throughout the epidermis, concomitant with a smaller reduction in the two TG6 splice variants. These observations have yet to be confirmed in a wider pool of patients and the function of this altered expression is not immediately apparent, possibly suggesting a secondary effect. With these antibodies now available it will be possible to investigate the potential involvement of TG6 and TG7 in other skin disorders such a psoriasis or lamellar ichthyosis, where other members of the TG family have already been implicated in the disease phenotype (Huber *et al.*, 1995; Russel *et* al., 1995; Candi *et al.*, 2002).

7.2 Identifying potential transglutaminase substrates

Preliminary experiments within this thesis do not support the hypothesised role of TG β-barrel domains in substrate selection. Similar profiles of ^{35}S labelled proteins were retrieved from cellular extracts using immobilised recombinant forms of TG5, 6 and 7. When considering regions of low homology between TG isoforms, the N-terminus is another region of high variability and may be at least partially responsible for substrate selectivity. A group working with the TG1 enzyme have carried out studies generating recombinant deletion constructs and *in vitro* cross-linking experiments with various synthetic peptides. Their findings revealed residues 62-92 are important in defining the substrate specificity of TG1 (Kim *et al.*, 1994). As a consequence they have postulated that this domain may have important implications on substrate selection *in vivo*.

Work to generate a full-length recombinant form of TG7 continues in our laboratory. If successful, this can be incorporated into *in vitro* cross-linking studies and is more likely to identify possible *in vivo* substrates than the C-terminus in isolation. The expression of TG7 within the human epidermis and its evident gradient from the basal cells suggests a potential function in keratinocyte differentiation (Chapter 3). TG1, TG3 and TG5 all have established roles in the formation of the CE structure following commitment of keratinocytes to terminal differentiation. Consequently envelope precursors such as involucrin (Rice and Green, 1979), loricrin (Mehrel *et al.*, 1990) and the small proline rich proteins (SPRs) (Steinert *et al.*, 1998) provide good candidates for *in vitro* cross-linking and double cross-linking studies with TG7. Double cross-linking studies establishing the ability of different TG isoforms to target distinct residues within the same substrates have been published by Candi *et al.* (2001). These have shown that following exhaustive cross-linking by one isoform, proteins can undergo further modification by a second. However, this is dependent on the temporal order in which TG isoforms are introduced. For example following exhaustive TG5 catalysed cross-linking of SPR3, the addition of TG1 or TG3 is capable of further modifying the protein as shown following resolution by SDS-PAGE. If however TG5 is added subsequent to TG1 or TG3 modification no change in the cross-linking profile is seen, reflecting the regulated order in which these isoforms are expressed *in vivo* (Candi *et al*, 2001).

7.3 Identifying a possible role for transglutaminase enzymes in corneocyte maturation

The generation of stratum corneum depth profiles in conjunction with Western blotting proved to be a useful tool for investigating altered TG levels and cleavage through this region of the epidermis. Within this Chapter of work, three pools of TG3 have been identified. This includes a Tris soluble fraction (cytoplasmic), a detergent soluble fraction (lipid associated) and an insoluble fraction. To date, available literature has considered this isoform to be a soluble enzyme, localising to the cytoplasm of the cell (Kim *et al.*, 1990; 1993; Hitomi *et al.*, 2003). It may be that TG3 translocates in the latter stages of keratinocyte differentiation, either as the result of protein interactions or post-translational modifications. To confirm whether distribution is unique to the stratum corneum, serial extractions could be carried out on keratinocytes cultured under proliferating conditions and at a series of time points following induction of differentiation. Alternatively *Ex vivo* samples could be utilised. The skin abrasion technique could be employed following the removal of the stratum corneum by sequential tape stripping. This would harvest the epidermal layers without contamination by dermal tissue.

This study has identified alterations in TG3 protein levels across the stratum corneum, which could implicate this isoform in the process of corneocyte maturation. It was found that the level of the 27 kDa (C-terminus) TG3 cleavage product increased in the more superficial corneocyte layers of forearm epidermis, at times this was accompanied by increased quantities of the 77 kDa proenzyme. However, the 50 kDa active fragment was not unambiguously identified due to the absence of a suitable positive control. The addition of such a control would benefit this project greatly. These results suggest TG3 could be undergoing activation in a region of the epidermis characterised by the continued modification of corneocytes by isopeptide bonds (Watkinson *et al.*, 2001). Interestingly, this TG3 profile was not reproduced when epidermis obtained from the back of the hand was included in this study. This region of skin suffers from extended environmental exposure and previous studies have shown it to retain the fragile envelope morphology. As discussed in Chapter 5, future studies incorporating this method would benefit from the inclusion of corresponding ratios of the immature fragile envelopes compared to the mature rigid envelopes.

Unfortunately, potential keratin cross-reactivity associated with other antibodies included in this work has limited the reliability of data concerning these isoforms. If alternative antibodies could be obtained this may help complete this area of work.

7.4 The effects of mesenchymal TG2 on keratinocyte migration, morphology and differentiation

This work utilised HCA2 human fibroblasts stably transfected with DNA vectors to produce high level constitutive expression of TG2 sense RNA, antisense RNA as well as a TG2 mutant RNA where the catalytic cysteine (Cys) residue was substituted with serine (Ser), thus removing the enzymes cross-linking activity but maintaining protein conformation. HCA2 cells transfected with an empty vector were included in experiments as a control (mock).

Attempts to generate a skin equivalent model incorporating HCA2 fibroblasts were unsuccessful. The tissue architecture and cell morphology observed in normal epidermis were completely absent. It was also found that skin equivalents generated by the insert method and incorporating the HCA2 transfectants did not generate an 'epidermis' greater than 2-7 layers in thickness. Greater success was achieved with murine 3T3 cells (work carried out at Unilever, Colworth) and primary oral fibroblasts. In these models, columnar basal cells were apparent, succeeded by a polygonal morphology in the spinous region and subsequent flattening of cells. However, neither of these models produced a recognisable granular layer or stratum corneum with the characteristic basket weave appearance. In addition to this, immunohistochemical analysis of the primary oral fibroblast-Ntert keratinocyte coculture did not demonstrate expression of differentiation markers as observed in native skin. In order to progress with this work it may be necessary to utilise a different cell line in the generation of new transfectants. It may also be pertinent to establish unequivocally that the keratinocytes seeded display characteristics of undifferentiated basal cells.

The development of a migration model for keratinocytes proved more opportune. However, significant sample variation is evident, probably a consequence of the heterogeneous nature of the dermal component. The growing of fibroblast cells to hyperconfluency most likely produced areas of regional variation. Attempts to counteract this involved the inclusion of large numbers of sample repeats. From the experiments included in this thesis, it became apparent that TG2 effects migration by a combination of mechanisms, a finding that might have been expected for this multifunctional enzyme. Delineation of soluble and cell effects would suggest that TG2 overexpression produced a direct inhibiting influence from fibroblast cells and a

promoting effect via an as yet unidentified soluble factor. Whether these effects are reliant on the transamidating activity of TG2 has not been unambiguously established by these studies. It is possible that cell effects occur via the integrin coreceptors situated on the cell surface. To expand on this, an incubation step of the transfected fibroblasts with the commercially available monoclonal anti-TG2 (CUB7402) could be included. This would aim to interfere with the binding properties of surface TG2. If the coreceptors are involved in the inhibitory effect, the Mock, Sense and $Cys^{277}Ser$ transfectants would be expected to demonstrate an increased rate of migration following this incubation step. In the case of the migration promoting soluble factor, it should be noted that only the active form of TG2 is secreted from the cell (Balklava *et al.*, 2002). In order to assess whether transamidating activity is indeed necessary for promoting keratinocyte migration, cell extracts containing the $Cys^{277}Ser$ mutant could be used to supplement antisense transfectant cultures. This conditioned media would then be used in combination with the generated extra cellular matrix (ECM) for further assays. Microarrays of the transfectants provide a possible method for identifying soluble factors involved in promoting keratinocyte migration. However, this technique has its limitations and would not encompass translational controls or alterations in protein activation. In fact a strong candidate for this function in keratinocyte migration is TGFβ. This soluble factor has been shown to promote keratinocyte migration (Nickoloff *et al.*, 1988) and in addition to this, its expression and activation from its latent form is induced by TG2 (Nunes *et al.*, 1997; Ritter *et al.*, 1998). Consequently it would seem sensible to expand this Chapter of work by investigating alterations in this proteins expression and activation within cultures of the four transfectants.

Finally, future studies should consider whether increases in the areas of keratinocyte spheroids correlate with the rate of mitogenesis. Previous studies have reported mitotic effects can be induced by soluble factors involved in the regulation of keratinocyte migration (Gibbs *et al.*, 2000; Galluci *et al.*, 2004) and TG2 has been reported to inhibit cell proliferation (Wu *et al.*, 2000). Such effects could be analysed by estimation of the Ki67 proliferation index (Gibbs *et al.*, 2000) or the extent of BrdU uptake (Galluci *et al.*, 2004).

To summarise; work carried out within this thesis has successfully generated antibodies against synthetic peptides designed using available data for TG6 and TG7 sequences. A combination of Western blotting and immunohistochemical studies has confirmed the expression of TG6L and TG7 within the cytosolic fraction of dermal fibroblasts and epidermal keratinocytes. There was also evidence of enzyme cleavage products, these were particularly prominent in the case of TG7 (~ 40 kDa). A protein correlating with the predicted full-length form of TG6S (70 kDa) was not detected within these studies. However a putative fragment was identified in the soluble extracts of keratinocytes (~ 35 kDa). Whether these constitute physiological fragments or are evidence of protein instability, has not been ascertained. Further to this, growing keratinocytes to confluency produced an altered pattern of cleavage products, possibly linked to differentiation in these cells.

Studies utilising truncated recombinant forms of TG5, 6 and 7, do not support the hypothesised role for the C-terminal β-barrel domains in substrate selection. In addition to this, results have indicated that this enzyme region is involved with actin binding in these isoforms.

Investigations of late stage corneocyte maturation, within the human stratum corneum, have identified a potential role for TG3 in catalysing this process through corresponding alterations in protein levels. Findings would suggest that the 27 kDa cleavage product of TG3 could be involved in the regulation of this enzyme.

Work was also begun to elucidate the role of dermal TG2 in mesenchymal-epithelial interactions. Using an *in vitro* model, this multifunctional enzyme was shown to produce opposing regulatory effects in keratinocyte migration. This included an inhibitory effect via direct fibroblast cell interactions and positive regulation by an as yet unidentified soluble factor.

To conclude, these studies have provided novel findings concerning the role of dermal TG2 and epidermal TG3 in normal skin homeostasis. Expansion of this work and elucidation of signalling pathways involved may facilitate "a potential route to healthy skin".

References

Achyuthan, K. E. and Greenberg, C. S. (1987) Identification of a guanosine triphosphate-binding site on guinea pig liver transglutaminase. Role for GTP and calcium ions in modulating activity. J. Biol. Chem. 262, 1901-6

Aeschlimann, D., Kaupp, O. and Paulsson, M. (1995) Transglutaminase catalysed matrix crosslinking in differentiating cartilage: identification of osteonectin as a major glutaminyl substrate. J. Cell Biol. 129, 881-92

Aeschlimann, D., Koeller, M-K., Allen-Hoffmann, B. L. and Mosher, D. F. (1998) Isolation of a cDNA encoding a novel member of the transglutaminase gene family from human keratinocytes. Detection and identification of transglutaminase gene products based on RT-PCR with degenerate primers. J. Biol. Chem. 273, 3452-3460

Aeschlimann, D. and Paulsson, M. (1991) Crosslinking of laminin-nidogen complexes by tissue transglutaminase: A novel mechanism for basement membrane stabilization. J. Biol. Chem. 266, 15308-17

Aeschlimann, D. and Paulsson, M. (1994) Transglutaminases: Protein cross-linking enzymes in tissues and body fluids. Thrombosis and Haemostasis 71 (4), 402-15

Aeschlimann, D., Paulsson, M., Mann, K. (1992) Identification of Gln^{726} in nidogen as the amine acceptor in transglutaminase-catalysed cross-linking of laminin-nidogen complexes. J. Biol. Chem. 267, 11316-21

Aeschlimann, D. and Thomazy, V. (2000) Protein Crosslinking in Assembly and Remodelling of Extracellular Matrices: The role of Transglutaminases. Connective Tissue Research 41 (1), 1-27 [may be written 1999]

Aeschlimann, D., Wetterwald, A., Fleisch, H. and Paulsson, M. (1993) Expression of tissue transglutaminase in skeletal tissues correlates with events of terminal differentiation of chondrocytes. J. Cell Biol. 120, 1461-70

Aho, S. (2004) Many faces of periplakin: domain-specific antibodies detect the protein throughout the epidermis, explaining the multiple protein-protein interactions. Cell Tissue Res. 316, 87-97.

Ahvazi, B., Boeshans, K. M., Idler, W., Baxa, V. and Steinert, P. M. (2003) Roles of calcium ions in the activation and activity of the transglutaminase 3 enzyme. J. Biol. Chem. 278 (6), 23834-41

Ahvazi, B., Boeshans, K. M., Idler, W., Baxa, U., Steinert, P. M. and Rastinejad, F. (2004) Structural basis for the coordinated regulation of transglutaminase 3 by guanine nucleotides and calcium/magnesium. J. Biol. Chem. 279, 7180-92

Ahvazi, B., Kim, H. C., Kee, S. H., Nemes, Z. and Steinert, P. M. (2002) Three-dimensional structure of the human transglutaminase 3 enzyme: Binding of calcium ions changes structure for activation. EMBO J. 21, 2055-67

Akimov, S.and Belkin, A. (2001) Cell-surface transglutaminase promotes fibronectin assembly via interaction with the gelatin-binding domain of fibronectin: a role in TGFβ-dependent matrix deposition. J. Cell Sci. 114, 2989-3000

Akimov, S. S., Krylov, D., Fleischmann, L. F. and Belkin, A. M. (2000) Tissue transglutaminase is an integrin-binding adhesion coreceptor for fibronectin. J. Cell Biol. 148, 825-38

Allen, T. D. and Potten, C. S. (1975) Desmosomal form, fate and function in mammalian epidermis. J. Ultrastruct. Res. 5, 94-105

Anderson, K. I. and Cross, R. (2000) Contact dynamics during keratinocyte motility. Curr. Biol. 10, 253-60

Anderson, K. I., Wang, Y. L. and Small, J. V. (1996) Coordination of protrusion and translocation of the keratinocyte involves rolling of the cell body. J. Cell Biol. 134, 1209-18

Ando, Y., Imamura, S., Owada, M. K. and Kannagi, R. (1991) Calcium-induced intracellular cross-linking of lipocortin I by tissue transglutaminase in A431 cells. Augmentation by membrane phospholipids. J. Biol. Chem. 266, 1101-18

Andreadis, S. T., Hamoen, K. E., Yarmush, M. L. and Morgan, J. R. (2001) Keratinocyte growth factor induces hyperproliferation and delays differentiation in a skin equivalent model system. FASEB J. 15, 898-906

Antonyak, M. A., Singh, U. S., Lee, D. A., Boehm, J. E., Combs, C., Zgola, M. M., Page, R. L. and Cerione, R. A. (2001) Effects of tissue transgluatmainse on retinoic acid-induced differentiation and protection against apoptosis. J. Biol. Chem. 276, 33582-7

Aragane, Y. Yamada, H., Schawrz, A., Poppelmann, B., Luger, T. A., Tezuka, T. and Schawrz, T. (1996) Transforming growth factor-alpha induces interleukin-6 in the human keratinocyte cell line HaCaT mainly by transcriptional activation. J. Invest. Dermatol. 106, 1192-7

Asselineau, D., Bernard, B. A., Bailly, C. Darmen, M. and Prunieras, M. (1986) Human epidermis reconstructed by culture: is it "normal"? J. Invest. Dermatol. 86, 181-6

Backendof, C. and Hohl, D. (1992) A common origin for cornified envelope proteins? Nat. Genet. 2, 91

Baek, K. J., Kang, S. K., Damron, D. S. and Im, M. J. (2001) PLCδ1 is a guanosine nucleotide exchanging factor for TG2 ($G\alpha_h$) and promotes α_{1B}-adrenoreceptor-mediated GTP binding and intracellular calcium release. J. Biol. Chem. 276, 5591-7

Bale, S. J., Russell, L. J., Lee, M. L., Compton, J. G., Digiovanna, J. J. (1996) Congenital recessive ichthyosis unlinked to loci for epidermal transglutaminases. J. Invest. Dermatol. 107, 808-11

Balklava, Z., Verderio, E., Collighan, R., Gross, S., Adams, J. and Griffin, M. (2002) Analysis of tissue transglutaminase function in the migration of Swiss 3T3 fibroblasts. J. Biol. Chem. 277 (19) 16567-75

Ballestar, E., Abad, C. and Franco, L. (1996) Core histones are glutaminyl substrates for tissue transglutaminase. J. Biol. Chem. 271, 18817-24

Ballestar, E., Boix-Chornet, M. and Franco, L. (2001) Conformational change in the nucleosome followed by the selective accessibility of histone glutamines in the transglutaminase reaction: effects of salt concentrations. Biochemistry 40, 1922-9

Banks-Schlegel, S. and Green, H. (1981) Involucrin synthesis and tissue assembly by keratinocytes in natural and cultured human epithelial. J. Cell Biol. 90, 732-37

Barker, J. N. (1991) The pathophysiology of psoriasis. Lancet 338, 227-30

Barrandon, Y. and Green, H. (1987) Cell migration is essential for sustained growth of keratinocyte colonies: the roles of transforming growth factor alpha and epidermal growth factor. Cell 50, 1131-7

Barsigian, C., Stem, A. M. and Martinez, J. (1991) Tissue type II transglutaminase covalently incorporates itself, fibrinogen or fibronectin into high molecular weight complexes on the extracellular surface of isolated hepatocytes. J. Biol. Chem. 266, 22501-9

Baumgartner, W., Golenhofen, N., Weth, A., Hiragi, T., Saint, R., Griffin, M. and Drenckhahn, D. (2004) Role of transglutaminase 1 in stabilisation of intercellular junctions of the vascular endothelium. Histochem. Cell Biol. 122, 17-25

Bell, E., Ehrlich, H. P., Buttle, D. J. and Nakatsuji, T. (1981a) Living tissue formed *in vitro* and accepted as skin-equivalent tissue of full thickness. Science 211, 1052-4

Bell, E., Ehrlich, H. P., Sher, S., Merrill, C., Sarber, R., Hull, B., Nakatsuji, T., Church, D. and Buttle, D. J. (1981b) Development and use of a living skin equivalent. Plast. Reconstr, Surg. 67, 386-92

Benz, J., Bergner, A., Hofmann, A., Demange, P., Gottig, P., Liemann, S., Huber, R. and Voges, D. (1996) The structure of recombinant human annexin VI in crystals and membrane-bound. J. Mol. Biol. 266, 638-43

Berbers, G. A., Feenstra, R. W., Van den Bos, R. Hoekman, W. A., Bloemendal, H. and De Jong, W. W. (1984) Lens transglutaminase selects specific β-crystallin sequences as substrate. Proc. Natl. Acad. U.S.A 81, 7017-20

Bernassola, F., Federici, M., Corazzari, M., Terrinoni, A., Hribal, M. L., De Laurenzi, V., Ranalli, M., Massa, O., Sesti, G., Mclean, W. H. I., Citro, G., Barbetti, F. and Melin, G. (2002) Role of transglutaminase 2 in glucose intolerance: Knockout mice studies and a putative mutation in a MODY patient. FASEB J. 16, 1371-8

Bikie, D., Ratnam, A., Mauro, T., Harris, J. and Pillai, S. (1996) Changes in calcium responsiveness and handling during keratinocyte differentiation. J. Clin. Invest. 97, 1085-93

Boelsma, E., Verhoeven, M. C. and Ponec, M. (1999) Reconstruction of a human skin equivalent using a spontaneously transformed keratinocyte cell line (HaCaT). J. Invest. Dermatol. 112, 489-98

Bowness, J. M., Folk, J. E. and Timpl, R. (1987) Identification of a substrate site for liver transglutaminase on the aminopropeptide of type III collagen. J. Biol. Chem. 262, 1022-4

Bowness, J. M., Tarr, A. H. and Wong, T. (1988) Increased transglutaminase activity during skin wound healing in rats. Biochim. Biophys. Acta. 967, 234-40

Bowness, J. M., Venditti, M., Tarr, A. H. and Taylor, J. R. (1994) Increase in ε(γ-glutamyl)lysine crosslinks in atherosclerotic aortas. Artherosclerosis 111, 247-53

Broome, A. M. and Eckert, R. L. (2004) Microtubule-dependent redistribution of a cytoplasmic cornified envelope precursor. J. Invest. Dermatol. 122, 29-38

Brown, G. L., Curtsinger, L., Brightwell, J. R., Ackerman, D. M., Tobin, G. R., Pock, H. C. Jr., George-Nascimento, C., Valenzuela, P. and Schultz, G. S. (1986) Epidermal regeneration by biosynthetic epidermal growth factor. J. Exp. Med. 163, 1319-24

Brown, G. L., Nanney, L. B., Griffin, J., Cramer, A., Yancey, J. M., Curtsinger, L. J., Holtzin, L., Scultz, G. S., Jurkiewizz, M. J. and Lynch, J. B. (1989) Enhancement of wound healing by topical treatment with epidermal growth factor. N. Engl. J., Med. 321, 76-9

Brunette, D. M. (1984) Cholera toxin and dibutyryl cyclic-AMP stimulate the growth of epithelial cells derived from epithelial rests from porcine periodontal ligament. Arch. Oral Biol. 29, 303-9

Burger, A., Berendes, R., Leimann, S., Benz, J., Hofmann, A., Gottig, P., Huber, R., Gerke, V., Thiel, C., Romisch, J. and Weber, K. (1996) The crystal structure and ion channel activity of human annexin II, a peripheral membrane protein. J. Mol. Biol. 257, 839-47

Butler, S. J. and Landon, M. (1981) Transglutaminase-catalyzed incorporation of putrescine into denatured cytochrome *c*. Biochim. Biophys. Acta 670, 214-21

Candi, E., Melino, G., Mei, G., Tarcsa, E., Chung, S-I., Marekov, L. N. and Steinert, P. M. (1995) Biochemical, structural, and transglutaminase substrate properties of human loricrin, the major epidermal cornified cell envelope protein. J. Biol. Chem. 270, 26382-90

Candi, E., Oddi, S., Paradis, A., Terrinon, A., Ranalli, M., Teofoli, P., Citro, G., Scarpato, S., Puddu, P. and Melino, G. (2002) Expression of transglutaminase 5 in normal and pathologic human epidermis. J. Invest. Dermatol. 119, 670-7

Candi, E., Oddi, S., Terrinoni, A., Paradisi, A., Ranalli, M., Finazzi-Agro, A. and Melino, G. (2001) Transglutaminase 5 cross-links loricrin, involucrin and small proline-rich proteins *in vitro*. J. Biol. Chem. 276, 35014-23

Candi, E., Paradisi, A., Terrinoni, A., Pietroni, V., Oddi, S., Cadot, B., Jogini, V., Meiyappan, M., Clardy, J., Finazzi-Agro, A., Melino, G. (2004) Transglutaminase 5 is regulated by guanine-adenine nucleotides. Biochem. J. 381, 313-9

Candi, E., Tarcsa, E., DiGiovanna, J. J., Compton, J. G., Elias, P. M., Marekov, L. N. and Steinert, P. M. (1998) A highly conserved lysine residue on the head domain of type II keratins is essential for the attachment of keratin intermediate filaments to the cornified cell envelope through isopeptide crosslinking by transglutaminases. Proc. Natl. Acad. Sci. U.S.A 95, 2067-72

Candi, E., Tarcsa, E., Idler, W. W., Kartasova, T., Marekov, L. N. and Steinert, P. M. (1999) Transglutaminase cross-linking properties of the small proline-rich 1 family of cornified cell envelope proteins. J. Biol. Chem. 274, 7226-37

Capon, F. B., Dallapiccola, B. and Novelli, G. (2000) Advances in the search for psoriasis susceptibility genes. Mol. Genet. Metab. 71, 250-5

Cariello, L., Ristoratore, F., Zanetti, L. (1997) A new transglutaminase-like from the ascidian *Ciona intestinalis*. FEBS Lett 408, 171-6

Carrell, N. A., Erickson, H. P., McDonagh, J. (1989) Electron microscopy and hydrodynamic properties of factor XIII subunits. J. Biol. Chem. 264, 551-6

Casadio, R., Polverini, E., Mariani, P., Spinozzi, F., Carsughi, F., Fontano, A., Polverino de Laureto, P., Matteurci, G. and Bergamini, C. M. (1999) The structural basis for the regulation of tissue transglutaminase by calcium ions. Eur. J. Biochem. 262, 67-9

Cha, D., O'Brien, P., O'Toole, E. A., Woodley, D. T. and Hudson, L. G. (1996) Ehanced modulation of keratinocyte motility by transforming growth facto-alpha (TGF-alpha) relative to epidermal growth factor (EGF). J. Invest. Dermatol. 106, 590-7

Chang, S. K. and Chung, S. I., (1986) The particulate-associated transglutaminase from chondrosarcoma and liver. J. Biol. Chem. 261, 8112-21

Chakravarty, R. and Rice, R. H. (1989) Acylation of keratinocyte transglutaminase and myristic acids in the membrane region. J. Biol. Chem. 264, 625-9

Chapman, S. J. and Walsh, A. (1990) Desmosomes, corneosomes and desquamation. An ultrastructural study of adult pig epidermis. Arch. Dermatol. Res. 282, 304-10

Chen, R. and Doolittle, R. F. (1971) γ-γ Cross-linking sites in human and bovine fibrin. Biochemistry 10, 4486-91

Chen, J. M., Sheldon, A. and Pincus, M. R., (1993) Structure-function correlations of calcium binding and calcium channel activities based on 3-dimensional models of human annexins I, II, III, V and VII. J. Biomol. Struct. Dyn. 10, 1067-89

Chung, S. I. and Folk, J. E. (1972) Transglutaminase from hair follicle of guinea pig. Proc. Natl. Acad. Sci. U.S.A 69, 303-8 TG3 50 KDa

Clark, R. A. F (1996), (Ed.) The molecular and Cellular Biology of wound repair. (Plenum, New York)

Clark, R. A. F, Lanigan, J. M., DellaPelle, P., Dvorak, H. F. and Colvin, R. B. (1982) Fibronectin and fibrin provide a provisional matrix for epidermal cell migration during wound reepithelialization. J. Invest. Dermatol. 79, 264-9

Clarke, D. D., Mycek, M. J., Neidle, A., Waelsch, H. (1957) The incorporation of amines into protein. Arch. Biochem. Biophys. 79, 338-54

Clement, S., Velasco, P. T., Murthy, S. N. P., Wilson, J. H., Lukas, T. J., Goldman, R. D. and Lorand, L. (1998) The intermediate filament protein, vimentin, in lens is a target for cross-linking by transglutaminase. J. Biol. Chem. 273, 7604-9

Cohen, C. M., Dotimas, E. and Korsgren, C. (1993) Human erythrocyte membrane protein band 4.2 (pallidin). Semin. Hematol. 30, 119-37

Cohen, I., Gerrard, J. M. and White, J. G. (1982) Ultrastructure of clots during isometric contraction. J. Cell Biol. 93, 775-87

Cohen, B. E., Lee, G., Arispe, N. and Pollard, H. B. (1995) Cyclic 3'-5'-adenosine monophosphate binds to annexin 1 and regulates calcium-dependent membrane aggregation and ion channel activity. FEBS Lett 377, 444-50

Cooper, A. J., Sheu, R. K., Burke, J. R., Onodera, O., Strittmatter, W. J., Roses, A. D. and Blass, J. P. (1997) Transglutaminase-catalyzed inactivation of glyceraldehydes 3-phosphate dehydrogenase and α-ketoglutarate dehydrogenase complex by polyglutamine domains of pathological length. Proc. Natl. Acad. Sci. U.S.A 94, 12604-9

Cooper, A. J., Wang, J., Pasternack, R., Fuchsbauer, H. L. Sheu, R. K. and Blass, J. P. (2000) lysine-rich histone (H1) is a lysyl substrate of tissue transglutaminase: possible involvement of transglutaminase in the formation of nuclear aggregates in (CAG)(n)/Q(n) expansion diseases. Dev. Neurosci. 22, 404-17

Corbett, S. A., Lee, L., Wilson, C. L. and Schwartzbauer, J. E. (1997) Covalent crosslinking of fibronectin to fibrin is required for maximal cell adhesion to a fibronectin-fibrin matrix. J. Biol. Chem. 272, 24999-25005

Cordella-Miele, E., Miele, L. and Mukherjee, A. B. (1990) A novel transglutaminase-mediated post-translational modification of phospholipase A_2 dramatically increases its catalytic activity. J. Biol. Chem. 265, 17180-8

Cotsarelis, G., Cheng, S., Dong, G., Sun, T-T. and Lavker, R. M. (1989) Existence of slow cycling limbal epithelial basal cells that can be preferentially stimulated to proliferate: Implications on epithelial stem cells. Cell 57, 201-9

Crish, J. F., Howard, J. M., Zaim, T. M., Murthy, S. and Eckert, R. L. (1993) Tissue-specific and differentiation-appropriate expression of the human involucrin gene in transgenic mice: An abnormal epidermal phenotype. Differentiation 53, 191-200

Croft, C. B. and Tarin, D. (1970) Ultrastructural studies of wound healing in mouse skin. I. Epithelial behaviour. J. Anat. 106, 63-77

Dale, B. A., Holbrook, K. A. and Steinert, P. M. (1978) Assembly of stratum corneum basic protein and keratin filaments in macrofibrils. Nature 276, 729-31

De Laurenzi, V. and Melino, G. (2000) Apoptosis. The little devil of death. Nature 406, 135-6

De Laurenzi, V. and Melino, G. (2001) Gene disruption of tissue transglutaminase. Mol. Cell Biol. 21, 148-55

Dickson, M. A., Hahn, W. C., Ino, Y., Ronfrad, V., Wu, J. Y., Weinberg, R. A., Louis, D. N., Li, F. P. and Reinwald, J. G. (2000) Human keratinocytes that express hTERT and also bypass a p16-^{INK4a}-enforced mechanism that limits life span become immortal yet retain normal growth and differentiation characteristics. Mol. Cell Biol. 20, 1436-47

Dieterich, W., Ehnis, T., Bauer, M., Donner, P., Volta, U., Riecken, E.O. and Schuppan, D. (1997) Identification of tissue transglutaminase as the autoantigen of coeliac disease. Nat. Med. 3, 797-801

Dijan, P., Easley, K. and Green, H. (2000) Targeted ablation of the murine gene. J. Cell. Biol. 151, 381-8

Dolynchuk, K. N., Bendor-Samuel, R. and Bowness, J. M. (1994) Effect of putrescine on tissue transglutaminase activity in wounds: decreased breaking strength and increased matrix fuco protein solubility. Plast. Reconstr. Surg. 93, 567-73

Donaldson, D. J. and Mahan, J. T. (1984) Epidermal cell migration on laminin-coated substrates: comparison with other extracellular matrix and non-matrix proteins. Cell Tissue Res. 235, 221-4

Donato, R. (1999) Functional roles of S100 proteins, calciym-binding proteins of the EF-hand type. Biochim. Biophys. Acta 1450, 191-231

Donoff, R. B., McLennon, J. E. and Grillo, H. C. (1971) Preparation and properties of collagenases from epithelium and mesenchyme of healing mammalian wounds. Biochim. Biophys. Acta 277, 239-53

Doolittle, R. T., Watt, K. W. K., Coltrell, B. A., Strong, D. D., Riley, M. (1979) The amino acid sequence of the α-chain of human fibrinogen. Nature 280, 464-8

Dotto, G. P. (2000) p21$^{WAF1/Cip1}$: More than a break to the cell cycle? Biochim. Biophys. Acta 87483: 1-14

Dunsmore, S. E., Rubin, J. S., Kovacs, S. O., Chedid, M., Parks, W. C. and Welgus, H. G. (1996) Mechanisms of hepatocyte growth factor stimulation of keratinocyte metalloproteinase production. J. Biol. Chem. 271, 24576-82

Eckert, R. L. (1989) Structure, function and differentiation of the keratinocyte. Physiol. Rev. 69, 1316-46

Eckert, R., Crish, J. and Robinson, N. (1997) The epidermal keratinocyte as a model for the study of gene regulation and cell differentiation. Physiol. Rev. 77, 397-424

Eckert, R. L. and Green, H. (1986) Structure and evolution of the human involucrin gene. Cell 46, 583-9

Eckert, R. L., Sturniolo, M. T., Broome, A-M., Ruse, M. and Rorke, E. A. (2005) Transglutaminase function in epidermis. J. Invest. Dermatol. 124, 481-92

Eckert, R. L., Yaffe, M. B., Crish, J. F., Murthy, S., Rorke, E. A. and Welter, J. F. (1993) Involucrin – structure and role in envelope assembly. J. Invest. Dermatol. 100, 613-7

Egberts, F., Heinrich, M., Jensen, J. M., Winoto-Morbach, S., Pfeiffer, S., Wickel, M., Schunck, M., Steude, J., Saftig, P., Proksch, E., Schutz, S. (2004) Cathepsin D is involved in the regulation of transglutaminase 1 and epidermal differentiation. J. Cell Sci. 117, 2295-307

Elias, P. M. and Menon, G. K. (1991) Structural and lipid biochemical correlates of the epidermal permeability barrier. In: Elias, P. M., (Ed.), Skin lipids, advances in lipid research. (Academic, San Diego) vol 24 pp 1-26

Elliott, G. and O'Hare, P. (1997) Intercellular trafficking and protein delivery by a herpesvirus structural protein. Cell 88, 223-33

Eriksson, A., Siegbahn, A., Westermark, B., Heldin, C. H. and Claesson-Welsh, L. (1992) PDGF alpha- and beta-receptors activate unique and common signal transduction pathways. EMBO J. 11, 543-56

Esposito, C. and Caputo, I (2004) Mammalian transglutaminase: Identification of substrates as a key to physiological function and physiopathological relevance. FEBS J. 272, 615-31

Esposito, C., Cozzolino, A., Mariniello, L., Stiuso, P., De Maria, S., Metafora, S., Ferranti, P. and Carteni-Farina, M. (1999) Enzymatic synthesis of vasoactive intestinal peptide analogs by transglutaminase. J. Peptide Res. 53, 626-32

Etoh, Y., Simon, M. and Green H. (1986) Involucrin acts as a transglutaminase substrate at multiple sites. Biochem. Biophys. Res. Commun. 136, 51-6

Fabbi, M., Marimpietri, D., Martini, S., Brancolini, C., Amoresano, A., Scaloni, A., Bargelles, A. and Cosulich, E. (1999) Tissue transglutaminase is a caspase substrate during apoptosis. Cleavage causes loss of transamidating function and is a biochemical marker of caspase 3 activation. Cell death and differentiation 6, 992-1001

Facchiano, F., Benfenati, F., Valtorta, F. and Luini, A. (1993) Covalent modification of synapsin I by tetnus toxin-activated transglutaminase. J. Biol. Chem. 268, 4588-91

Farbman, A. I. (1966) Plasma membrane changes during keratinisation. Anat. Rec. 156, 269-82

Feng, J. F., Rhee, S. G. and Im, M. J. (1996) Evidence that PLC-δ1 is the effector in the Gh/TG2-mediated signalling. J. Biol. Chem. 271, 16451-4

Festoff, B. W., SantaCruz, K., Arnold, P. M., Sebastion, C. T., Davies, P. J. A. and Citron, B. A. (2002) Injury-induced "switch" from GTP-regulated to novel GTP-independent isoform of tissue transglutaminase in the rat spinal cord. Journal of Neurochemistry 81, 708-18

Fesus, L., Metsis, M. L., Muszbek, L., Koteliansky, V. E. (1986) Transglutaminase-sensitive glutamine residues of human plasma fibronectin revealed by studying its proteolytic fragments. Eur. J. Biochem. 154, 371-4

Folk, J. E. (1980) Transglutaminases. Annu. Rev. Biochem. 49, 517-31

Folk, J. E. and Cole, P. W. (1965) Structural requirements of specific substrates for guinea pig liver transglutaminase. J. Biol. Chem. 240, 2951-60

Folk, J. E., Cole, P. W., Mullooly, J. P. (1967) Mechanism of action of guinea pig liver transglutaminase: The metal-dependent hydrolysis of p-nitrophenyl acetate; further observations on the role of metal in enzyme activation. J. Biol. Chem. 242, 2615-21

Folk, J. E. and Finlayson, J. S. (1977) The ε-(γ-glutamyl)lysine cross-link and the catalytic role of transglutaminases. Adv Protein Chem. 31, 1-133

Folk, J. E., Park, M. H., Chung, S. I., Schrode, J., Lester, E. P. and Cooper, H. L. (1980) Polyamines as physiological substrates for transglutaminases. J. Biol. Chem. 255, 3695-700

Folk, J. E., Park, M. H., Chung, S. I., Schrode, J., Lester, E. P. and Cooper, H. L. (1999) Polyamines as physiological substrates for transglutaminase enhances. J. Biol. Chem. 255, 3695-700

Forslind, B., Lindberg, M., Roomans, G. M., Pallon, J. and Werner-Linde, Y. (1997) Aspects on the physiology of human skin: studies using particle probe analysis. Microsc. Res. Tech. 38, 373-86

Fraij, B. M. and Gonzales, R. A. (1997) Organisation and structure of the human tissue transglutaminase gene. Biochim. Biophys. Acta. 1354, 65-71

Franceschi, R. T., Iyer, B. S. and Cui, Y. (1994) Effects of ascorbic acid on collagen matrix formation and osteoblast differentiation in murine MC3T3-E1 cells. J. Bone Miner. Res. 9, 843-54

Frenck, E. and Mevorah, B. (1977) The keratinisation disorder in collodion babies evolving into lamellar ichthyosis. J. Cutan. Pathol. 4, 329-37

Fry, L. (1995) Dermatitis herpetiformis. Bailliere. Clin. Gastr. 9, 371-94

Fuchs, E. and Byrne, C. (1994) The epidermis: Rising to the surface. Curr. Opin. Genet. Dev. 4, 725-36

Fuchs, E. and Green, H. (1980) Changes in keratin gene expression during terminal differentiation of the keratinocyte. Cell 19, 1033-42

Furcht, L. T., Wendelschafer-Crabb, G., Mosher, D. F. and Foldart, J. M. (1980) Ascorbic-induced fibroblast cell matrix: reaction of antibodies to procollagen I and III and fibronectin in an axial periodic fashion. Prog. Clin. Biol. Res. 41, 829-43

Gailit, J., Welch, M. P. and Clark, R. A. F. (1994) TGF-β1 stimulates expression of keratinocyte integrins during re-epithelialization of cutaneous wounds. J. Invest. Dermatol. 103, 221-7

Gallucci, R. M., Sloan, D. K., Heck, J. M., Murray, A. R. and O'Dell, S. J. (2004) Interleukin 6 indirectly induces keratinocyte migration. J. Invest. Dermatol. 122, 764-72

Garach-Jehoshua, O., Ravid, A., Liberman, U. A., Reichert, J, Glaser, T. and Koren, R (1998) Upregulation of the calcium-dependent protease, calpain, during keratinocyte differentiation. Br. J. Dermatol. 139, 950-7

Garlick, J. A. and Taichman, L. B. (1994) Fate of human keratinocytes during reepithelialization in an organic culture model. Lab. Invest. 70, 916-24

Gaudry, C.A., Verderio, E., Aeschlimann, D., Cox, A., Smith, C. and Griffin M. (1999) Cell surface localization of tissue transglutaminase is dependent on a fibronectin-binding site in its N-terminal β sandwich domain. J. Biol. Chem. 274, 30707-30714

Gentile, V., Saydak, M., Chiocca, E. A., Akande, O., Birckbichler, P. J., Lee, K. N., Stein, J. P. and Davies, P. J. A. (1991) J. Biol. Chem. 266, 478-83

Gentile, V., Thomazy, V., Piacentini, M., Fesus, L. and Davies, P. J. A. (1992) Expression of tissue transglutaminase in Balb-C 3T3 fibroblasts: effects on cellular morphology and adhesion. J. Cell Biol. 119, 463-74

Gerke, V. and Moss, S. E. (2002) Annexins: From structure to function. Physiol. Rev. 82, 331-71

Ghahary, A., Tredget, E. E., Chang, L. J., Scott, P. G. and Shen, Q. (1998) Genetically modified dermal keratinocytes express high levels of transforming growth factor-beta1. J. Invest. Dermatol. 110, 800-5

Ghalbzouri, A. E., Gibbs, S., Lamme, E., Van Blitterswijk, C. A. and Ponec, M (2002) Cutaneous Biology: Effect of fibroblasts on epidermal regeneration. Br. J., Dermatol. 147, 230-43

Ghalbzouri, A. E., Hensbergen, P., Gibbs, S., Kempenaar, J., Van der Schors, R. and Ponec, M. (2004) Fibroblasts facilitate re-epithelialization in wounded human skin equivalents. Laboratory Investigation 84, 102-12

Gibbs, S., Fijneman, R., Wiegant, J., Van Kessel, A. G., Van de Putte, P. and Backendorf, C. (1993) Molecular characterisation and evolution of the SPRR family of keratinocyte differentiation markers encoding small proline-rich proteins, Genomics 16, 630-7

Gibbs, S., Silva Pinto, A. N., Murli, S., Huber, M., Hohl, D. and Ponec, M. (2000) Epidermal growth factor and keratinocyte growth factor differentially regulate epidermal migration, growth, and differentiation. Wound Repair Regen. 8, 192-3

Gibbins, J. R. (1968) Migration of stratified squamous epithelium *in vivo*. The development of phagocyticability. Am., J. Pathol. 53, 929-51

Goldsmith, L. A., Baden, H. P., Roth, S. I., Colman, R., Lee, L. and Fleming, B. (1974) Vertebral epidermal transamidases. Biochim. Biophys. Acta 351, 113-25

Gorman, J. J. and Folk, J. E. (1981) Structural features of glutamine substrates for transglutaminases: Specificities of human plasma factor XIIIa and the guinea pig liver enzyme toward synthetic peptides. J. Biol. Chem. 256, 2712-5

Gorman, J. J. and Folk, J. E. (1984) Structural features of glutamine substrates for transglutaminases: Role of extended interactions in the specificity of human plasma factor XIIIa and the guinea pig liver enzyme. J. Biol. Chem. 259, 9007-10

Grant, F. J., Taylor, D. A, Sheppard, P. O., Mathewes, S. L., Lint, W., Vanaja, E., Bishop, P. D. and O'Hara, P. J. (1994) Molecular-cloning and characterisation of a novel transglutaminase cDNA from a human prostate cDNA library. Biochem. Biophys., Res. Commun. 203, 1117-23

Green, K. J. and Gaudry, C.A. (2000) Are desmosomes more than tethers for intermediate filaments? Nat. Rev. Mol. Cell Biol. 1, 208-16

Greenberg, C., S., Birkbichler, P. J. and Rice, R. H. (1991) Transglutaminases: Multifunctional cross-linking enzymes that stabilize tissues. Fed. Am. Soc. Exp. Biol. 5, 3071-7

Grenard, P., Bates, M. K. and Aeschlimann, D. (2001) Evolution of transglutaminase genes: identification of a transglutaminase gene cluster on human chromosome 15q15. Structure of the gene encoding transglutaminase x and a novel gene family member, transglutaminase z. J. Biol. Chem. 276, 33066-78

Griffin, M., Casadio, R. and Bergamini, C. M. (2002) Transglutaminases: nature's biological glues. Biochem. J. 368, 377-96

Grinnell, F. (1992) Wound repair, keratinocyte activation and integrin modulation. J. Cell Sci. 101, 1-5

Grinnell, F., Billingham, R. E. and Burgess, L. (1981) Distribution of fibronectin during wound healing *in vivo*. J. Invest. Dermatol. 76, 181-9

Groenen, P. J. T. A., Bloemendal, H. and De Jong, W. W. (1994) Lys-17 is the amino-donor substrate site for transglutaminase in βA3-crystallin. J. Biol. Chem. 269, 831-3

Grundmann, U., Amann, E., Zettlmeissl, G., Kupper, H. A. (1986) Characterization of cDNA encoding for human factor XIIIa. Proc. Natl. Acad. Sci. U.S.A 83, 8024-8

Guo, M, Toda, K. I. and Grinnell, F. (1990) Activation of human keratinocyte migration on type I collagen and fibronectin. J. Cell Sci. 96, 197-205

Haroon, Z. A., Hettasch, J. M., Lai, T-S., Dewhirst, M. W. and Greenberg, C. S. (1999) Tissue transglutaminase is expressed, active, and directly involved in rat dermal wound healing and angiogenesis. FASEB J. 13, 1787-95

Harsfalvi, J., Arato, G. and Fesus, L. (1987) Lipids associated with tissue transglutaminase. Biochim. Biophys. Acta 923, 42-5

Hashimoto, K. (1969) Cellular envelopes of keratinised cells of the human epidermis. Arch. Clin. Exp. Derm. 235, 374-85

Hauert, J., Patston, P. A. and Schapira, M. (2000) C1 inhibitor cross-linking by tissue transglutaminase. J. Biol. Che. 275, 14558-62

Hettasch, J. M., Bandarenko, N., Burchette, J. L., Lai, T. S., Marks, J. R., Haroon, Z. A., Peters, K., Dewhirst, M. W., Iglehart, J. D. and Greenberg, C. S. (1996) Tissue transglutaminase expression in human breast cancer. Lab. Invest. 75, 637-45

Hebda, P. A. (1988) Stimulatory effects of transforming growth factor-beta and epidermal growth factor on epidermal cell outgrowth from porcine skin explain cultures. J. Invest. Dermatol. 91, 440-5

Hennings, H., Michael, D., Cheng, C., Steinert, P., Holbrook, K. and Yuspa, S. H. (1980) Calcium regulation of growth and differentiation of mouse epidermal cells in culture. Cell 19, 245-54

Herbert, S. C. and Brown, E. M. (1995) The extracellular calcium receptor. Curr. Opin. Cell Biol. 7, 484-92

Hertle, M. D., Kubler, M-D., Leigh, I. M. and Watt, F. M. (1992) Aberrant integrin expression during epidermal wound healing and in psoriatic epidermis. J. Clin. Invest. 89, 1892-1901

Hinterhuber, G., Marquardt, Y., Diem, E., Rappersberge, K., Wolff, K. and Foedinger, D. (2002). Organotypic keratinocyte coculture using normal human serum: an immunomorphological study at light and electron microscope levels. Exp. Dermatol. 11, 413-20

Hitomi, K., Horio, Y., Ikura, K., Yamanishi, K. and Maki, M. (2001) Analysis of epidermal-type transglutaminase (TGase 3) expression in mouse tissues and cell lines. Int. J. Biol. Cell Biol. 33, 491-8

Hitomi, K., Presland, R. B., Nakayama, T., Fleckman, P., Dale, B. A. and Maki, M. (2003) Analysis of epidermal-type transglutaminase (transglutaminase 3) in human stratified epithelia and cultured keratinocytes using monoclonal antibodies. J. Dermatol. Sci. 32, 95-103

Hunter, I., Sigmundsson, K., Beauchemin, N. and Obrink, B. (1998) The cell adhesion molecule C-CAM is a substrate for tissue transglutaminase. FEBS Lett. 425, 141-4

Ho, K. C., Quarmby, V. E., French, F. S. and Wilson, E. M. (1992) Molecular cloning of rat prostate transglutaminase cDNA: The major androgen-related protein-DP1 of rat dorsal prostate and coagulating gland. J. Biol. Chem. 267, 12660-7

Hohenadl, C., Mann, K., Mayer, U., Timpl, R., Paulsson, M. and Aeschlimann, D. (1995) Two adjacent N-terminal glutamines of BM-40 (osteonectin, SPARC) act as amine acceptor sites in transglutamine$_c$-catalyzed modification. J. Biol. Chem. 270, 23415-20

Hohl, D., Mehrel, T., Lichti, U., Turner, M. L., Roop, D. R. and Steinert, P. M. (1991) Characterization of human loricrin: Structure and function of a new class of epidermal cell envelope proteins. J. Biol. Chem. 266, 6626-36

Holbrook, K. A. and Odland, G. F. (1975) The fine structure of developing human epidermis: Light scanning, and transmission electron microscopy of the periderm. J. Invest. Dermatol. 65, 16-38

Horikoshi, T., Igarashi, S., Uchiwa, H., Brysk, H. and Brysk, M. M. (1999) Role of endogenous cathepsin D-like and chymotrysin-like proteolysis in human epidermal desquamation. Br. J. Dermatol. 141, 453-9

Huber, M., Rettler, I., Bernasconik, K., Frenk, E., Lavrijsen, S. P., Ponec, M., Lautenschlager, S., Schorderet, D. F., Hohl, D. (1995) Mutations of keratinocyte transglutaminase in lamellar ichthyosis. Science 267, 525-8

Hubner, G., Brauche, M., Smola, H. and Madlener, M. (1996) Differential regulation of pro-inflammatory cytokines during wound healing in normal and glucacorticoid-treated mice. Cytokine 8, 548

Huff, T., Ballweber, E., Humeny, A., Bonk, T., Becker, C. M., Muller, C. S. G., Mannherz, H. G. and Hannappel, E. (1999) Thymosin β4 serves as a glutamyl substrate of transglutaminase. Labelling with fluorescent dansylcadaverine does not abolish interaction with G-actin. FEBS Lett. 464, 14-20

Hwang, K. C., Grey, C. D., Sivasubramanian, N. and Im, M-J. (1995) Interaction site of GTP binding G_h (transglutaminase II) with phospholipase C. J. Biol. Chem. 270, 27058-62

Hwang, K. C., Grey, C. D., Sweot, W. E., Moravec, C. S. and Im, M-J. (1996) (alpha)1-Adrenergic receptor coupling with Gh in the failing human heart. Circulation 94, 718-26

Ichikawa, A., Ohashi, Y., Terada, S., Natsuka, Y. and Ikura, K. (2004) *In vitro* modification of betaine-homocysteine S-methyltransferase by tissue-type transglutaminase. Int. J. Biochem. Cell Biol. 36, 1991-2002

Ichinose, A., Hendrickson, L. E., Fujikawa, K., Davie, E. W. (1986) Amino acid sequence of the a-subunit of human factor XIII. Biochemistry 25, 6900-6

Iismaa, S. E., Wu, M. J., Nanda, N., Church, W. B. and Graham, R. M. (2000) GTP binding and signalling by G_h/transglutaminase II involves distinct residues in a unique binding pocket. J. Biol. Chem. 275, 18259-65

Iizuka, R., Chiba, K., Imajoh-Ohmi, S. (2003) A novel approach for the detection of proteolytically activated transglutaminase 1 in epidermis using cleavage site-directed antibodies. J. Invest. Dermatol. 121 (3) 457-64

Ikura, K., Kita, K., Fujita, I., Hashimoto, H. and Kawabata, N. (1998) Identification of amine acceptor acceptor protein substrates of transglutaminase in liver extracts: use of 5-(biotinamido)pentylamine as a probe. Arch. Biochem. Biophys. 356, 280-6

Ikura, K., Nasu, T., Yokota, H., Tsuchiya, T., Sasaki, R., Chiba, H. (1988) Amino acid sequence of guinea pig liver transglutaminase from its cDNA sequence. Biochemistry 27, 2898-905

Ikura, K., Shinagawa, R., Suto, N. and Sasaki, R. (1994) Increase caused by interleukin-6 in promoter activity of guinea pig liver transglutaminase gene. Biosci. Biotechnol. Biochem. 58, 1540-1

Inada, R., Matsuki, M., Yamada, K., Morishima, Y., Shen, S-C., Kuramoto, N., Yasuno, H., Takahashi, K., Miyachi, Y. and Yamanishi, K. (2000) Facilitated wound healing by activation of the transglutaminase 1 gene. Am. J. Pathol. 157 (6) 1875-87

Ishida-Yamamoto, A., Hohl, D., Roop, D. R., Iizuka, H. and Eady, R. A. J. (1993) Loricrin immunoreactivity in human skin: Localisation to specific granules (L-granules) in acrosyringia. Arch. Dermatol. Res. 285, 491-8

Isobe, M., Katsuramaki, T., Hirata, K., Kimura, H.,Nagayamo, M. and Matsuno, T. (1999) Beneficial effects of inducible nitric oxide synthase inhibitor on reperfusion injury in the pig liver. Transplantation 68, 803-13

Jensen, P. H., Sorensen, E. S., Petersen, T. E., Glieman, J. and Rasmussen, L. K. (1995) Residue in the synuclein consensus motif of the alpha-synuclein fragment. NAC, participate in transglutaminase-catalyzed cross-linking to Alzheimer-disease amyloid beta A4 peptide. Biochem. J. 310, 91-4

Jeon, S., Djian, P. and Green, H. (1998) Inability of keratinocytes lacking their specific transglutaminase to form cross-linked envelopes: absence of envelopes as a simple diagnostic test for lamellar icthyosis. Proc. Natl. Acad. Sci. U.S.A 95, 687-90

Jeong, J-M., Murthy, S. N. P., Radek, J. T. and Lorand, L.(1995) The fibronectin-binding domain of transglutaminase. J. Biol. Chem. 270, 5654-8

Jiang, C. K., Magnaldo, T., Ohtsuki, M., Freedberg, I. M., Bernerd, F. and Blumenberg, M. (1993) Epidermal growth factor and transforming growth factor alpha specifically induce the activation- and hyperproliferation-associated keratins 6 and 16. Proc. Natl. Acad. Sci. U.S.A 90, 6786-90

Jimenez, P. A. and Rampy, M. A. (1999) Keratinocyte growth factor-2 accelerates wound healing in incisional wounds. J. Surg. Res. 81, 238-42

Johnson, T. S., Knight, C. R. L., El-Alaoui, S., Mian, S., Rees, R. C., Gentile, V., Davies, P. J. A. and Griffin, M. (1994) Transfection of tissue transglutaminase into highly malignant hamster fibrosarcoma leads to a reduced incidence of primary tumour growth. Oncogene 9, 2935-42

Johnson, T. S., Griffin, M., Thomas, G. L., Skill, J., Cox, A., Yang, B., Nicholas, B., Birckbichler, P. J., Muchaneta-Kubara, C. and El Nahas, A. M. (1997) The role of transglutaminase in the rat subtotal nephrectomy model of renal fibrosis. J. Clin. Invest. 99, 2950-60

Jones, R. A., Nicholas, B., Mian, S., Davies, P. J. A. and Griffin, M. (1997) Reduced expression of tissue transglutaminase in a human endothelial cell line leads to changes in cell spreading, cell adhesion and reduced polymerisation of fibronectin. J. Cell Sci. 110, 2461-72

Kaartinen, M. T. and Mckee, M. D. (2002) Tissue transglutaminase and its substrates in calcified tissues: bone and teeth. Minerva Biotec. 14, 206

Kaartinen, M. T., Pirhonen, A., Linnala-Kankkunen, A. and Maenpaa, P. H. (1997) Transglutaminase catalysed cross-linking of osteopontin is inhibited by osteocalcin. J. Biol. Chem. 272, 22736-41

Kalinin, A. E., Kajava, A. V. and Steinert, P. M. (2002) Epithelial barrier function: Assembly and structural features of the cornified cell cell envelope. Bioessays 24, 789-800

Kanaji, T., Ozaki, H., Takao, T., Kawajiri, H., Ide, H., Motoki, M. and Shimonishi, Y. (1993) Primary structure of microbial transglutaminase from Streptoverticillium sp. Strain s-8112. J. Biol. Chem. 268, 11565-72

Katz, S. I., Falchuk, Z. M., Dahl, M. V., Rogentine, G. N. and Strober, W. (1972) HL-A8: A genetic link between dermatitis herpetiformis and gluten sensitive enteropathy. J. Clin. Invest. 51, 2977-80

Kaur, P. and Carter, W. G. (1992) Integrin expression and differentiation in transformed human epidermal cells is regulated by fibroblasts. J. Cell Sci. 103, 755-63

Kim, S. Y., Chung, S. I., Steinert, P. M. (1995a) Highly active soluble processed forms of the transglutaminase 1 enzyme in epidermal keratinocytes J. Biol. Chem. 270 (30), 18026-35

Kim, S. Y., Chung, S. I., Yoneda, K. and Steinert, P. M. (1995b) Expression of transglutaminase 1 in human epidermis. J. Invest. Dermatol. 104, 211-7

Kim, I. G., Gorman, J. J., Lee, S. C., Park, S. C., Chung, S. I. and Steinert, P. M. (1993) The deduced sequence of the novel protransglutaminase E (TGase 3) of human and mouse. J. Biol. Chem. 268 12682-90

Kim, H-C., Idler, W. W., Kim, I. G., Han, J. H., Chung, S. I. and Steinert, P. M. (1991) The complete amino acid sequence of the human transglutaminase K enzyme deduced from the nuclei acid sequence of cDNA clones. J. Biol. Chem. 266, 536-9

Kim, S. Y., Kim, I. G., Chung, S. I. and Steinert, P. M. (1994) The structure of the transglutaminase 1 enzyme. Deletion cloning reveals domains that regulate its specific activity and substrate specificity. J. Biol. Chem. 269, 27979-86

Kim, H. C., Lewis, M. S., Gorman, J. J., Park, S. C., Girad, J. E., Folk, J. E. and Chung, S. I. (1990) Protransglutaminase E from guinea pig skin. Isolation and partial characterisation. J. Biol. Chem. 265, 21971-8

Kleman, J. P., Aeschlimann, D., Paulsson, M. and Van der Rest, M. (1995) Transglutaminase-catalyzed cross-linking of fibrils for collagen V/XI in A204 rhabdomyosarcoma cells. Biochemistry 34, 13768-775

Knox, P., Crooks, S. and Rimmer, C. S. (1986) Role of fibronectin in the migration of fibroblasts into plasma clots. J. Cell. Biol. 102, 2318-2323.

Kobayashi, K., Hashiguchi, K., Yokozeki, K., Yamanaka, S. (1998) Molecular cloning of the transglutaminase gene from *Bacillus subtilis* and its expression in *Escherichia coli*. Biosci. Biotechnol. Biochem. 62, 1109-14

Koch, P. J., De Viragh, P. A., Sharer, E., Bundman, D., Longley, M. A., Bickenbach, J., Kawachi, Y., Suga, Y., Zhou, Z., Huber, M., Hohl, D., Kartasov, T., Jarnik, M., Steven, A. C. and Roop, D. R. (2000) Lessons from loricrin-deficient mice: compensatory mechanisms maintaining skin barrier function in the absence of a major cornified envelope protein. J. Cell Biol. 151, 389-400

Kojima, S., Inui, T., Muramatsu, H., Suzuki, Y., Kadomatsu, K., Yoshizawa, M., Hirose, S., Kimura, T., Sakakibara, S. and Muramatsu, T. (1997) Dimerization of midkine by tissue transglutaminase and its functional implication. J. Biol. Chem. 272, 9410-16

Kojima, S., Nara, K. and Rifkin, D. B. (1993) Requirement for transglutaminase in the activation of latent transforming growth factor-beta in bovine endothelial cells. J. Cell Biol. 121, 439-48

Korff, T. and Augustin, H. G. (1998) Integration of endothelial cells in multicellular spheroids prevents apoptosis and induces differentiation. J. Cell Biol. 143, 1341-52

Korsgren, C., Lawler, J., Lambert, S., Speicher, D. and Cohen, C. M. (1990) Complete amino acid sequence and homologies of human erythrocyte membrane protein band 4.2. Biochemistry 87, 613-7

Koseki-Kuno, S., Yamakawa, M., Dickneite, G. and Ichinose, A. (2003) Factor XIII A subunit-deficient mice developed severe uterine bleeding events and subsequent spontaneous miscarriages. Blood 102, 4410-2

Krieg, P., Schuppler, M., Koesters, R., Mincheva, A., Lichter, P. and Marks, F. (1997) Repetin (Rptn) a new member of the "fused gene" subgroup within the S100 gene family encoding a murine epidermal differentiation protein. Genomics 43 339-48

Kubilus, J., Kvedar, J. and Baden, H. P. (1987) Identification of new components of the cornified envelope of human and bovine epidermis. J. Invest. Dermatol. 89, 44-50

Kuchler, K. and Thorner, J. (1990) Membrane translocation of proteins without hydrophobic signal peptides. Curr. Opin. Cell. Biol. 2 617-24

Kuncio, G. S., Tsyganskaya, M., Zhu, J., Liu, S. L., Nagy, L., Thomazy, V., Davies, P. J. and Zern, M. A. (1998) TNF-alpha modulates expression of the tissue transglutaminase gane in liver cells. Am. J. Physiol. 274, G240-5

LaCelle, P. T., Lambert, A., Ekambaram, M. C., Robinson, N. A. and Eckert, R. L. (1998) *In vitro* cross-linking of recombinant human involucrin. Skin Pharmacol. Appl. Skin Physiol. 13, 17-30

Lai, T. S., Slaughter, T. F., Koropehak, C. M., Haroon, Z. A. and Greenberg, C. S. (1996) C-terminal deletion of human tissue transglutaminase enhances magnesium-dependent GTP/ATPase activity. The American Society for biochemistry and molecular biology

Landmann, L. (1986) Epidermal permeability barrier: Transformation of lamellar granule-disks into intercellular sheets by a membrane-fusion process, a freeze-fracture study. J. Invest. Dermatol. 87, 202-9

Lauer, P., Metzner, H. J., Zettlmeissl, G., Li, M., Smith, A. G., Lathe, R. and Dickneite, G. (2002) Targeted inactivation of the mouse locus encoding coagulation factor XIII-A: Hemostatic abnormalities in mutant mice and characterisation of the coagulation deficit. Thromb. Haemost. 88, 967-74

Lavker, R. M. (1976) Membrane coating granules: The fate of the discharged lamellae. J. Ultrastruct. Res. 55, 79-86

Lavker, R. M. and Matoltsy, A. G. (1971) Substructure of keratohyalin granules of the epidermis as revealed by high resolution electron microscopy. J. Ultrastruct. Res. 1971 35, 575-81

Lee, J-H., Jang, S-I., Yong, J-M., Markova, N. G. and Steinert, P. M. (1996) The proximal promoter of the human transglutaminase 3 gene: stratified squamous epithelial-specific expression in cultured cells is mediated by the binding of Sp1 and ets transcription factors to a proximal promoter element. J. Biol. Chem. 271, 4561-8

Lee, J., Leonard, M., Oliver, T., Ishihara, A. and Jacobson, K. (1994) Traction forces generated by locomoting keratinocytes. J. Cell Biol. 127, 1957-64

Lee, K. N., Maxwell, M. D., Patterson, M. K., Birckbichler, P. J. and Conway, E. (1992) Identification of transglutaminase substrates in HT29 colon cancer cells: use of 5-biotin-amidopentylamine as a transglutaminase-specific probe. Biochim. Biophys. Acta 1136, 12-16

Lichti, U. and Yuspa, S. H. (1998) Modulation of tissue and epidermal transglutaminases in mouse epidermal cells after treatment with 1-O-tetradecaroylphorbol-13-acetate and/or retinoic acid *in vivo* and in culture. Cancer Research 48 (1) 74-81

Liu, S., Cerione, R. A. and Clardy, J. (2002) Structural basis for the guanine nucleotide-binding activity of tissue transglutaminase and its regulation of transamidation activity. Proc. Natl. Acad. Sci. U.S.A 99, 2738-42

Lobitz, C. J. and Buxman, M. M. (1982) Characterization and localization of bovine epidermal transglutaminase substrate. J. Invest. Dermatol. 78, 150-4

Long, S., and Rogers, J. S. (1996) A rapid, sensitive assay for transglutaminase activity in tape strips (Unilever – internal circulation)

Lorand, L. and Conrad, S. M. (1984) Transglutaminases. Mol. Cell. Biochem. 58, 9-35

Lorand, L. and Graham, M. (2003) Transglutaminase: Crosslinking enzymes with pleiotropic functions. Nat. Rev. 4, 140-56

Lu, S., Saydak, M. Gentile, V., Stein, J. and Davies, P. J. A. (1995) Isolation and characterization of the human tissue transglutaminase gene promoter. J. Biol. Chem. 270, 9748-56

Maccioni, R. B. and Arechaga, J. (1986) Transglutaminase (TG) involvement in early embryogenesis. Exp. Cell Res. 167, 266-70

Mack, D. H., Vartikar, J., Pipas, J. M. and Laimins, L. A. (1993) Specific repression of TATA-mediated but not initiator-mediated transcription by wild-type p53. Nature 363, 81-3

Mahoney, S. A., Wilkinson, M., Smith, S. and Haynes, L. W. (2000) Stabilization of neuritis in cerebellar granule cells by transglutaminase activity: identification of midkine and galactin-3 as substrates. Neuroscience 101, 141-55

Makarova, K. S., Aravind, L., Koonin, E. V. (1999) A superfamily of archeal, bacterial, and eukaryotic proteins homologous to animal transglutaminases. Protein Sci. 8, 1714-19

Manabe, M., Hirotani, T., Negi, M., Hattori, M. and Ogawa, H. (1981) Isolation and characterization of the membraneous fraction in human stratum corneum. J. Dermatol. 8, 329-33

Marekov, L. N. and Steinert, P. M. (1998) Ceramides are bound to structural proteins of the human foreskin epidermal cornified cell envelope. J. Biol. Chem. 273, 17763-70

Markova, N. G., Marekov, L. N., Chipev, C. C., Gan, S. Q., Idler, W. W. and Steinert, P. M. (1993) Profilaggrin is a major epidermal calcium-binding protein. Mol. Cell Biol. 13, 613-25

Marks, R. and Barton, S. P. (1983) The significance of the size and shape of corneocytes. In: Marks, R. and Plewig, G., (Ed.), Stratum corneum, (Springer-Verlag, Berlin) pp 175-180

Marks, R., Lawson, A. and Nicholls, S. (1983) Age-related changes in stratum corneum, structure and function. In: Marks, R. and Plewig, G., (Ed.), Stratum corneum, (Springer-Verlag, Berlin) pp 175-180

Martin, P. (1997) Wound Healing – Aiming for perfect skin regeneration. Science 276, 75-81

Martinet, N., Beninati, S., Nigra, T. P. and Folk, J. E. (1990) N^1,N^8-bis(γ-glutamyl)spermidine cross-linking in epidermal-cell envelopes. Comparison of cross-link levels in normal and psoriatic cell envelopes. Biochem. J. 271, 305-8

Martinez, J., Chalupowiez, D. G, Roush, R. K., Sheth, A. and Barsigian, C. (1994) Transglutaminase-mediated processing of fibronectin by endothelial cell monolayers. Biochemistry 33, 2538-45

Mass-Szabowski, N., Stark, H. J. and Fusenig, N. E. (2000) Keratinocyte growth regulation in defined organotypic cultures through IL-1 induced KGF expression in resting fibroblasts. J. Invest. Dermatol. 114, 1075-84

Mass-Szabowski, N., Szabowski, A., Stark, H. J., Andrecht, S., Kolbus, A., Schorpp-Kistner, M., Angel, P. and Fusenig, N. E. (2001) Organotypic cocultures with genetically modified mouse fibroblasts as a tool to dissect molecular mechanisms regulating keratinocyte growth and differentiation. J. Invest. Dermatol.116, 816-20

Matoltsy, A. G. (1966) Membrane coating granules of the epidermis. J. Ultrastruct Res. 15, 510-5

Matoltsy, A. G. and Balsamo, C. A. (1955) A study of the components of the cornified epithelium of human skin. J. Biophysic and Biochem. Cytol. 1 (4), 339-6

Matoltsy, A. G. and Matoltsy, M. N. (1970) The chemical nature of keratohyalin granules of epidermis. J. Cell Biol. 47, 593-603

Matoltsy, A. G. and Matoltsy, M. N. (1966) The membrane protein of horny cells. J. Invest. Dermatol. 46, 127-9

Matsuki, M., Yamashita, F., Ishida-Yamamoto, A., Yamada, K., Kinoshita, C., Fushiki, S., Ueda, E., Morishima, Y., Tabata, K., Yasuno, H., Hashida, M., Iizuka, H., Ikawa, M., Okabe, M., Kondoh, G., Kinoshita, T., Takeda, J. and Yamanishi, K. (1998) Defective stratum corneum and early neonatal death in mice lacking the gene for transglutaminase 1 (keratinocyte transglutaminase). Proc. Natl. Acad. Sci. U.S.A 95, 1044-9

Matsumoto, K., Hashimoto, K., Yoshikawa, K. and Nakamura, T. (1991) Marked stimulation of growth and motility of human keratinocytes by hepatocyte growth factor. Exp. Cell Res. 196, 114-20

McCarthy, D. W., Downing, M. T., Brigstock, D. R., Luquette, M. H., Brown, K. D., Abad, M. S. and Besner, G. E. (1996) Production of heparin-binding epidermal growth factor (HB-EGF) at sites of thermal injury in paediatric patients. J. Invest. Dermatol. 106, 49-56

McCawley, L. J., O'Brien, P. and Hudson, L. G. (1998) Epidermal growth factor (EGF)-and scatter factor/hepatocyte growth factor (SF/HGF)-mediated keratinocyte migration is coincident with induction of matrix metalloproteinase (MMP)-9. J. Cell Physiol. 176, 255-65

Mearns, B., Nanda, N., Michalicek, J., Iismaa, S. and Graham, R. (2002) Impaired wound healing and altered fibroblast cytoskeletal dynamics in Gh knockout mice. (Presented at 7th International Conference on Protein Crosslinking Reactions, Ferrara, Italy, 2002). Minerva Biotechnologica 14, 218

Mehrel, T., Hohl, D., Rothnagel, J. A., Longley, M. A., Bundman, D., Cheng, C., Lichti, U., Bisher, M. E., Steven, P. M., Yuspa, S. H. and Roop, D. R. (1990) Identification of a major keratinocyte cell envelope protein, loricrin. J. Cell Biochem. 61, 1103-12

Melino, G., Annicchiarico-Petruzzelli, M., Piredda, L., Candi, E., Gentile, V., Davies, P. J. A. and Piacentini, M. (1994) Tissue transglutaminase and apoptosis: sense and antisense transfection studies with human neuroblastoma cells. Mol. Cell Biol. 14, 6584-6596

Menon, G. K., Feingold, K. R., Man, M-Q., Schaude, M. and Elias, P. M. (1992) Structural basis for the barrier abnormality following inhibition of HMG CoA reductase in murine epidermis. J. Invest. Dermatol. 98, 209-19

Michel, S., Bernerd, F., Jetten, A. M., Floyd, E., Shroot, B. and Reichert, U. (1992) Expression of keratinocyte transglutaminase mRNA revealed by *in situ* hybridisation. J. Invest. Dermatol. 98, 364-8

Michel, S. and Demarchez, M. (1988) Localization and *in vivo* activity of epidermal transglutaminase. J. Invest. Dermatol. 90, 472-4

Michel, S. and Juhlin, L. (1990) Cornified envelopes in congenital disorders of keratinisation. Br. J. Dermatol. 122, 15-21

Michel, S., Schmidt, R., Robinson, S. M., Shroot, B. and Reichert, U. (1987) Identification and subcellular distribution of cornified envelope precursor proteins in the transformed human keratinocyte line SV-K14. J. Invest. Dermatol. 88, 301-5

Milakovic, T., Tucholski, J., McCoy, E. and Johnson, G. V. W. (2004) Intracellular localization and activity state of tissue transglutaminase differentially impacts cell death. J. Biol. Chem 279, 8715-22

Mimotopes, A Mitokor Company (2001) Antipeptide Antibodies 1-15

Mirza, A., Liu, S-L., Frizell, E., Zhu, J., Maddukuri, S., Martinez, J., Davies, P., Schwarting, R., Norton, P. and Zern, M. A. (1997) A role for tissue transglutaminase in hepatic injury and fibrogenesis, and its regulation by NF-κB. Am. J. Physiol. 272, G281-8

Mishcke, D., Korge, B. P., Marenholz, I., Volz, A. and Ziegler, A. (1996) Genes encoding structural proteins of epidermal cornification and S100 calcium-binding proteins from a gene complex ("epidermal differentiation complex") on human chromosome 1q21. J. Invest. Dermatol. 106, 989-92

Morioka, S., Lazarus, G. S., Baird, J. C. and Jensen, P. J. (1987) Migrating keratinocytes express urokinase-type plasminogen activator. J. Invest. Dermatol. 83, 445-7

Mosher, D. F., Fogerty, F. J., Chernousov, M. A. and Barry, E. L. (1991) Assembly of fibronectin into extracellular matrix. Ann. N Y Acad. Sci. 614, 167-180

Muesch, A., Hartmann, E., Rohde, K., Rubartelli, A., Sitia, R. and Rapoport, T. A. (1990) A novel pathway for secretory proteins ? Trends Biochem. Sci. 15, 86-8

Mukherjee, A. B., Cordella-Miele, E., Kikukawa, T. and Miele, L. (1988) Modulation of cellular response to antigen by uteroglobin and transglutaminase. Adv. Exp. Med. Biol. 231, 135-52

Murthy, S. N. P., Iismaa, S., Begg, G., Freyman, D. M., Graham, R. M and Lorand, L. (2002) Conserved tryptophan in the core domain of transglutaminase is essential for catalytic activity. Proc. Natl. Acad. Sci. U.S.A 99 (5), 2738-42

Murthy, S. N., Wilson, J. H., Lukas, T. J., kuret, J. and Lorand, L. (1998) Cross-linking sites of the human tau protein, probed by reactions with human transglutaminase. J. Neurochem. 71, 2607-14

Murthy, S. N., Wilson, J. H., Zhang, Y. and Lorand, L. (1994) Residue Gln-30 of human erythrocyte anion transporter is a prime site for reaction with intrinsic transglutaminase. J. Biol. Chem. 269, 22907-11

Nadeau, O. W., Traxler, K. W. and Carlson, G. M. (1998) Zero-length crosslinking of the beta subunit of phosphorylase kinase to the N-terminal half of its regulatory alpha subunit. Biochem. Biophys. Res. Commun. 251, 637-41

Nagae, S., Lichti, O., De Luca, L. and Yuspa, S. H. (1987) Effect of retinoic acid on cornified envelope formation; difference between spontaneous envelope formation *in vivo* or *in vitro* and expression of envelope competence. J. Invest. Dermatol. 89, 51-8

Nakagawa, S., Pawalek, P. and Grinell, F. (1989) Extracellular matrix organization modulates fibroblast growth and growth factor responsiveness. Exp. Cell Res. 182, 572-82

Nakaoka, H., Perez, D. M., Baek, K. J., Das, T., Hussain, A., Misono, K., Im, M. J. and Graham, R. M. (1994) G_h: A GTP-binding protein with transglutaminase activity and receptor signalling function. Science 264, 1593-6

Nanda, N., Iismaa, S. E., Owens, W. A., Hussain, A., Mackay, F. and Graham, R. M. (2001) Targeted inactivation of G_h/tissue transglutaminase II. J. Biol. Chem. 276, 20673-8

Nara, K., Ito, S., Ito, T., Suzuki, Y., Ghoneim, M. A., Tachibana, S. and Hirose, S. (1994) Elastase inhibitor elafin is a new type of proteinase inhibitor which has a transglutaminase-mediated anchoring sequence termed 'cementoin'. J. Biochem. 115, 441-8

Nemes, Z., Adany, R., Balazs, M., Boross, P. and Fesus, L. (1997) Identification of cytoplasmic actin as an abundant glutaminyl substrate for tissue transglutaminase in HL-60 and U937 cells undergoing apoptosis. J. Biol. Chem. 272, 20577-83

Nemes, Z., Marekov, L., Fesus, L. and Steinert, P. (1999a) A novel function for transglutaminase 1: Attachment of long-chain ω-hydroxyceramides to involucrin by ester bond formation. Proc. Natl. Acad. Sci. U.S.A 96 (15) 8402-7

Nemes, Z., Marekov, L. N. and Steinert, P. M. (1999b) Involucrin cross-linking by transglutaminase 1: binding to anionic membranes directs residue specificity. J. Biol. Chem. 274, 11013-21

Nemes, Z. and Steinert, P. M. (1999) Bricks and mortar of the epidermal barrier. Exp. Mol. Med. 31, 5-19

Nicholas, B., Svethurst, P., Verdeno, B., Jones, R. and Griffin M (2003) Crosslinking of cellular proteins by tissue transglutaminase during necrotic cell death: A mechanism for maintaining tissue integrity. Biochem. J. 371, 413-22

Nicklolff, B. J., Mitra, R. S., Riser, B. L., Dixit, V. M. and Varani, J. (1988) Modulation of keratinocyte motility. Correlation with production of extracellular matrix molecules in response to growth promoting and antiproliferative factors. American Journal of Pathology 132, 543-51

Nunes, I., Gleizes, P. E., Metz, C. N. and Rifkin, D. B. (1997) Latent transforming growth factor β binding protein domains involved in activation and transglutaminase-dependent cross-linking of latent transforming growth factor-beta. J. Cell. Biol. 136, 1151-63

O'Keefe, E. J., Payne, R. E., Russel, N. and Woodley, D. T. (1985) Spreading and enhanced motility of human keratinocytes on fibronectin. J. Invest. Dermatol. 85, 125-30

Obedencio, G. P., Nuccitelli, R. and Isseroff, R. R. (1999) Involucrin-positive keratinocytes demonstrate decreased migration speed but sustained directional migration in a DC electric field. J. Invest. Dermatol. 113, 851-5

Odland, G. and Ross, R. (1968) Human wound repair. I. Epidermal regeneration. J. Cell Biol. 39, 135-51

Ogawa, H. and Goldsmith, L. A. (1976) Human epidermal transglutaminase: preparation and properties. J. Biol. Chem. 251, 7281-8

Oliverio, S., Amendola, A., Disan, F., Farrace, M. G., Fesus, L., Nemes, Z., Piredda, L., Spinedi, A. and Piacentini, M. (1997) Tissue transglutaminase dependent posttranslational modification of the retinoblastoma gene product in promonocytic cells undergoing apoptosis. Mol. Cell. Biol. 17, 6040-8

Oliverio, S., Amendola, A., Rodolfo, C., Spinedi, A. and Piacentini, M. (1999) Inhibition of "tissue" transglutaminase increases cell survival by preventing apoptosis. J. Biol. Chem. 274, 34123-8

Orru, S., Caputo, I., D'Amato, A., Ruoppolo, M. and Esposito, C. (2003) Proteomics identification of acyl-acceptor and acyl-donor substrates for transglutaminase in human intestinal epithelial cell line. J. Biol. Chem. 278, 31766-73

Paramesworan, K. N., Cheng, X-F, Chen, E. C., Velasco, P. T., Wilson, J. H. and Lorand, L. (1997) Hydrolysis of γ.ε isopeptides by cytosolic transglutaminases and by coagulation factor $XIII_a$. J. Biol. Chem. 272 10311-7

Parmentier, L., Blanchet-Bardon, C., Nguyen, S., Prud'homme, J. F., Dubertret, L. and Weissenbach, J. (1995) Autosomal recessive lamellar ichthyosis: identification of a new mutation in transglutaminase 1 and evidence for heterogeneity. Hum. Mol. Genet. 4, 1391-5

Parmentier, L., Lakholar, H., Blanchet-Bardon, C., Marchand, S. Dubertret, L. and Weissenbach, J. (1996) Mapping of a second locus for lamellar ichthyosis to chromosome 2q33-35. Hum. Mol. Genet. 5, 555-9

Pearton, D. J., Dale, B. A. and Presland, R. B. (2002) Functional analysis of the profilaggrin N-terminal peptide: Identification of domains that regulate nuclear and cytoplasmic distribution. J. Invest. Dermatol. 119, 661-9

Pedersen, L. C., Yee, V. C., Bishop, P. D., Le Trong, I., Teller, D. C. and Stenkamp, R. E. (1994) Transglutaminase factor XIII uses proteinase-like catalytic triad to cross-link macromolecules. Protein Sci. 3, 1131-5

Peng, X., Zhang, Y., Zhang, H., Graner, S., Williams, J. F., Levitt, M. L. and Lokshin, A. (1999) Interaction of tissue transglutaminase with nuclear transport protein importin-α3. FEBS Lett 446, 35-9

Phillips, M. A., Jessen, B. A., Lu, Y., Qin, Q., Stevens, M. E. and Rice, R. H. (2004) A distal region of the human TGM1 promoter is required for expression in transgenic mice and cultured keratinocytes. BMC Dermatology 4,

Phillips, M. A., Qin, Q., Mehrpouyan, M. and Rice, R. H. (1993) Keratinocyte transglutaminase membrane anchorage: Analysis of site-directed mutants. Biochemistry 32, 11057-63

Piacentini, M., Martinet, N., Beninati, S. and Folk, J. E. (1988b) Free and protein-conjugated polyamines in mouse epidermal cells. Effect of high calcium and retinoic acid. J. Biol. Chem. 263, 3790-4

Piredda, L., Amendola, A., Colizzi, V., Davies, P. J. A., Farrace, M. G., Maurizio, F., Gentile, V., Uray, I., Piacentini, M. and Fesus, L. (1997) Lack of "tissue" transglutaminase protein cross-linking leads to leakage of macromolecules from dying cells: relationship to development of autoimmunity in MRL1pr/1pr mice. Cell Death Differ. 4, 463-72

Pisano, J. J., Finlayson, J. S., and Peyton, M. P. (1986) Cross-link in fibrin polymerised by factor XIII ε(γ-glutamyl)lysine. Science 160, 892-3

Poon, M-C, Russel, J. A., Low, S., Sinclair, G. D., Jones, A. R., Blahey, W., Ruether, B. A., Hoer, D. I. (1989) Hemopoietic origin of factor XIII a-subunits in platelets, monocytes and plasma. Evidence from bone marrow transplantation studies. J. Clin. Invest. 84, 787-92

Porta, R., Esposito, C., Metafora, S., Pucci, P., Malorni, A. and Marino, G. (1988) Substance P as a transglutaminase substrate: identification of the reaction products by fast atom bombardment mass spectrometry. Anal. Biochem. 172, 499-503

Presland, R. B., Haydock, P. V., Fleckman, P., Nirunsuksiri, W. and Dale, B. A. (1992) Characterization of the human epidermal profilaggrin gene. Genomic organization and identification of an S-100-like calcium binding domain at the amino terminus. J. Biol. Chem. 267, 23772-81

Presland, R. B., Kimball, J. R., Kautsky, M. B., Lewis, S. P. Lo, C. Y. and Dale, B. A. (1997) Evidence for specific proteolytic cleavage of the N-terminal domain of human profilaggrin during epidermal differentiation. J. Invest. Dermatol. 108, 170-8

Prunieras, M., Regnier, M., Woodley, D. (1983) Methods for cultivation of keratinocytes with an air-liquid interface. J. Invest. Dermatol. 81, S28-33

Pucci, P., Malorni, A., Marino, G., Metafora, S., Esposito, C. and Porta, R. (1988) β-Endorphin modification by transglutaminase *in vitro*: identification by FAB/MS of glutamine-11 and lysine-29 as acyl donor and acceptor sites. Biochem. Biophys. Res. Commun. 154, 735-40

Putnins, E. E., Firth, J. D., Lohachitranont, A., Uitto, V. J. and Larjava, H. (1999) Keratinocyte growth factor (KGF) promotes keratinocyte cell attachment and migration on collagen and fibronectin. Cell Adhes. Commun. 7, 211-21

Quash, G. A., Paret, M. J., Wilson, M. B., Poncet, A., Joly, M. O. and Andre, J. (2000) Tissue transglutaminase (tTG) inserts polyamines into seminal fluid (sf) prostate specific antigen (PSA) enzymically active sfPSA has bound polyamines. Conference on Transglutaminase and Protein Crosslinking Reactions, September 16-19, Lyon, France.

Raghunath, M., Hopfner, B., Aeschlimann, D., Luthi, U., Meuli, M., Altermatt, S., Gobet, R., Bruckner-Tuderman, L. and Steinmann, B. (1996) Crosslinking of the dermo-epidermal junction of skin regenerating from keratinocyte autografts. J. Clin. Invest. 98, 1174-84

Rahman, S. A. and Tsuyama, S. (1993) Immunohistochemical study of cell proliferation and differentiation in epidermis of mice after administration of cholera toxin. Arch. Dermatol. Res. 285, 27-31

Rasmussen, L. K., Ellgaard, L., Jensen, P. H. and Sorensen, E. S. (1999) Localization of a single transglutaminase-reactive glutamine in the third domain of RAP, the alpha2-macroglobulin receptor-associated protein. J. Protein Chem. 18, 69-73

Rasmussen, L. K., Esben, S. S., Torben, E. P., Gliemann, J. and Jensen, P. H. (1994) Identification of glutamine and lysine residues in Alzheimer amyloid β-A4 peptide responsible for transglutaminase-catalyzed homopolymerization and cross-linking to αM receptor. FEBS Lett. 338, 161-6

Regauer, S. and Compton, C. C. (1990) Cultured keratinocyte sheets enhance spontaneous re-epithelialization in a dermal explant model of partial-thickness wound healing. J. Invest. Dermatol. 95, 341-6

Reichert, U., Michel, S. and Schmidt, R. (1993) The cornified cell envelope: A key structure of terminally differentiating keratinocytes. In: Darmon, M. and Blumberg, M., (Ed.), Molecular Biology of the Skin. (San Diego, CA: Academic Press, Inc.) pp 107-50

Reif, S. and Lerner, A. (2004) Tissue transglutaminase – the key player in celiac disease: A review. Autoimmun. Rev. 3, 40-5

Rety, S., Osterich, D., Arie, J. P., Tabaries, S., Seeman, J., Russo-Marie, F., Gerke, V. and Lewit-Bentley, A. (2000) Structural basis of the Ca^{2+}-dependent association between S100C (S100A11) and its target, the N-terminal part of annexin 1. Structure Fold. Des. 8, 175-84

Rice, R. H. and Green, H. (1977) The cornified envelope of terminally differentiated human epidermal keratinocytes consists of cross-linked protein. Cell 11, 417-22

Rice, R. H. and Green, H. (1979) Presence in human epidermal cells of a soluble protein precursor of the cross-linked envelope: Activation of the cross-linking by calcium ions. Cell 18, 681-94

Rice, R., Mehrpouyan, M., Qin, Q., Phillips, M. and Lee, Y. (1996) Identification of phosphorylation sites in keratinocyte transglutaminase. Biochem. J. 320, 547-50

Rice, R. H., Rong, X. and Chakravarty, R. (1990) Proteolytic release of keratinocyte transglutaminase. Biochem J. 265, 351-7

Ridley, A. J., Cornoglio, P. M. and Hall, A. (1995) Regulation of scatter factor/hepatocyte growth factor responses by Ras, Rac and Rho in MDCK cells. Mol. Cell Biol. 15, 1110-22

Ridley, A. J., Paterson, H. F., Johnston, C. L., Diekman, D. and Hall, A. (1992) The small GTP-binding protein rac regulates growth factor-induced membrane ruffling. Cell 70, 401-10

Ritchie, H., Lawrie, L. C., Crombie, P. W., Mosesson, M. W. and Booth, N. A. (2000) Cross-linking of plasminogen activator inhibitor 2 and α_2-antiplasminin to fibrin(ogen). J. Biol. Chem. 275, 24915-20

Ritter, S. J. and Davies, P. J. (1998) Identification of a transforming growth factor-beta/bone morphogenic protein 4 (TGF-beta/BMP4) response element within the mouse tissue transglutaminase gene promoter. J. Biol. Chem. 263, 4586-92

Robinson, N. A. and Eckert, R. L. (1998) Identification of transglutaminase-reactive residues in S100A11. J. Biol. Chem. 273, 2721-8

Robinson, N. A., Lapic, S., Welter, J. F. and Eckert, R. L. (1997) S100A11, S100A10, annexin 1, desmosomal proteins, small proline-rich proteins, plasminogen activator inhibitor-2, and involucrin are components of the cornified envelope of cultured human epidermal keratinocytes. J. Biol. Chem. 272, 12035-46

Roop, O. (1995) Defects in the barrier. Science 267, 474-75

Rufini, A., Vilbois, F., Paradisi, A., Oddi, S., Tartaglione, R., Leta, A., Bagetta, G., Guerrier, G., Finazzi-Agro, A., Melino, G. and Candi, E. (2004) Transglutaminase 5 is acetylated at the N-terminal end. Amino Acids 26, 425-30

Ruoppolo, M., Orru, S., Francese, S., Caputo, I. and Esposito, C. (2003) Structural characterization of transglutaminase-catalyzed cross-linking between glyceraldehydes 3-phosphate dehydrogenase and polyglutamine repeats. Protein Sci. 12, 170-9

Ruse, M., Lambert, A., Robinson, N., Ryan, D., Shon, K-J. and Eckert, R. L. (2001) S100A7, S100A10, and S100A11 are transglutaminase substrates. Biochemistry 40, 3167-73

Russell, L. J., Di Giovanna, J. J., Rogers, G. R., Steinert, P. M., Hashem, N., Compton, J. G., Bale, S. J. (1995) Mutations in the gene for transglutaminase 1 in autosomal recessive lamellar ichthyosis. Nat. Genet. 9, 279-83

Saber-Lichtenberg, Y., Brix, K., Schmitz, A., Heuser, J. E., Wilson, J. H., Lorand, L. and Herzog, V. (2000) Covalent cross-linking of secreted bovine thyroglobulin by transglutaminase. FASEB J. 14, 1005-14

Safer, D., Sosnick, T. R. and Elzinga, M. (1997) Thymosin β4 binds actin in an extended conformation and contacts both the barbed and pointed ends. Biochemistry 36, 5806-16

Saffer, J. D., Jackson, S. P., Annarella, M. B. (1991) Developmental expression of Sp1 in the mouse. Mol. Cell Biol. 11, 2189-99

Sakai, K., Busby, W. H., Clarke, J. B. and Clemmons, D. R. (2001) Tissue transglutaminase facilitates the polymerisation of insulin-like growth factor-binding protein 1 (IGFBP-1) and leads to loss of IGFBP-1's ability to inhibit insulin-like growth factor-I-stimulated protein synthesis. J. Biol. Chem. 276, 8740-5

Sane, D. C., Moser, T. L., Pippen, A. M. M., Parker, C. J., Achyuthan, K. E. and Greenberg, C. S. (1988) Vitronectin is a substrate for transglutaminases. Biochem. Biophys. Res. Commun. 157, 115-20

Santibanez, J. F., Quintanilla, M. and Martinez, J. (2000) Genistein and curcumin block TGF-beta 1-induced u-PA expression and migratory and invasive phenotype in mouse epidermal keratinocytes. Nutr. Cancer 37, 49-54

Sardy, M., Karpati, S., Merkl, B., Paulsson, M. and Smyth, N. (2002) Epidermal transglutaminase (TGase 3) is the autoantigen of dermatitis herpetiformis. J. Exp. Med. 195, 747-57

Sarret, Y., Woodley, D. T., Grigsby, K., Wynn, K. and O'Keefe, E. J. (1992) Human keratinocyte locomotion: The effect of selected cytokines. J. Invest. Dermatol. 98, 12-16

Sato, C., Tsuboi, R., Shi, C. M., Rubin, J. S. and Ogawa, H. (1995) Comparative study of hepatocyte growth factor/scatter factor and keratinocyte growth factor effects on human keratinocytes. J. Invest. Dermatol. 104, 958-63

Schmidt, G., Selzrer, J., Lerm, M. and Aktories, K. (1998) The Rho-deamidating cytotoxic necrotizing factor 1 from *Escherichia coli* possesses transglutaminase activity. Cysteine 866 and histidine 881 are essential for enzymic activity. J. Biol. Chem. 273, 13669-74

Schultz, G. S., White, M., Mitchell, R., Brown, G., Lynch, J., Twerdzik, D. R. and Todaro, G. J. (1987) Epithelial wound healing enhanced by transforming growth factor alpha and vaccinia growth factor. Science 235, 350-2

Schurer, N. T. and Elias, P. M. (1991) The biochemistry and function stratum corneum lipids. In skin lipids. Advances in skin lipid research (P. M. Elias, ed) pp 27-56, Academic Press, San Diego

Seitz, J. Keppler, C., Huntemann, S., Rausch, U. and Aumuller, G. (1991) Purification and molecular characterisation of a secretory transglutaminase from coagulating gland of the rat. Biochim. Biophys. Acta 1078, 139-46

Seitz, J. Keppler, C., Rausch, U. and Aumuller, G. (1990) Immunohistochemistry of secretory transglutaminase from rodent prostate. Histochemistry 93, 525-30

Selkoe, D. J., Abraham, C. and Ihara, Y. (1982) Brain transglutaminase: *in vitro* crosslinking of human neurofilament proteins into insoluble polymers. Proc. Natl. Acad. Sci. U.S.A 79, 6070-4

Shainoff, J. R., Urbanic, D. A. and Di Bello, P. M. (1991) Immunoelectrophoretic characterizations of the cross-linking of fibrinogen and fibrin by factor XIIIa and tissue transglutaminase. J. Biol. Chem. 266, 6429-37

Shenping, L., Cerione, R. A and Clardy, J. (2001) Structural basis for the guanine nucleotide-binding activity of tissue transglutaminase and its regulation of transamidation activity. Proc. Natl. Acad. Sci. U.S.A 99, 2743-7

Simon, M. and Green, H. (1984) Participation of membrane-associated proteins in the formation of the cross-linked envelope of the keratinocyte. Cell 36, 827-34

Simon, M. and Green, H. (1985) Enzymatic cross-linking of involucrin and other proteins by keratinocyte particulates *in vitro*. Cell 40, 677-83

Simon, M. and Green, H. (1988) The glutamine residues reactive in transglutaminase-catalyzed cross-linking of involucrin. J. Biol. Chem. 263, 18093-98

Singh, U. S., Erickson, J. W. and Cerione, R. A. (1995) Identification and biochemical characterization of an 80 kilodalton GTP-binding/transglutaminase from rabbit liver nuclei. Biochemistry 34 15863-71

Singh, U. S., Kunor, M. T., Kao, Y-L. and Baker, K. M. (2001) Role of transglutaminase II in retinoic acid-induced activation of RhoA-associated Kinase-2. EMBO J. 20, 2413-2423

Smethurst, P. and Griffin, M. (1996) Measuremnet of tissue transglutaminase activity in a permeabilised cell system: its regulation by Ca^{2+} and nucleotides. Biochem. J. 313, 803-8

Smith, A. D., Streilein, R. D. and Hall, R. P. (2002) Neutrophil CD 11b, L-Selectin and Fc IgA receptors in patients with dermatitis herpetiformis. Br. J. Dermatol. 147, 1109-17

Smola, H., Thiekotter, G. and Fusenig, N. E. (1993) Mutual induction of growth factor gene expression by epidermal-dermal cell interaction. J. Cell Biol. 122, 417-29

Sollid, L. M. (2000) Molecular basis of celiac disease. Ann. Rev. Immunol. 18 53-81

Sorensen, E. S., Rasmussen, L. K., Moller, L., Jensen, P. H., Hojrup, P. and Petersen, T. E. (1994) Localization of transglutaminase-reactive glutamine residues in bovine osteopontin. Biochem. J. 304, 13-16

Steinert, P. M. (1995) A model for the hierachical structure of the cornified cell envelope. Cell Death Different. 2, 33-40

Steinert, P. M. (2000) The complexity and redundancy of epithelial barrier function. J. Cell Biol. 151, F5-7

Steinert, P. M., Candi, E., Kartasova, T., Marekov, L. (1998) Small proline-rich proteins are cross-bridging proteins in the cornified cell envelopes of stratified squamous epithelial. J. Struct. Biol. 122, 76-85

Steinert, P. M., Candi, E., Taresa, E., Marekov, L. N., Sette, M., Paci, M., Ciani, B., Guerrieri, P. and Melino, G. (1999) Transglutaminase crosslinking and structural studies of the human small proline rich 3 protein. Cell Death Differ 6, 916-30

Steinert, P. M., Chung, S. I., Kim, S. Y. (1996a) Inactive zymogen and highly active proteolytically processed membrane-bound forms of the transglutaminase 1 enzyme in human epidermal keratinocytes. Biochem. Biophys. Res. Commun. 221, 101-6

Steinert, P. M., Kim, S. Y., Chung, S. I. and Marekov, L. N. (1996b) The transglutaminase 1 enzyme is variably acylated by myristate and palmitate during differentiation in epidermal keratinocytes. J. Biol. Chem. 271 26242-26250

Steinert, P. M. and Marekov, L. N. (1995) The proteins elafin, filaggrin, keratinocyte intermediate filaments, loricrin, and small proline-rich proteins 1 and 2 are isopeptide crosslinked components of the human epidermal cornified cell envelope. J. Biol. Chem. 270, 17702-11

Steinert, P. M. and Marekov, L. N. (1997) Direct evidence that involucrin is a major early isopeptide crosslinked component of the keratinocyte cornified cell envelope. J. Biol. Chem. 272, 2021-30

Steinhardt, R. A., Bi, G. and Alderton, J. M. (1994) Cell membrane resealing by a vesicular mechanism similar to neurotransmitter release. Science 263 390-3

Stephens, P., Grenard, P., Aeschlimann, P., Langley, M., Blain, E., Errington, R., Kipling, D., Thomas, D. and Aeschlimann, D. (2004) Cross-linking and G-protein functions of transglutaminase 2 contribute differentially to fibroblast would healing responses. J. Cell. Sci. 117 (15), 3389-403

Steven, A. C., Bisher, M. E., Roop, D. R. and Steinert, P. M. (1990) Biosynthetic pathways of filaggrin and loricrin – two major proteins expressed by terminally differentiated epidermal keratinocytes. J. Struct. Biol. 104, 150-62

Sun, T. T. and Green, H. (1976) Differentiation of the epidermal keratinocyte in cell culture: formation of the cornified envelope. Cell 9, 511-21

Swartzendruber, D. C., Kitko, D. J., Wertz, P. W., Madison, K. C. and Downing, D. T. (1988) Isolation of corneocyte envelopes from porcine epidermis. Arch. Dermatol. Res. 280, 424-9

Swartzendruber, D. C., Wertz, P. W., Kitko, D. J., Madison, K. C. and Downing, D. T. (1989) Molecular models of the intercellular lipid lamellae in mammalian stratum corneum. J. Invest. Dermatol. 92, 251-7

Swartzendruber, D. C., Wertz, P. W., Madison, K. C. and Downing, D. T. (1987) Evidence that the corneocyte has a chemically bound lipid envelope. J. Invest. Dermatol. 88, 709-13

Taenaka, N., Hibino, T., Fukuda, M., Mishima, H. and Shimomura, Y. (2003) Tissue transglutaminase modulates the proliferation and attachment of keratinocytes. (Presented at the Association for Research in Vision and Ophthalmology, 2003 Meeting). Invest. Ophthalmol. Vis. Sci. 44, E-Abstract 881

Takagi, T. and Doolittle, R. F. (1974) Amino acid studies on factor XIII and the peptide released during its activation by thrombin. Biochemistry, 13, 750-6

Takahashi, N., Takahashi, Y. and Putnam, F. W. (1986) Primary structure of blood coagulation factor XIIIa (fibrinoligase, transglutaminase) from human placenta. Proc. Natl. Acad. Sci. U.S.A 83, 8019-23

Takahashi, M., Tezuka, T., Kakegawa, H. and Katunuma, N. (1994) Linkage between phosphorylated cystatin alpha and filaggrinn by epidermal transglutaminase as a model of cornified envelope and inhibition of cathepsin L activity by cornified envelope and the conjugated cystatin alpha. FEBS Lett 340, 173-6

Takashima, A. and Grinnell, F. (1985) Fibronectin-mediated keratinocyte migration and initiation of fibronectin receptor function *in vitro*. J. Invest. Dermatol. 85, 304-8

Tamaki, T. and Aoki, N. (1982) Crosslinking of α_2- plasmin inhibitor to fibrin catalysed by activated fibrin-stabilizing factor. J. Biol. Chem. 257 (14) 14767-14772

Tarcsa, E., Candi, E., Kartasova, T., Idler, W. W., Marekov, L. N. and Steinert, P. M. (1998) Structural and transglutaminase substrate properties of the small proline-rich 2 family of cornified cell envelope proteins. J. Biol. Chem. 273, 23297-303

Tesfaigizi, J. and Carlson, D. M. (1999) Expression, regulation, and function of the SPR family of proteins. A review. Cell Biochem. Biophys. 30, 243-65

Thacher, S. M. (1989) Purification of keratinocyte transglutaminase and its expression during squamous differentiation. J. Invest. Dermatol. 92, 578-84

Tharaud, C., Ribet, A. M., Costes, C. and Gaillardin, C. (1992) Secretion of human blood coagulation factor-XIIIa by the yeast Yarrowia-Lipolytica. Gene 121, 111-9

Thomas, H. (2004) Characterisation of a novel transglutaminase, transglutaminase 6, and determination of its expression pattern. PhD thesis, University of Wales, Cardiff.

Thomazy, V. and Fesus, L. (1989) Differential expression of tissue transglutaminase in human cells: an immunohistochemical study. Cell Tissue Res. 255, 215-24

Toda, K. and Grinnell, F. (1987) Activation of human keratinocyte fibronectin receptor function in relation to other ligand-receptor interactions. J. Invest. Dermatol. 88, 412-7

Tokunaga, F., Muta, T., Iwaanga, S., Ichinose, A., Davie, E. W., Kuma, K. and Miyata, T. (1993) Limulus hemocyte transglutaminase, cDNA cloning, amino acid sequence, and tissue localisation. J. Biol. Chem. 268, 262-8

Trask, B. C., Broekelmann, T., Ritty, T. M., Trask, T. M., Tisdale, C. and Mecham, R. P. (2001) Posttranslational modifications of microfibril associated glycoprotein-1 (MAGP-1). Biochemistry 40, 4372-80

Traupe, H., Kolde, G. and Happle, R. (1984) Autosomal dominant lamellar ichthyosis: A new skin disorder. Clin. Genet. 26, 457-61

Trejo-Skalli, A. V., Velasco, P. T., Murthy, S. N. P., Lorand, L. and Goldman, R. D. (1995) Association of transglutaminase-related antigen with intermediate filaments. Proc. Natl. Acad. Sci. U.S.A 92, 8940-4

Tsai, Y. H., Lai, W. F. T., Wu, Y. W. and Johnson, L. R. (1998) Two distinct classes of rat intestinal mucosal enzymes incorporating putrescine into protein. FEBS Letters 435, 251-6

Tsuboi, R., Sato, C., Kurita, Y., Ron, D., Rubin, J. S. and Ogawa, H. (1993) Keratinocyte growth factor (FGF-7) stimulates migration and plasminogen activator activity of normal human keratinocytes. J. Invest. Dermatol. 101, 49-53

Tsuboi, R., Sato, C., Shi, C. M., Ogawa, H. (1992) Stimulation of keratinocyte migration by growth factors. J. Dermatol. 19, 652-3

Tuan, T. L., Keller, L. C., Sun, D., Nimni, M. E. and Cheung, D. (1994) Dermal fibroblasts activate keratinocyte outgrowth on collagen gels. J. Cell Sci. 107, 2285-9

Tucholski, J. and Johnson, G. V. (2002) Tissue transglutaminase differentially modulates apoptosis in a stimuli-dependent manner. J. Neurochem. 81, 780-91

Upchurch, H. F., Conway, E., Patterson, M. K., Jr. and Maxwell, M. P. (1991) Localization of cellular transglutaminase on the extracellular matrix after wounding: Characteristics of the matrix bound enzyme. J. Cell Physiol. 149, 375-82

Vasylyk, B., Hahn, S. L. and Giovane, A. (1993) The Ets family of transcription factors. Eur. J. Biochem 211, 7-18 ets TFs function in larger complexes

Verderio, E., Johnson, T. and Griffin, M. (2005) Transglutaminases in wound healing and inflammation. Mehta, K., Echert, R. (eds): Transglutaminases. Prog. Exp. Turn. Res. Basel, Karger. 38, 89-114

Verderio, E., Nicholas, B., Gross, S. and Griffin, M. (1998) Regulated expression of tissue transglutaminase in Swiss 3T3 fibroblasts: Effects on the processing of fibronectin, cell attachment and cell death. Exp. Cell Res. 239, 119-38

Verderio, E., Telci, D., Okoye, A., Melino, G. and Griffin, M. (2003) A novel RGD-independent cell adhesion pathway mediated by fibronectin-bound tissue transglutaminase rescues cells from anoikis. J. Biol. Chem. 278, 42604-14

Vollberg, T. M., George, M. D., Nervi, C. and Jetten, A. M. (1992) Regulation of type I and type II transglutaminase in normal human bronchial epithelial and lung carcinoma cells. Am. J. Respir. Cell. Mol. Biol. 7, 10-8

Volz, A., Korge, B. P., Compton, J. G., Ziegler, A., Steinert, P. M. and Mischke, D. (1993) Physical mapping of a functional cluster of epidermal differentiation genes on chromosome 1q21. Genomics 18, 92-9

Walts, A. E., Said, J. W., Siegei, M. B. and Banks-Schlegel, S. (1985) Involucrin, a marker of squamous and urothelial differentiation. An immunohistochemical study on its distribution in normal and neoplastic tissues. J. Pathol. 145, 329-40

Warhol, M. J., Roth, J., Lucocq, J. M., Pinkus, G. S. and Rice, R. H. (1985) Immunoultrastructural localization of involucrin in squamous epithelium and cultured keratinocytes. J. Histochem. Cytochem. 33, 141-9

Watkinson, A., Harding, C. and Rawlings, T. (2001) The cornified envelope: Its role in stratum corneum structure and maturation (Unilever – internal circulation)

Watt, F. M., Kubler, D., Hotchin, N. A., Nicholson, L. J. and Adams, J. C. (1993) Regulation of keratinocyte terminal differentiation by integrin-extracellular matrix interactions. J. Cell Sci. 106, 175-82

Weinberg, J. B., Pippen, A. M. and Greenberg, C. S. (1991) Extravascular fibrin formation and dissolution in synovial tissue of patients with osteoarthritis and rheumatoid arthritis. Arthritis Rheum. 34, 996-1005

Weisberg, L.J., Shui, D. T., Conkling, P. R. and Shuman, M. A. (1987) Identification of normal human peripheral blood monocytes and liver as sites of synthesis of coagulation factor a-chain. Blood 70, 579-582

Weinstein, G. D., McCullough, J. L. and Ross, P. A. (1985) Cell kinetic basis for pathophysiology of psoriasis. J. Invest. Dermatol. 85, 579-83

Weiss, K., Meizner, H. J. and Hilgenfield, R. (1998) Two non-proline *cis* peptide bonds may be important for factor XIII function. FEBS Letters 423, 291-6

Wertz, P. W. and Downing, D. T. (1987) Covalently bound omega-hydroxy-acyl-sphingosine in the stratum corneum. Biochim. Biophys. Acta 917, 108-11

Wertz, P. W., Swartzendruber, D. C. Kitko, D. J., Madison, K. C. and Downing, D. T. (1989) The role of corneocyte lipid envelopes in cohesion of the stratum corneum. J. Invest. Dermatol. 93, 169-72

White, R. A., Peters, L. L., Adjison, L. R., Korsgen, C., Cohen, C. M. and Lux, S. E. (1992) The murine pallid mutation is a platelet storage pool disease associated with the protein 4.2 (pallidin) gene. Nature Genetics 2, 80-3

Williams, M. L. (1992) Ichthyosis: mechanisms of disease. Pedeatr. Dermatol. 9, 365-8

Williams, M. L. and Elias, P. M. (1985) Heterogeneity in autosomal recessive ichthyosis. Clinical and biochemical differentiation of lamellar ichthyosis and nonbullous congenital ichthyosiform erythroderma. Arch. Dermatol. 121, 477-88

Williams-Ashman (1984) Transglutaminases and the clotting of mammalian seminal fluids. Mol Cell Biochem 58, 51-61

Wilson, E. M. and French, F. S. (1980) Biochemical homology between rat dorsal prostate and coagulating gland. J. Biochem 255, 10946-53

Winter, D. G. (1972) Epidermal regeneration studied in the domestic pig. In: Maibach, H. I. and Rovec, D. T., (Ed.), Epidermal wound healing. (Chicago, Yearbook Med Publications) pp 71-112

Woodley, D. T., O'Keefe, E. J. and Prunieras, M. (1985) Cutaneous wound healing: a model for cell-matrix interactions. J. Am. Acad. Dermatol. 12, 420-33

Wu, J., Liu, S-H., Zhu, J-L., Norton, P. A., Nojiri, S., Hoek, J. B. and Zerm, M. A. (2000) Roles of tissue transglutaminase in ethanol-induced inhibition of hepatocyte proliferation and α-1 adrenergic signal transduction. J. Biol. Chem. 275, 22213-19

Ya-Xian, Z., Suekate, T. and Tagami, H. (1999) Number of cell layers of the stratum corneum in normal skin-relationship to the anatomical location on the body, age, sex and physical parameters. Arch. Dermatol. Res. 291, 555-9

Yaffe, Beegan, H. and Eckert, R. L. (1992) Biophysical characterization of involucrin reveals a molecule ideally suited to function as an intermolecular cross-bridge of the keratinocyte cornified envelope. J. Biol. Chem. 267, 12233-8

Yamada, K., Matsuki, M., Morishima, Y., Ueda, E., Tabata, K., Yasuno, H., Suzuki, M. and Yamanishi, K. (1997) Activation of the human transglutaminase 1 promoter in transgenic mice: terminal differentiation-specific expression of the TGM1-lacZ transgene in keratinised stratified squamous epithelia. Hum. Mol. Genet. 6, 2223-31

Yao, Y., Lamkin, M. S. and Oppenheim, F. G. (2000) Pellicle precursor protein crosslinking characterization of an adduct between acidic proline-rich protein (PRP-1) and statherin generated by transglutaminase. J. Dent. Res. 79, 930-8

Yang, F., Sun, X., Beech, W., Teter, B., Wu, S., Sigel, J., Vinters, H. V., Frautschy, S. A. and Cole, G. M. (1998) Antibody to caspase-cleaved actin detects apoptosis in differentiated neuroblastoma and plaque-associated neurons and microglia in Alzheimer's disease. Am. J. Pathol. 152, 379-89

Yee, V. C., Le Trong, I., Bishop, P. D., Pedersen, L. C., Stenkamp, R. E. and Teller, D. C. (1996) Structure and function studies of FXIIIa by X-ray crystallography. Sem. Thromb. Hemostasis 22, 377-384

Yee, V. C., Pedersen, L. C., Le Trong, I., Bishop, P. D., Stenkamp, R. E. and Teller, D. C. (1994) Three-dimensional structure of a transglutaminase: Human blood coagulation factor XIII. Proc. Natl. Acad. Sci. U.S.A 91, 7296-300

Yoneda, K. and Steinert, P. M. (1993) Overexpression of human loricrin in transgenic mice produces a normal phenotype. Proc. Natl. Acad. Sci. U.S.A 90, 10754-8

Zambruno, G., Marchisio, P. C., Marconi, A., Vaschieri, C., Melchiori, A., Giannetti, A. and De Luca, M. (1995) Transforming growth factor-beta 1 modulates beta 1 and beta 5 integrin receptors and induces the *de novo* expression of alpha 5 beta 6 heterodimer in normal human keratinocytes: Implications for wound healing. J. Cell Biol. 129, 853-65

Zettergren, J. G., Peterson, L. L. and Wuepper, K. D. (1984) Keratolinin: The soluble substrate of epidermal transglutaminase from human and bovine tissue. Proc. Natl. Acad. Sci. U. S. A 81, 238-42

Zeeuwen, P. L., Vlijmen-Willems, I. M., Olthuis, D., Johansen, H. T., Hitomi, K., Hara-Nishimura, I., Powers, J. C., James, K. E., Op den Camp, H. J., Lemmens, R. and Schalkwijk, J. (2004) Evidence that unrestricted legumain activity is involved in disturbed epidermal cornification in cystatin M/E deficient mice. Hum. Mol. Genet. 13, 1069-79

Zemaitaitis, M. O., Kim, S-Y., Halverson, R. A., Trancoso, J. C., Lee, J. M. and Muma, N. A. (2002) Transglutaminase activity, protein, and mRNA expression are increased in progressive supranuclear palsy. Journal of Neuropathy and experimental neurology 62, 173-84

Zhang, L. X., Mills, K. J., Dawson, M. I., Collins, S. J. and Jetten, A. M. (1995) Evidence for the involvement of retinoic acid receptor RAR_{α}-dependent signalling pathway in the induction of tissue transglutaminase and apoptosis by retinoids. J. Biol. Chem. 270, 6022-9

Ziyadeh, F. N., Hoffman, B. B., Han, D. C., Iglesias-De La Cruz, M. C., Hong, S. W., Isonon, M., Chen, S., McGowan, T. A. and Sharma, K. (2000) Long-term prevention of renal insufficiency, excess matrix gene expression, and glomerular mesangial matrix expansion by treatment with monoclonal antitransforming growth factor-beta antibody in db/db diabetic mice. Proc. Natl. Acad. Sci. U. S. A. 97, 8015-20

Appendix 1

Sequence data

Sequencing of PCRII/C-fragment construct

Clone 5

M13 primer: 1069-1460 bp

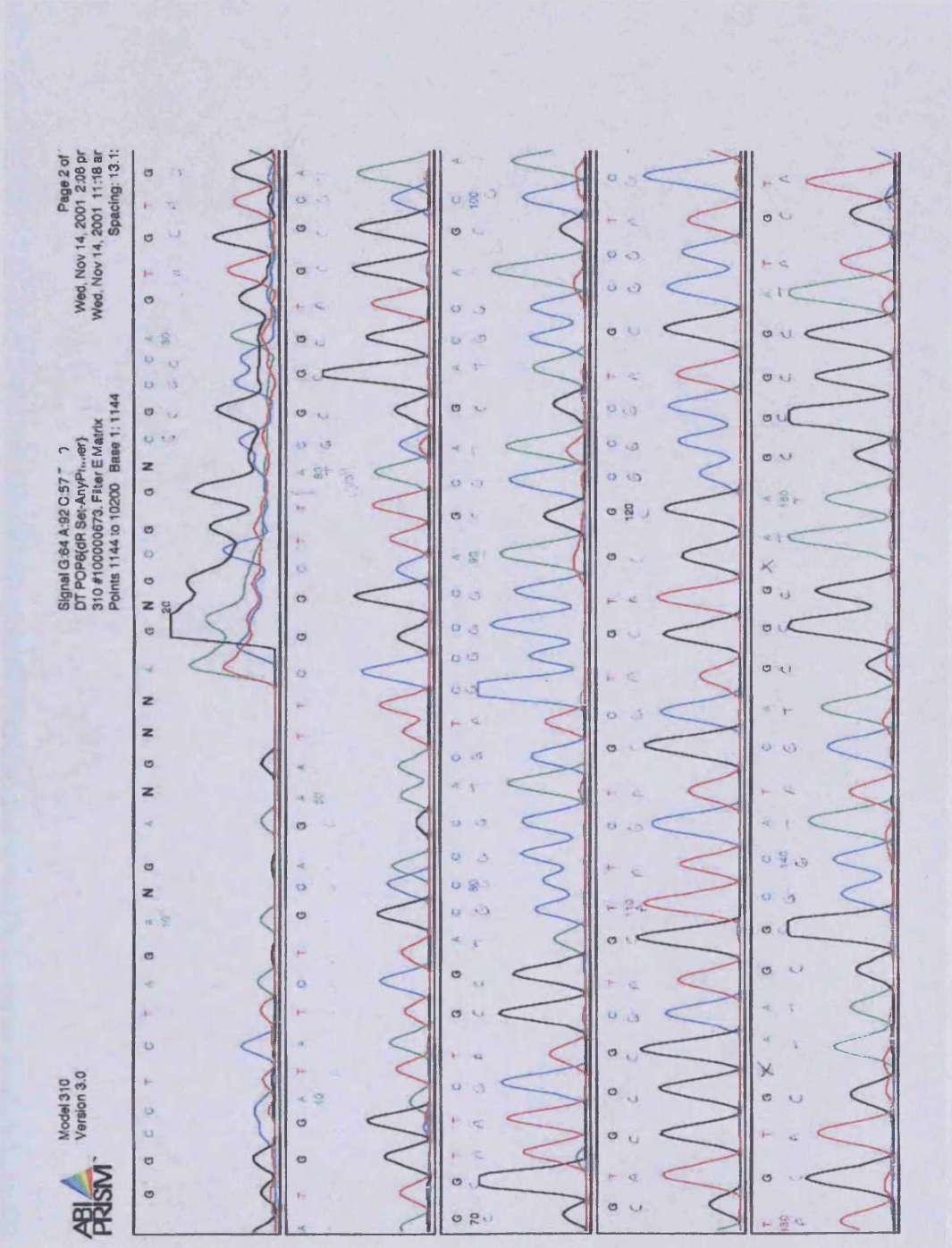

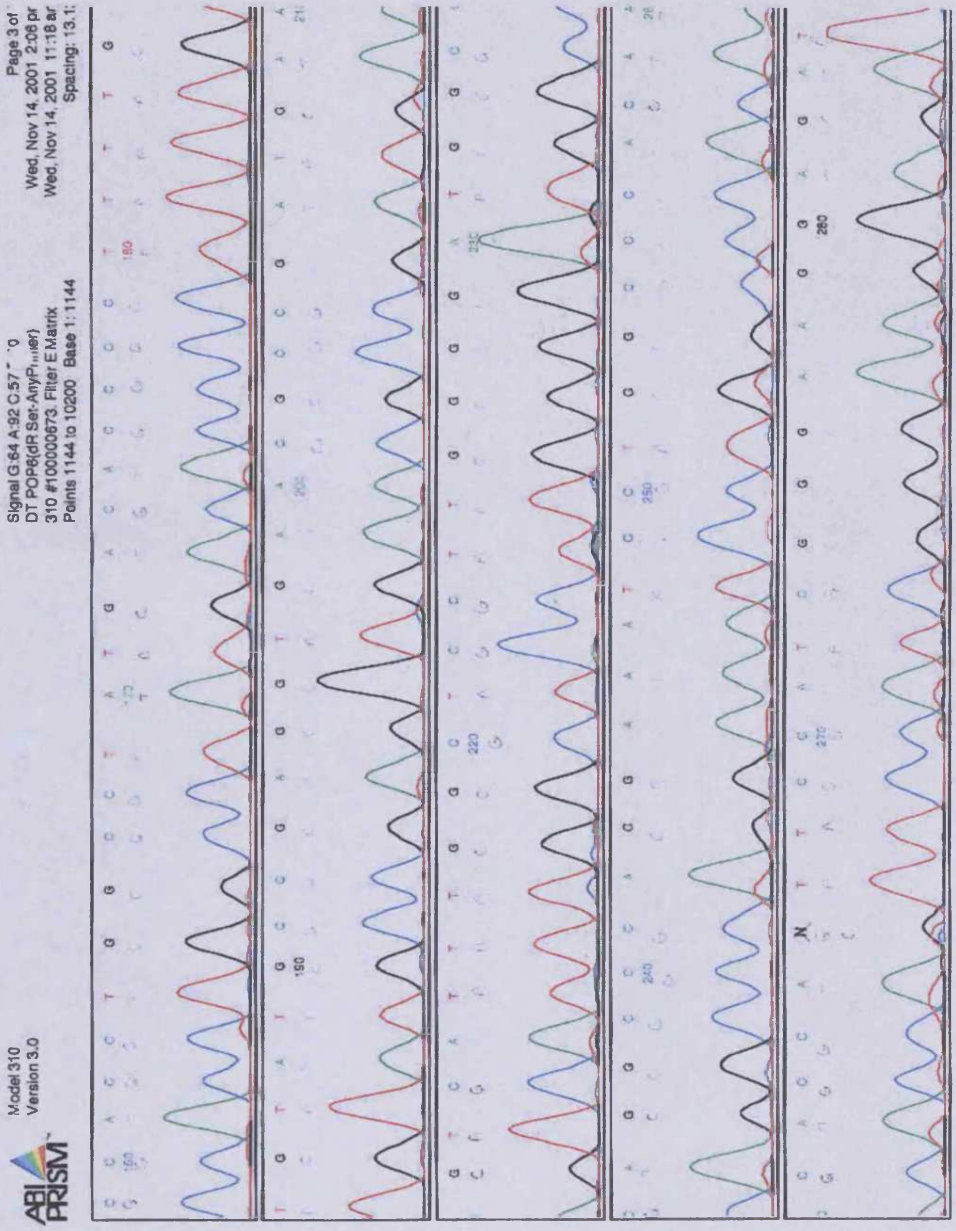
ABI PRISM
Model 310
Version 3.0
Signal G:64 A:92 C:57 T:0
DT POP6(dR Set-AnyPrimer)
310 #1000000673, Filter E Matrix
Points 1144 to 10200 Base 1: 1144
Wed, Nov 14, 2001 2:08 pr
Wed, Nov 14, 2001 11:18 ar
Spacing: 13.1
Page 3 of

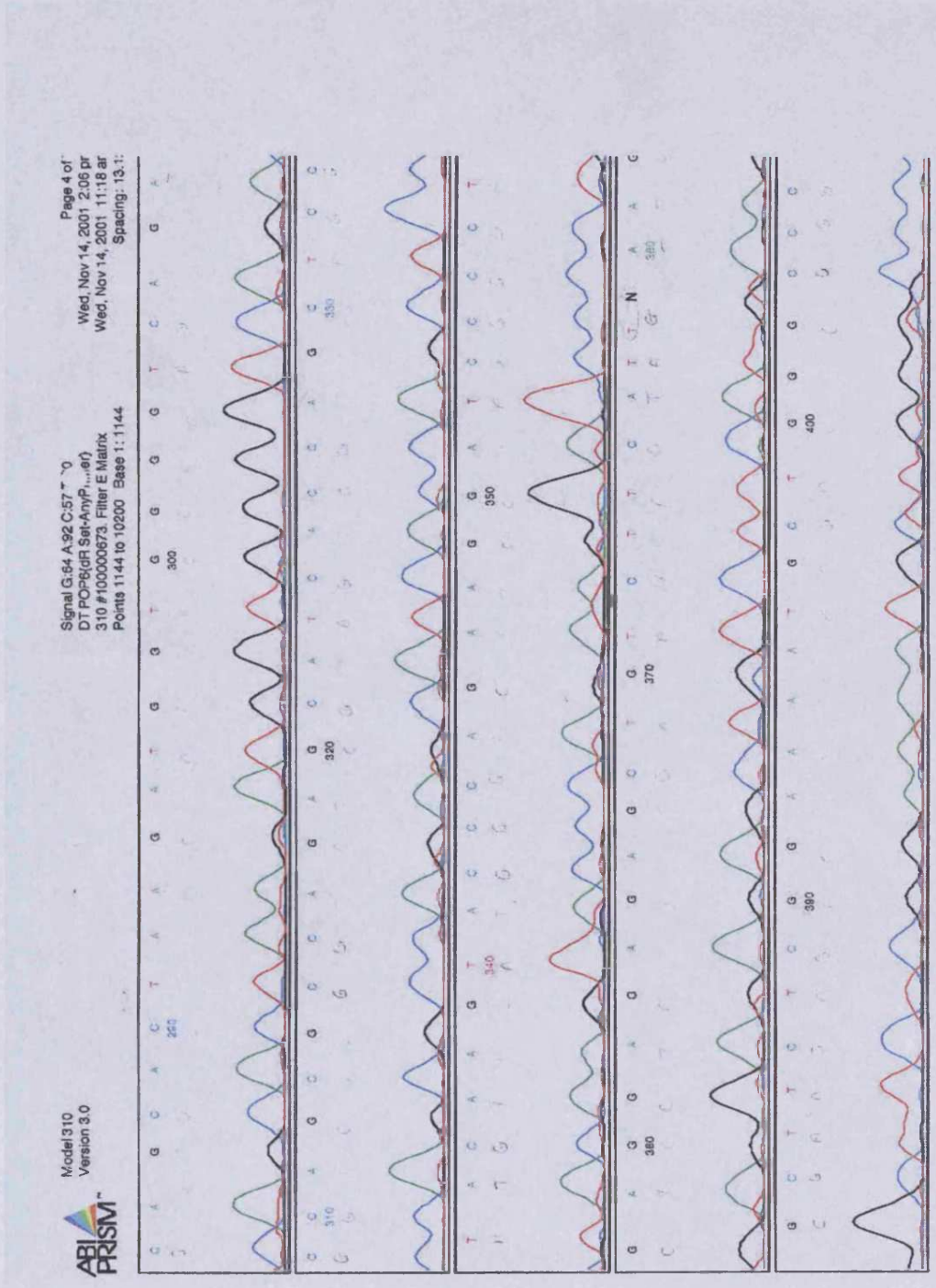
ABI PRISM
Model 310
Version 3.0
Signal G:64 A:92 C:57 T:0
DT POP6(dR Set-AnyP...er)
310 #100000673. Filter E Matrix
Points 1144 to 10200 Base 1: 1144
Wed, Nov 14, 2001 2:06 pr
Wed, Nov 14, 2001 11:18 ar
Spacing: 13.1:
Page 4 of

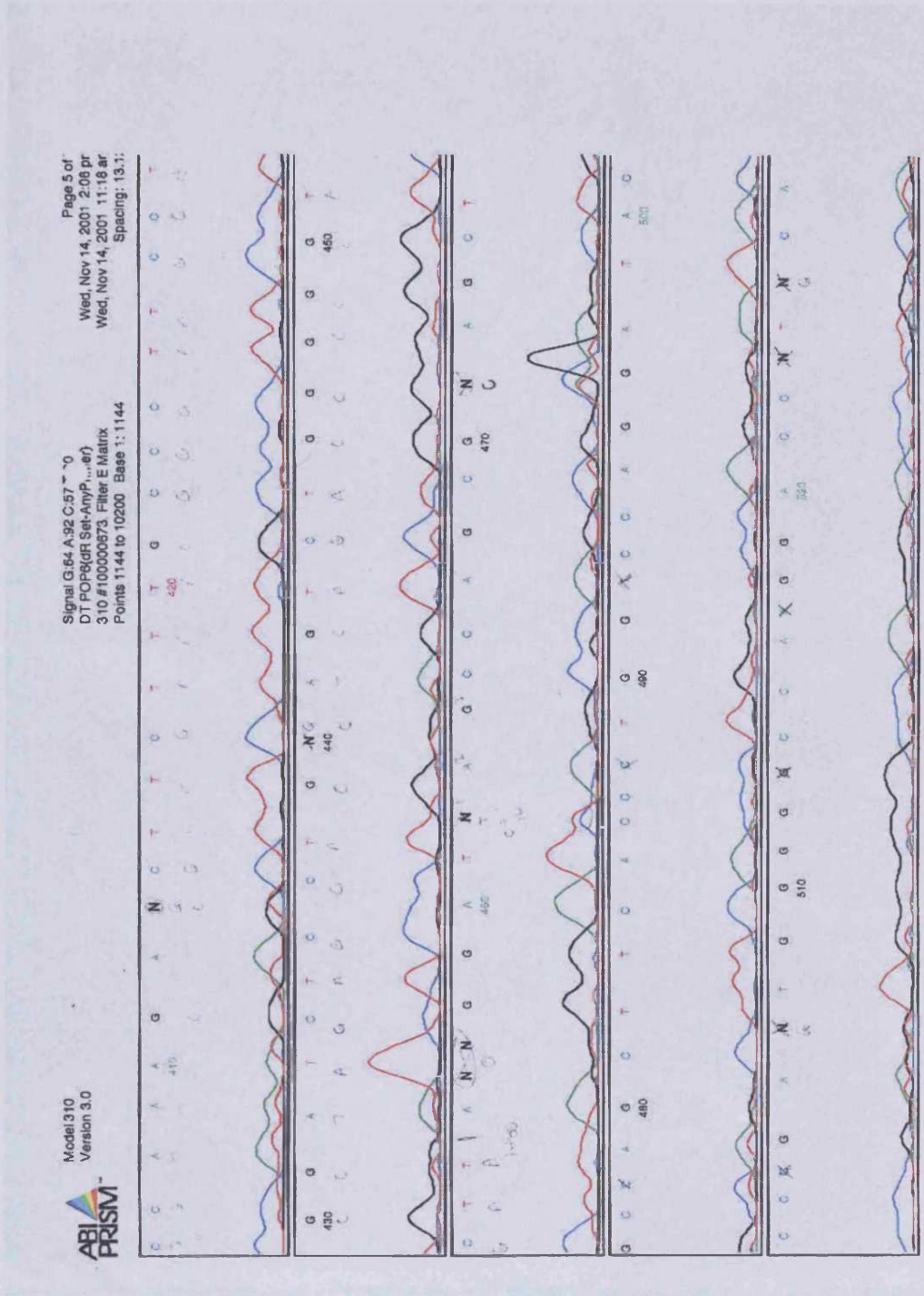
ABI PRISM
Model 310
Version 3.0
Signal G:64 A:92 C:57
DT POP6(dR Set-AnyP,...e)
310 #100000873 Filter E Matrix
Points 1144 to 10200 Base 1:1144
Wed, Nov 14, 2001 2:06 pr
Wed, Nov 14, 2001 11:18 ar
Spacing: 13.1
Page 5 of

TG7 Up 11: 1349-1853 bp

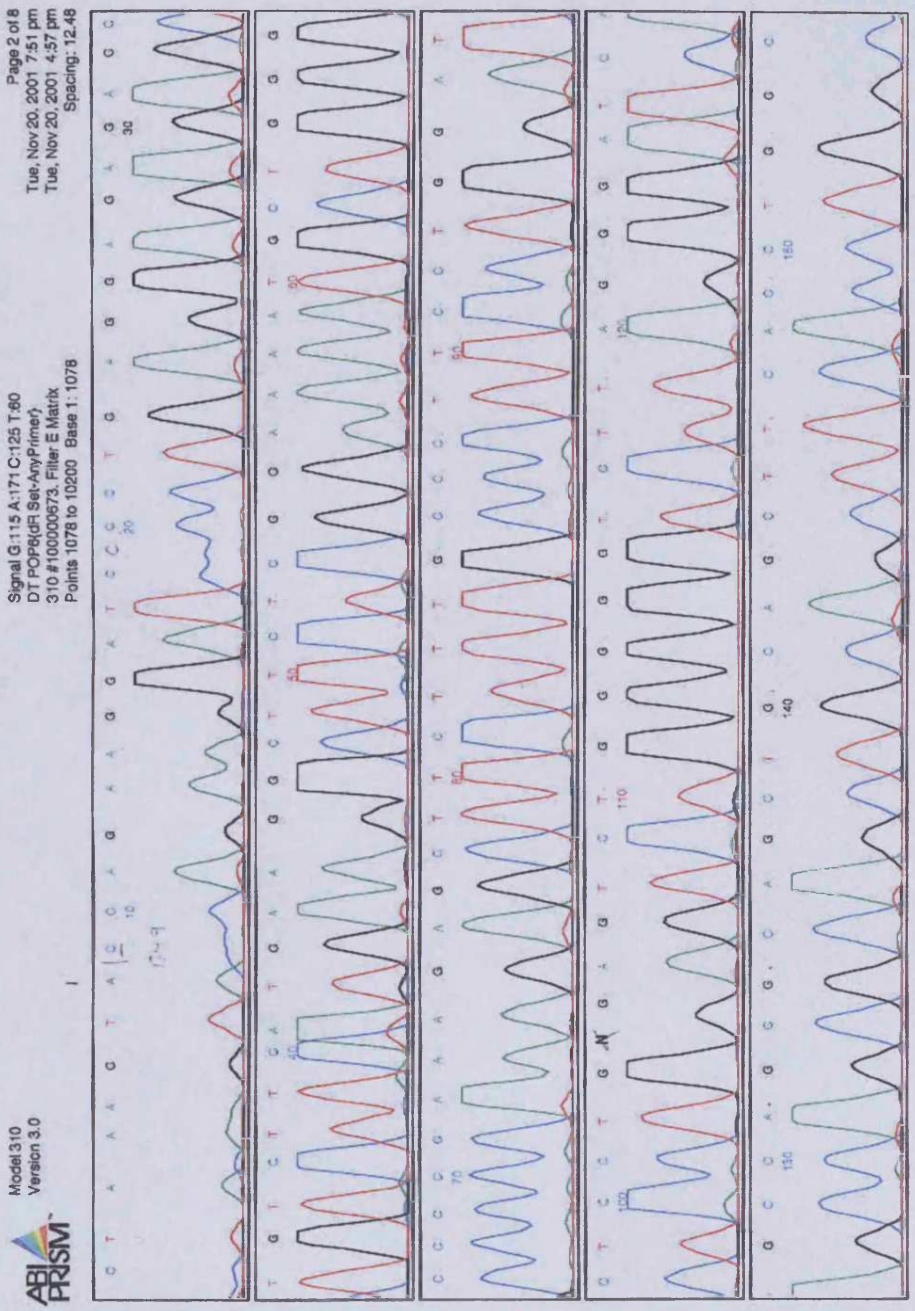

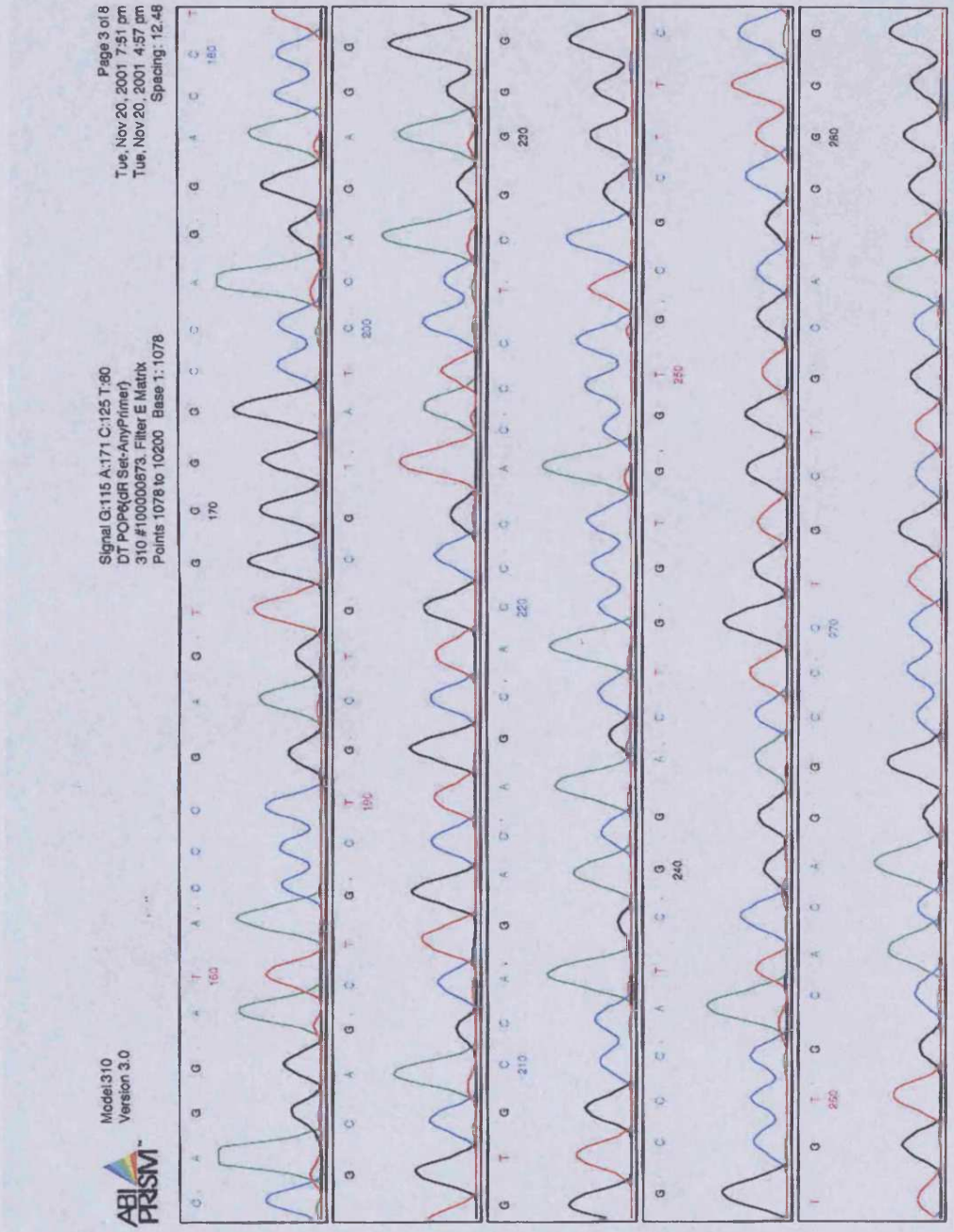
ABI PRISM
Model 310
Version 3.0
Signal G:115 A:171 C:125 T:80
DT POP6(dR Set-AnyPrimer)
310 #100000673. Filter E Matrix
Points 1078 to 10200 Base 1: 1078
Page 3 of 8
Tue, Nov 20, 2001 7:51 pm
Tue, Nov 20, 2001 4:57 pm
Spacing: 12.48

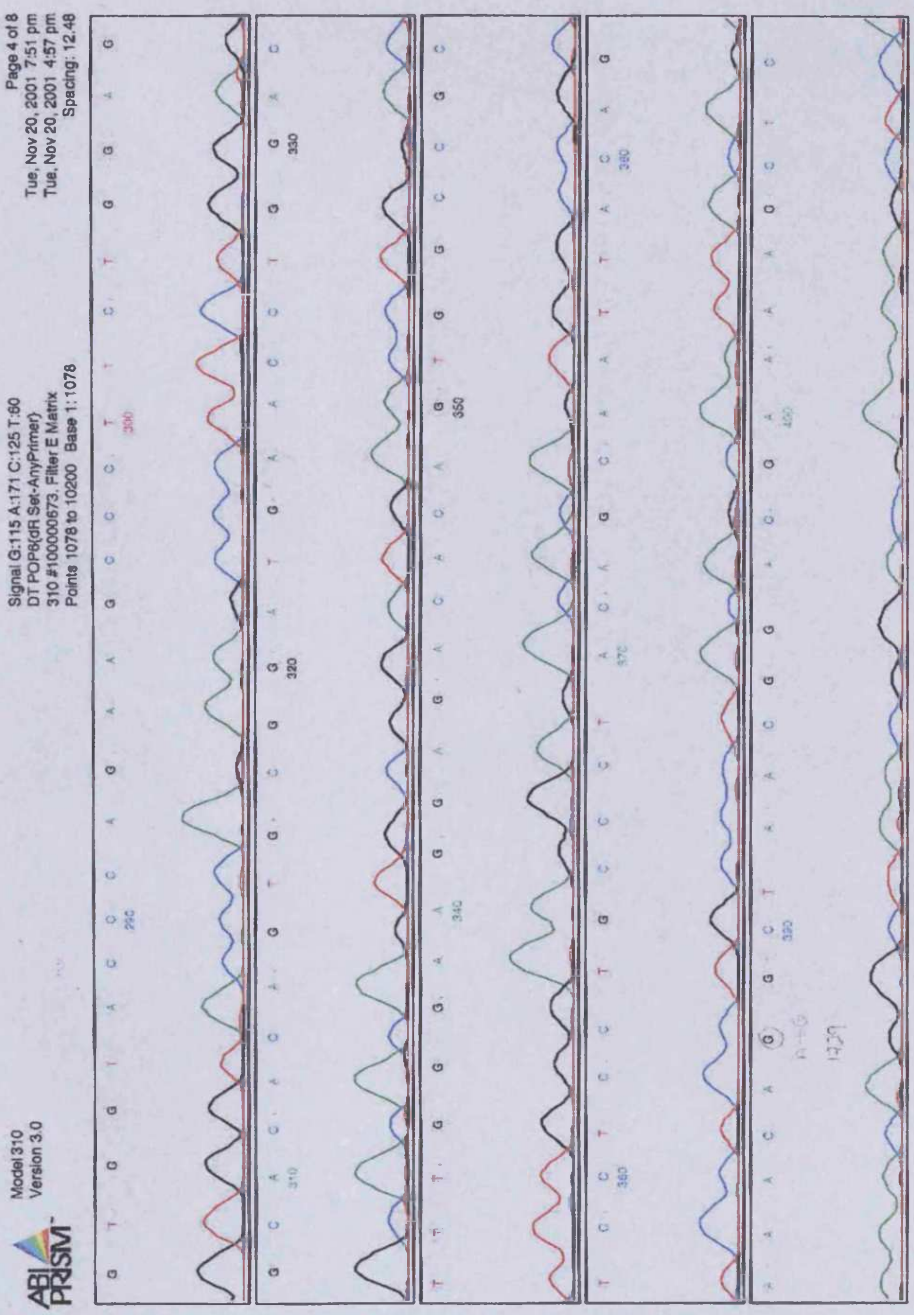
ABI PRISM
Model 310
Version 3.0
Signal G:115 A:171 C:125 T:60
DT POP6(dR Set-AnyPrimer)
310 #100000673. Filter E Matrix
Points 1078 to 10200 Base 1:1078
Page 4 of 8
Tue, Nov 20, 2001 7:51 pm
Tue, Nov 20, 2001 4:57 pm
Spacing: 12.48

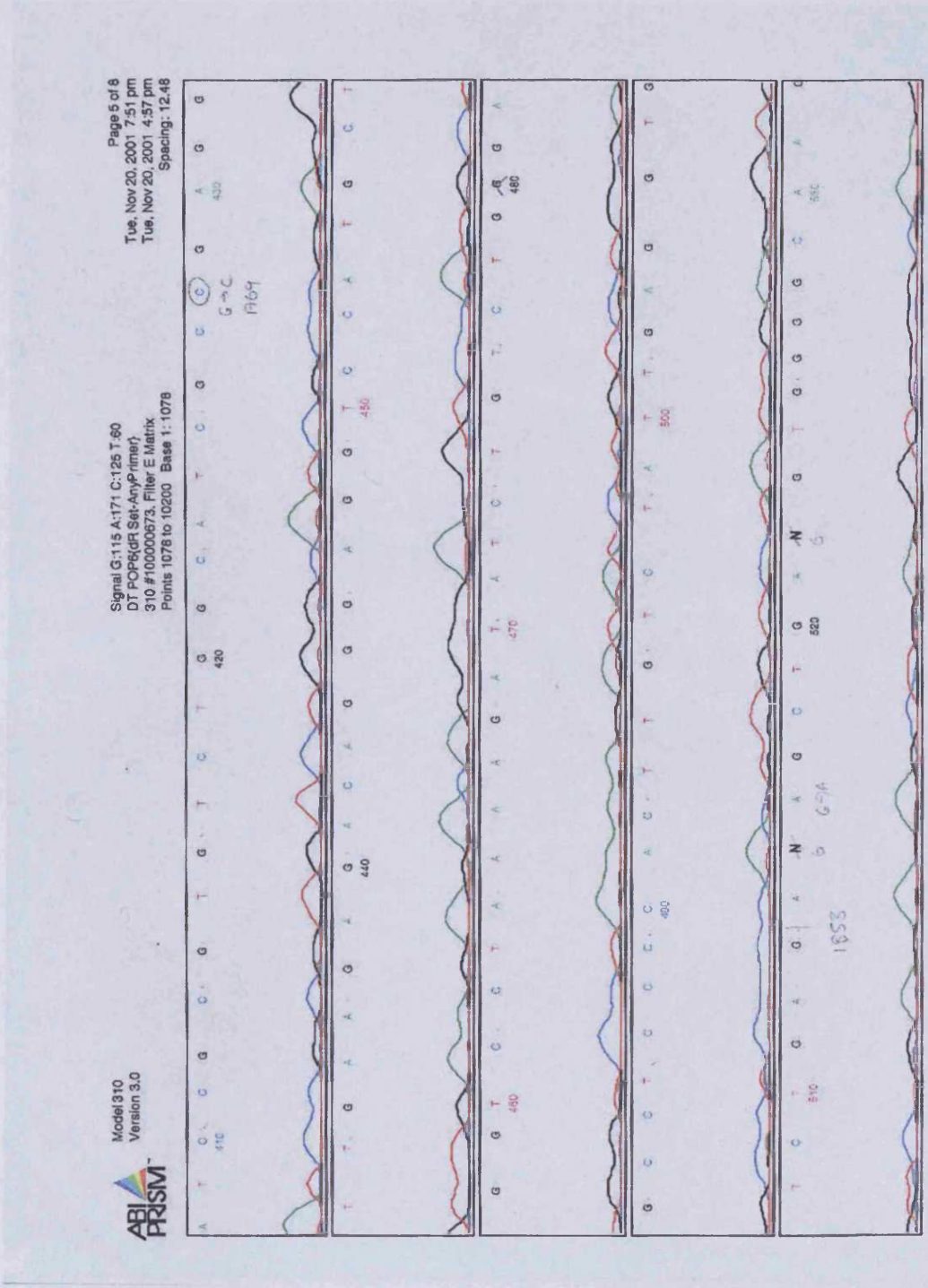
ABI PRISM
Model 310
Version 3.0
Signal G:115 A:171 C:125 T:80
DT POP6(dR Set-AnyPrimer)
310 #100000673, Filter E Matrix
Points 1078 to 10200 Base 1:1078
Page 5 of 8
Tue, Nov 20, 2001 7:51 pm
Tue, Nov 20, 2001 4:57 pm
Spacing: 12.48
G→C
1969
1853
G→A

TG7 Up 9: 1485-1769 bp

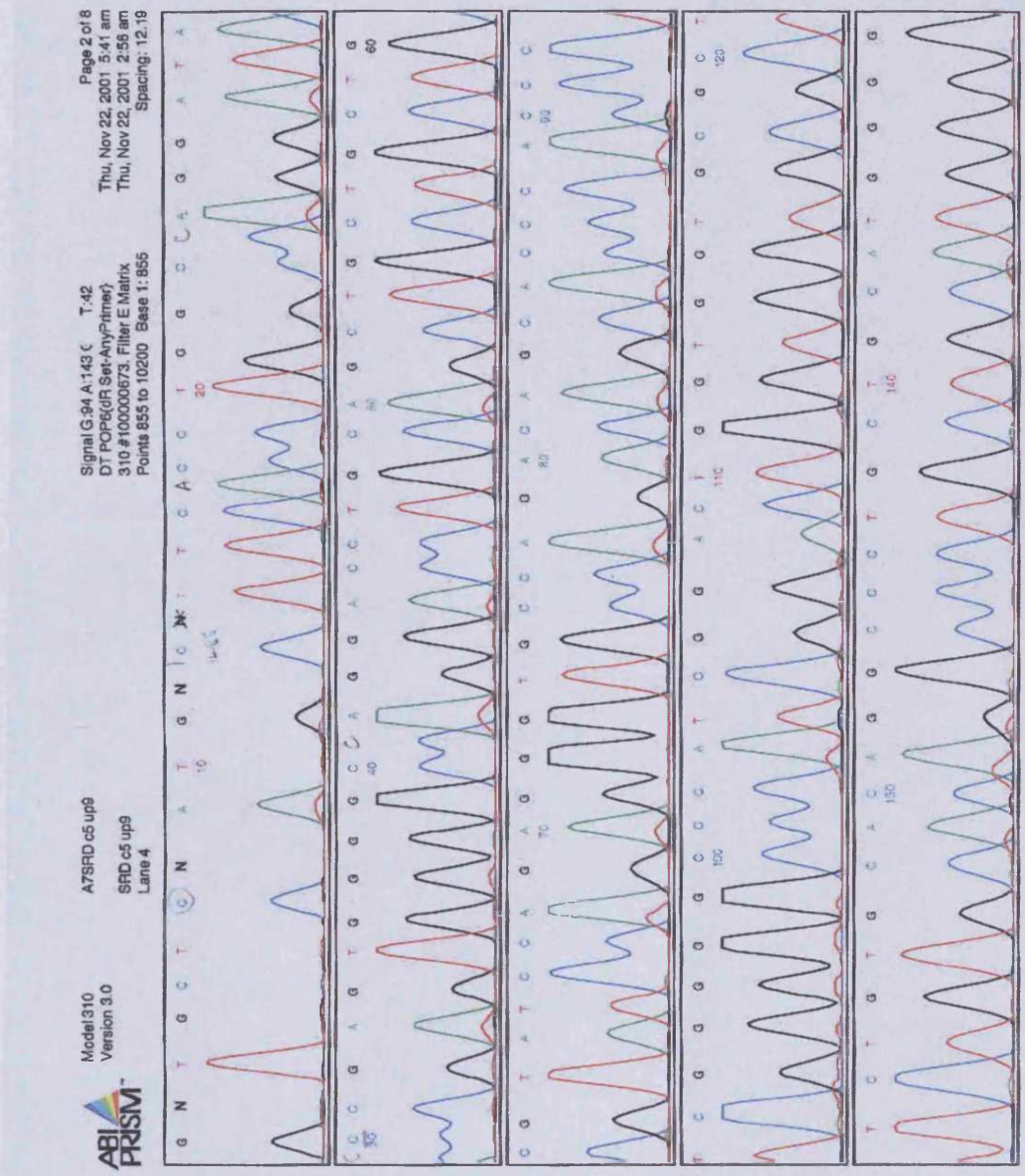

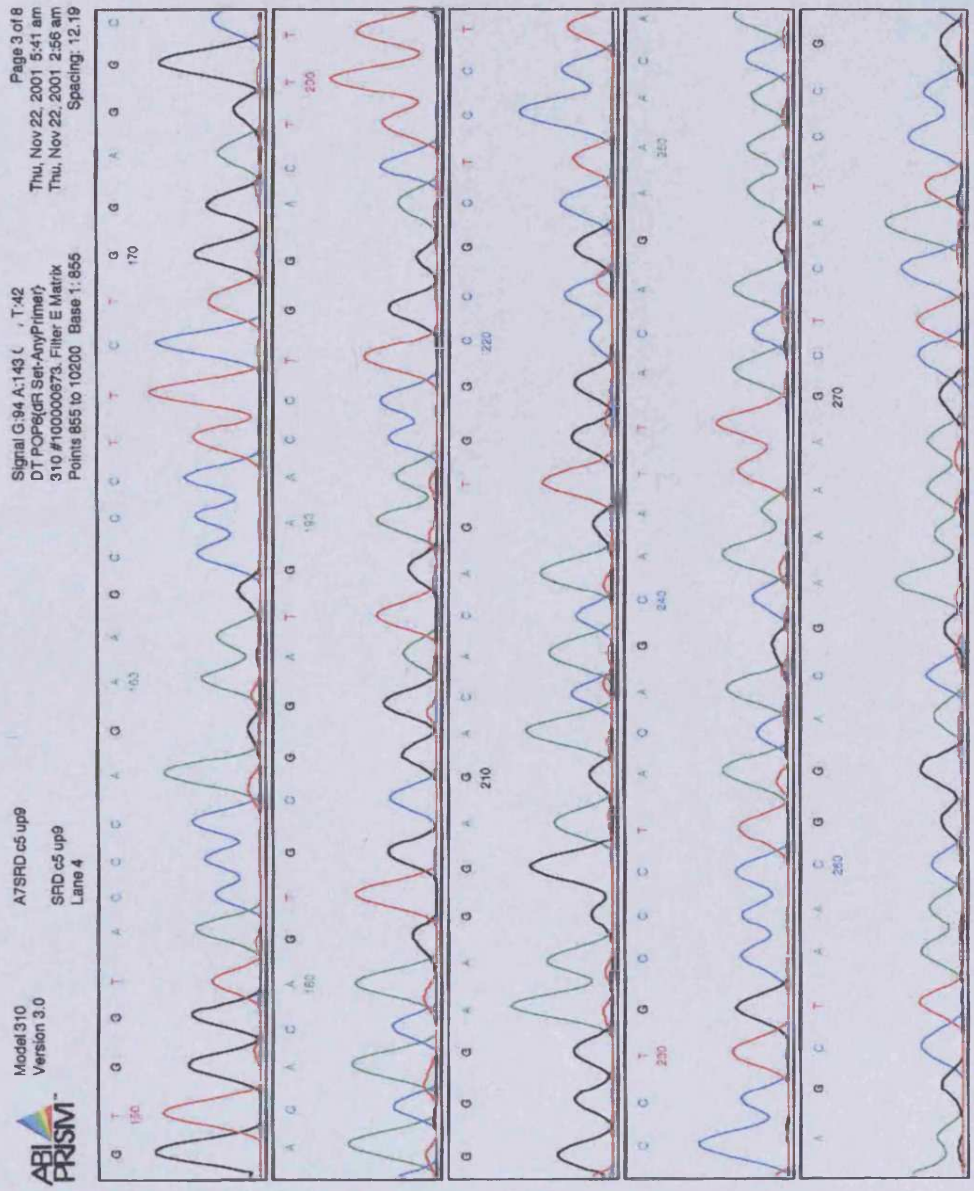
ABI PRISM
Model 310
Version 3.0
A7SRD c5 up9
SRD c5 up9
Lane 4
Signal G:94 A:143 C , T:42
DT POP6(dR Set-AnyPrimer)
310 #100000873. Filter E Matrix
Points 855 to 10200 Base 1: 855
Page 3 of 8
Thu, Nov 22, 2001 5:41 am
Thu, Nov 22, 2001 2:56 am
Spacing: 12.19

ABI PRISM
Model 310
Version 3.0
A7SRD c5 up9
SRD c5 up9
Lane 4
Signal G:94 A:143 C T:42
DT POP6(dR Set-AnyPrimer)
310 #100000673. Filter E Matrix
Points 855 to 10200 Base 1: 855
Page 4 of 8
Thu, Nov 22, 2001 5:41 am
Thu, Nov 22, 2001 2:56 am
Spacing: 12.19

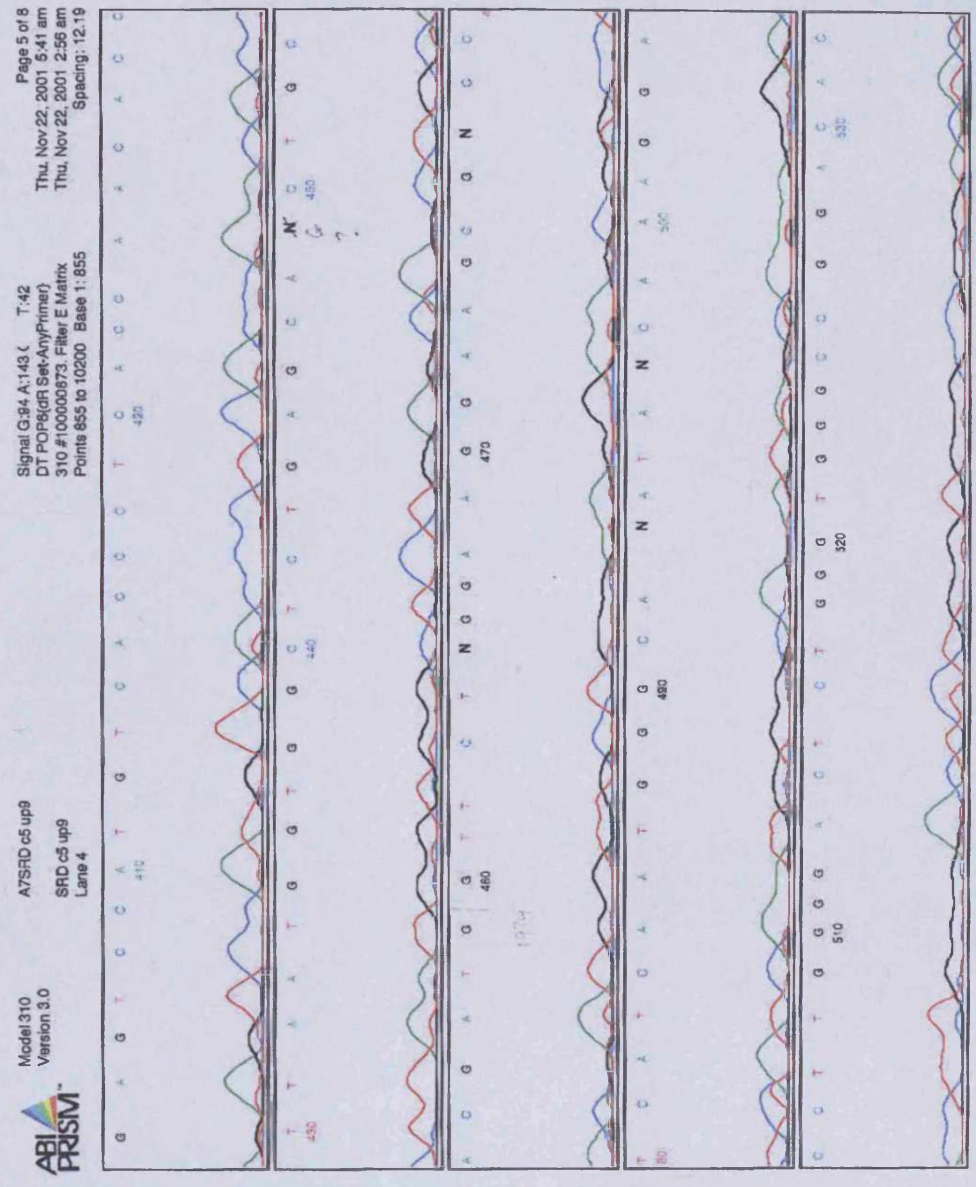
ABI PRISM
Model 310
Version 3.0
A7SRD c5 up9
SRD c5 up9
Lane 4
Signal G:94 A:143 C T:42
DT POP6(dR Set-AnyPrimer)
310 #100000873. Filter E Matrix
Points 855 to 10200 Base 1: 855
Page 5 of 8
Thu, Nov 22, 2001 5:41 am
Thu, Nov 22, 2001 2:56 am
Spacing: 12.19

TG7 Up 1: 1904-2253 bp

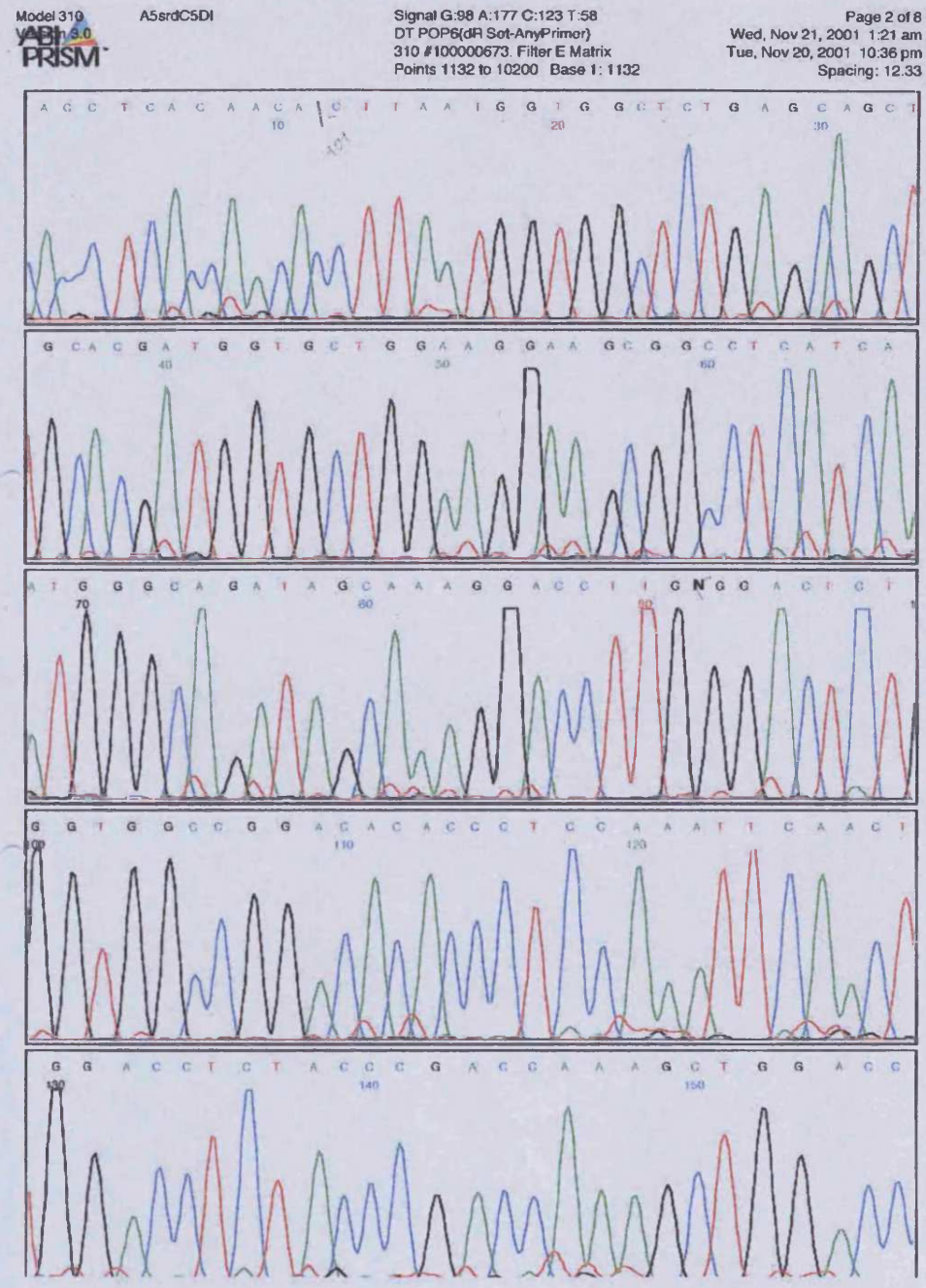

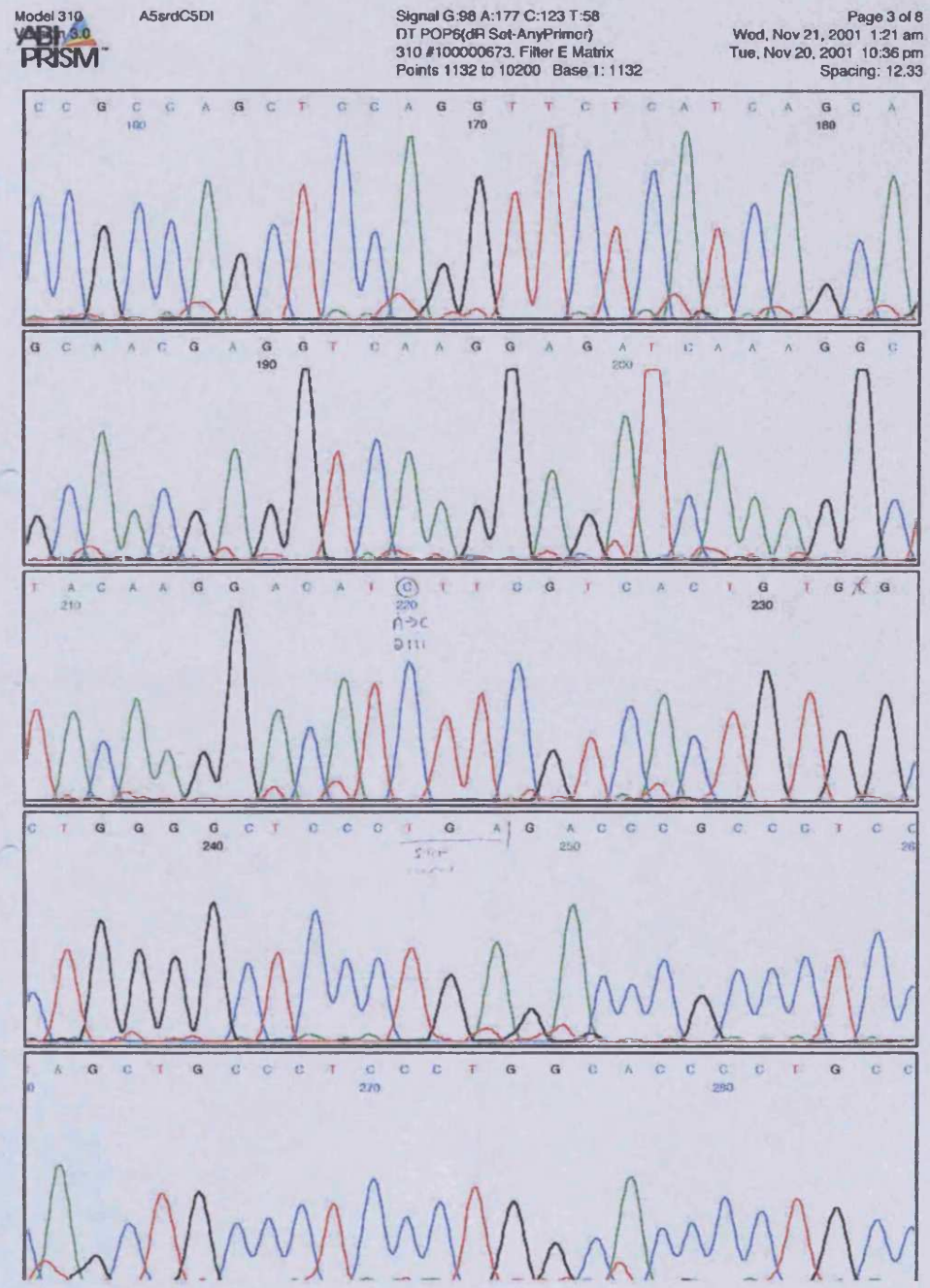
Model 310
A5srdC5DI
Signal G:98 A:177 C:123 T:58
DT POP6(dR Set-AnyPrimer)
310 #100000673. Filter E Matrix
Points 1132 to 10200 Base 1: 1132
Page 3 of 8
Wed, Nov 21, 2001 1:21 am
Tue, Nov 20, 2001 10:36 pm
Spacing: 12.33

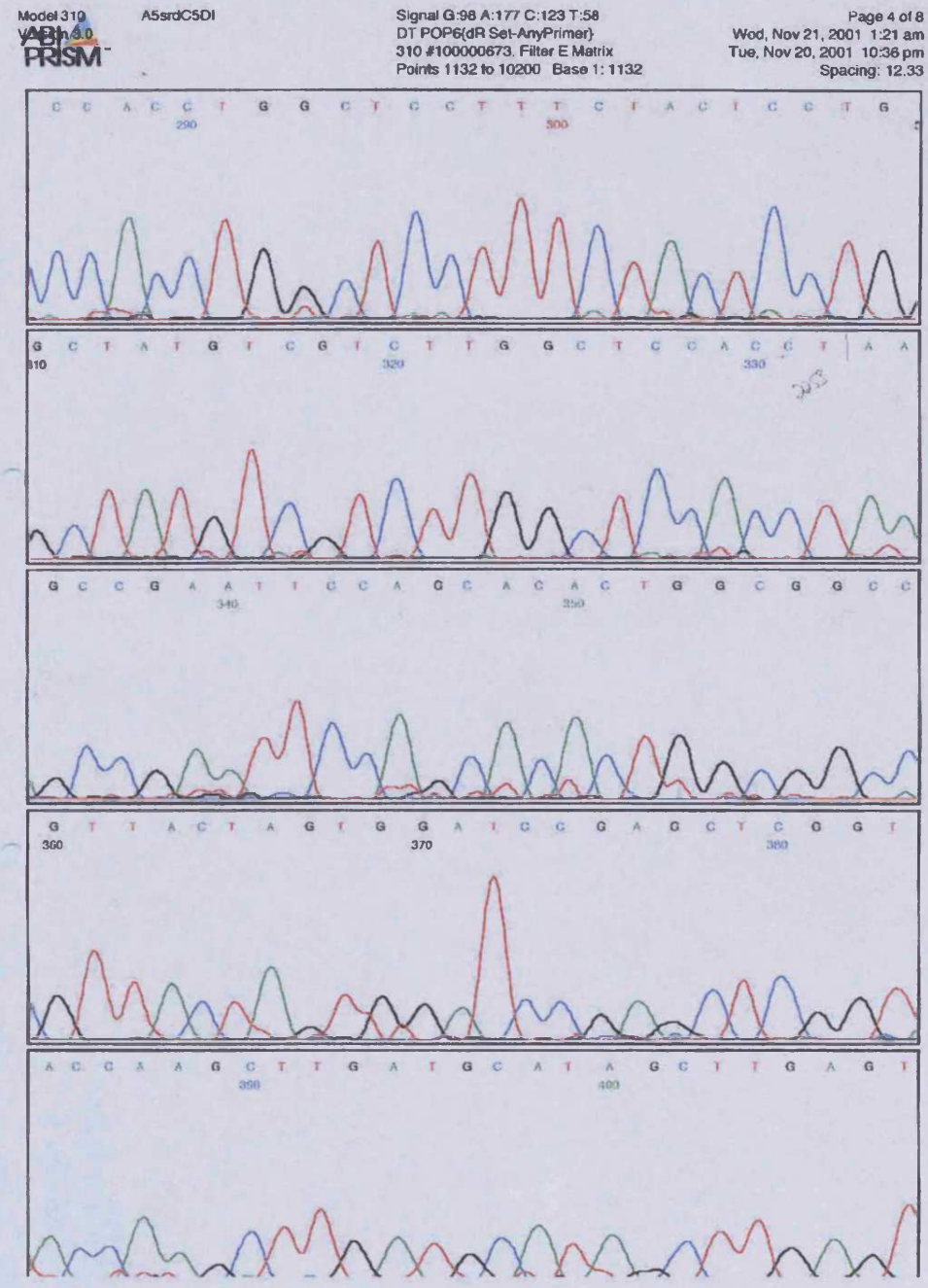
Model 310
A5srdC5DI
Signal G:98 A:177 C:123 T:58
DT POP6{dR Set-AnyPrimer}
310 #100000673. Filter E Matrix
Points 1132 to 10200 Base 1: 1132
Page 4 of 8
Wed, Nov 21, 2001 1:21 am
Tue, Nov 20, 2001 10:36 pm
Spacing: 12.33

Sequencing of pGEX-2T/TG7 construct

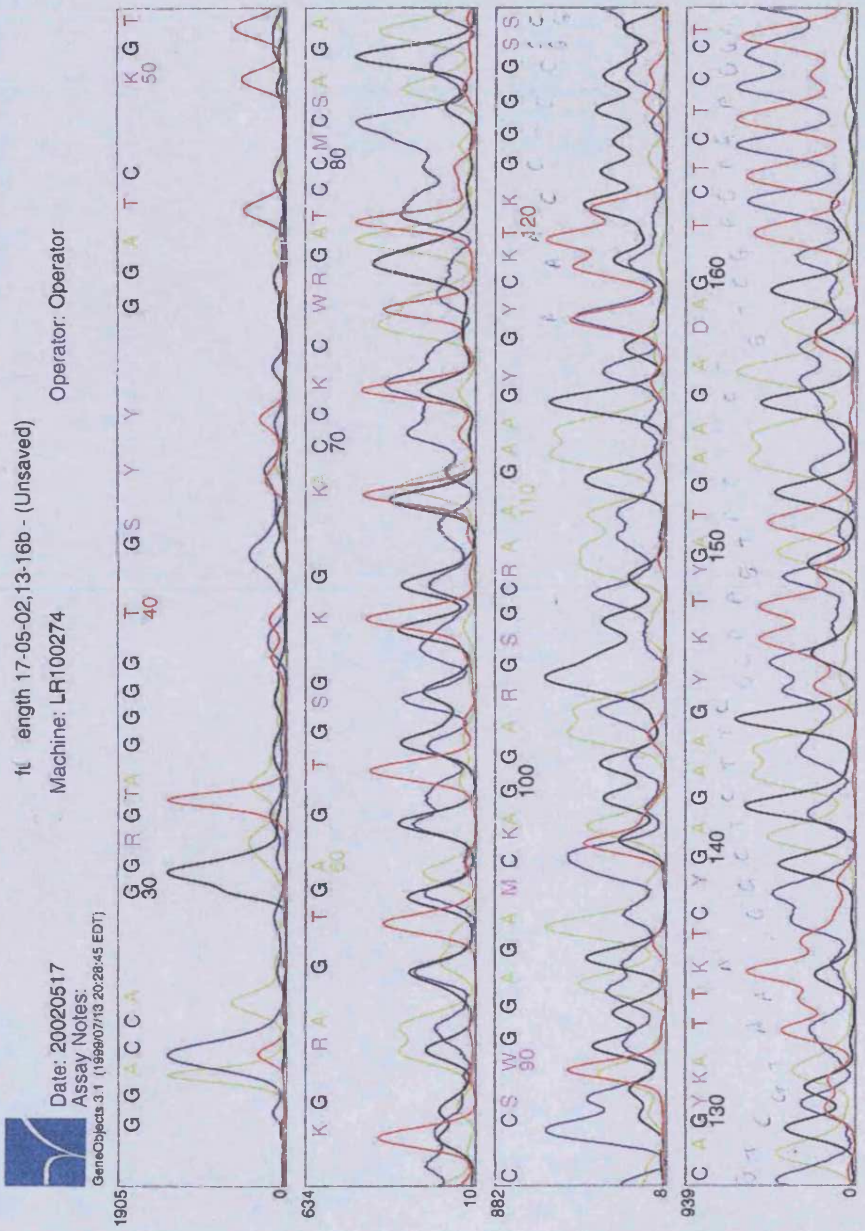

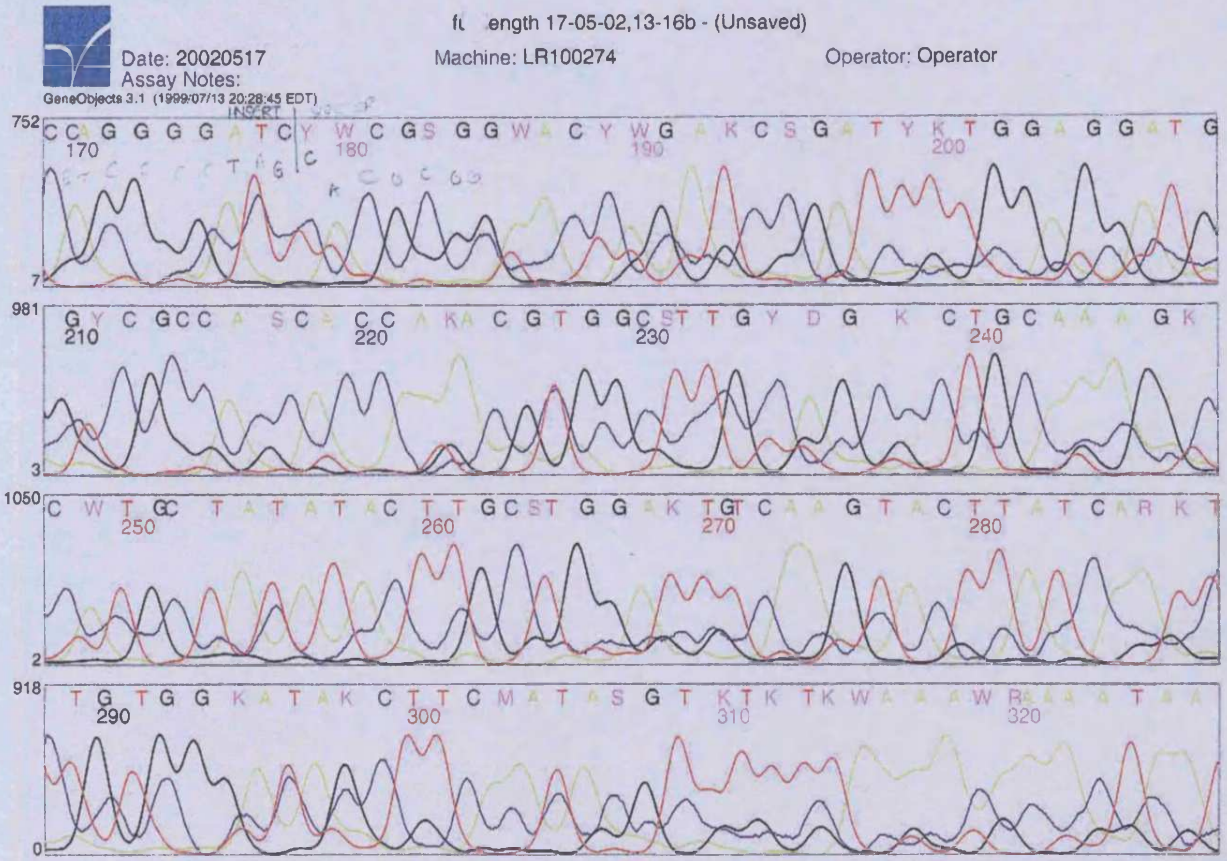

File: full length 17-05-02,13-16b

P6S incorporates a sequence unique to the short form of TG6

Nucleotide and deduced amino acid for the short form of TG6 (TG6S). The active site Cys residue is shown in red, and the His and Asp residues of the catalytic triad are in pink. Residues involved in Ca^{2+}-binding are shown in blue. The sequence difference between the two alternatively spliced variants (TG6L and TG6S) is shown in **bold** and the region involved in the design of the peptide P6S is underlined (H. Thomas Thesis, 2004)

```
                                                                      5
                                                                  AA CCC

          14          23          32          41          50          59
ATG ACC CAG GGG ATC AGA GTC ACC AAG GTG GAC TGG CAG CGG TCG AGG AAT GGC
 M   T   Q   G   I   R   V   T   K   V   D   W   Q   R   S   R   N   G

          68          77          86          95          104         113
GCT GCC CAC CAC ACC CAG GAG TAC CCC TGC CCT GAG CTG GTG GTT CGC AGG GGC
 A   A   H   H   T   Q   E   Y   P   C   P   E   L   V   V   R   R   G

         122         131         140         149         158         167
CAG TCG TTC AGC CTC ACG CTG GAG CTG AGC AGA GCC CTG GAC TGT GAG GAG ATC
 Q   S   F   S   L   T   L   E   L   S   R   A   L   D   C   E   E   I

         176         185         194         203         212         221
CTC ATC TTC ACG GTG GAG ACA GGA CCC CGG GCT TCT GAG GCC CTC CAC ACC AAA
 L   I   F   T   V   E   T   G   P   R   A   S   E   A   L   H   T   K

         230         239         248         257         266         275
GCT GTG TTC CAG ACA TCG GAG CTG GAG CGG GGT GAG GGC TGG ACA GCA GCA AGG
 A   V   F   Q   T   S   E   L   E   R   G   E   G   W   T   A   A   R

         284         293         302         311         320         329
GAG GCT CAG ATG GAG AAA ACT CTG ACC GTC AGT CTC GCC AGC CCT CCC AGT GCT
 E   A   Q   M   E   K   T   L   T   V   S   L   A   S   P   P   S   A

         338         347         356         365         374         383
GTC ATT GGC CGC TAC CTG CTG AGC ATC AGG CTT TCC TCT CAC CGC AAA CAC AGC
 V   I   G   R   Y   L   L   S   I   R   L   S   S   H   R   K   H   S

         392         401         410         419         428         437
AAC CGG AGG CTG GGC GAG TTT GTT CTC CTT TTC AAC CCA TGG TGT GCA GAG GAC
 N   R   R   L   G   E   F   V   L   L   F   N   P   W   C   A   E   D

         446         455         464         473         482         491
GAT GTG TTT CTG GCC TCA GAG GAG GAG AGA CAG GAG TAC GTG CTC AGC GAC AGC
 D   V   F   L   A   S   E   E   E   R   Q   E   Y   V   L   S   D   S

         500         509         518         527         536         545
GGC ATC ATC TTC CGA GGC GTG GAG AAG CAC ATA CGA GCC CAG GGC TGG AAC TAC
 G   I   I   F   R   G   V   E   K   H   I   R   A   Q   G   W   N   Y

         554         563         572         581         590         599
GGG CAG TTT GAG GAG GAC ATC CTG AAC ATC TGC CTC TCC ATC CTG GAT CGA AGC
 G   Q   F   E   E   D   I   L   N   I   C   L   S   I   L   D   R   S

         608         617         626         635         644         653
CCC GGT CAC CAA AAC AAC CCA GCC ACC GAC GTG TCC TGC CGC CAC AAC CCC ATC
 P   G   H   Q   N   N   P   A   T   D   V   S   C   R   H   N   P   I

         662         671         680         689         698         707
```

```
TAC GTC ACC AGG GTC ATC AGT GCC ATG GTG AAC AGC AAC AAC GAC CGA GGT GTG
 Y   V   T   R   V   I   S   A   M   V   N   S   N   N   D   R   G   V

        716         725         734         743         752         761
GTG CAA GGA CAG TGG CAG GGC AAG TAC GGC GGC GGC ACC AGC CCG CTG CAC TGG
 V   Q   G   Q   W   Q   G   K   Y   G   G   G   T   S   P   L   H   W

        770         779         788         797         806         815
CGC GGC AGC GTG GCC ATT CTG CAG AAG TGG CTC AAG GGC AGG TAC AAG CCA GTC
 R   G   S   V   A   I   L   Q   K   W   L   K   G   R   Y   K   P   V

        824         833         842         851         860         869
AAG TAC GGC CAG TGC TGG GTC TTC GCC GGA GTC CTG TGC ACA GTC CTC AGG TGC
 K   Y   G   Q   C   W   V   F   A   G   V   L   C   T   V   L   R   C

        878         887         896         905         914         923
TTG GGG ATA GCC ACA CGG GTC GTG TCC AAC TTC AAC TCA GCC CAC GAC ACA GAC
 L   G   I   A   T   R   V   V   S   N   F   N   S   A   H   D   T   D

        932         941         950         959         968         977
CAG AAC CTG AGT GTG GAC AAA TAC GTG GAC TCC TTC GGG CGG ACC CTG GAG GAC
 Q   N   L   S   V   D   K   Y   V   D   S   F   G   R   T   L   E   D

        986         995        1004        1013        1022        1031
CTG ACA GAA GAC AGC ATG TGG AAT TTC CAT GTC TGG AAT GAG AGC TGG TTT GCC
 L   T   E   D   S   M   W   N   F   H   V   W   N   E   S   W   F   A

       1040        1049        1058        1067        1076        1085
CGG CAG GAC CTA GGC CCC TCT TAC AAT GGC TGG CAG GTT CTG GAT GCC ACC CCC
 R   Q   D   L   G   P   S   Y   N   G   W   Q   V   L   D   A   T   P

       1094        1103        1112        1121        1130        1139
CAG GAG GAG AGT GAA GGT GTG TTC CGG TGC GGC CCA GCC TCA GTC ACC GCC ATC
 Q   E   E   S   E   G   V   F   R   C   G   P   A   S   V   T   A   I

       1148        1157        1166        1175        1184        1193
CGC GAG GGT GAT GTG CAC CTG GCT CAC GAT GGC CCC TTC GTG TTT GCG GAG GTC
 R   E   G   D   V   H   L   A   H   D   G   P   F   V   F   A   E   V

       1202        1211        1220        1229        1238        1247
AAC GCC GAC TAC ATC ACC TGG CTG TGG CAC GAG GAT GAG AGC CGG GAG CGT GTA
 N   A   D   Y   I   T   W   L   W   H   E   D   E   S   R   E   R   V

       1256        1265        1274        1283        1292        1301
TAC TCA AAC ACG AAG AAG ATT GGG AGA TGC ATC AGC ACC AAG GCG GTG GGC AGT
 Y   S   N   T   K   K   I   G   R   C   I   S   T   K   A   V   G   S

       1310        1319        1328        1337        1346        1355
GAC TCC CGC GTG GAC ATC ACT GAC CTC TAC AAG TAT CCG GAA GGG TCC CGG AAA
 D   S   R   V   D   I   T   D   L   Y   K   Y   P   E   G   S   R   K

       1364        1373        1382        1391        1400        1409
GAG AGG CAG GTG TAC AGC AAG GCG GTG AAC AGG CTG TTC GGC GTG GAA GCC TCT
 E   R   Q   V   Y   S   K   A   V   N   R   L   F   G   V   E   A   S

       1418        1427        1436        1445        1454        1463
GGA AGG AGA ATC TGG ATC CGC AGG GCT GGG GGT CGC TGT CTC TGG CGT GAC GAC
 G   R   R   I   W   I   R   R   A   G   G   R   C   L   W   R   D   D

       1472        1481        1490        1499        1508        1517
CTC CTG GAG CCT GCC ACC AAG CCC AGC ATC GCT GGC AAG TTC AAG GTG CTA GAG
 L   L   E   P   A   T   K   P   S   I   A   G   K   F   K   V   L   E

       1526        1535        1544        1553        1562        1571
CCT CCC ATG CTG GGC CAC GAC CTG AGA CTG GCC CTG TGC TTG GCC AAC CTC ACC
 P   P   M   L   G   H   D   L   R   L   A   L   C   L   A   N   L   T

       1580        1589        1598        1607        1616        1625
TCC CGG GCC CAG CGG GTG AGG GTC AAC CTG AGC GGT GCC ACC ATC CTC TAT ACC
```

```
 S   R   A   Q   R   V   R   V   N   L   S   G   A   T   I   L   Y   T

       1634        1643        1652        1661        1670        1679
CGC AAG CCA GTG GCA GAG ATC CTG CAT GAA TCC CAC GCC GTG AGG CTG GGG CCG
 R   K   P   V   A   E   I   L   H   E   S   H   A   V   R   L   G   P

       1688        1697        1706        1715        1724        1733
CAA GAA GAG AAG AGA ATC CCA ATT ACA ATA TCT TAC TCT AAG TAT AAA GAA GAC
 Q   E   E   K   R   I   P   I   T   I   S   Y   S   K   Y   K   E   D

       1742        1751        1760        1769        1778        1787
CTG ACA GAG GAC AAG AAG ATC CTG TTG GCT GCC ATG TGC CTT GTC ACC AAA GGA
 L   T   E   D   K   K   I   L   L   A   A   M   C   L   V   T   K   G

       1796        1805        1814        1823        1832        1841
GAG AAG CTT CTG GTG GAG AAG GAC ATT ACT CTA GAG GAC TTC ATC ACC ATC AAG
 E   K   L   L   V   E   K   D   I   T   L   E   D   F   I   T   I   K

       1850        1859        1868        1877        1886        1895
CGT GCC TAC CCT GGA GCC TCA GGA GAG GGC CTC AGT CCA GTT TGA CAT CAC CCC
 R   A   Y   P   G   A   S   G   E   G   L   S   P   V   *

       1904        1913        1922        1931        1940        1949
CTC CAA AAG TGG CCC AAG GCA GCT GCA GGT GGA CCT TGT AAG CCC TCA CTT CCC

       1958        1967        1976        1985        1994        2003
GGA CAT CAA GGG CTT TGT GAT CGT CCA TGT GGC CAC TGC CAA GTG ATG GAT CAT

       2012        2021        2030        2039        2048        2057
GAG GGA CTG AGA GGG GTG GAT TTG GCC CCT GTC CTC CTC CTG CCC ATT CTT TGT

       2066        2075        2084        2093        2102
CTC TTC CAC ATG GGA GCC AGG AGG CCT CAG TTA ATC CTG CCT CAA CCT
```

Peptide synthesis

TG6L

hTG6l (large + small isoform)

SIGMA GENOSYS — QUALITY ASSURANCE DOCUMENTATION

Customer Number: 101721
Peptide #: 72073-2
Lot #: B6601-004

M_r without C-term: 1715.9
pI 4.56

Sequence: CGWRDDLLEPVTKPS
Length: 15 Mgs Shipped: 12.8
Molecular Weight: 1714.9781494141 Final Purity 90

OD_{280} 0.1% ~3.316

GRAVY -0.707

Peptide Name PEP2
Notes: N-Term:[H] C-Term:[NH2]

Column: Discovery Bio Wide Pore C-18, 250mmX4.6mm, 5μm
Mobile Phase: A=0.1% TFA/Water
B=0.1% TFA/Acetronitrile
Gradient: 0 to 2 min.: 100% A
2 to 20 min.: 0 to 67.5% B
Detection: 214nm
Storage Conditions: -20 C for Long Term
4 C for Short Term

Sigma-Genosys makes no claims to the peptide's ability to function in the specific application of the customer. All peptides are shipped lyophilized and as gross weight. Peptide for research use only.

Analytical HPLC and Mass Spectral analyses are enclosed.

Handling & Storage of Peptides

Resuspension

1. Hydrophilic peptides: Resuspend the peptide in distilled or deionized water. Make sure that the pH of the solution is around pH 7.0, and adjust the pH if necessary to improve solubility.
2. Hydrophobic peptides: Dissolve the peptide in a minimum volume of DMF, DMSO (if the sequence does not have Cys, Met or Trp), IPA, ethanol, or other organic solvents that can be tolerated in the experiment. Add the peptide solution slowly (dropwise) into a stirred buffer of your choice. For non-biological studies, stronger solvents like TFA, formic acid or acetic acid may be used for initial solubilization.

Storage

Peptides are supplied lyophilized. For maximum stability, the lyophilized peptide should be stored at -20°C. Most peptides will be stable in solutions for several days at 4°C. Avoid repeated freeze/thaw cycles if using frozen solutions. Upon removal from the freezer, bring the peptide vial to room temperature before opening and weighing to avoid moisture condensation.

Peptides containing W, M, and C are prone to oxidation and should be stored in a lyophilized state under an inert gas. These peptides should be degassed and stored in aliquots at -80°C if they will be stored in solution.

• Peptides containing Q and N are susceptible to deamidation and should be stored at -80°C. Additionally, peptides containing a Q at the N-terminus will cyclize to pyroglutamate under dilute acid conditions.

Sigma-Genosys
1442 Lake Front Circle
The Woodlands, Texas 77380-3600
1-800-234-5362

Sigma-Genosys Ltd.
London Road, Pampisford
Cambridge CB2 4EF, UK
(+44) (0) 1223 839000

Sigma-Genosys Japan K.K.
777-13 Nishi-I, Shin-Ko, Ishikari
Hokkaido, Japan
81 133 73 5005

Sigma-Aldrich Pty Ltd.
Unit 2, 14 Anella Avenue
Castle Hill NSW 2154
Australia
1-800-800-097

Cashmere Scientific Company
No. 2-1, 2F, Lane 40
Chang-An W. Road
Taipei, Taiwan 104
886-2-25416188

Sigma-Aldrich Korea
Samhan Camus Annex, 10th Floor
17-26 Yoido-dong, Yungdeungpo-ku
Seoul, Korea
82 2 783 5211

Sigma-Aldrich Canada Ltd.
2149 Winston Park Drive
Oakville, Ontario L6H 6J8
CANADA (905) 829-9500

Sigma-Aldrich Pte., Ltd.
102E Pasir Panjong Road
#08-01 Citilink Warehouse
118529, Republic of Singapore
65 271 1089

Current Date 6/2/03

Sample Information

SampleName 72073-3b6601-5
Vial 69
Injection 1
System Name SCOOBYDOO2
Run Time 30.00 Minutes

Date Acquired 5/30/03 11:50:46 PM
Acq Method Set STANDARD
Processing Method Auto Integration
Date Processed 6/2/03 10:26:34 AM
Injection Volume 20.00 ul

Auto-Scaled Chromatogram at 214 nm

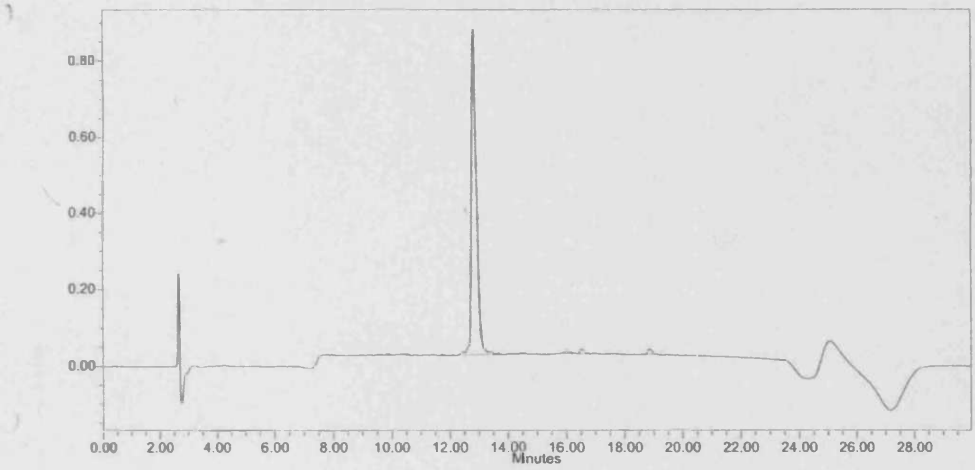

Integration Results

	RT	Area	Height	% Area	% Height
1	8.921	8212	1332	0.07	0.14
2	9.182	15246	1787	0.14	0.19
3	9.590	18353	2122	0.17	0.23
4	9.875	21940	2751	0.20	0.30
5	10.402	52886	3705	0.48	0.40
6	11.386	12727	1983	0.11	0.21
7	11.742	23610	2711	0.21	0.29
8	12.462	86066	7711	0.78	0.83
9	12.781	10326559	854660	93.30	92.27
10	13.371	84636	7789	0.76	0.84

Integration Results

	RT	Area	Height	% Area	% Height
11	18.851	209492	19465	0.68	1.09

Voyager Spec #1=>SM5[BP = 1714.7, 965]

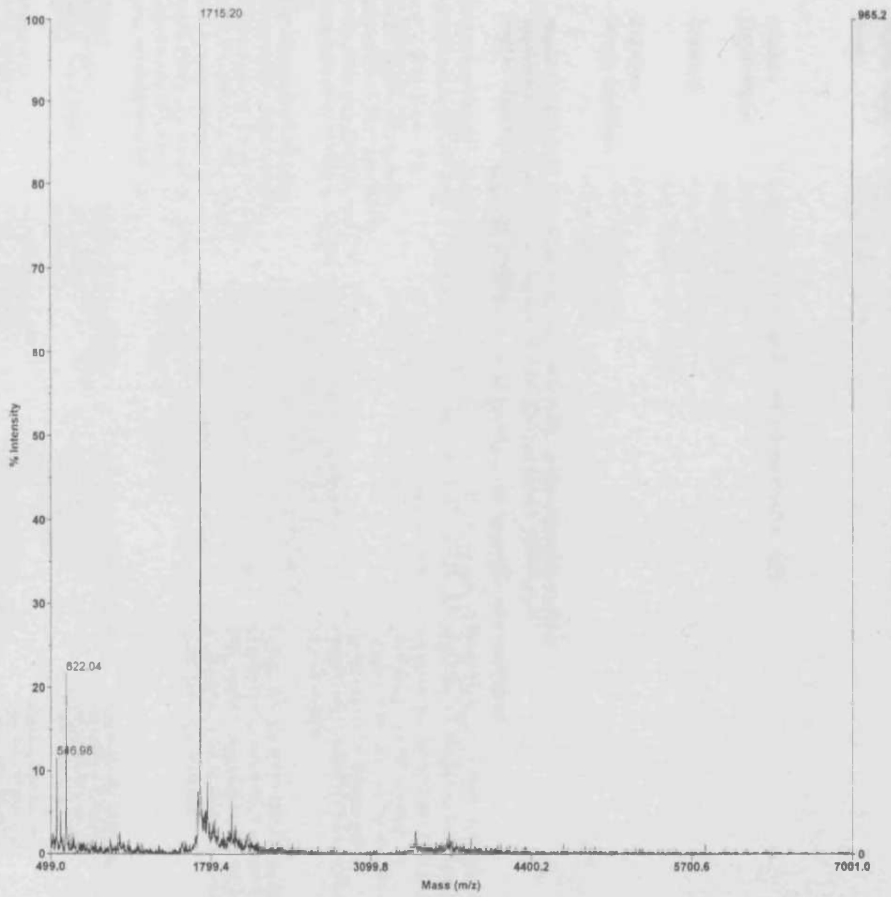

Mode of operation:	Linear
Extraction mode:	Delayed
Polarity:	Negative
Acquisition control:	Manual
Accelerating voltage:	20000 V
Grid voltage:	94.5%
Guide wire 0:	0.04%
Extraction delay time:	150 nsec
Acquisition mass range:	500 – 7000 Da
Number of laser shots:	60/spectrum
Laser intensity:	1484
Laser Rep Rate:	3.0 Hz
Calibration type:	External – D:\Voyager\Calibrate\April03Lo.cal
Calibration matrix:	a-Cyano-4-hydroxycinnamic acid
Low mass gate:	400 Da
Digitizer start time:	14.686
Bin size:	2 nsec
Number of data points:	19895
Vertical scale:	200 mV
Vertical offset:	0%
Input bandwidth:	150 MHz
Sample well:	17
Plate ID:	100 WELL PLATE
Serial number:	1105
Instrument name:	Voyager-DE
Plate type filename:	C:\Voyager\100 well plate.pit
Lab name:	GENOSYS BIOTECHNOLOGIES
Absolute x-position:	32067.9
Absolute y-position:	42226.3
Relative x-position:	0.390508
Relative y-posititon:	-1.19115
Shots in spectrum:	60
Source pressure:	6.427e-007
Mirror pressure:	0
TC2 pressure:	0.01778
TIS gate width:	30
TIS flight length:	940

Acquired: 17:40:00, May 30, 2003
Sample Description: 72073-2B6601-4
D:\Voyager\Data\Peptides\MAY\30May03_0021.dat

Printed: 17:40, May 30, 2003

TG6S

SIGMA GENOSYS QUALITY ASSURANCE DOCUMENTATION hTG6S (short form)

Customer Number: 101721
Peptide #: 72073-1
Lot #: D6619-002
Sequence: TIRAYPGASGEGLSP
Length: 15 Mgs Shipped: 10.9
Molecular Weight: 1474.6500244141 Final Purity 79
Peptide Name PEP1
Notes: N-Term:[H] C-Term:[NH2]

M_r (w/o NH_2 at C) 1475.6
pI: 5.66
$A^{1\%}_{280}$ = 0.867
GRAVY -0.273

Column: Discovery Bio Wide Pore C-18, 250mmX4.6mm, 5µm
Mobile Phase: A=0.1% TFA/Water
B=0.1% TFA/Acetronitrile
Gradient: 0 to 2 min.: 100% A
2 to 20 min.: 0 to 67.5% B
Detection: 214nm
Storage Conditions: -20 C for Long Term
4 C for Short Term

Sigma-Genosys makes no claims to the peptide's ability to function in the specific application of the customer. All peptides are shipped lyophilized and as gross weight. Peptide for research use only.

Analytical HPLC and Mass Spectral analyses are enclosed.

Handling & Storage of Peptides

Resuspension

1. Hydrophilic peptides: Resuspend the peptide in distilled or deionized water. Make sure that the pH of the solution is around pH 7.0, and adjust the pH if necessary to improve solubility.
2. Hydrophobic peptides: Dissolve the peptide in a minimum volume of DMF, DMSO (if the sequence does not have Cys, Met or Trp), IPA, ethanol, or other organic solvents that can be tolerated in the experiment. Add the peptide solution slowly (dropwise) into a stirred buffer of your choice. For non-biological studies, stronger solvents like TFA, formic acid or acetic acid may be used for initial solubilization.

Storage

Peptides are supplied lyophilized. For maximum stability, the lyophilized peptide should be stored at -20°C. Most peptides will be stable in solutions for several days at 4°C. Avoid repeated freeze/thaw cycles if using frozen solutions. Upon removal from the freezer, bring the peptide vial to room temperature before opening and weighing to avoid moisture condensation.

Peptides containing W, M, and C are prone to oxidation and should be stored in a lyophilized state under an inert gas. These peptides should be degassed and stored in aliquots at -80°C if they will be stored in solution.

Peptides containing Q and N are susceptible to deamidation and should be stored at -80°C. Additionally, peptides containing a Q at the N-terminus will cyclize to pyroglutamate under dilute acid conditions.

Sigma-Genosys
1442 Lake Front Circle
The Woodlands, Texas 77380-3600
1-800-234-5362

Sigma-Genosys Ltd.
London Road, Pampisford
Cambridge CB2 4EF, UK
(+44) (0) 1223 839000

Sigma-Genosys Japan K.K.
777-13 Nishi-I, Shin-Ko, Ishikari
Hokkaido, Japan
81 133 73 5005

Sigma-Aldrich Pty Ltd.
Unit 2, 14 Anella Avenue
Castle Hill NSW 2154
Australia
1-800-800-097

Cashmere Scientific Company
No. 2-1, 2F, Lane 40
Chang-An W. Road
Taipei, Taiwan 104
886-2-25416188

Sigma-Aldrich Korea
Samhan Camus Annex, 10th Floor
17-26 Yoido-dong, Yungdeungpo-ku
Seoul, Korea
82 2 783 5211

Sigma-Aldrich Canada Ltd.
2149 Winston Park Drive
Oakville, Ontario L6H 6J8
CANADA (905) 829-9500

Sigma-Aldrich Pte., Ltd.
102E Pasir Panjong Road
#08-01 Citilink Warehouse
118529, Republic of Singapore
65 271 1089

Current Date 6/6/03

Sample Information

SampleName 72073-1D6619-2RR
Vial 12
Injection 1
System Name SCOOBYDOO2
Run Time 30.00 Minutes

Date Acquired 6/6/03 2:43:42 PM
Acq Method Set STANDARD
Processing Method Auto Integration
Date Processed 6/6/03 3:24:21 PM
Injection Volume 5.00 ul

Auto-Scaled Chromatogram at 214 nm

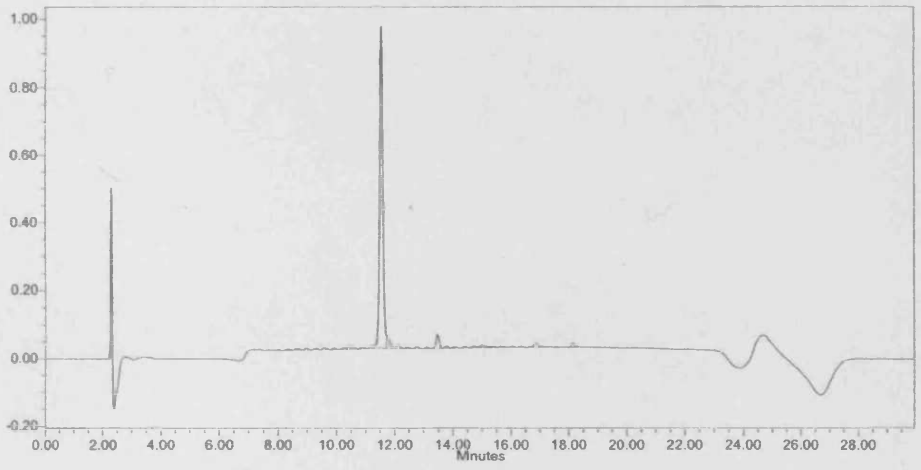

Integration Results

	RT	Area	Height	% Area	% Height
1	8.051	20093	2404	0.22	0.21
2	8.360	24797	2801	0.27	0.24
3	8.641	35322	3873	0.39	0.33
4	8.988	43684	4881	0.48	0.42
5	9.291	32021	4107	0.35	0.35
6	9.604	59887	6619	0.65	0.57
7	9.932	41598	4727	0.45	0.41
8	10.236	41297	4891	0.45	0.42
9	10.407	77496	9121	0.84	0.78
10	10.569	57285	6993	0.62	0.60

	RT	Area	Height	% Area	% Height
11	10.881	30620	4055	0.33	0.35
12	11.237	67361	7974	0.73	0.69
13	11.537	7333793	950030	79.96	81.69
14	11.717	261031	37841	2.85	3.25
15	12.139	88462	10386	0.96	0.89
16	12.431	22200	2363	0.24	0.20
17	12.770	41532	5423	0.45	0.47
18	13.123	30858	3658	0.34	0.31
19	13.463	312301	40611	3.41	3.49
20	13.776	63772	6874	0.70	0.59

Integration Results

	RT	Area	Height	% Area	% Height
21	14.076	25332	3240	0.28	0.28
22	14.385	28302	2871	0.31	0.25
23	15.007	125331	6426	1.37	0.55
24	15.358	32250	2997	0.35	0.26
25	15.697	29979	2345	0.33	0.20
26	16.068	25567	2320	0.28	0.20
27	16.363	17012	2249	0.19	0.19
28	16.847	116010	10551	1.26	0.91
29	18.133	86610	10335	0.94	0.89

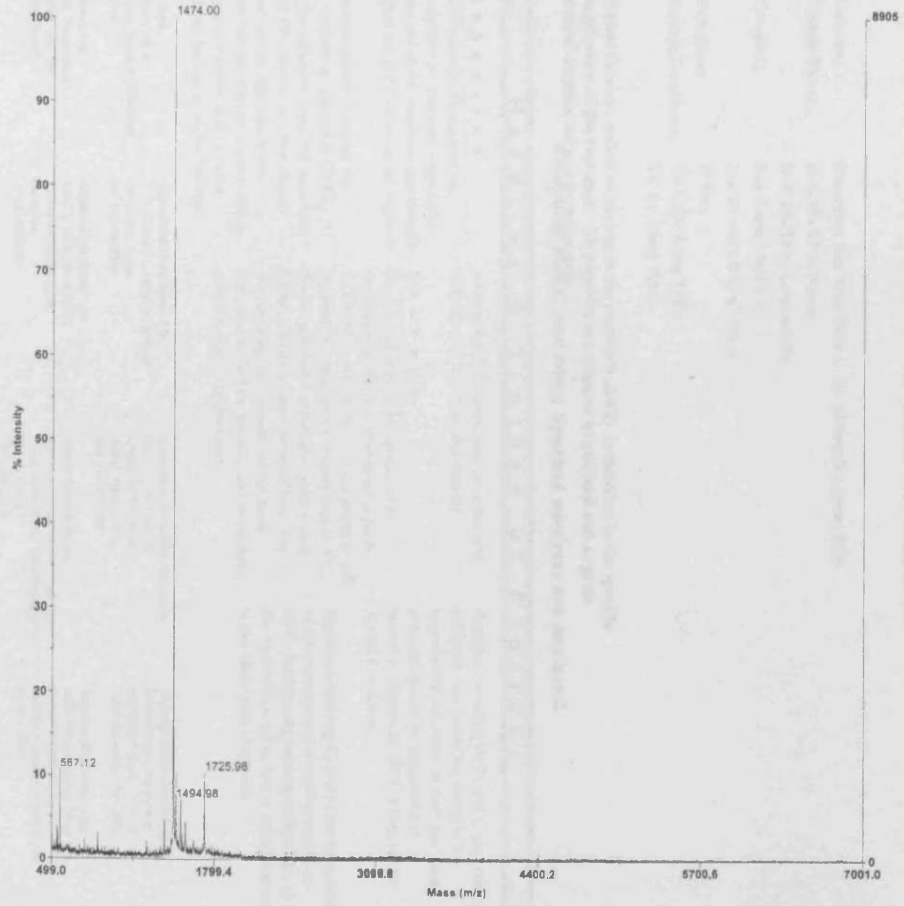

Mode of operation:	Linear
Extraction mode:	Delayed
Polarity:	Positive
Acquisition control:	Manual
Accelerating voltage:	20000 V
Grid voltage:	94.5%
Guide wire 0:	0.04%
Extraction delay time:	150 nsec
Acquisition mass range:	500 – 7000 Da
Number of laser shots:	60/spectrum
Laser intensity:	1598
Laser Rep Rate:	3.0 Hz
Calibration type:	External – D:\Voyager\Calibrate\April03Lo.cal
Calibration matrix:	a-Cyano-4-hydroxycinnamic acid
Low mass gate:	400 Da
Digitizer start time:	14.684
Bin size:	2 nsec
Number of data points:	19893
Vertical scale:	200 mV
Vertical offset:	0%
Input bandwidth:	150 MHz
Sample well:	19
Plate ID:	100 WELL PLATE
Serial number:	1105
Instrument name:	Voyager-DE
Plate type filename:	C:\Voyager\100 well plate.plt
Lab name:	GENOSYS BIOTECHNOLOGIES
Absolute x-position:	42226.7
Absolute y-position:	42228.3
Relative x-position:	-0.787619
Relative y-posititon:	0.797121
Shots in spectrum:	60
Source pressure:	6.018e-007
Mirror pressure:	0
TC2 pressure:	0.01658
TIS gate width:	30
TIS flight length:	940

Acquired: 18:53:00, June 05, 2003
Sample Description: 72073-1D6619-2
D:\Voyager\Data\Peptides\June\05JUNE03_0118.dat

Printed: 18:53, June 05, 2003

TG7

hTG7

SIGMA GENOSYS QUALITY ASSURANCE DOCUMENTATION

Customer Number: 101721
Peptide #: 72073-3
Lot #: B6601-005
Sequence: ESGGLRDQPAQLQL
Length: 14 Mgs Shipped: 14.1
Molecular Weight: 1510.6839599609 Final Purity 93
Peptide Name PEP3
Notes: N-Term:[H] C-Term:[NH2]

Pf. Sigma w/o C-Term. MW: 1511.6
pI: 4.57
Gravy: -0.857

Column:	Discovery Bio Wide Pore C-18, 250mmX4.6mm, 5µm
Mobile Phase:	A=0.1% TFA/Water
	B=0.1% TFA/Acetronitrile
Gradient:	0 to 2 min.: 100% A
	2 to 20 min.: 0 to 67.5% B
Detection:	214nm
Storage Conditions:	-20 C for Long Term
	4 C for Short Term

Sigma-Genosys makes no claims to the peptide's ability to function in the specific application of the customer. All peptides are shipped lyophilized and as gross weight. Peptide for research use only.

Analytical HPLC and Mass Spectral analyses are enclosed.

Handling & Storage of Peptides

Resuspension

1. Hydrophilic peptides: Resuspend the peptide in distilled or deionized water. Make sure that the pH of the solution is around pH 7.0, and adjust the pH if necessary to improve solubility.
2. Hydrophobic peptides: Dissolve the peptide in a minimum volume of DMF, DMSO (if the sequence does not have Cys, Met or Trp), IPA, ethanol, or other organic solvents that can be tolerated in the experiment. Add the peptide solution slowly (dropwise) into a stirred buffer of your choice. For non-biological studies, stronger solvents like TFA, formic acid or acetic acid may be used for initial solubilization.

Storage

Peptides are supplied lyophilized. For maximum stability, the lyophilized peptide should be stored at -20°C. Most peptides will be stable in solutions for several days at 4°C. Avoid repeated freeze/thaw cycles if using frozen solutions. Upon removal from the freezer, bring the peptide vial to room temperature before opening and weighing to avoid moisture condensation.

Peptides containing W, M, and C are prone to oxidation and should be stored in a lyophilized state under an inert gas. These peptides should be degassed and stored in aliquots at -80°C if they will be stored in solution.

Peptides containing Q and N are susceptible to deamidation and should be stored at -80°C. Additionally, peptides containing a Q at the N-terminus will cyclize to pyroglutamate under dilute acid conditions.

Sigma-Genosys
1442 Lake Front Circle
The Woodlands, Texas 77380-3600
1-800-234-5362

Sigma-Genosys Ltd.
London Road, Pampisford
Cambridge CB2 4EF, UK
(+44) (0) 1223 839000

Sigma-Genosys Japan K.K.
777-13 Nishi-I, Shin-Ko, Ishikari
Hokkaido, Japan
81 133 73 5005

Sigma-Aldrich Pty Ltd.
Unit 2, 14 Anella Avenue
Castle Hill NSW 2154
Australia
1-800-800-097

Cashmere Scientific Company
No. 2-1, 2F, Lane 40
Chang-An W. Road
Taipei, Tanwan 104
886-2-25416188

Sigma-Aldrich Korea
Samhan Camus Annex, 10th Floor
17-26 Yoido-dong, Yungdeungpo-ku
Seoul, Korea
82 2 783 5211

Sigma-Aldrich Canada Ltd.
2149 Winston Park Drive
Oakville, Ontario L6H 6J8
CANADA (905) 829-9500

Sigma-Aldrich Pte., Ltd.
102E Pasir Panjong Road
#08-01 Citilink Warehouse
118529, Republic of Singapore
65 271 1089

Current Date 6/2/03

Sample Information

SampleName 72073-3b6601-5
Vial 69
Injection 1
System Name SCOOBYDOO2
Run Time 30.00 Minutes

Date Acquired 5/30/03 11:50:46 PM
Acq Method Set STANDARD
Processing Method Auto Integration
Date Processed 6/2/03 10:26:34 AM
Injection Volume 20.00 ul

Auto-Scaled Chromatogram at 214 nm

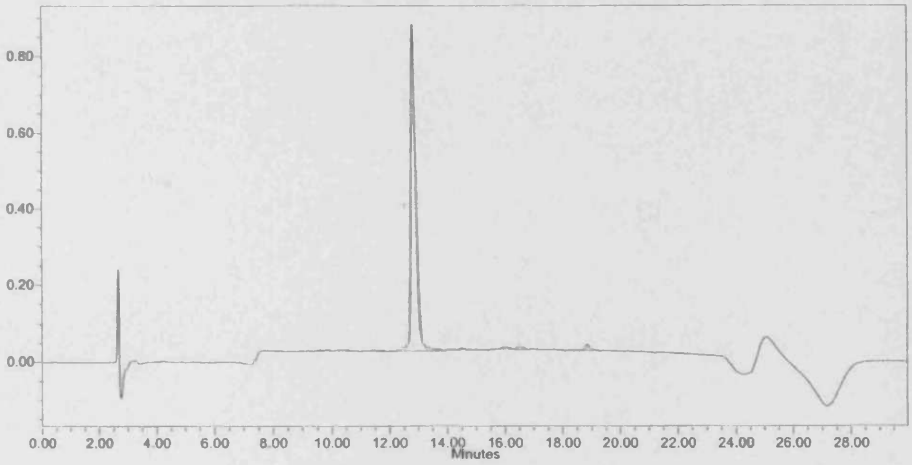

Integration Results

	RT	Area	Height	% Area	% Height
1	8.921	8212	1332	0.07	0.14
2	9.182	15246	1787	0.14	0.19
3	9.590	18353	2122	0.17	0.23
4	9.875	21940	2751	0.20	0.30
5	10.402	52886	3705	0.48	0.40
6	11.386	12727	1983	0.11	0.21
7	11.742	23610	2711	0.21	0.29
8	12.462	86066	7711	0.78	0.83
9	12.781	10326559	854660	93.30	92.27
10	13.371	84636	7789	0.76	0.84

Integration Results

	RT	Area	Height	% Area	% Height
11	13.651	34451	4261	0.31	0.46
12	14.474	29356	3290	0.27	0.36
13	15.987	92430	7672	0.84	0.83
14	16.500	113684	10668	1.03	1.15
15	18.829	147428	13817	1.33	1.49

Acquired: 17:41:00, May 30, 2003
Sample Description: 72073-3B6601-5
D:\Voyager\Data\Peptides\MAY\30May03_0022.dat

Mode of operation:	Linear
Extraction mode:	Delayed
Polarity:	Negative
Acquisition control:	Manual
2889.0Accelerating voltage:	20000 V
Grid voltage:	94.5%
Guide wire 0:	0.04%
Extraction delay time:	150 nsec
Acquisition mass range:	500 – 7000 Da
Number of laser shots:	60/spectrum
Laser intensity:	1484
Laser Rep Rate:	3.0 Hz
Calibration type:	External – D:\Voyager\Calibrate\April03Lo.cal
Calibration matrix:	a-Cyano-4-hydroxycinnamic acid
Low mass gate:	400 Da
Digitizer start time:	14.686
Bin size:	2 nsec
Number of data points:	19895
Vertical scale:	200 mV
Vertical offset:	0%
Input bandwidth:	150 MHz
Sample well:	18
Plate ID:	100 WELL PLATE
Serial number:	1105
Instrument name:	Voyager-DE
Plate type filename:	C:\Voyager\100 well plate.plt
Lab name:	GENOSYS BIOTECHNOLOGIES
Absolute x-position:	37148.9
Absolute y-position:	42228.9
Relative x-position:	1.38989
Relative y-position:	1.37909
Shots in spectrum:	60
Source pressure:	6.0556e-007
Mirror pressure:	0
TC2 pressure:	0.01757
TIS gate width:	30
TIS flight length:	940

Printed: 17:42, May 30, 2003

APPENDIX 2

Anti-TG2 immunoprecipitation of a 58 KDa protein from HCA2 fibroblasts allowed to spread on collagen I

MATRIX SCIENCE **Mascot Search Results**

```
User           : Michael Morton
Email          : mortonms@cf.ac.uk
Search title   : SALLYTDSRD1210904F2
Database       : NCBInr 20040916 (2026219 sequences; 679922428 residues)
Timestamp      : 21 Sep 2004 at 16:23:15 GMT
Top Score      : 228 for gi|4507895, vimentin [Homo sapiens]
```

Probability Based Mowse Score

Ions score is -10*Log(P), where P is the probability that the observed match is a random event.
Protein scores greater than 76 are significant (p<0.05).

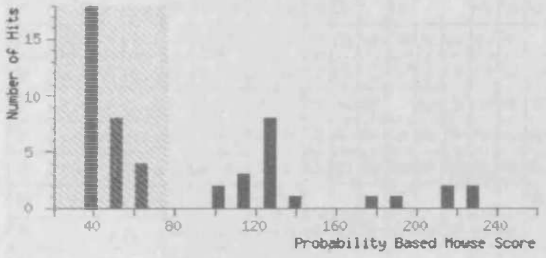

Protein Summary Report

Format As [Protein Summary] Help

Significance threshold p< [0.05] Max. number of hits [20]

Overview Table

Click on column header to jump to entry in results list.
Move mouse over any indicator to highlight identical peptides.
Click on an indicator to see details of individual match.
Use check boxes to select sub-set of queries for new search.

Mouse over: [-Query-] [-Accession-] [-Sequence-]

Hit:	1	2	3	4	5	6	7	8	9	10	11	12	13	14	15	16	17	18	19	20
☑ 825.16 (1+)																				
☑ 839.12 (1+)																				
☑ 845.14 (1+)																				

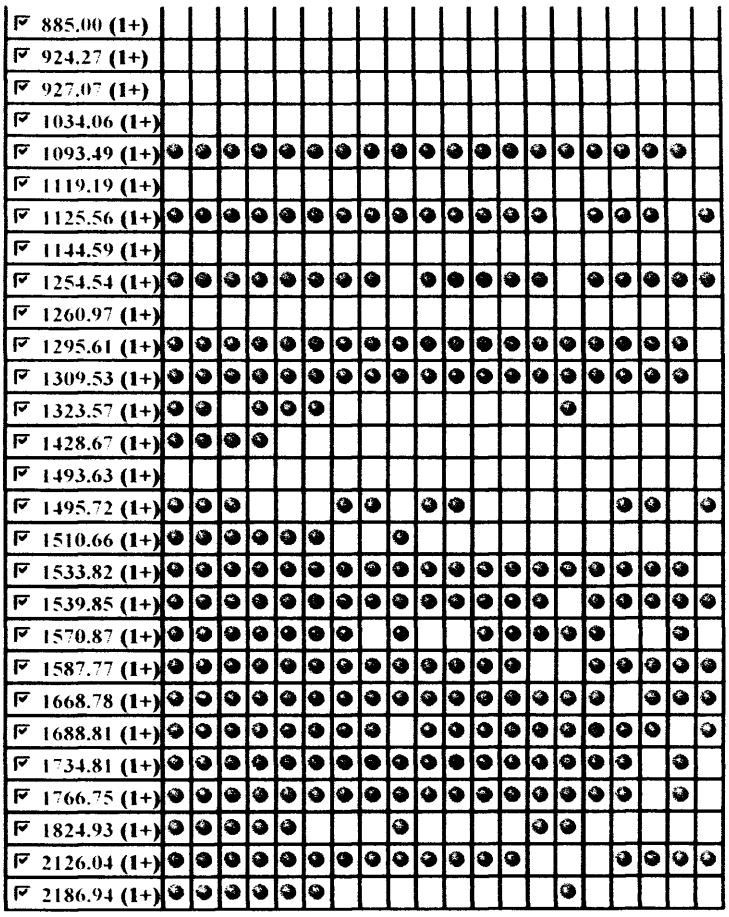

Select All | Select None | Search Selected

Index

	Accession	Mass	Score	Description
1.	gi|4507895	53710	228	vimentin [Homo sapiens]
2.	gi|44890587	53676	228	Vimentin [Homo sapiens]
3.	gi|47115317	53604	211	VIM [Homo sapiens]
4.	gi|340219	53738	209	vimentin
5.	gi|21757045	52463	193	unnamed protein product [Homo sapiens]
6.	gi|16552261	47516	180	unnamed protein product [Homo sapiens]
7.	gi|14389299	53757	140	vimentin [Rattus norvegicus]

42 KDa protein retrieved from Ntert keratinocyte extract through binding of TG5 β-barrel domains

Mascot Search Results

```
User            : Michael Morton
Email           : mortonms@cf.ac.uk
Search title    : SALLYTDSRD4b210904F4
Database        : NCBInr 20040916 (2026219 sequences; 679922428 residues)
Taxonomy        : Homo sapiens (human) (119915 sequences)
Timestamp       : 21 Sep 2004 at 16:38:42 GMT
Top Score       : 72 for gi|15277503, ACTB protein [Homo sapiens]
```

Probability Based Mowse Score

Ions score is -10*Log(P), where P is the probability that the observed match is a random event.
Protein scores greater than 63 are significant (p<0.05).

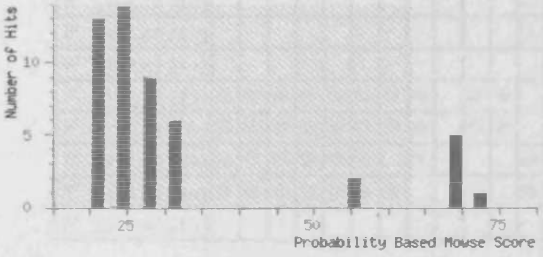

Protein Summary Report

Format As [Protein Summary] Help

Significance threshold p< [0.05] Max. number of hits [20]

Overview Table

Click on column header to jump to entry in results list.
Move mouse over any indicator to highlight identical peptides.
Click on an indicator to see details of individual match.
Use check boxes to select sub-set of queries for new search.

Mouse over: [-Query-] [-Accession-] [-Sequence-]

Hit:	1	2	3	4	5	6	7	8	9	10	11	12	13	14	15	16	17	18	19	20
☑ 824.18 (1+)																				
☑ 845.15 (1+)																				
☑ 861.12 (1+)																				

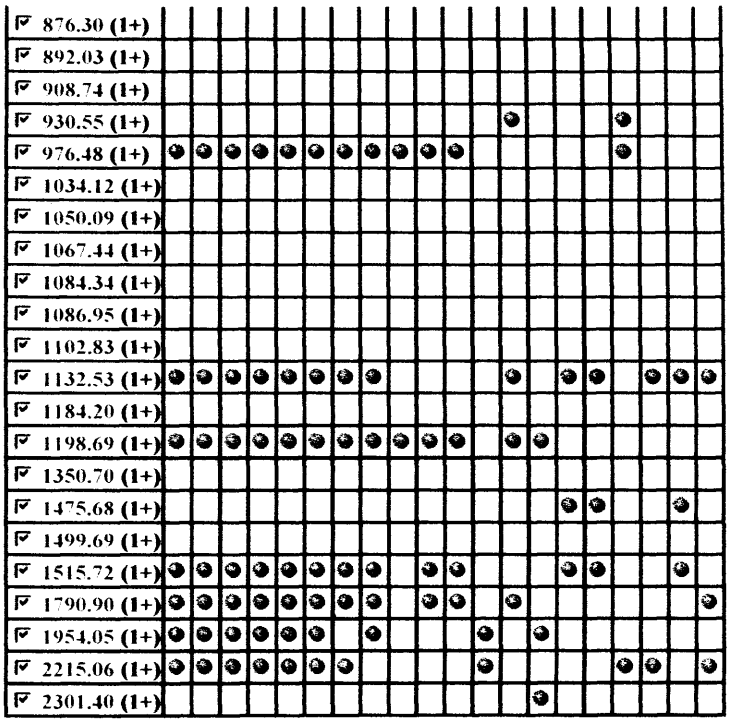

Select All | Select None | Search Selected

Index

	Accession	Mass	Score	Description
1.	gi|15277503	40536	72	ACTB protein [Homo sapiens]
2.	gi|14250401	41321	70	actin, beta [Homo sapiens]
3.	gi|71625	41977	70	actin gamma - bovine (tentative sequence)
4.	gi|16924319	40819	69	Unknown (protein for IMAGE:3538275) [Homo sapiens]
5.	gi|17511847	42108	69	ACTG1 protein [Homo sapiens]
6.	gi|21070355	42052	69	beta actin [Cavia porcellus]
7.	gi|16359158	42078	55	Beta actin [Homo sapiens]
8.	gi|28336	42128	54	mutant beta-actin (beta'-actin) [Homo sapiens]
9.	gi|998468	2420	32	48 kda histamine receptor subunit peptide 1 [internal
10.	gi|14192922	42334	31	actin, alpha, cardiac; alphac-actin [Mus musculus]
11.	gi|33563240	42366	31	actin, alpha 1, skeletal muscle [Mus musculus]
12.	gi|13171508	6570	30	immunoglobulin heavy chain variable region [Homo sapi
13.	gi|51492803	42226	30	PREDICTED: hypothetical protein XP_499543 [Homo sapie
14.	gi|28279429	24499	30	Similar to UDP-Gal:betaGlcNAc beta 1,4- galactosyltra
15.	gi|229361	17099	29	myoglobin
16.	gi|230638	17038	29	Myoglobin Mutant With Lys 45 Replaced By Arg And Cys
17.	gi|7020984	22277	29	unnamed protein product [Homo sapiens]

Appendix 3

QPCR assay including cDNA reverse transcribed from 12 ng total RNA

Well	Type	Name	Detector	Ct	StdDev Ct	Qty	Mean Qty	StdDev Qty
A1	Unknown	A tg2	htg2	33.04	0.574	2.38	3.26	1.236
A2	Unknown	B tg2	htg2	34.43	1.151	9.29E-01	6.18E-01	4.39E-01
A3	Unknown	C tg2	htg2	33.58	2.181	4.51	2.53	2.793
A4	NTC	NTC tg2	htg2	32.25	0.12			
A5	Standard	tg2 50 pg	htg2	18.24	0.318	50000		
A6	Standard	tg2 5 pg	htg2	21.88	0.155	5000		
A7	Standard	tg2 500 fg	htg2	25.67	0.508	500		
A8	Standard	tg2 50 fg	htg2	28.95	0.159	50		
A9	Standard	tg2 5 fg	htg2	31.49	0.138	5		
B1	Unknown	A tg2	htg2	32.23	0.574	4.13		
B2	Unknown	B tg2	htg2	34.68	0	7.87E-01	3.26	1.236
B3	Unknown	C tg2	htg2	35.19	2.181	5.58E-01	6.18E-01	4.39E-01
B4	NTC	NTC tg2	htg2	32.08	0.12		2.53	2.793
B5	Standard	tg2 50 pg	htg2	17.79	0.318	50000		
B6	Standard	tg2 5 pg	htg2	22.1	0.155	5000		
B7	Standard	tg2 500 fg	htg2	23.96	0.508	500		
B8	Standard	tg2 50 fg	htg2	26.72	0.159	50		
B9	Standard	tg2 5 fg	htg2	31.69	0.138	5		
C1	Unknown	A tg1	htg1	31.5	0.255	3.8	4.24	6.31E-01
C2	Unknown	B tg1	htg1	31.66	1.689	3.46	2.16	1.845
C3	Unknown	C tg1	htg1	33.58	0.397	1.12	1.34	3.09E-01
C4	NTC	NTC tg1	htg1	34.75	0			
C5	Standard	tg1 50 pg	htg1	15.46	0.009	50000		
C6	Standard	tg1 5 pg	htg1	19.39	0.308	5000		
C7	Standard	tg1 500 fg	htg1	22.5	0.852	500		
C8	Standard	tg1 50 fg	htg1	26.51	0.628	50		
C9	Standard	tg1 5 fg	htg1	30.99	0.307	5		
D1	Unknown	A tg1	htg1	31.14	0.255	4.69	4.24	6.31E-01
D2	Unknown	B tg1	htg1	34.05	1.689	8.53E-01	2.16	1.845
D3	Unknown	C tg1	htg1	33.02	0.397	1.56	1.34	3.09E-01
D4	Standard	tg1 50 pg	htg1	15.47	0.009	50000		
D5	Standard	tg1 5 pg	htg1	18.95	0.308	5000		
D6	Standard	tg1 500 fg	htg1	23.7	0.852	500		
D7	Standard	tg1 50 fg	htg1	27.4	0.628	50		
D8	Standard	tg1 5 fg	htg1	31.43	0.307	5		
D9	Unknown	A 1:10	RP S26	34.1	0.405	4.31	3.2	1.57
D10	Unknown	S9 1:10	RP S26	invalid				
E1	Standard	C 1:10	RP S26	33.11	0.451	549.22		
E2	Standard	C 1:30	RP S26	34.22	0.484	9		
E3	Standard	C 1:90	RP S26	34.92	0.354	1		
E4	NTC	NTC HK	RP S26	36.94	1.129			
E5	Unknown	A 1:10	RP S26	34.68	0.405	2.09	3.2	1.57
E6	Unknown	S9 1:10	RP S26	32.26	0	44.32		
E7	Standard	C 1:10	RP S26	33.75	0.451	9		
E8	Standard	C 1:30	RP S26	34.91	0.484	3		
E9	Standard	C 1:90	RP S26	35.42	0.354	1		
E10	NTC	NTC HK	RP S26	38.54	1.129			

QPCR assay including cDNA reverse transcribed from 50 ng total RNA

Well	Type	Name	Detector	Ct	StdDev Ct	Qty	Mean Qty	StdDev Qty
A1	Unknown	A tg2	htg2	32.64	2.825	1.84E-01	2.39	3.123
A2	Unknown	F tg2	htg2	30.34	1.235	1.17	2.97	2.55
A3	Unknown	G tg2	htg2	27.93	1.274	8.2	5.06	4.443
A4	NTC	ntc tg2	htg2	28.98	2.352			
A5	Standard	tg2 50 pg	htg2	17.19	0.442	50000		
A6	Standard	tg2 5 pg	htg2	20.31	0.639	5000		
A7	Standard	tg2 500 fg	htg2	24.17	0.26	500		
A8	Standard	tg2 50 fg	htg2	27.75	4.422	50		
A9	Standard	tg2 5 fg	htg2	28.4	0.534	5		
B1	Unknown	A tg2	htg2	28.64	2.825	4.6	2.39	3.123
B2	Unknown	F tg2	htg2	28.6	1.235	4.78	2.97	2.55
B3	Unknown	G tg2	htg2	29.73	1.274	1.92	5.06	4.443
B4	NTC	ntc tg2	htg2	32.3	2.352			
B5	Standard	tg2 50 pg	htg2	16.56	0.442	50000		
B6	Standard	tg2 5 pg	htg2	19.41	0.639	5000		
B7	Standard	tg2 500 fg	htg2	23.8	0.26	500		
B8	Standard	tg2 50 fg	htg2	21.5	4.422	50		
B9	Standard	tg2 5 fg	htg2	29.16	0.534	5		
C1	Unknown	A tg1	htg1	26.23	0.766	3.76	2.66	1.549
C2	Unknown	F tg1	htg1	26.39	0.569	3.3	2.51	1.113
C3	Unknown	G tg1	htg1	23.44	1.779	35.63	20.15	21.892
C4	NTC	ntc tg1	htg1	25.28	0.278			
C5	Standard	tg1 50 pg	htg1	14.2	0.048	50000		
C6	Standard	tg1 5 pg	htg1	16.81	0.179	5000		
C7	Standard	tg1 500 fg	htg1	21.15	0.462	500		
C8	Standard	tg1 50 fg	htg1	24.29	0.716	50		
C9	Standard	tg1 5 fg	htg1	26.09	1.437	5		
D1	Unknown	A tg1	htg1	27.31	0.766	1.57	2.66	1.549
D2	Unknown	F tg1	htg1	27.2	0.569	1.72	2.51	1.113
D3	Unknown	G tg1	htg1	25.96	1.779	4.67	20.15	21.892
D4	NTC	ntc tg1	htg1	25.68	0.278			
D5	Standard	tg1 50 pg	htg1	14.27	0.048	50000		
D6	Standard	tg1 5 pg	htg1	17.06	0.179	5000		
D7	Standard	tg1 500 fg	htg1	20.5	0.462	500		
D8	Standard	tg1 50 fg	htg1	23.28	0.716	50		
D9	Standard	tg1 5 fg	htg1	24.05	1.437	5		
E1	Unknown	A RP S26	RP S26	19.86	1.366	702.7	424.91	392.852
E2	Unknown	F RP S26	RP S26	20.43	0.513	442.85	344.45	139.162
E3	Standard	G RP S26	RP S26	22.3	0.272	100		
E4	Standard	G 1:10	RP S26	25.44	0.238	10		
E5	Standard	G 1:30	RP S26	27.31	0.752	3.33		
E6	Standard	G 1:90	RP S26	27.2	0	1.11		
E7	NTC	ntc RP S26	RP S26	27.73	0			
E8	Unknown	A RP S26	RP S26	21.79	1.366	147.12	424.91	392.852
E9	Unknown	F RP S26	RP S26	21.15	0.513	246.04	344.45	139.162
E10	Standard	G RP S26	RP S26	21.92	0.272	100		
F1	Standard	G 1:10	RP S26	25.1	0.238	10		
F2	Standard	G 1:30	RP S26	26.25	0.752	3.33		
F3	Standard	G 1:90	RP S26	27.2	0	1.11		